DETERMINACIÓN DE LAS PROPIEDADES DE TRANSPORTE EN MEZCLAS MULTICOMPONENTES

MIREN LARRAÑAGA SERNA

Director de Tesis:

M. Mounir Bou-Ali Saidi

Tesis dirigida a la obtención del título de

Doctor por Mondragon Unibertsitatea

Departamento de Mecánica y Producción Industrial

Mondragon Unibertsitatea

23 octubre 2015

AGRADECIMIENTOS

Durante la tesis el tiempo pasa cada vez más y más rápido. Tras pasar los últimos meses inmersa en la redacción de la memoria, con las prisas por cumplir los plazos previstos, las correcciones de última hora, los altibajos en el ánimo y en la inspiración… parece que el final, o al menos el final de la memoria, haya llegado de golpe. Y en estos momentos se hace hasta raro parar y echar la vista atrás, recordar lo vivido estos últimos años y todas las personas que de una manera u otra han dejado huella en esta tesis. En estas líneas me gustaría poder transmitir mi agradecimiento a todas esas personas que me han ayudado y enseñado, y especialmente, a todos los que me han hecho reír.

En primer lugar, he de darle las gracias a Mounir. Gracias por persuadirme para hacer la tesis, y por haberme acompañado en todos estos años. Gracias por la confianza que has depositado en mí, y por todo lo que he aprendido contigo, en cada reunión, en cada discusión y en cada conversación, en las dificultades y en los logros.

Seguidamente, quiero dar las gracias a Lander. Por todo. Por apoyarme, por animarme, por escucharme siempre, hasta cuando no puedo parar de hablar y no me acuerdo ni dónde había empezado la conversación. Por interesarte por lo que hago y querer explicar a todos qué es eso de la termodifusión. Por todo lo que nos reímos juntos. Eskerrik asko.

Me gustaría dar las gracias también a mi familia y en especial a mis aitas. Vosotros me habéis educado y me habéis inculcado el valor del trabajo. Es en gran parte gracias a vosotros que he llegado hasta aquí. Gracias por apoyarme y confiar en mí, por seguir preocupándoos por mí y por interesaros por mis experimentos y por esos coeficientes ternarios de los que tanto he hablado.

Quisiera dar las gracias a todos los miembros del grupo de Fluidos, por su ayuda en diferentes momentos y por el buen ambiente que ha habido en estos años. Particularmente, me gustaría dar las gracias a aquellos con los que he pasado más tiempo. Por una parte, a Alain, David, Joanes y Manex por todo lo que me han enseñado y ayudado en mis comienzos en Fluidos, y por todos los buenos momentos compartidos. En especial, he de darle las gracias a David por enseñarme a utilizar todos los equipos del laboratorio y por estar siempre dispuesto a echarme una mano. Por otra parte, a Estela, Iker y Ion. Mila esker zuen laguntzagatik eta elkarrekin pasatu ditugun momentu guztiengatik. Gracias por los necesarios ratos de charla y de procrastinación y sobre todo por haberme aguantado y apoyado en estos últimos meses en los que unas risas o un abrazo son el empujón que necesitas para llegar al final. No quisiera olvidarme de Leire, Karmele, Maialen, Joxemi, Pedro… Eskerrik asko nirekin konpartitu duzuen denboragatik. Me gustaría extender estos agradecimientos al resto de personal de Eskola que ha ayudado a sacar adelante este trabajo: Nagore, Ángel, Gotzon…

También quiero dar las gracias a los compañeros doctorandos y becarios con los que he coincidido en estos años. En especial quisiera acordarme de aquellos con los que llevo más tiempo y con los que más he compartido: Ione, Joseba y Torrano. Gracias por todos los buenos momentos que hemos pasado juntos, por todo lo que me he reído con vosotros, por las inquietudes compartidas y los viajes con conversaciones filosóficas que sólo

acaban porque hemos llegado y hay que salir del coche. Además, gracias a todos con los que he compartido incontables cafés y conversaciones de pasillo, de las que hemos aprendido y con las que nos hemos reído, y que en general, ayudan a ver las cosas desde otra perspectiva. Eskerrik asko Elías, Txino, Maider, Arkaitz, Iñigo, Arakama… Mención especial para "los Christians", a quienes me alegro mucho de haberme acoplado para comer los viernes de este último año. Mila esker barre guztiengatik eta zuekin ikasi dudanagatik.

Un último agradecimiento para todos los que habéis estado en los momentos de desconexión y recarga de pilas en estos años. Gracias a mi kuadrilla de Vitoria, y a la kuadrilla de la uni. Eskerrik asko Maite, Iñaki, Antonia y demás familia BIN. Y gracias a Manu y demás monitores, porque el deporte es terapéutico.

Volviendo al ámbito más científico, quisiera dar las gracias por sus aportes a esta tesis a diferentes personas y grupos con las que he tenido la oportunidad de trabajar. Muchas gracias a los catedráticos de la UPV Joseba Madariaga y Carlos Santamaría por todas sus aportaciones a esta tesis y por haber compartido conmigo su experiencia y sus conocimientos sobre la termodifusión.

Thank you to Professor Andrew Rees for his kindness and willingness to accept me in the University of Bath, and for his collaboration to the work done in this thesis.

Thank you also to the participating teams of the project DCMIX I have had the pleasure of working and learning with. Specially, I would like to thank to the team of Professor Valentina Shevtsova (ULB) and to the team of Professor Werner Köhler (Universität Bayreuth), with which I have had the opportunity to work more closely.

Además, he de dar las gracias al Gobierno Vasco por la beca predoctoral BFI-2011-295 que me ha permitido desarrollar este trabajo.

RESUMEN

En esta tesis doctoral se han analizado las propiedades de transporte en mezclas ternarias. El objetivo general de la misma es la determinación de los coeficientes de termodifusión, difusión molecular y Soret en mezclas ternarias. Por una parte se han determinado los coeficientes de termodifusión tanto en mezclas binarias como ternarias, mediante la técnica termogravitacional. Por otra parte, se han determinado los coeficientes de difusión molecular en mezclas binarias y ternarias mediante la técnica *sliding symmetric tubes* (SST). Los coeficientes Soret tanto de mezclas binarias como ternarias se han determinado a partir de la combinación de los coeficientes de termodifusión y difusión molecular.

Durante esta tesis doctoral se ha desarrollado una nueva metodología experimental para determinar los coeficientes de difusión molecular en mezclas ternarias mediante la técnica SST. Esto, junto con la medición de los coeficientes de termodifusión, ha hecho posible la determinación de los coeficientes Soret en mezclas ternarias. Concretamente, se han medido estos coeficientes para las seis concentraciones de la mezcla ternaria formada por 1,2,3,4-Tertrahidronaftalina (THN), Isobutilbenceno (IBB) y n-Dodecano (nC$_{12}$), correspondientes al proyecto DCMIX1. Además, dentro de este proyecto, se ha llevado a cabo el primer *benchmark* en mezclas ternarias junto con otros cinco equipos a escala internacional. En este trabajo de *benchmark* se han medido los coeficientes de transporte de la mezcla THN-IBB-nC$_{12}$ a concentración másica de 0,80-0,10-0,10 y a 25°C mediante diferentes técnicas experimentales y en diferentes condiciones de gravedad. Los resultados han mostrado en general un buen acuerdo, lo que ha supuesto un gran avance en el estudio del fenómeno de la termodifusión en mezclas ternarias.

Además, se han determinado los coeficientes de termodifusión de la mezcla ternaria formada por 1-Metilnaftaleno (MN), Tolueno (Tol) y n-Decano (nC$_{10}$) a ocho concentraciones y a 25°C. El estudio del coeficiente de termodifusión de estas dos mezclas ternarias ha propiciado el desarrollo de una regla de combinación que permite predecir los coeficientes de termodifusión en mezclas ternarias a partir de estos coeficientes en las mezclas binarias correspondientes.

Por otra parte, se ha continuado con el estudio de las mezclas binarias. En concreto, se han analizado 13 sistemas binarios formados por MN, Tol y nC$_i$ (para i = 6, 8, 10, 12, 14 y 16) a 25°C. Se ha medido el coeficiente de termodifusión de estos sistemas a varias concentraciones (77 mezclas) mediante la técnica termogravitacional. Además, se han determinado los coeficientes de difusión molecular mediante la técnica SST para estos 13 sistemas a concentración másica de 0,50. Por último, se han determinado los coeficientes Soret correspondientes a estas 13 mezclas binarias.

Los resultados experimentales en mezclas binarias han permitido realizar un análisis del efecto de las propiedades de la mezcla como viscosidad o masa molecular, sobre los coeficientes de termodifusión, difusión molecular y Soret.

LABURPENA

Tesi-doktoretza honetan garraio propietateak aztertu dira nahasketa hirutarretan. Lanaren helburu orokorra, nahasketa hirutarretan termodifusioko, difusio molekularreko eta Soret koefizienteak zehaztea da. Alde batetik, termodifusioko koefizienteak neurtu dira teknika termograbitazionalaren bidez, nahasketa bitarretan eta hirutarretan. Bestetik, difusio molekularreko koefizienteak zehaztu dira *sliding symmetric tubes* (SST) teknikaren bidez, bai nahasketa bitarretan bai hirutarretan. Soret koefizienteak zehaztu dira temodifusio eta difusio molekularreko koefizienteen konbinaziotik.

Tesi-doktoretza honetan metodologia esperimental berri bat garatu da, nahasketa hirutarretan difusio molekularreko koefizienteak zehazteko SST teknikaren bidez. Honek, temodifusioko koefizienteen neurketarekin batera, Soret koefizientearen zehaztapena nahasketa hirutarretan ahalbidetu du. Konkretuki, koefiziente hauek neurtu dira DCMIX1 proiektuaren nahasketa hirutarraren sei konposaketarako. Nahasketa hau 1,2,3,4-Tertrahidronaftalinak (THN), Isobutilbentzenoak (IBB) eta n-Dodekanoak (nC$_{12}$) osatzen dute. Gainera, proiektu honen egituran, lehenengo *benchmark*-a nahasketa hirutarretan burutu da, beste bost nazioarteko taldeekin. Lan honetan, THN-IBB-nC$_{12}$ nahasketaren garraio koefizienteak zehaztu dira 0,80-0,10-0,10 kontzentraziorako eta 25°C-etan, hainbat teknika esperimentalen bitartez eta grabitate baldintza ezberdinetan. Emaitzak bat datoz, aurrerapen garrantzitsua ekarriz termodifusio fenomenoaren ikerketari.

Gainera, termodifusioko koefizienteak neurtu dira 1-Metilnaftalenoak (MN), Toluenoak (Tol) eta n-Dekanoak (nC$_{10}$) osatzen duten nahasketarako, zortzi kontzentrazio ezberdinetarako eta 25°C-etan. Bi sistema hauen termodifusioko koefizientearen ikerketak, korrelazio berri baten garapena bideratu du. Korrelazio honek, nahasketa hirutarren termodifusioko koefizienteak, nahasketa bitarren koefizienteetatik kalkulatzea ahalbidetzen du.

Bestalde, nahasketa bitarren ikerketarekin jarraitu da. Konkretuki, 13 sistema bitarrak aztertu dira, MN-k, Tol-k eta nC$_i$-k (non i = 6, 8, 10, 12, 14 eta 16) osatuta, 25°C-etan. Termodifusioko koefizienteak neurtu dira hainbat kontzentrazioetara (guztira 77 nahasketa), teknika termograbitazionalaren bitartez. Halaber, difusio molekularreko koefizienteak neurtu dira 13 sistema hauetarako, 0,50-eko kontzentrazio masikoan. Azkenik, Soret koefizienteak zehaztu dira 13 nahasketa hauetarako.

Nahasketa bitarretan lortu diren emaitza esperimentalak erabili dira nahasketen propietateek (adibidez, biskositatea edo masa molekularra) termodifusioko, difusio molekularreko eta Soret koefizienteetan daukaten eragina aztertzeko.

ABSTRACT

In this doctoral thesis the transport properties in ternary mixtures are analysed. The general objective of the work, is the determination of the thermodiffusion, molecular diffusion and Soret coefficients in ternary mixtures. On the one hand, we measure the thermodiffusion coefficients in both binary and ternary mixtures, by the thermogravitational technique. On the other hand, we ascertain the molecular diffusion coefficients in binary and ternary mixtures by the sliding symmetric tubes (SST) technique. The Soret coefficients in both binary and ternary mixtures are determined by the combination of the results for the thermodiffusion and molecular diffusion coefficients.

In this work, we develop a new experimental methodology to determine the molecular diffusion coefficients in ternary mixtures by the SST technique. This, together with the measurement of the thermodiffusion coefficients, makes possible the determination of the Soret coefficients in ternary mixtures. Specifically, we measure these coefficients for the six compositions of the ternary mixture formed by 1,2,3,4-Tertrahydronaphtaline (THN), Isobutylbenzene (IBB) and n-Dodecane (nC$_{12}$), related to the project DCMIX1. In addition, in the framework of this project, we have conducted the first benchmark in ternary mixtures, in collaboration with other five teams at international level. In this benchmark work each team measures the transport coefficients of the mixture THN-IBB-nC$_{12}$ at mass fraction of 0.80-0.10-0.10 and at 25°C, by different experimental techniques and in different gravity conditions. The results show a good agreement in general, which comes as a great breakthrough in the study of the thermodiffusion phenomenon in ternary mixtures.

In addition, we determine the thermodiffusion coefficients of the ternary mixture composed by 1-Methylnaphtalene (MN), Toluene (Tol) and n-Decane (nC$_{10}$) at eight different compositions and at 25°C. The study of these two ternary mixtures results in a combination rule which enables the prediction of the thermodiffusion coefficients in ternary mixtures from the thermodiffusion coefficients of the corresponding binaries.

Moreover, we continue with the study of binary mixtures. Specifically, we analyse 13 binary systems composed by MN, Tol and nC$_i$ (for i = 6, 8, 10, 12, 14 and 16), at 25°C. We measure the thermodiffusion coefficient of these systems at different mass fractions (77 mixtures) by the thermogravitational technique. Additionally, we determine the molecular diffusion coefficients by the SST technique for the equimass composition of these 13 binary mixtures.

With the experimental results in binary mixtures, we analyse the effect of different properties of the mixtures, such as viscosity or molecular weight, on the thermodiffusion, molecular diffusion and Soret coefficients.

INDICE

ÍNDICE DE TABLAS

ÍNDICE DE FIGURAS

GLOSARIO

m_T	Masa total de la mezcla, kg.
m_i	Masa del componente *i* en la mezcla, kg.
M_m	Masa molecular, uma.
M_i	Masa molecular del componente *i*, uma.
c_i	Concentración másica del componente *i* en la mezcla.
ρ	Densidad, kg/m^3.
n_D	Índice de refracción, RIU.
α	Coeficiente de expansión térmica, K^{-1}.
T	Temperatura, K.
β	Coeficiente de expansión másica.
k_i	Coeficiente de calibración correspondiente a la densidad, kg/m^3.
$k_i^{'}$	Coeficiente de calibración correspondiente al índice de refracción.
μ	Viscosidad dinámica, Pa·s.
t	Tiempo, s.
D_T	Coeficiente de termodifusión en una mezcla binaria, m^2/sK.
$D_{T,i}^{'}$	Coeficiente de termodifusión del componente *i* en una mezcla ternaria, m^2/sK.
ν	Viscosidad cinemática, m^2/s.
L_x	Espesor del gap de la columna termogravitacional, m.
L_z	Longitud del gap de la columna termogravitacional, m.
g	Aceleración de la gravedad, m/s^2.
$c^{up/low}\Big\vert_m$	Concentración media en el tubo superior/inferior.
$c_0^{up/low}$	Concentración inicial en el tubo superior/inferior.
D	Coeficiente de difusión molecular en una mezcla binaria, m^2/s.

D_{ij}	Coeficientes de difusión molecular en una mezcla ternaria, m^2/s.
$\hat{D}_i$	Valores propios de la matriz de difusión en una mezcla ternaria, m^2/s.
L	Longitud, m.
t_r	Tiempo de relajación, s.
$S_i^{up\ /\ low}$	Pendiente formada por la variación de la concentración del componente *i* en función de la raíz cuadrada del tiempo en el tubo superior/inferior, s^2.
S_T	Coeficiente Soret de una mezcla binaria, K^{-1}.
$S_{T,i}^{'}$	Coeficiente Soret del componente *i* en una mezcla ternaria, K^{-1}.

1. INTRODUCCIÓN

Los fenómenos de transporte de masa en mezclas líquidas analizados en esta tesis doctoral son los debidos a un gradiente de concentración (difusión molecular), a un gradiente térmico (termodifusión) y a la combinación de ambos (efecto Soret). Estos fenómenos toman parte en múltiples procesos de diferentes campos desde la biología humana [1] hasta la energía nuclear [2]. Por ello, actualmente existe un interés creciente por esta temática y cada día son más las aplicaciones donde se demuestra que la difusión es un fenómeno a tener en cuenta.

El objetivo general de esta tesis doctoral se ha enfocado en el estudio experimental de los fenómenos de termodifusión, difusión molecular y Soret en mezclas líquidas multicomponentes. Para ello se han empleado diferentes técnicas como la técnica termogravitacional y la técnica *sliding symmetric tubes*. Con ello se espera contribuir al estudio y compresión de estos mecanismos de transporte

1.1. Estado del arte

A principios del siglo XIX Graham descubrió la difusión en los líquidos mediante ensayos experimentales, pero fue Fick quien posteriormente desarrolló la primera relación cuantitativa para expresar la difusión, conocida hoy como la ley de Fick [3]. Combinando esta ecuación con la ley de conservación de la masa se obtiene la segunda ley de Fick:

$$\frac{\partial c}{\partial t} = D\frac{\partial^2 c}{\partial z^2}. \tag{1.1}$$

Por otra parte, en 1856 Ludwig descubrió experimentalmente el fenómeno de la termodifusión [4]. Posteriormente y de forma independiente, Soret también descubrió este fenómeno y continuó estudiándolo [5, 6]. Es en reconocimiento a estos esfuerzos iniciales que hoy en día se conoce como efecto Soret o Ludwig-Soret a la separación que se produce en una mezcla debido al efecto de un gradiente térmico.

Estos fenómenos de transporte de masa, resultan de gran interés en la comunidad científica por los numerosos campos en los que juegan un rol importante, como en métodos de separación [7, 8], procesos de combustión [9], caracterización de campos geológicos [10]…

En macromoléculas y coloides la termodifusión es importante por su potencial para caracterizar polímeros y partículas [11]. Además, su estudio es fundamental para entender algunos aspectos relacionados con la ciencia de la vida [12]. De hecho, la termodifusión se ha presentado como un posible mecanismo de transporte biológico [13] e incluso en [14] se muestra cómo el efecto Soret pudo tomar parte en el origen de la vida. En esta serie de aplicaciones biotecnológicas, recientemente se ha mostrado que la termodifusión puede ser un parámetro importante en la optimización de microdispositivos en forma de T [8].

Por otra parte, este fenómeno despierta un gran interés en el sector de la industria petrolífera [15]. El conocimiento de los coeficientes de transporte permite una óptima explotación y exploración de los pozos petrolíferos, ayudando a predecir el estado inicial de las reservas [16-18].

El caso de las mezclas binarias ha sido ampliamente estudiado, y a día de hoy existen diversas técnicas contrastadas para determinar las propiedades de transporte en estas mezclas. Algunas de ellas emplean métodos ópticos como por ejemplo: *Thermal Diffusion Forced Rayleigh Scattering* (TDFRS) [19], mediante la cual se puede determinar simultáneamente el coeficiente de difusión molecular y el coeficiente Soret; *Optical Beam Deflection* (OBD) [20], que permite determinar los coeficientes Soret y de termodifusión y difusión molecular; y *Optical Digital Interferometry* (ODI) [20], mediante la cual se determina el coeficiente Soret.

También existen técnicas que no emplean métodos ópticos y permiten determinar los coeficientes de transporte de manera independiente. Entre ellas se puede encontrar la técnica *Open Ended Capillary* (OEC) [21], que permite determinar el coeficiente de difusión molecular; la técnica *Sliding Symmetric Tubes* (SST) [22] que se emplea en el laboratorio de Fluidomecánica de Mondragon Goi Eskola Politeknikoa para determinar el coeficiente de difusión molecular; para determinar el coeficiente de difusión molecular también se emplean técnicas basadas en el principio de dispersión de Taylor [23]. Por otra parte, la técnica termogravitacional [24], utilizada en el laboratorio de Fluidomecánica de Mondragon Goi Eskola Politeknikoa, se emplea para determinar el coeficiente de termodifusión

Hoy en día es necesario continuar analizando mezclas binarias pues el conocimiento obtenido de su estudio es la base para poder comprender el comportamiento de los fenómenos de transporte en mezclas ternarias. Con el fin de avanzar en el desarrollo de nuevos modelos numéricos de predicción, según la teoría de la termodinámica de no equilibrio [25] o como base de la dinámica molecular [26], varios equipos científicos de carácter experimental, han tratado de desarrollar nuevas correlaciones cuantitativas. Por ejemplo, en [27, 28] se expresa el coeficiente Soret de una mezcla binaria en función de la masa molecular y la inercia de los componentes. Por otra parte, en mezclas binarias de alcanos, se han desarrollado correlaciones que permiten predecir los coeficientes de termodifusión [29], difusión molecular [22] y Soret [30] a partir de propiedades más simples de la mezcla.

Además de correlaciones cuantitativas, también se han realizado diversos estudios sobre la influencia de ciertas propiedades de la mezcla sobre el coeficiente de difusión térmica. Por ejemplo en [21, 31] se analizan los conceptos de similitud y movilidad de las moléculas.

Actualmente, el mayor interés de la comunidad científica se encuentra en el estudio de los fenómenos de transporte en mezclas ternarias. En la mayoría de aplicaciones las mezclas en las que interviene el fenómeno de la termodifusión son multicomponentes, por lo que el estudio de las mezclas ternarias parece un paso lógico antes de avanzar hacia sistemas más complejos. Sin embargo, a día de hoy no existe una teoría rigurosa y unificada; por ejemplo, a la hora de determinar el coeficiente de difusión térmica, el modelo desarrollado para definir el flujo de masa debido al gradiente de temperatura en los trabajos de Ghorayeb y Firoozabadi [32] es diferente al presentado por Kempers [33]. De hecho, la falta de una base de datos experimentales para mezclas ternarias o superiores obstaculiza el avance en el desarrollo de los diferentes modelos basados en la termodinámica de no equilibrio o en la dinámica molecular.

En los últimos años se han publicado varios trabajos individuales en los que se determinan los diferentes coeficientes de transporte en mezclas ternarias. En dichos trabajos se han empleado la técnica termogravitacional [34, 35], la técnica SST [36], la técnica OBD [37], la técnica TDT [38, 39], o la técnica OEC [40, 35]. A su vez, también se han realizado simulaciones en base a la dinámica molecular [41] y modelos de predicción [42]. No obstante, y debido a la falta de más resultados experimentales, no han podido contrastarse completamente.

Los tímidos esfuerzos individuales de cada equipo indicaban la necesidad de aunar el potencial de cada grupo en un proyecto común. En este punto, cabe destacar el proyecto *Diffusion Coefficients measurements in ternary MIXtures* (DCMIX) de la Agencia Espacial Europea (ESA) en el que participa el grupo de Mecánica de Fluidos de Mondragon Goi Eskola Politeknikoa. Este proyecto está coordinado por la Prof. V. Shevtsova (*Microgravity Research Center* de la *Université Libre de Bruxelles*, Bélgica) y por el Prof. Z. Saghir (*Ryerson University*, Canadá). En él participan los equipos del Prof. W. Köhler (Universität Bayreuth, Alemania), del Prof. A. Mojtabi (*Université Paul Sabatier*, Francia), del Prof. A. Komiya (*Tohoku University*, Japón), del Dr. I. Ryzhkov (*Institute of Computational Modelling* SB RAS, Rusia), del Prof. S. Van Vaerenbergh (*Université Libre de Bruxelles*, Bélgica), de la Prof. T. Lyubimova (*Intitute of Continuous Media*, Rusia), del Dr. M Eslamian (*University of Toronto*, Canadá), del Dr. H. Bataller (*Université de Pau et des Pays de l'Adour*, Francia), del Prof. S. Semenov (*Russian Academy of Sciences*, Rusia), de la Prof. S. Wiegand (*Forschungszentrum Jülich*, Alemania) y del Prof. J. M. Ortiz de Zarate (Universidad Complutense de Madrid, España).

El objetivo del proyecto DCMIX es analizar el fenómeno de la termodifusión en mezclas ternarias, tanto en condiciones terrestres como de microgravedad. Para ello, se realizan experimentos en los laboratorios terrestres y también a bordo de la Estación Espacial Internacional (ISS). En ella se encuentra la instalación *Selectable Optical Diagnostic Instrument* (SODI) empleada para determinar los coeficientes Soret en condiciones de microgravedad. En el capítulo 5 de esta memoria se incluye una descripción del funcionamiento de este dispositivo.

Durante esta tesis doctoral se ha analizado la mezcla correspondiente a la primera misión del proyecto DCMIX (DCMIX1), formada por 1,2,3,4-Tetrahidronaftalina (THN), Isobutilbenceno (IBB) y n-Dodecano (nC$_{12}$), a las 6 concentraciones que se marcan en la Figura 1.1 (a). Los resultados obtenidos han contribuido a la organización del primer *benchmark* en mezclas ternarias [43], en el que seis equipos del proyecto DCMIX han analizado la mezcla THN-IBB-nC$_{12}$ a concentración de 0,80-0,10-0,10 y a 25°C mediante diferentes técnicas experimentales y en diferentes condiciones de gravedad. El capítulo 5 de esta memoria incluye todos los detalles de este trabajo colaborativo que ha supuesto un gran avance en el estudio del fenómeno de la termodifusión en mezclas líquidas ternarias.

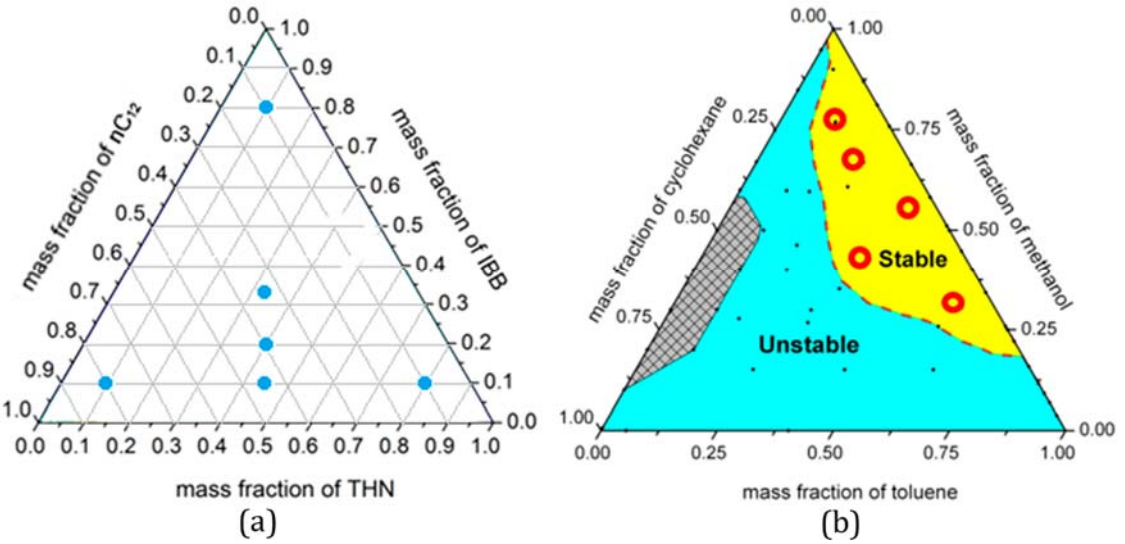

Figura 1.1. Triángulos de concentración para las mezclas ternarias (a) THN-IBB-nC$_{12}$ y (b) Tol-M-CH, a 25°C.

En DCMIX2 (la segunda misión), Figura 1.1 (b), la mezcla analizada está formada por Tolueno (Tol), Metanol (M) y Ciclohexano (CH) a cinco concentraciones diferentes. Esta mezcla se caracteriza por el cambio de signo del coeficiente Soret y además, porque la mezcla es inmiscible en un amplio rango de concentración. Actualmente se están procesando los resultados obtenidos en microgravedad y se están realizando los experimentos en los laboratorios terrestres.

En la tercera misión del proyecto DCMIX y que corresponde a DCMIX3 se ha propuesto una mezcla ternaria acuosa. Se compone de Agua, Etanol y Trietilenglicol a cinco concentraciones. Actualmente se están realizando los experimentos en condiciones terrestres y se está preparando el experimento para enviar las mezclas a analizar en la Estación Espacial Internacional. La campaña experimental de DCMIX3 se vio retrasada el pasado octubre de 2014 debido a la explosión del cohete no tripulado Antares [44]. En ella se perdió la célula que contenía las mezclas de este proyecto junto con otra serie de experimentos científicos.

En el futuro cercano se prevén las campañas DCMIX4 y DCMIX5, para las que aún no se han definido las mezclas a analizar.

1.2. Motivación y objetivos

La motivación de esta tesis doctoral es llegar a conocer y comprender los mecanismos de transporte de no equilibrio en mezclas multicomponentes, para así, profundizar en el funcionamiento de los mismos y poder sacar el máximo rendimiento en sus posibles aplicaciones.

El objetivo final de esta tesis es por tanto determinar los coeficientes de transporte tanto de primer como de segundo orden en mezclas ternarias. Este objetivo general puede desglosarse en los siguientes objetivos operativos:

- Determinar el coeficiente de termodifusión en mezclas binarias y ternarias mediante la técnica termogravitacional.
- Desarrollar una metodología para determinar experimentalmente el coeficiente de difusión molecular en mezclas ternarias mediante la técnica de *Sliding symmetric tubes*.
- Determinar el coeficiente Soret de manera indirecta tanto en mezclas binarias como ternarias.
- Recuperar y analizar los resultados experimentales obtenidos en condiciones de microgravedad a bordo de la ISS y compararlos con los obtenidos en este trabajo y en otros laboratorios en condiciones terrestres.
- Validar y ampliar los modelos de predicción de los fenómenos de transporte en mezclas multicomponentes.

Los objetivos descritos se ven representados mediante el diagrama de la Figura 1.2. Además de estos objetivos, existen otros como la difusión, explotación de los resultados, generación de nuevas colaboraciones y estancias en otros centros.

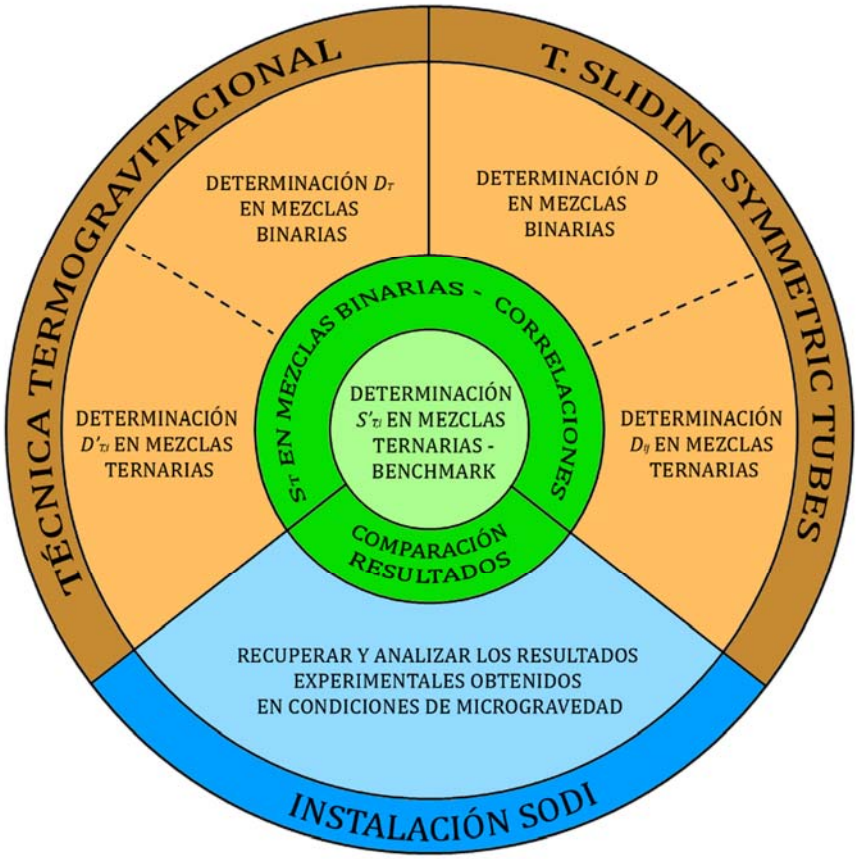

Figura 1.2. Diagrama de objetivos de la tesis doctoral.

Para llevar a cabo estos objetivos se han analizado varias mezclas binarias y ternarias formadas por los componentes que se presentan en la Tabla 1.1. En ella se muestran también las propiedades termofísicas de los componentes puros empleados.

Tabla 1.1. Propiedades de los componentes puros correspondientes a las mezclas analizadas en esta tesis doctoral, a 25°C.

Componente	M_m	ρ (kg/m^3)	nD	μ x 10^{-3} (Pa·s)	α x 10^{-3} (K^{-1})
Tolueno	92,14	862,288	1,49382	0,554	1,080
1,2,3,4-Tetrahidronaftalina	132,21	964,791	1,53870	1,971	0,813
Isobutilbenceno	134,22	849,060	1,48381	0,955	0,952
1-Metilnaftaleno	142,20	1018,542	1,61800	3,005	0,733
n-Hexano	86,18	655,197	1,37260	0,323	1,386
n-Octano	114,23	698,753	1,39514	0,513	1,157
n-Decano	142,28	726,111	1,40946	0,838	1,041
n-Dodecano	170,34	745,161	1,41939	1,327	0,973
n-Tetradecano	198,39	759,160	1,42670	2,034	0,929
n-Hexadecano	226,44	770,213	1,43242	2,995	0,899

2. TÉCNICAS EXPERIMENTALES

En este capítulo se describen las técnicas empleadas durante esta tesis doctoral para determinar los coeficientes de termodifusión, difusión molecular y Soret tanto en mezclas líquidas binarias como ternarias. Los coeficientes de termodifusión se han medido mediante la técnica termogravitacional (TG). Los coeficientes de difusión molecular se han determinado mediante la técnica *Sliding symmetric tubes* (SST). Durante esta tesis también se han desarrollado las ecuaciones de trabajo para poder determinar los coeficientes de difusión molecular en mezclas ternarias mediante la técnica SST. Los coeficientes Soret se determinan de manera indirecta a partir de los resultados obtenidos para los coeficientes de termodifusión y difusión molecular.

Cabe destacar que las columnas termogravitacionales y la instalación de *Sliding symmetric tubes* han sido diseñadas y construidas íntegramente en Mondragon Goi Eskola Politeknikoa (MGEP).

2.1. Técnica termogravitacional

En este trabajo se ha utilizado la técnica termogravitacional (TG) para determinar el coeficiente de termodifusión. En esta técnica se introduce una mezcla entre dos paredes a diferentes temperaturas, siendo una de ellas la pared fría y la otra, la pared caliente. Debido al gradiente de temperatura, se crea una separación horizontal ya que, generalmente, las moléculas más densas tienden a desplazarse hacia la pared fría y las menos densas hacia la pared caliente. A causa de esta separación horizontal, aparece un gradiente de concentración y se genera un flujo de masa en el sentido contrario debido al fenómeno de la difusión molecular. Además, el efecto de la gravedad genera flujos convectivos que amplifican la separación a lo largo de la columna (Figura 2.1).

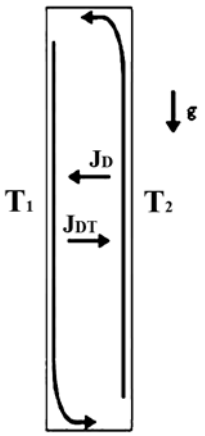

Figura 2.1. Diagrama de flujos en la técnica termogravitacional

El análisis de la distribución de la concentración en estado estacionario a lo largo de la columna permite la determinación del coeficiente de termodifusión. Para ello se emplea la expresión (2.1) [45-47] que se basa en la teoría para gases de Furry, Jones y Onsager (F.J.O.) [48] y que fue extendida a disoluciones concentradas por Majumdar [49].

$$\Delta c_i = -\frac{504 L_z}{g L_x^4} \frac{D'_{T,i} \nu}{\alpha} c_i c_j \,. \qquad (2.1)$$

Además de la separación a lo largo de la columna, otro parámetro a tener en cuenta es el tiempo de relajación; es decir, el tiempo que tarda la mezcla en llegar al estado estacionario. Generalmente, el tiempo de equilibrio de un ensayo es cinco veces el tiempo de relajación. Este parámetro depende tanto de las propiedades de la mezcla analizada como de las dimensiones de la columna termogravitacional empleada, y viene dado por la siguiente expresión [47]:

$$t_r = \frac{9! L_z^{\,2} \mu^2 D}{\left(\pi \Delta T g \rho \alpha L_x^{\,3}\right)^2}. \qquad (2.2)$$

En este trabajo se han empleado dos columnas termogravitacionales planas, que pueden verse en la Figura 2.2. Como se ha comentado anteriormente, estas dos columnas han sido diseñadas y construidas íntegramente en MGEP, considerando los límites de validez de la teoría F.J.O. [50, 51] a la hora de dimensionar la relación de aspecto (el gap y la altura).

Figura 2.2. Instalación termogravitacional formada por las dos columnas planas de L_z = 500 mm y de L_z = 980 mm

Ambas columnas están compuestas por dos placas paralelas de aluminio, a través de las cuales circula el agua atemperada que genera el gradiente de temperatura. Una placa de Keltron Peek-1000 hace de separador entre las dos placas de aluminio. Este material tiene una conductividad térmica muy baja, con lo que la mezcla situada en el gap es sometida únicamente a un gradiente térmico horizontal. El agua que circula por las placas de aluminio está controlada por dos baños termostáticos de la casa Lauda, que permiten un ajuste de la temperatura de ±0,01 °C. La temperatura generada en el fluido analizado se mide mediante una sonda Pt 100. Esto otorga un control del gradiente térmico generado en la mezcla de ±0,1 °C.

La diferencia principal entre las dos columnas planas empleadas en este trabajo se encuentra en las dimensiones del espacio de trabajo, concretamente en su longitud. Una de las columnas (STC) tiene el gap de espesor 1±0,005 mm y longitud 500 mm, mientras que la otra (LTC), de construcción más reciente, tiene un gap de espesor 1,02±0,005 mm y

longitud 980 mm. La anchura del gap es la misma en ambos casos, 50 mm. Además, la columna STC tiene cuatro puntos de extracción mientras que la columna LTC tiene cinco.

Esta diferencia en la longitud del gap tiene influencia principalmente en la separación relativa a lo largo de la altura de la columna, que es proporcional a esta dimensión. Es decir, en la columna de mayor longitud aumenta la sensibilidad a la hora de medir la separación estacionaria. Esto es de especial interés en el caso de las mezclas ternarias, en las que la separación de los componentes es generalmente más reducida. Además, como es lógico, el volumen de muestra necesario en la columna LTC es aproximadamente el doble del necesario en la columna STC, que son del orden de 60 ml y 30 ml respectivamente.

La columna STC, cuya validez ha sido demostrada anteriormente en varios trabajos [34, 52], se ha empleado principalmente para determinar los coeficientes de termodifusión de las mezclas binarias estudiadas en esta tesis.

La columna LTC se ha empleado principalmente para determinar los coeficientes de termodifusión de las mezclas ternarias. Previamente, esta columna fue validada [53] con las mezclas binarias correspondientes al *benchmark* de Fontainebleau [54]. En la siguiente Tabla 2.1 puede verse la comparación entre los valores *benchmark* y los resultados obtenidos con la columna LTC.

Tabla 2.1. Comparación entre los valores *benchmark* del coeficiente de termodifusión y los medidos mediante la LTC a 25°C.

Mezcla	D_T x 10^{-12} (m^2/sK) LTC	D_T x 10^{-12} (m^2/sK) *Bench*	Dif. (%)
THN-IBB (0.5)	2,73 ± 0,05	2,80 ± 0,10	2,5
IBB-*n*C_{12} (0.5)	3,64 ± 0,06	3,70 ± 0,20	1,6
THN-*n*C_{12} (0.5)	6,10 ± 0,10	5,90 ± 0,30	2,5

2.1.1. Mezclas binarias

En el caso de las mezclas binarias, la separación en estado estacionario se obtiene a partir de la medida de la densidad de las muestras extraídas a lo largo de la altura de la columna. La variación de la densidad con respecto a la altura presenta un comportamiento lineal, como puede observarse en la Figura 2.3, en el ejemplo correspondiente a la mezcla MN-*n*C_8 a concentración másica de 0,60 de MN y a 25°C. Conociendo la pendiente de esta regresión lineal y las propiedades termofísicas de la mezcla, el coeficiente de termodifusión se determina mediante la siguiente expresión [52]:

$$D_T = -\frac{gL_x^4}{504}\frac{\alpha}{c_i c_j \beta \mu}\frac{\partial \rho}{\partial z}. \qquad (2.3)$$

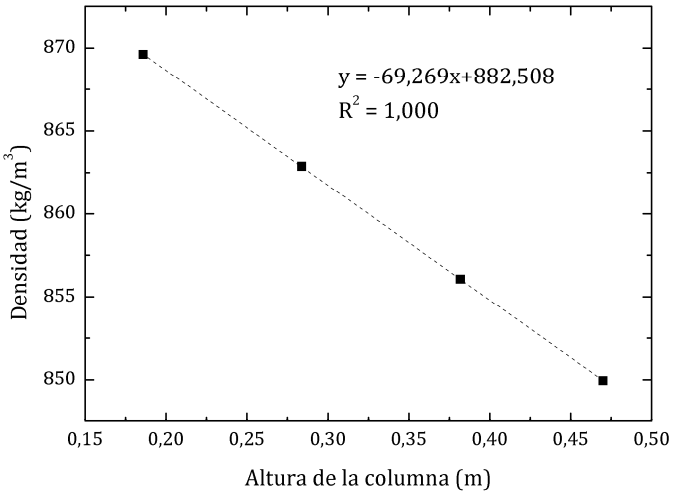

Figura 2.3. Variación de la densidad en función de la altura de la columna en estado estacionario, para la mezcla MN-*n*C_8 a concentración másica de 0,60 de MN y a 25°C, obtenida mediante la columna STC.

Para conocer el error experimental correspondiente a la determinación del coeficiente de termodifusión de una mezcla binaria se han considerado los errores sistemáticos y experimentales relativos a todos los parámetros de la expresión (2.3). Así pues, se puede observar que la variable que tiene una mayor influencia es el espesor del gap, que es propio de la instalación y repercutirá en todos los ensayos. Además, tienen efecto la precisión del densímetro y del viscosímetro y la determinación de los coeficientes de expansión térmica y másica. Por último, el error experimental del ensayo en sí mismo se ve reflejado en la precisión de la regresión lineal formada por la variación de la densidad con respecto a la altura de la columna.

Aunque se calcula específicamente para cada ensayo, el error experimental en la determinación del coeficiente de termodifusión de una mezcla binaria mediante la columna STC se encuentra generalmente en torno al 4%, mientras que para el caso de la columna LTC es inferior al 2%. Esta diferencia es gracias a la mayor sensibilidad en la determinación de la separación que proporciona la columna LTC.

2.1.2. Mezclas ternarias

En el caso de las mezclas ternarias, es necesario medir tanto la densidad como el índice de refracción para poder determinar las concentraciones de los tres componentes a lo largo de la altura de la columna en estado estacionario. Como se puede observar en la Figura 2.4 la variación de estas propiedades en función de la altura de la columna es lineal.

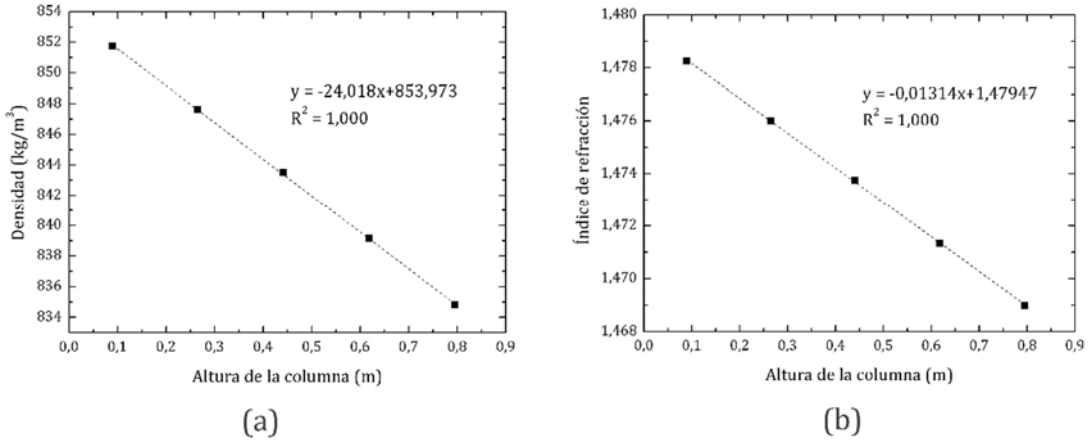

Figura 2.4. Variación de la densidad (a) y del índice de refracción (b) en función de la altura de la columna LTC, en estado estacionario, para la mezcla ternaria THN-IBB-nC$_{12}$ a concentración de 0,40-0,20-0,40 y a 25°C.

En el apartado 3.2.3 se describe cómo se determina la variación de la concentración de cada componente a lo largo de la altura de la columna mediante la combinación de las mediciones de densidad e índice de refracción y la condición de que la suma de las tres concentraciones es igual a la unidad. En la Figura 2.5 se muestra que esta variación también es lineal. A partir de estas variaciones pueden determinarse los coeficientes de termodifusión de cada componente, mediante la siguiente expresión [55]:

$$D'_{T,i} = -\frac{L_x^4}{504 L_z}\frac{\alpha g}{\nu}\Delta c_i \,. \qquad (2.4)$$

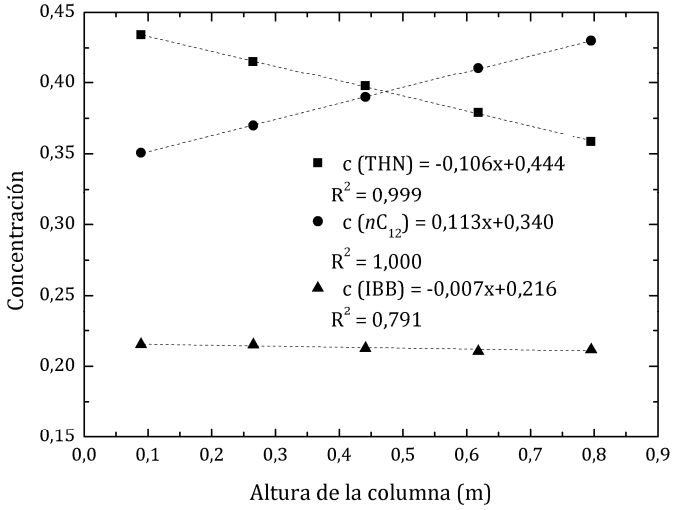

Figura 2.5. Variación de la concentración de cada componente en función de la altura de la columna LTC en estado estacionario, para la mezcla ternaria THN-IBB-nC$_{12}$ a concentración de 0,40-0,20-0,40 y a 25°C.

La ecuación (2.4) se emplea para determinar los coeficientes de termodifusión de los componentes 1 y 3, es decir, los de mayor y menor densidad. El coeficiente correspondiente al componente 2, se determina sabiendo que la suma de los tres coeficientes de termodifusión debe ser cero.

El error experimental de los coeficientes de termodifusión en mezclas ternarias se calcula de la misma forma que para el caso de las mezclas binarias. En el caso de las medidas realizadas mediante la columna LTC, el error experimental se encuentra alrededor del 4%. En el caso de la columna STC, se puede lograr un error similar al de la columna LTC [56], siempre y cuando se elimine uno de los puntos de la recta de separación y se realicen un mayor número de ensayos.

2.2. Técnica *sliding symmetric tubes*

En este trabajo se ha empleado la técnica *sliding symmetric tubes* (SST) para determinar el coeficiente de difusión molecular en mezclas binarias y ternarias. Esta instalación fue diseñada y construida en MGEP con el fin de cubrir las carencias detectadas en la técnica *Open Ended Capillary* [46], utilizada hasta el momento en MGEP.

Esta instalación se compone de varios conjuntos de tubos (Figura 2.6.a) que tienen dos posiciones: tubos enfrentados y tubos separados. En la posición de tubos enfrentados, el contenido de ambos tubos está en contacto, mientras que en la posición de tubos separados el contenido de cada tubo está aislado.

En un ensayo, estando los conjuntos en posición de tubos separados, se introduce en cada uno de ellos la mezcla de estudio con una pequeña diferencia de concentración (generalmente c_i ± 3% en mezclas binarias y c_i ± 5% en mezclas ternarias) entre el tubo superior e inferior. Con el fin de evitar la convección, la mezcla más densa se introduce en el tubo inferior. Todos los conjuntos se introducen en un baño con agua regulada mediante un baño termostático con control de la temperatura de ±0,1°C. De esta forma, se mantendrá la temperatura de la mezcla constante durante todo el ensayo (Figura 2.6. b). Cuando los tubos se han atemperado, todos los conjuntos se pasan a posición de tubos enfrentados y, debido al gradiente de concentración, aparece un flujo difusivo entre los dos tubos.

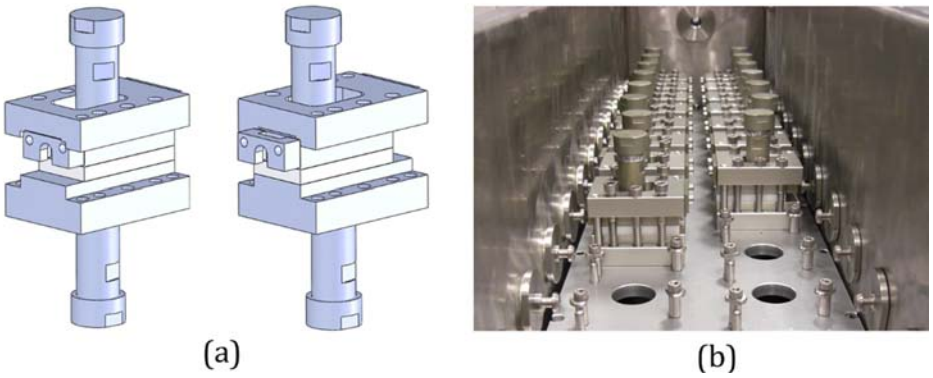

Figura 2.6. Instalación *sliding symmetric tubes*. (a) Representación de los conjuntos de tubos. (b) Posicionamiento de los conjuntos de tubos en el baño.

Cada cierto tiempo, se pasa cada conjunto a posición de tubos separados, deteniendo el proceso difusivo entre esos dos tubos. El contenido de cada tubo se extrae y se analiza para conocer su composición. Por consiguiente, al final de un ensayo se conoce la variación de la concentración de la mezcla en función del tiempo (Figura 2.7), lo que a su vez permite determinar el coeficiente de difusión molecular. Como puede observarse en la Figura 2.7, la variación de la concentración en el tubo superior e inferior ocurre de manera simétrica, siendo el eje de simetría la concentración media de la mezcla.

Hay varios factores que pueden variar en cada ensayo dependiendo de la mezcla analizada: el número de conjuntos utilizados, la diferencia de concentración inicial y el tiempo entre la separación de cada conjunto.

Cuando se analiza una mezcla nueva es importante prever si tendrá un coeficiente de difusión alto o bajo (en comparación a otras mezclas ya estudiadas) a la hora de planificar el ensayo mediante la técnica SST. No obstante, el hecho de trabajar con conjuntos independientes permite adaptar los tiempos de extracción durante la propia realización del ensayo.

2.2.1. Mezclas binarias

En el caso de las mezclas binarias se mide la densidad de cada tubo para conocer la concentración de la mezcla en ese conjunto. En la Figura 2.7 se muestra la variación de la concentración en función del tiempo para la mezcla MN-*n*C_8 a concentración másica de 0,50 de MN y a 25°C.

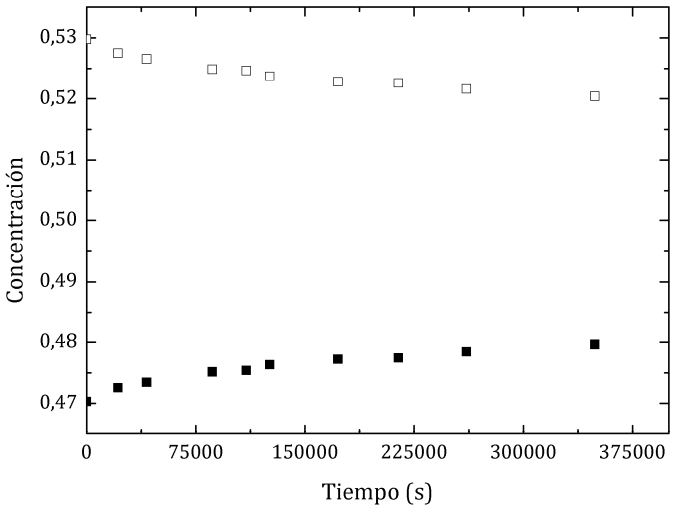

Figura 2.7. Variación de la concentración en función del tiempo en el tubo superior (símbolo relleno) e inferior (símbolo vacío), determinada mediante la técnica SST para la mezcla formada por MN-*n*C_8 a concentración másica de 0,50 de MN y a 25°C.

Al resolver la segunda ley de Fick para las condiciones de contorno de la técnica SST se obtiene que la concentración es una función de la forma:

$$c(z,t) = \frac{c_0^{low} + c_0^{up}}{2} - \frac{2(c_0^{up} - c_0^{low})}{\pi} \sum_{m=1}^{\infty} \frac{1}{m} \sin\left(\frac{m\pi}{2}\right) \cos\left(\frac{m\pi z}{2L}\right) \exp\left(-\frac{m^2\pi^2}{4L^2} Dt\right) \quad (2.5)$$

Esta ecuación representa el perfil de concentración a lo largo de los tubos y en función del tiempo. A partir de ella, se puede obtener la expresión de la concentración media para cada tubo en función del tiempo [22]:

$$c^{\text{low}}\Big|_{\text{m}}(t) - \frac{c_0^{\text{low}} + c_0^{\text{up}}}{2} = \frac{4}{\pi^2}\left(c_0^{\text{low}} - c_0^{\text{up}}\right) \sum_{n=0}^{\infty} \frac{\exp\left(-\left(n+\frac{1}{2}\right)^2 \frac{\pi^2}{L^2} Dt\right)}{(2n+1)^2},$$

$$c^{\text{up}}\Big|_{\text{m}}(t) - \frac{c_0^{\text{low}} + c_0^{\text{up}}}{2} = \frac{4}{\pi^2}\left(c_0^{\text{up}} - c_0^{\text{low}}\right) \sum_{n=0}^{\infty} \frac{\exp\left(-\left(n+\frac{1}{2}\right)^2 \frac{\pi^2}{L^2} Dt\right)}{(2n+1)^2}. \quad (2.6)$$

Las ecuaciones del tubo superior e inferior son linealmente dependientes, por lo que se tiene una ecuación y una incógnita. Además, la concentración varía en los tubos superiores e inferiores de forma simétrica, por lo que se debe obtener el mismo resultado para el coeficiente de difusión con ambas ecuaciones. Las expresiones (2.6) se resuelven mediante el método de mínimos cuadrados con ayuda del programa *Matlab*. Para asegurar un buen ajuste a lo largo de toda la curva de concentración, especialmente en los tiempos iniciales, se emplea un número de términos n = 1000. Además, se realizan 100 iteraciones del ajuste para garantizar la convergencia del resultado.

2.2.2. Mezclas ternarias

Como se ha comentado anteriormente, para determinar la concentración de una mezcla ternaria, es necesario medir tanto la densidad como el índice de refracción. La Figura 2.8 muestra la variación de la concentración de cada componente en los tubos superior e inferior para la mezcla ternaria formada por THN-IBB-nC$_{12}$ a concentración de 0,45-0,10-0,45 y a 25°C.

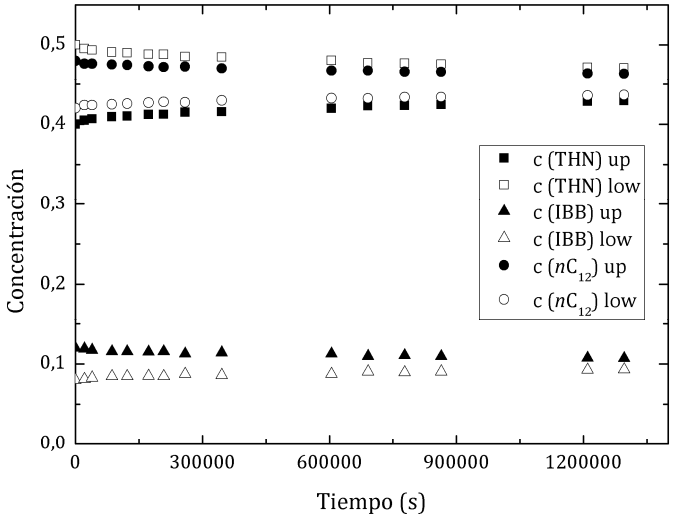

Figura 2.8. Variación de la concentración de cada componente en función del tiempo en los tubos superiores e inferiores obtenida mediante la técnica SST, para la mezcla ternaria formada por THN-IBB-nC$_{12}$ a concentración de 0,45-0,10-0,45 y a 25°C.

En el caso de las mezclas ternarias se tiene una matriz de difusión con cuatro coeficientes, por lo que la determinación de los mismos se complica de forma considerable. Uno de los principales objetivos de esta tesis ha sido resolver la determinación de los coeficientes de difusión molecular y los valores propios de la matriz de difusión, en mezclas ternarias mediante la técnica SST. Los valores propios de la matriz de difusión se definen mediante la siguiente expresión:

$$\hat{D}_1 = \frac{D_{11} + D_{22} - \sqrt{\left(D_{11} - D_{22}\right)^2 + 4D_{12}D_{21}}}{2},$$

$$\hat{D}_2 = \frac{D_{11} + D_{22} + \sqrt{\left(D_{11} - D_{22}\right)^2 + 4D_{12}D_{21}}}{2}. \qquad (2.7)$$

Inicialmente, como se muestra en el Apéndice C [57], se desarrolló una solución analítica para mezclas ternarias siguiendo el mismo procedimiento que para el caso de mezclas binarias (Ec. (2.6)). Las ecuaciones obtenidas para la nueva variable de concentración, ϕ_i, son las siguientes:

$$\phi_j^{\text{low}}\Big|_{\text{m}}(t) - \frac{\phi_{0,j}^{\text{low}} + \phi_{0,j}^{\text{up}}}{2} = \frac{4}{\pi^2}\left(\phi_{0,j}^{\text{low}} - \phi_{0,j}^{\text{up}}\right)\sum_{n=0}^{\infty}\frac{\exp\left(-\left(n+\frac{1}{2}\right)^2\frac{\pi^2}{L^2}\hat{D}_j t\right)}{(2n+1)^2},$$

$$\phi_j^{\text{up}}\Big|_{\text{m}}(t) - \frac{\phi_{0,j}^{\text{low}} + \phi_{0,j}^{\text{up}}}{2} = \frac{4}{\pi^2}\left(\phi_{0,j}^{\text{up}} - \phi_{0,j}^{\text{low}}\right)\sum_{n=0}^{\infty}\frac{\exp\left(-\left(n+\frac{1}{2}\right)^2\frac{\pi^2}{L^2}\hat{D}_j t\right)}{(2n+1)^2}, \qquad (2.8)$$

para *j*=1, 2.

La solución de estas ecuaciones requería un ajuste no lineal de dos ecuaciones con cuatro incógnitas para poder determinar los coeficientes de difusión. Los ajustes de cuatro parámetros no son siempre estables; por ello, en el trabajo [57] se analizó el efecto de diferentes métodos de ajuste, en colaboración con el grupo de la Prof. Shevtsova del *Microgravity Research Center* de la Universidad de Bruselas. Sin embargo, la complejidad de las ecuaciones hizo que no se pudieran obtener resultados fiables que además, dependían fuertemente de los parámetros iniciales de ajuste.

Todo ello impulsó un nuevo desarrollo analítico para poder determinar los coeficientes de difusión molecular en mezclas ternarias, presentado en el Apéndice D (difusión Bath). Este trabajo se llevó a cabo en colaboración con el Prof. D. Andrew S. Rees del departamento de Ingeniería Mecánica de la Universidad de Bath, y se publicó en [36]. La nueva solución analítica está basada en la conocida solución autosimilar de la ecuación de Fourier para un sólido calentado impulsivamente, que se puede encontrar en Carslaw y Jaeger [58]. A continuación se describe el desarrollo, en primer lugar para mezclas binarias y posteriormente para mezclas ternarias.

Nueva solución analítica para mezclas binarias

Se parte de resolver la segunda ley de Fick (1.1) para tiempos relativamente cortos, es decir, cuando la zona entre las dos concentraciones en la que se da la difusión (de aquí en adelante, zona de difusión) no ha alcanzado los extremos de los tubos. De esta forma, la zona de difusión satisface una solución autosimilar para lo cual se necesitan los siguientes cambios de variable:

$$\eta = \frac{z}{2\sqrt{Dt}}, \tag{2.9}$$

$$\tau = \sqrt{t}, \tag{2.10}$$

donde *z* es la variable vertical. En el régimen autosimilar, la derivada con respecto al tiempo puede despreciarse, por lo que se obtiene la siguiente ecuación para la concentración:

$$\frac{\partial^2 c}{\partial \eta^2} + 2\eta \frac{\partial c}{\partial \eta} = 0. \tag{2.11}$$

Las condiciones de contorno en este caso, considerando la transformación de las variables, son las siguientes:

$$c \to c_0^{\text{low}} \quad \text{para } \eta \to -\infty,$$

$$c \to c_0^{\text{up}} \quad \text{para } \eta \to +\infty. \tag{2.12}$$

Resolviendo la ecuación (2.11) se obtiene la siguiente expresión para la concentración:

$$c(z,t) = c_0^{\text{up}} + \frac{c_0^{\text{low}} - c_0^{\text{up}}}{2}\,\text{erfc}(\eta)\,, \tag{2.13}$$

siendo erfc (η) la función error complementaria de η [58].

Al integrar la expresión (2.13) y dividirla por la longitud del tubo se obtiene la concentración media en cada tubo.

$$\frac{1}{L}\int_0^L c\;\mathrm{d}z = c_0^{\text{up}} + \frac{\left(c_0^{\text{low}} - c_0^{\text{up}}\right)}{L}\sqrt{\frac{Dt}{\pi}}\,. \tag{2.14}$$

Es importante remarcar que la ecuación (2.14) es válida para tiempos relativamente cortos, es decir, hasta el momento en que la zona de difusión llega al final de los tubos. Al superar este límite de tiempo, la ecuación basada en la *error function* (2.13) ya no reproduce fielmente el perfil de concentración a lo largo de los tubos (representado por la ecuación exponencial (2.5)), por lo que no es posible calcular los coeficientes de difusión mediante la misma. En la Figura 2.9 se representa como ejemplo el perfil de concentración para la mezcla MN-nC$_8$ a 0,50 de concentración y a 25°C, obtenido mediante las ecuaciones (2.13) y (2.5). Se puede observar cómo para tiempos cortos (por ejemplo, menos de 350.000 s) el perfil de concentración es el mismo, pero para tiempos largos (por ejemplo, 800.000 s) aparecen desviaciones entre las representaciones de las dos ecuaciones. Por lo tanto, para poder utilizar la ecuación basada en la *error function* (2.13) se precisa identificar los límites de tiempo en cada ensayo.

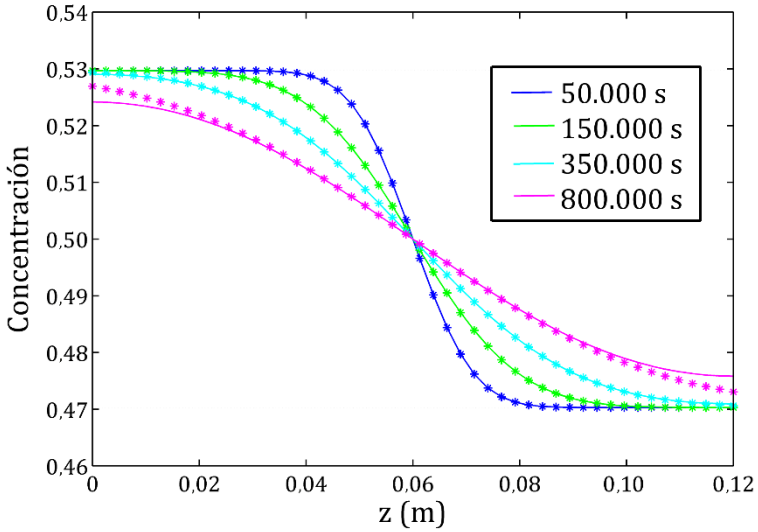

Figura 2.9. Perfil de concentración a lo largo de los tubos, para la mezcla MN-nC$_8$ a 0,50 de concentración másica de MN y a 25°C, obtenido mediante la ecuación (2.5) (representada por línea) y mediante la ecuación (2.13) (representada por asteriscos), a diferentes tiempos de difusión.

La ecuación (2.14) muestra que la concentración media varía linealmente con respecto a $(t)^{1/2}$. En la Figura 2.10 se muestra experimentalmente esta variación lineal de las concentraciones superior e inferior en función de la raíz cuadrada del tiempo.

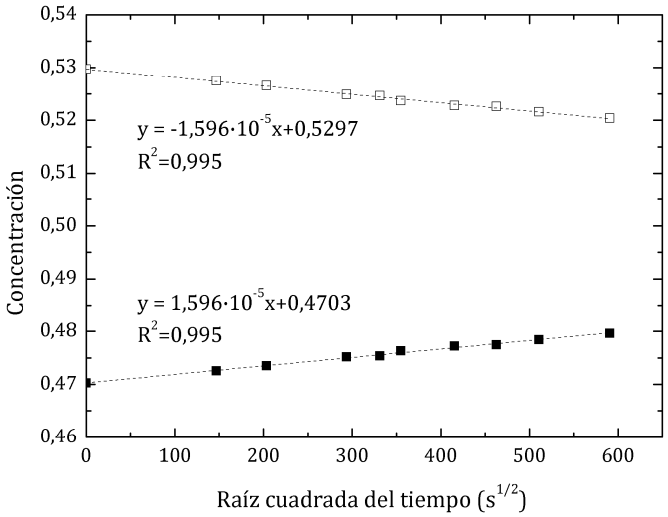

Figura 2.10. Variación de la concentración en función de la raíz cuadrada del tiempo, en el tubo superior (símbolo relleno) e inferior (símbolo vacío), determinada mediante la técnica SST para la mezcla formada por MN-*n*C_8 a concentración másica de 0.50 de MN y a 25°C

Como se puede observar, las variaciones son lineales y por tanto el coeficiente de difusión molecular dado por los datos correspondientes al tubo superior puede determinarse mediante la siguiente expresión:

$$S^{\mathrm{up}} = \frac{\left(c_0^{\mathrm{low}} - c_0^{\mathrm{up}}\right)}{L}\sqrt{\frac{D}{\pi}}\,. \tag{2.15}$$

En caso de tomarse la pendiente formada por los puntos de concentración en el tubo inferior, el resultado es el mismo en cuanto al coeficiente de difusión molecular.

Con el fin de validar este nuevo método analítico, se han comparado los resultados obtenidos mediante la solución clásica (ecuación (2.6)) y la nueva (ecuación (2.15)) para las conocidas mezclas binarias del *benchmark* de Fontainebleau formadas por THN, IBB y *n*C_{12} a 0,50 de concentración másica, y para el sistema de Agua-Isopropanol a diferentes concentraciones (Mialdun *et al*. [52]). Como se puede observar en la Figura 2.11, el acuerdo entre los resultados obtenidos mediante los dos métodos analíticos es muy bueno.

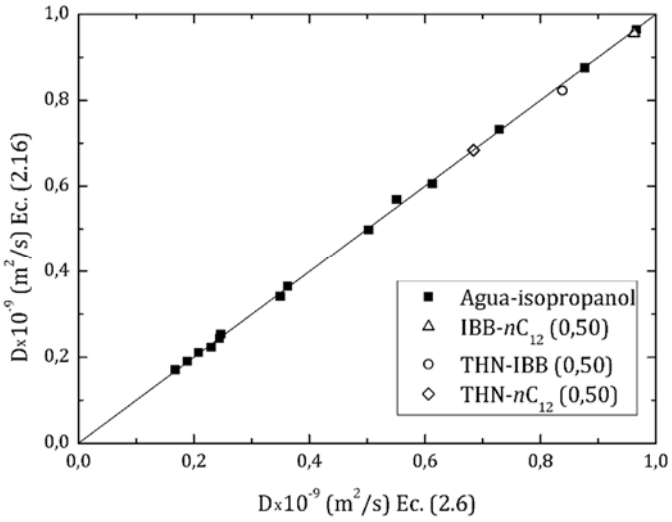

Figura 2.11. Comparación entre los resultados obtenidos mediante el método analítico clásico (ecuación (2.6)) y el nuevo método analítico basado en la *error function* (ecuación (2.15)), para las mezclas binarias formadas por THN, IBB y nC$_{12}$ a concentración de 0,50 y para el sistema binario de Agua-Isopropanol a diferentes concentraciones, en todos los casos a 25°C.

Nueva solución analítica para mezclas ternarias

En el caso de las mezclas ternarias el proceso es similar, aunque es necesario aplicar un segundo cambio de variable debido a que se dispone de una matriz de difusión de 2x2. La segunda ley de Fick para mezclas ternarias es:

$$\frac{\partial c_1}{\partial t} = D_{11}\frac{\partial^2 c_1}{\partial z^2} + D_{12}\frac{\partial^2 c_2}{\partial z^2},$$

$$\frac{\partial c_2}{\partial t} = D_{21}\frac{\partial^2 c_1}{\partial z^2} + D_{22}\frac{\partial^2 c_2}{\partial z^2}. \qquad (2.16)$$

Los cambios de variable aplicados en este caso son los siguientes:

$$\eta = \frac{z}{2\sqrt{t}},$$

$$\tau = \sqrt{t},$$

$$\lambda = \gamma\eta. \qquad (2.17)$$

Una vez más, se asume que la zona de difusión no ha llegado al extremo final de los tubos y por lo tanto, se obtienen las siguientes ecuaciones autosimilares para las concentraciones de los componentes 1 y 2:

$$D_{11}\gamma^2\frac{\partial^2 c_1}{\partial\lambda^2}+2\lambda\frac{\partial c_1}{\partial\lambda}+D_{12}\gamma^2\frac{\partial^2 c_2}{\partial\lambda^2}=0,$$

$$D_{21}\gamma^2\frac{\partial^2 c_1}{\partial\lambda^2}+2\lambda\frac{\partial c_2}{\partial\lambda}+D_{22}\gamma^2\frac{\partial^2 c_2}{\partial\lambda^2}=0. \qquad (2.18)$$

Las condiciones de contorno son similares a las del caso de mezclas binarias:

$$c_1\to c_{0,1}^{\text{low}} \text{ y } c_2\to c_{0,2}^{\text{low}} \quad \text{para } \eta\to-\infty,$$

$$c_1\to c_{0,1}^{\text{up}} \text{ y } c_2\to c_{0,2}^{\text{up}} \quad \text{para } \eta\to+\infty, \qquad (2.19)$$

Resolviendo las expresiones (2.18) se obtienen las siguientes expresiones para las concentraciones de los componentes 1 y2:

$$c_1(z,t)=A\,\text{erfc}(\lambda_1)+B\,\text{erfc}(\lambda_2)+c_{0,1}^{\text{up}},$$

$$c_2(z,t)=A\left(\frac{1-D_{11}\gamma_1^2}{D_{12}\gamma_1^2}\right)\text{erfc}(\lambda_1)+B\left(\frac{1-D_{11}\gamma_2^2}{D_{12}\gamma_2^2}\right)\text{erfc}(\lambda_2)+c_{0,2}^{\text{up}}, \qquad (2.20)$$

donde las constantes *A* y *B* dependen de los coeficientes de difusión y las concentraciones iniciales de los componentes 1 y 2 en los tubos superior e inferior, y vienen dadas por:

$$A=\frac{D_{12}\gamma_1^2\gamma_2^2\left(c_{0,2}^{\text{low}}-c_{0,2}^{\text{up}}\right)-\gamma_1^2\left(c_{0,1}^{\text{low}}-c_{0,1}^{\text{up}}\right)\left(1-D_{11}\gamma_2^2\right)}{2\left(\gamma_2^2-\gamma_1^2\right)},$$

$$B=\frac{D_{12}\gamma_1^2\gamma_2^2\left(c_{0,2}^{\text{low}}-c_{0,2}^{\text{up}}\right)-\gamma_2^2\left(c_{0,1}^{\text{low}}-c_{0,1}^{\text{up}}\right)\left(1-D_{11}\gamma_1^2\right)}{2\left(\gamma_1^2-\gamma_2^2\right)}, \qquad (2.21)$$

las variables γ_1 y γ_2 son proporcionales a los autovalores de la matriz de difusión, y se definen como:

$$\gamma_1=\sqrt{\frac{-\left(D_{11}+D_{22}\right)-\sqrt{\left(D_{11}+D_{22}\right)^2+4\left(D_{12}D_{21}-D_{11}D_{22}\right)}}{2\left(D_{12}D_{21}-D_{11}D_{22}\right)}},$$

$$\gamma_2=\sqrt{\frac{-\left(D_{11}+D_{22}\right)+\sqrt{\left(D_{11}+D_{22}\right)^2+4\left(D_{12}D_{21}-D_{11}D_{22}\right)}}{2\left(D_{12}D_{21}-D_{11}D_{22}\right)}}, \qquad (2.22)$$

y

$$\lambda_1=\gamma_1\eta,$$

$$\lambda_2=\gamma_2\eta. \qquad (2.24)$$

Al igual que en el caso de las mezclas binarias, las expresiones (2.22) se integran y después se dividen por la longitud del tubo para obtener la concentración media para cada componente en cada tubo:

$$\frac{1}{L}\int_0^L c_1 \mathrm{d}z = c_{0,1}^{\mathrm{up}} + \frac{2}{L}\sqrt{\frac{t}{\pi}}\left(\frac{A}{\gamma_1}+\frac{B}{\gamma_2}\right),$$

$$\frac{1}{L}\int_0^L c_2 \mathrm{d}z = c_{0,2}^{\mathrm{up}} + \frac{2}{L}\sqrt{\frac{t}{\pi}}\left(\frac{A}{\gamma_1}\left(\frac{1-D_{11}\gamma_1^2}{D_{12}\gamma_1^2}\right)+\frac{B}{\gamma_2}\left(\frac{1-D_{11}\gamma_2^2}{D_{12}\gamma_2^2}\right)\right). \qquad (2.24)$$

Las ecuaciones (2.24) muestran que en el caso de las mezclas ternarias, la concentración de cada componente también varía de forma lineal con respecto a la raíz cuadrada del tiempo (Figura 2.12). Por tanto, la pendiente de la línea correspondiente puede escribirse como:

$$S_1 = \frac{2}{L\sqrt{\pi}}\left(\frac{A}{\gamma_1}+\frac{B}{\gamma_2}\right),$$

$$S_2 = \frac{2}{L\sqrt{\pi}}\left(\frac{A}{\gamma_1}\left(\frac{1-D_{11}\gamma_1^2}{D_{12}\gamma_1^2}\right)+\frac{B}{\gamma_2}\left(\frac{1-D_{11}\gamma_2^2}{D_{12}\gamma_2^2}\right)\right). \qquad (2.25)$$

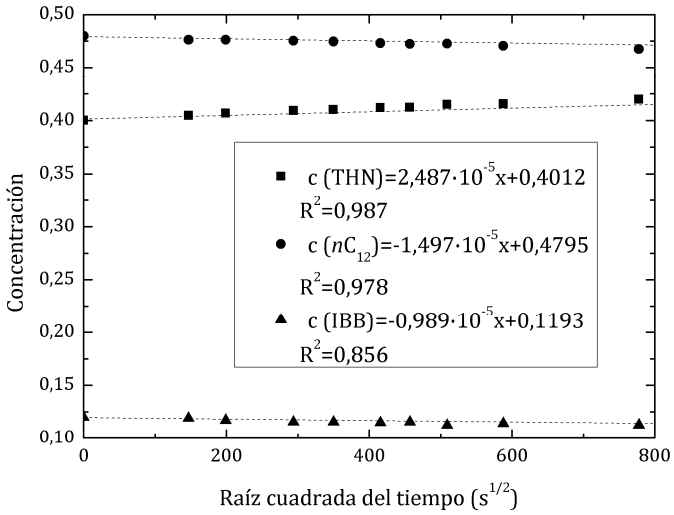

Figura 2.12. Variación de la concentración de cada componente en función de la raíz cuadrada del tiempo en el tubo superior obtenida mediante la técnica SST, para la mezcla ternaria formada por THN-IBB-*n*C_{12} a concentración de 0,45-0,10-0,45 y a 25°C.

Para determinar los coeficientes de difusión molecular en una mezcla ternaria, es necesario realizar dos experimentos independientes con concentraciones iniciales diferentes. De esta manera se obtiene un sistema con cuatro ecuaciones (las expresiones (2.25) para dos experimentos) y cuatro incógnitas (los cuatro coeficientes de difusión). Para resolver este sistema se ha empleado el método de Newton-Raphson.

En definitiva, este nuevo método analítico permite determinar los coeficientes de difusión molecular tanto en mezclas binarias como ternarias. No obstante, el tiempo del ensayo viene a ser un tema muy delicado, ya que hay que llegar a un compromiso entre la técnica experimental y el método analítico. Por una parte, como se ha comentado, hay un límite de tiempo para cada ensayo a partir del cual no es posible emplear el nuevo método analítico. Por otra parte, con el fin de evitar la influencia de las posibles perturbaciones que pueden surgir al cambiar la posición de los tubos en la técnica SST, es importante emplear tiempos de ensayo medianamente largos.

En la Figura 2.13 se muestra la variación de la concentración en función de la raíz cuadrada del tiempo, calculada mediante la ecuación exponencial que representa la evolución de la concentración, y mediante la ecuación basada en la *error function*. Como se puede observar, en tiempos cortos (menos de 350.000 s) ambas funciones dan un perfil de concentración idéntico, pero en tiempos largos (más de 640.000 s) el perfil basado en la *error function* se desvía claramente. En tiempos intermedios (alrededor de 500.000 s), la solución basada en la *error function* aún puede considerarse una buena aproximación, pues la desviación es muy pequeña. Es en este tiempo intermedio donde debe establecerse el límite de tiempo para determinar los coeficientes de difusión molecular mediante el nuevo método analítico aplicado a la técnica SST.

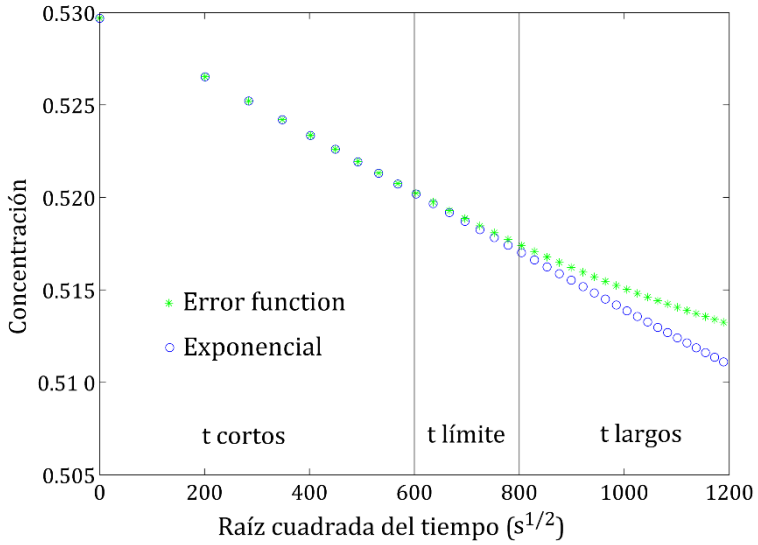

Figura 2.13. Concentración en función de la raíz cuadrada del tiempo, para la mezcla MN-*n*C_8 a 0,50 de concentración y a 25°C, en el tubo superior, determinada mediante la ecuación exponencial (2.5) y la basada en la *error function* (2.13).

Para determinar el límite de tiempo es necesario conocer el coeficiente de difusión de la mezcla. Por ello, inicialmente se calcula el límite de tiempo de ensayo con un coeficiente aproximado y tras determinar el coeficiente de difusión de esa mezcla, se vuelve a calcular el límite de tiempo para comprobar que se ha operado en el régimen adecuado.

2.3. Determinación del coeficiente Soret

Actualmente, en el laboratorio de Fluidomecánica de MGEP únicamente se determina el coeficiente Soret mediante el método indirecto; es decir, a partir de los coeficientes de termodifusión y difusión molecular.

2.3.1. Mezclas binarias

El coeficiente Soret viene dado por la relación entre el coeficiente de termodifusión y el coeficiente de difusión molecular [52, 54]:

$$S_T = \frac{D_T}{D}. \tag{2.25}$$

El error experimental en la determinación del coeficiente Soret viene dado por la suma de los errores experimentales correspondientes a los coeficientes de termodifusión y difusión molecular.

2.3.2. Mezclas ternarias

En el caso de mezclas ternarias, la expresión utilizada para determinar los coeficientes Soret a partir de los coeficientes de termodifusión y difusión molecular es la siguiente [43, 55, 59]:

$$S'_{T,i} = \frac{D'_{T,i} D_{jj} - D'_{T,j} D_{ij}}{D_{ii} D_{jj} - D_{ij} D_{ji}}. \tag{2.26}$$

En una mezcla ternaria hay tres coeficientes de Soret, correspondientes a cada uno de los tres componentes de la mezcla. En este caso también se determinan los coeficientes de los componentes 1 y 3 mediante la expresión (2.26), y el coeficiente correspondiente al componente 2 se calcula a partir de la condición de que los tres coeficientes deben sumar cero.

Al igual que en el caso de las mezclas binarias, el error experimental correspondiente viene dado por la suma de los errores experimentales de los coeficientes de termodifusión y difusión molecular

3. PROCEDIMIENTO EXPERIMENTAL

En este capítulo se describen los procedimientos experimentales aplicados para poder determinar los coeficientes de transporte mediante las técnicas descritas en el capítulo anterior. Por una parte, se describe el método de análisis necesario para determinar la concentración de los componentes en una mezcla. Por otra parte, se muestran los procedimientos y dispositivos utilizados para medir las propiedades de la mezcla necesarias para calcular el coeficiente de termodifusión mediante las expresiones (2.3) o (2.4).

3.1. Preparación de muestras

La composición de las mezclas que se analizan es un factor muy influyente en la medición de las propiedades de transporte, por lo que resulta fundamental que el proceso de preparación de las muestras se realice con precisión. En este caso, las mezclas se preparan mediante la concentración másica de cada componente utilizando balanzas de precisión.

Para preparar las mezclas analizadas en esta tesis se ha empleado una balanza GRAM VXI 310 (Figura 3.1), la cual tiene una resolución de 0,0001 g y un fondo de escala de 310 g.

Figura 3.1. Balanza GRAM VXI 310

Al preparar las mezclas, tanto binarias como ternarias, los componentes se añaden en orden decreciente de densidad. Conocida la concentración másica de cada uno de los componentes de la mezcla, se añade la masa que corresponde, la cual se calcula por medio de la siguiente expresión:

$$m_T = \frac{m_i}{c_i}, \quad i = 1, 2, 3. \tag{3.1}$$

3.2. Medida de la densidad e índice de refracción

La densidad se mide mediante un densímetro ANTON PAAR 5000 (Figura 3.2). Este aparato es capaz de calcular la densidad de un fluido con una resolución de 10^{-6} gr/cm^3 y una precisión de $5 \cdot 10^{-6}$ gr/cm^3. Además consta de un control de temperatura mediante elementos Peltier, que permite realizar mediciones con una resolución de temperatura de 10^{-3} °C. El volumen de muestra necesario para realizar una medición de densidad es de 2 ml.

El densímetro DMA 5000 dispone de un tubo de cuarzo en forma de "U" en el que se introduce el fluido a analizar. Un excitador piezoeléctrico hace vibrar el tubo y unos acelerómetros ópticos registran el período de vibración, P, con el que se puede determinar la densidad de la muestra mediante la expresión:

$$\rho = A_\rho \cdot P^2 - B_\rho . \qquad (3.2)$$

El densímetro se calibra regularmente con el fin de determinar las dos constantes de calibración A_ρ y B_ρ. Para ello se utilizan siempre aire y agua bidestilada, dos fluidos cuyas propiedades son conocidas y han sido ampliamente estudiadas en la literatura.

El índice de refracción se mide con un refractómetro RXA 156 de ANTON PAAR (Figura 3.2), que se acopla al densímetro ANTON PAAR DMA 5000. Este acoplamiento permite la medición simultánea de densidad e índice de refracción, lo cual resulta de gran utilidad en el estudio de mezclas ternarias, para las que se precisa conocer ambas propiedades.

Figura 3.2. Densímetro ANTON PAAR DMA 500 y refractómetro ANTON PAAR RXA 156

Este refractómetro es capaz de realizar medidas del índice de refracción con una precisión de $2 \cdot 10^{-5}$ nD y también permite un control de la temperatura de $3 \cdot 10^{-2}$ °C durante la medición, mediante elementos Peltier.

Al introducir la mezcla en el refractómetro, un LED genera un haz de luz, con una longitud de onda de 589,3±0,1 nm, que incide sobre la muestra. El ángulo de reflexión, que se mide mediante un conjunto de sensores de alta resolución, es utilizado para determinar el índice de refracción de la mezcla. El refractómetro se calibra a la vez que el densímetro, utilizando igualmente aire y agua bidestilada.

El proceso para medir estas propiedades es idéntico en el caso de mezclas binarias y mezclas ternarias.

3.2.1. Coeficiente de expansión térmica (α)

Esta propiedad se determina de igual manera tanto para mezclas binarias como ternarias, y expresa la variación de la densidad de la mezcla en función de la temperatura. El coeficiente α puede calcularse mediante la siguiente expresión:

$$\alpha = -\frac{1}{\rho}\frac{\partial \rho}{\partial T}. \tag{3.3}$$

En la Figura 3.3 se muestra la variación de la densidad con respecto a la temperatura para la mezcla formada por MN y nC$_8$ a concentración másica de 0,60 de MN y 25°C de temperatura. Como se puede observar, esta relación es lineal.

El error experimental correspondiente a la determinación de α viene dado por la precisión del densímetro junto con el error del ajuste lineal.

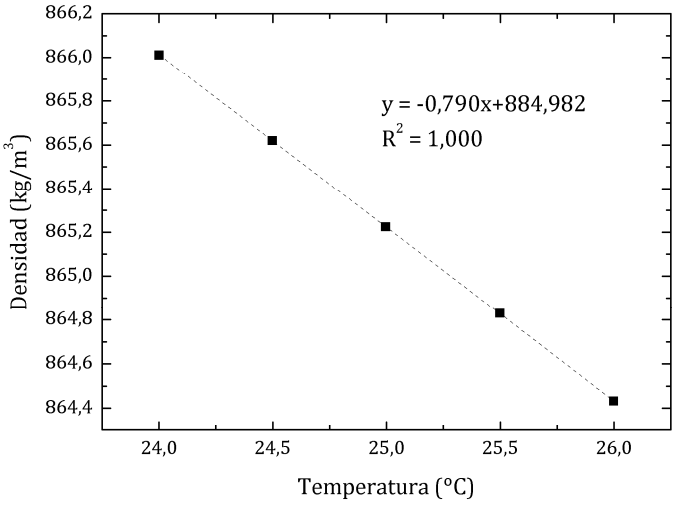

Figura 3.3. Variación de la densidad con respecto a la temperatura para la mezcla MN-nC$_8$ a concentración másica de 0,60 de MN.

3.2.2. Coeficiente de expansión másica (β)

Esta propiedad se define como la variación de la densidad de la mezcla con respecto a la concentración del componente más denso. Se puede representar mediante la siguiente ecuación:

$$\beta = \frac{1}{\rho}\frac{\partial \rho}{\partial c}. \tag{3.4}$$

Para obtener este coeficiente se determina la densidad de cinco muestras cuya concentración se encuentra alrededor de la concentración de estudio. Así se obtiene la relación entre la densidad y la concentración de los componentes, que como se puede apreciar en el ejemplo correspondiente a la mezcla MN-nC$_8$ a concentración másica de 0,60 de MN y a 25°C (Figura 3.4), es una relación lineal.

El error experimental correspondiente a la determinación de β viene dado por la precisión del densímetro además del error del ajuste lineal.

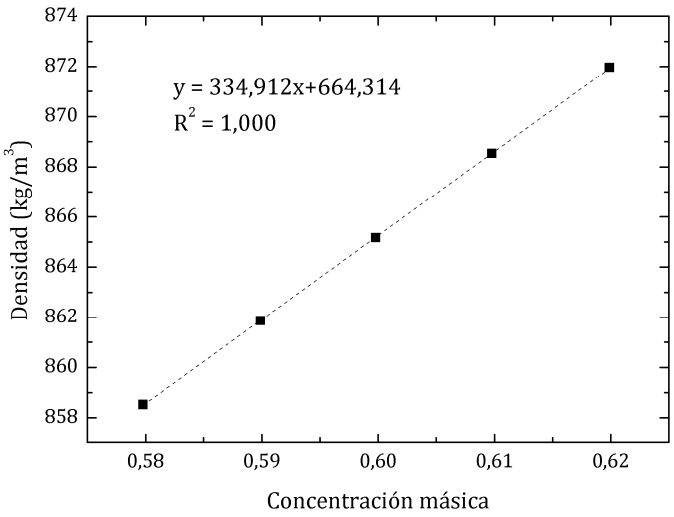

Figura 3.4. Variación de la densidad con la concentración de MN, para la mezcla MN-nC$_8$ a concentración másica de 0,60 de MN y a 25°C.

3.2.3. Calibración en mezclas ternarias

En el caso de las mezclas ternarias, es necesario conocer dos propiedades de la mezcla para poder determinar la concentración de sus componentes. En nuestro caso se emplean la densidad y el índice de refracción, que como se muestra en [59, 60], permiten la determinación más precisa de la concentración de los componentes en la mezcla. Resolviendo el siguiente sistema de ecuaciones se determina la concentración de los componentes de una mezcla ternaria:

$$c_1 = \frac{k_2^{'}(\rho - k_0) - k_2(n_D - k_0^{'})}{k_1 k_2^{'} - k_1^{'} k_2}, \tag{3.5}$$

$$c_2 = \frac{k_1(n_D - k_0^{'}) - k_1^{'}(\rho - k_0)}{k_1 k_2^{'} - k_1^{'} k_2}, \tag{3.6}$$

$$c_3 = 1 - c_1 - c_2 . \tag{3.7}$$

Para cada mezcla ternaria que se quiere analizar, se preparan 25 mezclas alrededor de la concentración de estudio y se miden su densidad e índice de refracción. Con estos datos se crean los planos que se presentan en la Figura 3.5, que a su vez nos permiten calcular los coeficientes de calibración.

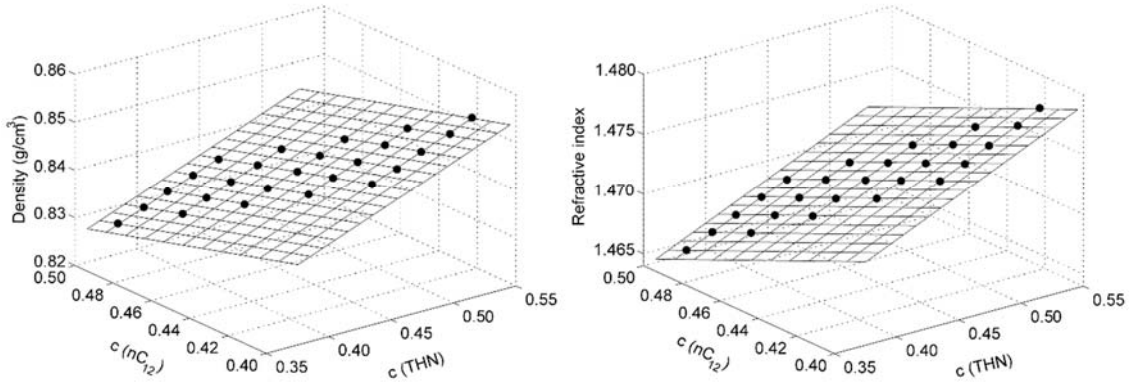

Figura 3.5. Planos de calibración correspondientes a la mezcla ternaria THN-IBB-nC$_{12}$ a concentración de 0,45-0,10-0,45 y a 25°C.

La calibración es una tarea delicada que debe realizarse cuidadosamente. Los pequeños errores cometidos en la preparación de las 25 mezclas se traducen en una menor precisión en la determinación de la concentración de cada componente en una mezcla ternaria. Esto a su vez aumenta el error experimental cometido en la determinación de los coeficientes de termodifusión y difusión molecular.

3.3. Viscosidad dinámica

La viscosidad dinámica es otro de los parámetros necesarios para determinar el coeficiente de termodifusión mediante la técnica termogravitacional. En el laboratorio de Fluidomecánica de MGEP se dispone de dos dispositivos que permiten medir la viscosidad dinámica: el viscosímetro de caída de bola Haake y el microviscosímetro ANTON PAAR AMVn. Ambos se basan en la Ley de Stoke de caída de un cuerpo sumergido en un fluido. Esta Ley relaciona la viscosidad dinámica de un fluido con el tiempo de caída a velocidad constante de un cuerpo sumergido en el mismo, mediante la siguiente expresión:

$$\mu = K_b(\rho_b - \rho)\Delta t\,. \tag{3.8}$$

siendo K_b y ρ_b la constante y la densidad relativas al cuerpo sumergido.

3.3.1. Viscosímetro de caída de bola Haake

Este viscosímetro está compuesto por dos cilindros: el interior, en el que se introduce la mezcla, y el exterior, por el que circula el agua controlada por un baño termostático con un control de temperatura de 0,1°C. En el cilindro en el que está la muestra se introduce a su vez una bola calibrada (Figura 3.6). El tiempo de caída se determina de forma manual con una desviación inferior a ±0,2 s.

Figura 3.6. Viscosímetro de caída de bola HAAKE

El rango de viscosidades medibles varía en función de la bola utilizada. En este trabajo, se han empleado dos bolas de borosilicato de diferente diámetro que han permitido un intervalo de viscosidades de 0,2 a 2,5 mPa·s. Ambas bolas han sido calibradas con varios líquidos de viscosidades ampliamente conocidas.

El volumen de mezcla necesario para realizar una medición es de 40 ml.

3.3.2. Microviscosímetro ANTON PAAR AMVn

El microviscosímetro (Figura 3.7) permite determinar la viscosidad dinámica de una muestra de manera automática con precisión de ±0,002 s. Consta de elementos Peltier integrados que permiten controlar la temperatura durante la medición con una precisión de 0,05°C.

Figura 3.7. Microviscosímetro ANTON PAAR AMVn

El conjunto capilar-bola puede ser intercambiado, dando así la posibilidad de medir diferentes rangos de viscosidades. El conjunto empleado en este trabajo permite analizar un rango de viscosidades de 0,3 a 10 mPa·s. Además, permite seleccionar los ángulos de caída a los que se realiza la medición. Tiempos de caída demasiado elevados o reducidos dan lugar a que aumente la incertidumbre de la medición. El volumen de muestra necesario en este caso es de 150 µl, considerablemente menor que en el caso del viscosímetro HAAKE.

4. MEZCLAS BINARIAS

Como se ha comentado en la introducción de esta memoria, el fenómeno de la termodifusión en mezclas binarias ha sido ampliamente estudiado. En la bibliografía se pueden encontrar trabajos sobre diferentes tipos de mezclas [11, 22, 29, 30, 61-64]. Y en los que además se emplean técnicas y métodos diferentes tanto de carácter experimental como teórico o numérico [26, 52, 54, 65, 66].

Generalmente, en todos los procesos naturales o industriales en los que intervienen estos fenómenos de transporte las mezclas están formadas por más de dos componentes. Por esta razón, el reto actualmente se encuentra en el análisis de las mezclas ternarias. No obstante, las mezclas binarias son menos complejas que las mezclas multicomponentes y por ello es de vital importancia continuar investigándolas. Estas mezclas sirven como guía para comprender los mecanismos fundamentales que rigen los fenómenos de transporte de masa en mezclas líquidas. Además, permiten estudiar la relación entre éstos y otras propiedades de las mezclas, como densidad, masa molecular, forma y tamaño de las moléculas, viscosidad… Asimismo, para poder desarrollar y validar modelos teóricos o numéricos se precisa de un gran volumen de datos experimentales. Esto queda patente en trabajos como el publicado por Hartmann *et al*. [28], en el que plantearon una serie de combinaciones de mezclas binarias que no pudieron medir en su totalidad, a pesar de haber cubierto una gran parte de las mismas.

En el grupo de Mecánica de Fluidos de MGEP se han analizado en profundidad las mezclas binarias cuasi ideales de n-alcanos en trabajos previos a esta tesis. Caben destacar las correlaciones cuantitativas desarrolladas que permiten predecir los coeficientes de termodifusión [29], difusión molecular [22] y Soret [30]. En este trabajo también se ha examinado la validez de estas correlaciones en mezclas formadas por un n-alcano y un anillo aromático, y a su vez se han discutido modelos de comportamiento para diferentes mezclas binarias.

Con este fin, se han estudiado 13 sistemas binarios a diferentes concentraciones másicas y a 25°C en todos los casos. Concretamente, las mezclas binarias analizadas durante esta tesis doctoral se presentan en la Tabla 4.1.

Tabla 4.1. Mezclas binarias analizadas durante esta tesis, compuestas de Tolueno (Tol), 1-Metilnaftaleno (MN) y n-Alcanos (nC$_i$, siendo i el número de carbonos).

Sistema	c (Tol)	Sistema	c (MN)
Tol-nC$_6$	0,20/0,40/0,50/0,60/0,80	MN-nC$_6$	0,20/0,40/0,50/0,60/0,80
Tol-nC$_8$	0,20/0,40/0,50/0,60/0,80	MN-nC$_8$	0,20/0,40/0,50/0,60/0,80
Tol-nC$_{10}$	0,20/0,40/0,50/0,60/0,80	MN-nC$_{10}$	0,20/0,40/0,50/0,60/0,80
Tol-nC$_{12}$	0,20/0,40/0,50/0,60/0,80	MN-nC$_{12}$	0,20/0,40/0,50/0,60/0,80
Tol-nC$_{14}$	0,20/0,40/0,50/0,60/0,70/0,80	MN-nC$_{14}$	0,20/0,40/0,50/0,60/0,80
Tol-nC$_{16}$	0,20/0,40/0,50/0,60/0,70/0,80	MN-nC$_{16}$	0,20/0,40/0,50/0,60/0,80
		MN-Tol	0,20/0,40/0,50/0,60/0,80

Los coeficientes de termodifusión se han medido a todas las concentraciones analizadas de cada sistema. Los coeficientes de difusión molecular y Soret, sin embargo, se han determinado únicamente para la concentración equimásica de cada sistema.

4.1. Coeficiente de termodifusión

Como se ha descrito en la sección 2 de esta memoria, los coeficientes de termodifusión se han determinado mediante la técnica termogravitacional; concretamente, en el caso de las mezclas binarias, se han medido mediante la columna STC.

En primer lugar se han medido las propiedades de la mezcla necesarias para determinar el coeficiente de termodifusión mediante la ecuación (2.3). Los resultados obtenidos se muestran en la Tabla 4.2 para la serie de Tol-*n*C_i, en la Tabla 4.3 para la serie de MN-*n*C_i y en la Tabla 4.4 para el sistema MN-Tol.

En el caso de las mezclas Tol-*n*C_{12}, Tol-*n*C_{14} y Tol-*n*C_{16} a bajas concentraciones no ha sido posible determinar el coeficiente de termodifusión en la columna STC dado que la separación en estos casos es demasiado pequeña y entra dentro del error experimental de la columna.

Los resultados presentados son la media de al menos tres experimentos para cada mezcla. La desviación estándar entre las repeticiones es generalmente inferior al 3%.

Tabla 4.2. Propiedades termofísicas y coeficientes de termodifusión para todas las mezclas de la serie Tol-nC$_i$ analizadas a 25°C.

Sistema	c	ρ (kg/m^3)	α x 10^{-3} (K^{-1})	β	μ x 10^{-3} (Pa·s)	D_T x 10^{-12} (m^2/sK)
Tol-nC$_6$	0,20	688,333	1,327	0,254	0,323	13,7 ± 0,5
	0,40	725,100	1,266	0,267	0,355	13,6 ± 0,6
	0,50	745,100	1,235	0,274	0,382	13,6 ± 0,5
	0,60	765,843	1,204	0,279	0,399	14,2 ± 0,6
	0,80	811,142	1,141	0,296	0,469	14,0 ± 0,5
Tol-nC$_8$	0,20	725,399	1,144	0,193	0,492	6,5 ± 0,3
	0,40	754,798	1,133	0,203	0,490	7,6 ± 0,4
	0,50	770,404	1,120	0,209	0,489	8,1 ± 0,3
	0,60	786,906	1,117	0,215	0,497	8,8 ± 0,4
	0,80	822,529	1,100	0,231	0,516	9,8 ± 0,5
Tol-nC$_{10}$	0,20	748,482	1,052	0,156	0,721	3,3 ± 0,1
	0,40	773,011	1,059	0,165	0,655	4,3 ± 0,2
	0,50	786,100	1,064	0,171	0,624	5,3 ± 0,3
	0,60	800,143	1,068	0,176	0,592	5,7 ± 0,3
	0,80	829,507	1,075	0,188	0,566	7,3 ± 0,3
Tol-nC$_{12}$	0,20	764,503	0,995	0,132	1,010	-----
	0,40	785,657	1,015	0,141	0,830	2,5 ± 0,1
	0,50	796,913	1,025	0,143	0,749	3,3 ± 0,1
	0,60	808,709	1,037	0,151	0,695	3,8 ± 0,2
	0,80	834,032	1,058	0,158	0,605	5,6 ± 0,3
Tol-nC$_{14}$	0,20	776,199	0,957	0,115	1,372	----
	0,40	794,804	0,987	0,121	0,998	----
	0,50	804,685	0,999	0,127	0,875	2,0 ± 0,1
	0,60	815,095	1,014	0,130	0,777	2,8 ± 0,1
	0,70	825,975	1,031	0,135	0,707	3,5 ± 0,2
	0,80	837,485	1,046	0,139	0,636	4,5 ± 0,2
Tol-nC$_{16}$	0,20	785,150	0,929	0,101	1,770	----
	0,40	801,762	0,962	0,108	1,200	----
	0,50	810,653	0,980	0,112	1,020	1,3 ± 0,1
	0,60	819,996	0,998	0,116	0,870	1,9 ± 0,1
	0,70	829,779	1,017	0,120	0,760	2,7 ± 0,1
	0,80	839,998	1,039	0,125	0,680	3,4 ± 0,2

Tabla 4.3. Propiedades termofísicas y coeficientes de termodifusión para todas las mezclas de la serie MN-nC$_i$ analizadas a 25°C.

Sistema	c	ρ (kg/m^3)	α x 10^{-3} (K^{-1})	β	μ x 10^{-3} (Pa·s)	D_T x 10^{-12} (m^2/sK)
MN-nC$_6$	0,20	708,981	1,250	0,405	0,377	26,0 ± 1,0
	0,40	770,899	1,116	0,430	0,495	23,6 ± 0,8
	0,50	805,806	1,051	0,442	0,574	21,6 ± 0,6
	0,60	842,715	0,988	0,454	0,729	19,7 ± 0,7
	0,80	920,000	0,860	0,483	1,298	14,7 ± 0,7
MN-nC$_8$	0,20	747,506	1,078	0,350	0,593	15,6 ± 0,5
	0,40	802,684	0,995	0,366	0,748	14,7 ± 0,5
	0,50	833,702	0,955	0,381	0,897	12,7 ± 0,5
	0,60	865,290	0,914	0,387	1,081	12,3 ± 0,4
	0,80	936,822	0,825	0,409	1,613	10,0 ± 0,4
MN-nC$_{10}$	0,20	711,469	0,990	0,312	0,942	10,4 ± 0,3
	0,40	822,480	0,932	0,326	1,123	9,8 ± 0,4
	0,50	851,121	0,902	0,341	1,229	9,5 ± 0,3
	0,60	879,894	0,870	0,347	1,417	9,0 ± 0,3
	0,80	944,790	0,806	0,367	1,916	7,6 ± 0,4
MN-nC$_{12}$	0,20	788,355	0,936	0,290	1,422	7,0 ± 0,3
	0,40	836,526	0,892	0,304	1,562	6,7 ± 0,2
	0,50	863,199	0,862	0,317	1,643	6,8 ± 0,3
	0,60	890,465	0,844	0,321	1,819	6,6 ± 0,2
	0,80	951,160	0,791	0,339	2,200	6,3 ± 0,2
MN-nC$_{14}$	0,20	800,072	0,899	0,272	2,051	5,1 ± 0,2
	0,40	846,558	0,865	0,287	2,095	5,2 ± 0,2
	0,50	871,731	0,846	0,295	2,147	5,3 ± 0,1
	0,60	897,720	0,826	0,301	2,232	5,3 ± 0,2
	0,80	955,150	0,782	0,318	2,490	5,3 ± 0,3
MN-nC$_{16}$	0,20	809,968	0,877	0,253	2,820	4,1 ± 0,2
	0,40	854,113	0,846	0,273	2,690	4,2 ± 0,1
	0,50	878,450	0,830	0,282	2,620	4,4 ± 0,2
	0,60	903,279	0,810	0,288	2,650	4,4 ± 0,2
	0,80	958,123	0,774	0,304	2,730	4,6 ± 0,2

Tabla 4.4. Propiedades termofísicas y coeficientes de termodifusión para todas las mezclas del sistema MN-Tol analizadas a 25°C.

Sistema	c	ρ (kg/m^3)	α x 10^{-3} (K^{-1})	β	μ x 10^{-3} (Pa·s)	D_T x 10^{-12} (m^2/sK)
MN-Tol	0,20	890,898	1,009	0,166	0,667	8,6 ± 0,6
	0,40	921,129	0,926	0,168	0,859	7,1 ± 0,3
	0,50	936,677	0,899	0,170	1,014	6,4 ± 0,3
	0,60	952,750	0,865	0,171	1,168	5,9 ± 0,2
	0,80	986,026	0,790	0,173	1,786	4,5 ± 0,2

4.1.1. Dependencia de D_T con la concentración

En primer lugar, se ha analizado la variación del coeficiente de termodifusión en función de la concentración del componente de referencia (el más denso en cada sistema).

En la Figura 4.1 se muestran los resultados correspondientes a las series de Tol-nC$_i$, junto con los publicados por Alonso de Mezquía *et al.* [67] para las mezclas Tol-nC$_6$ y Tol-nC$_{12}$ a varias concentraciones. Como se puede observar, ambos grupos de resultados muestran un acuerdo excelente.

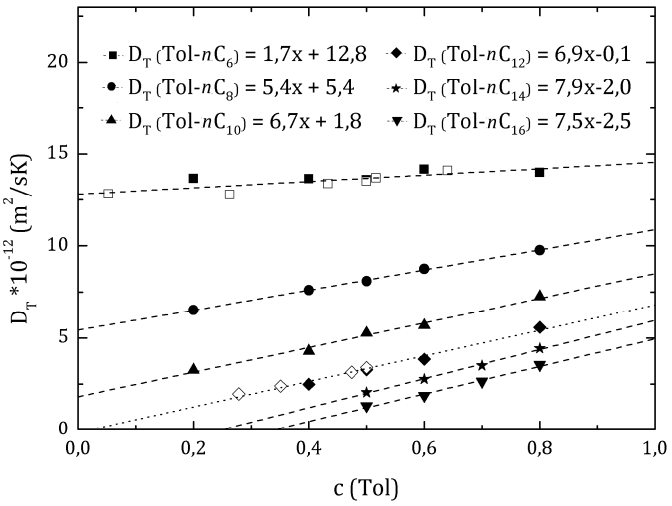

Figura 4.1. Variación del coeficiente de termodifusión con respecto a la concentración de tolueno para la serie de mezclas binarias Tol-nC$_i$ a 25°C. Los símbolos vacíos corresponden a los resultados publicados por Alonso de Mezquía *et al.* [67].

En la gráfica se puede ver que la variación del coeficiente de termodifusión con respecto a la concentración de tolueno es lineal para todas las mezclas, tal y como ocurría también en las mezclas binarias de alcanos [29]. Además, para todas las mezclas de esta serie el coeficiente de termodifusión aumenta al aumentar la concentración de tolueno. No obstante, la dependencia del coeficiente de termodifusión con la concentración de la mezcla (representada por la pendiente de la regresión lineal) es más débil a medida que disminuye el número de carbonos del n-alcano.

Por otra parte, se ha observado que para las mezclas de nC$_6$, nC$_8$ y nC$_{10}$ el coeficiente de termodifusión es positivo para todo el rango de concentraciones. Sin embargo, para los

alcanos con $i > 12$ se da una concentración a la que $D_T = 0$. Esta concentración aumenta a medida que aumenta la masa molecular del alcano. En estas mezclas y de acuerdo con las regresiones lineales, se prevé que para bajas concentraciones de tolueno el coeficiente de termodifusión será negativo, mientras que para altas concentraciones es positivo (Figura 4.1).

Además, al comparar los resultados entre las diferentes mezclas se puede ver cómo al aumentar la masa molecular del alcano, el coeficiente de termodifusión disminuye. Esto es debido a que al aumentar el número de carbonos del alcano disminuye la movilidad de la molécula, por lo que su capacidad de movimiento frente a un gradiente térmico disminuye.

Los coeficientes de termodifusión correspondientes a la serie MN-nC$_i$ en función de la concentración de MN se muestran en la Figura 4.2. También se han incluido los resultados publicados por Leahy-Dios *et al.* en [21, 31] para las mezclas de MN-nC$_i$ a diferentes concentraciones, medidos también mediante la técnica termogravitacional. Como se puede observar, el acuerdo con los resultados obtenidos en este trabajo es bueno.

En esta serie también se da que la variación de los coeficientes de termodifusión con respecto a la concentración de la mezcla es lineal. No obstante en este caso, la pendiente de esta variación es negativa para los alcanos con $i < 12$. Esta pendiente va aumentando su valor hasta que pasa a ser positiva para las mezclas de nC$_{14}$ y nC$_{16}$. Este comportamiento puede explicarse con la influencia de la viscosidad de los componentes de la mezcla. A medida que disminuye la diferencia entre las viscosidades de los dos componentes de la mezcla, disminuye la pendiente de variación de D_T con la concentración. En la serie de Tol-nC$_i$ se puede observar una tendencia similar.

Por su parte, en el caso de la serie de MN-nC$_i$, el coeficiente D_T es positivo durante todo el rango de concentración de todas las mezclas de la serie.

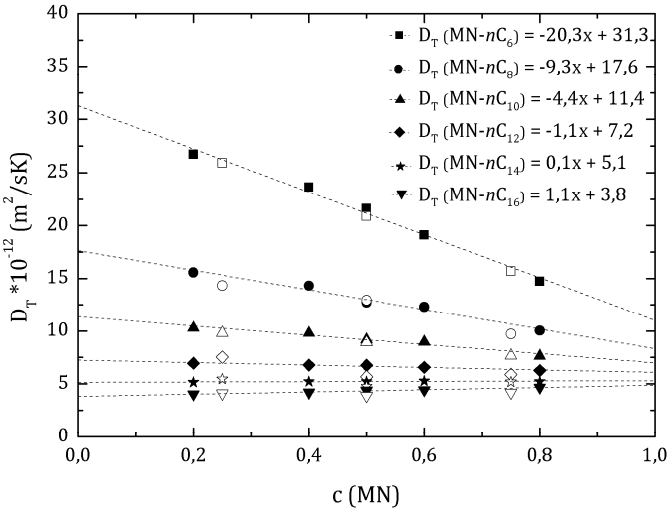

Figura 4.2. Variación del coeficiente de termodifusión con respecto a la concentración de MN para la serie de mezclas binarias MN-nC$_i$ a 25°C. Los símbolos vacíos corresponden a los resultados publicados por Leahy-Dios *et al.* en [21, 31].

Si se comparan los resultados entre las diferentes mezclas, en este caso también se observa que a medida que aumenta la masa molecular del alcano, el coeficiente de termodifusión disminuye.

Para la mezcla MN-Tol se cumple también que la variación del coeficiente de termodifusión en función de la concentración de MN es lineal, en este caso con pendiente descendente, tal y como se aprecia en la Figura 4.3.

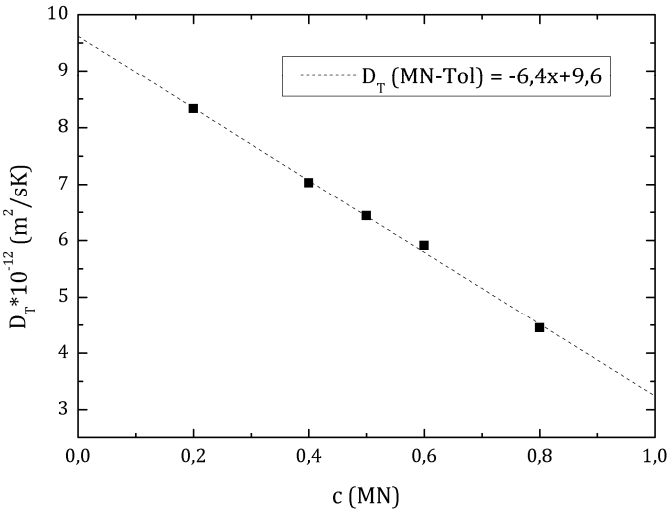

Figura 4.3. Variación del coeficiente de termodifusión con respecto a la concentración de MN para la serie de mezclas binarias de MN-Tol, a 25°C.

4.1.2. Influencia de la forma y el tamaño de las moléculas

Leahy-Dios y Firoozabadi [21] sugerían que la forma y el tamaño de las moléculas tienen influencia en el coeficiente de termodifusión, y se presenta mediante dos conceptos: la movilidad y la similitud de las moléculas. Como ya se ha visto, la movilidad de las moléculas se ve afectada negativamente por la masa molecular de la misma. Por otra parte, la similitud referida a la forma de las moléculas, también hace que disminuya el coeficiente de termodifusión. Es decir, si dos moléculas tienen una forma similar, reaccionarán de igual manera frente a un gradiente de temperatura, por lo que el coeficiente de termodifusión será menor.

En la Figura 4.4 se presentan los coeficientes de termodifusión correspondientes a las mezclas al 50% de concentración másica, en función de la masa molecular relativa de la mezcla. La masa molecular relativa de la mezcla, *MWn*, se define como el ratio de la masa molecular del alcano entre la masa molecular del solvente. En la gráfica se presentan los resultados correspondientes a las dos series de mezclas analizadas en este trabajo, además de los valores para las mezclas de alcanos nC$_6$-nC$_i$, nC$_{10}$-nC$_i$, nC$_{12}$-nC$_i$ publicados por Blanco *et al.* [24] y los publicados por Leahy-Dios y Firoozabadi [21] para las mezclas de MN-nC$_i$ y nC$_{10}$-nC$_i$. Como se puede observar, los resultados de nuestro grupo muestran un buen acuerdo con los de Leahy-Dios y Firoozabadi.

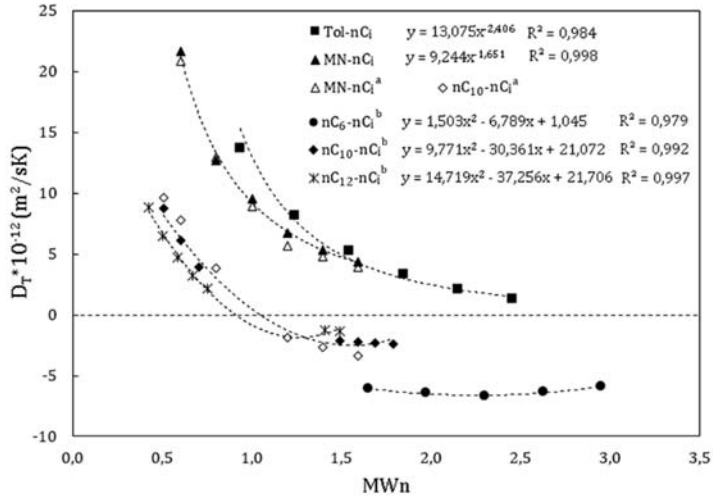

Figura 4.4. Coeficientes de termodifusión en función de la masa molecular relativa de la mezcla, para las mezclas al 50% de concentración másica y 25°C. [a]Resultados publicados por Leahy-Dios y Firoozabadi [21]. [b]Resultados publicados por Blanco *et al*. [24].

Como se sugería en Leahy-Dios y Firoozabadi [21] las mezclas formadas por un aromático (Tol y MN) y un n-alcano pueden describirse con un ajuste potencial. Este comportamiento también se observó en las series de benceno y n-alcanos presentadas por Polyakov y Wiegand [68]. Se puede ver nuevamente cómo al aumentar la masa molecular del soluto, el coeficiente de termodifusión disminuye.

En el caso de los n-alcanos, las tres series se describen mediante un ajuste polinómico de segundo orden, pero sólo dentro del rango estudiado. En general, las series formadas por dos n-alcanos presentan coeficientes de termodifusión menores que las series formadas por un n-alcano con Tol o con MN. Este comportamiento puede justificarse mediante el concepto de similitud entre las moléculas.

4.1.3. Soluciones diluidas

Extrapolando los resultados presentados en las Figura 4.1 y Figura 4.2 a la concentración $c_1 = 1$ ($c_2 = 0$), se puede determinar el coeficiente de termodifusión, D_T^0, para las soluciones diluidas de n-alcanos en Tol y en MN. Los resultados obtenidos se muestran en la Tabla 4.5.

Tabla 4.5. Coeficientes de termodifusión para la solución diluida de n-alcanos en Tol y MN a 25°C.

Sistema	D_T^0 x10^{-12} (m^2/sK)	Sistema	D_T^0 x10^{-12} (m^2/sK)
Tol-*n*C$_6$	14,5	MN-*n*C$_6$	11,0
Tol-*n*C$_8$	10,9	MN-*n*C$_8$	8,3
Tol-*n*C$_{10}$	8,5	MN-*n*C$_{10}$	7,0
Tol-*n*C$_{12}$	6,8	MN-*n*C$_{12}$	6,1
Tol-*n*C$_{14}$	6,0	MN-*n*C$_{14}$	5,3
Tol-*n*C$_{16}$	5,0	MN-*n*C$_{16}$	4,9

Como se puede observar, D_T^0 decrece con la masa molecular del n-alcano para ambos solventes (Tol y MN), y es menor para el solvente con mayor masa molecular (MN). Teniendo en cuenta la dependencia en la masa molecular del soluto observada en trabajos previos para mezclas diluidas de n-alcanos [69], se han representado en la Figura 4.5 los valores de D_T^0 con respecto al inverso del producto de las masas moleculares de los componentes de la mezcla. Los datos de ambas series presentan una tendencia lineal con la misma pendiente en los dos casos. Por tanto, D_T^0 puede escribirse como:

$$D_T^0 = a + \frac{b}{M_1}\left(\frac{1}{M_2}\right), \tag{4.1}$$

donde *b* es una constante independiente del solvente y *a* representa un valor estable de D_T^0 para valores altos de M_2 que depende del solvente considerado. Stadelmaier, Rauch y Köhler [69, 70] también observaron la dependencia del inverso de la masa molecular del soluto en polímero diluido y soluciones de n-alcanos en diferentes solventes. Por otra parte, los modelos teóricos desarrollados por Würger [71, 72] y las simulaciones de *reverse nonequilibrium molecular dynamics* (RNEMD) [73] también indican esta dependencia de D_T^0 con el inverso de la masa molecular del soluto.

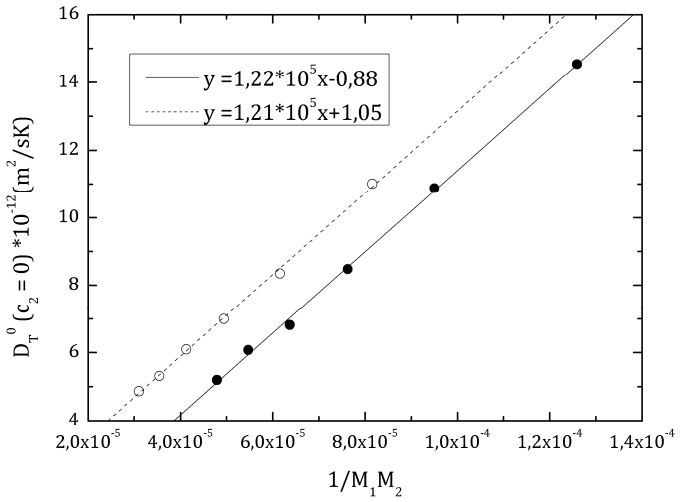

Figura 4.5. Coeficiente de termodifusión de las mezclas de n-alcanos diluidas en Tol y MN en función del inverso del producto de las masas moleculares.

A otras concentraciones de las mezclas, se ha observado que esta relación lineal no se cumple y que se ajusta con un polinomio de segundo grado.

4.2. Coeficiente de difusión molecular

Como se ha comentado anteriormente, el coeficiente de difusión molecular se ha determinado mediante la técnica SST para la concentración equimásica de todas las mezclas analizadas. Los coeficientes de difusión se han determinado con la nueva expresión (2.15). Por ello, se ha comprobado en todos los casos que el tiempo de ensayo

estaba dentro del límite de tiempos cortos. Los resultados obtenidos se muestran en la Tabla 4.6.

Tabla 4.6. Coeficientes de difusión molecular para la concentración equimásica de las mezclas binarias analizadas, determinados mediante la técnica SST

Sistema	D x 10^{-9} (m^2/s)	Sistema	D x 10^{-9} (m^2/s)
Tol-nC$_6$	2,90 ± 0,10	MN-nC$_8$	0,81 ± 0,02
Tol-nC$_8$	2,06 ± 0,03	MN-nC$_{10}$	0,56 ± 0,02
Tol-nC$_{10}$	1,69 ± 0,06	MN-nC$_{12}$	0,42 ± 0,01
Tol-nC$_{12}$	1,39 ± 0,03	MN-nC$_{14}$	0,32 ± 0,01
Tol-nC$_{14}$	1,22 ± 0,03	MN-nC$_{16}$	0,27 ± 0,02
Tol-nC$_{16}$	0,97 ± 0,02	MN-Tol	1,15 ± 0,04

En la Figura 4.6 se muestran los resultados obtenidos en función de la masa molecular del n-alcano para cada sistema. Esta relación queda representada por un ajuste potencial. Además se incluyen los resultados publicados por Leahy-Dios y Firoozabadi [21] para la serie MN-nC$_i$. Como se puede observar, para los n-alcanos más pequeños existen discrepancias entre nuestros resultados y los de Leahy-Dios y Firoozabadi. No obstante, para los n-alcanos más grandes el acuerdo es bueno. En todos los casos se observa una disminución del coeficiente de difusión a medida que aumenta la masa molecular del n-alcano. Se presentó una tendencia muy similar en las mezclas de benceno y n-alcanos analizadas por Polyakov y Wiegand [68].

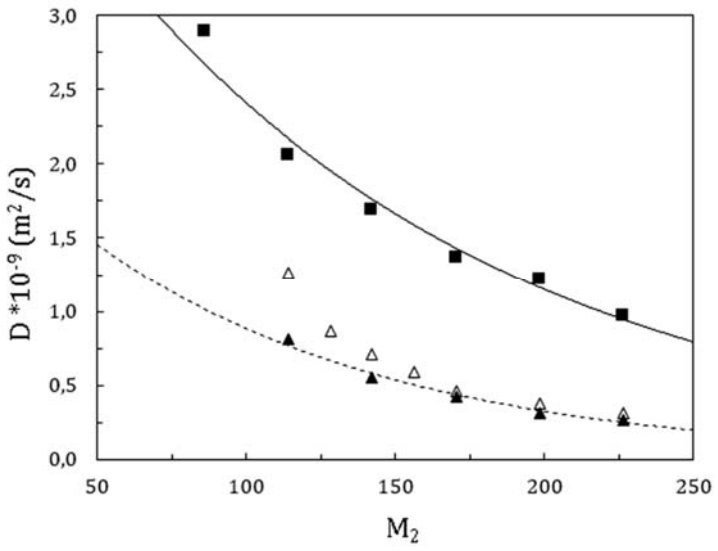

Figura 4.6. Coeficientes de difusión molecular para la concentración equimásica de las mezclas MN-nC$_i$ (triángulos) y Tol-nC$_i$ (cuadrados), determinados mediante la técnica SST, en función de la masa molecular del n-alcano. Los símbolos vacíos corresponden a los resultados de Leahy-Dios y Firoozabadi [21].

4.2.1. Dependencia de *D* con la viscosidad

En el trabajo publicado por Alonso de Mezquía *et al.* [22] se mostró que en mezclas binarias de n-alcanos se puede correlacionar el coeficiente *D* con la viscosidad. Este comportamiento se puede extender a los sistemas formados por Tol-nC$_i$ y MN-nC$_i$. En la Figura 4.7 se muestra la variación de los coeficientes de difusión molecular con respecto al inverso de la viscosidad dinámica de la mezcla. En esta figura también se presentan los resultados correspondientes a las mezclas binarias de n-alcanos (nC$_6$-nC$_i$, nC$_{10}$-nC$_i$, nC$_{12}$-nC$_i$) publicados en [22].

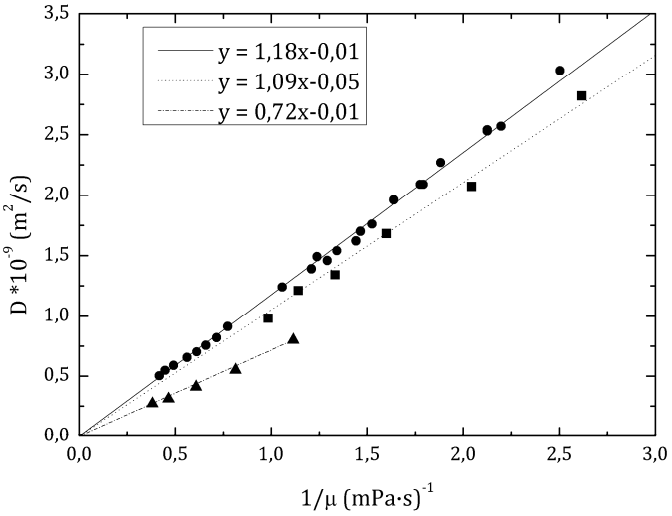

Figura 4.7. Coeficientes de difusión molecular en función del inverso de la viscosidad dinámica de la mezcla, para las mezclas de nC$_i$- nC$_i$ (círculos), Tol- nC$_i$ (cuadrados) y MN-nC$_i$ (triángulos) a 25°C.

Como se puede observar, esta relación se puede ajustar para cada sistema mediante una línea que cruza el origen. Por tanto, se puede escribir la siguiente relación lineal:

$$D = k / \mu . \tag{4.2}$$

Se podría deducir que el valor de la constante k depende en cierta medida de la morfología de los componentes de la mezcla. Así pues, para todas las mezclas equimásicas de n-alcanos el valor de k es el mismo, k = 1,18·10^{-12} kg·m/s^2. En el caso de las series de Tol-nC$_i$, el valor de la constante es k = 1,09·10^{-12} kg·m/s^2. Finalmente, para el caso de las mezclas de MN-nC$_i$, el valor es k = 0,7·10^{-12} kg·m/s^2. En conclusión, el producto $D\mu$ para una mezcla equimásica es una constante para cada serie y su valor depende de la morfología de los componentes de la mezcla.

4.3. Coeficiente Soret

A partir de los resultados obtenidos para los coeficientes de termodifusión y difusión molecular, se han calculado los coeficientes Soret para las concentraciones equimásicas de las mezclas analizadas. En la Tabla 4.7 se presentan los resultados. Para poder determinar

el coeficiente Soret correspondiente a la mezcla MN-nC$_6$, el coeficiente de difusión molecular de la mezcla se ha calculado mediante la ecuación (4.2) a partir del ajuste presentado en la Figura 4.7.

Tabla 4.7. Coeficientes Soret para las concentraciones equimásicas de cada mezcla, determinados de forma indirecta a 25°C.

Sistema	S_T x 10^{-3} (K^{-1})	Sistema	S_T x 10^{-3} (K^{-1})
Tol-nC$_6$	4,7 ± 0,4	[a]MN-nC$_6$	17,0 ± 1,0
Tol-nC$_8$	3,9 ± 0,2	MN-nC$_8$	16,0 ± 1,0
Tol-nC$_{10}$	3,1 ± 0,3	MN-nC$_{10}$	17,0 ± 1,0
Tol-nC$_{12}$	2,4 ± 0,1	MN-nC$_{12}$	16,0 ± 1,0
Tol-nC$_{14}$	1,7 ± 0,1	MN-nC$_{14}$	17,0 ± 1,0
Tol-nC$_{16}$	1,4 ± 0,1	MN-nC$_{16}$	16,0 ± 2,0
		MN-Tol	5,6 ± 0,4

[a]Para determinar este coeficiente Soret se ha calculado el coeficiente de difusión correspondiente a partir de la ecuación presentada en la Figura 4.7.

4.3.1. Dependencia de S_T con la masa molecular

En la Figura 4.8 se presentan los resultados correspondientes en función de la masa molecular del n-alcano, para las series de Tol-nC$_i$ y MN-nC$_i$ a 0,50 de concentración másica y a 25°C.

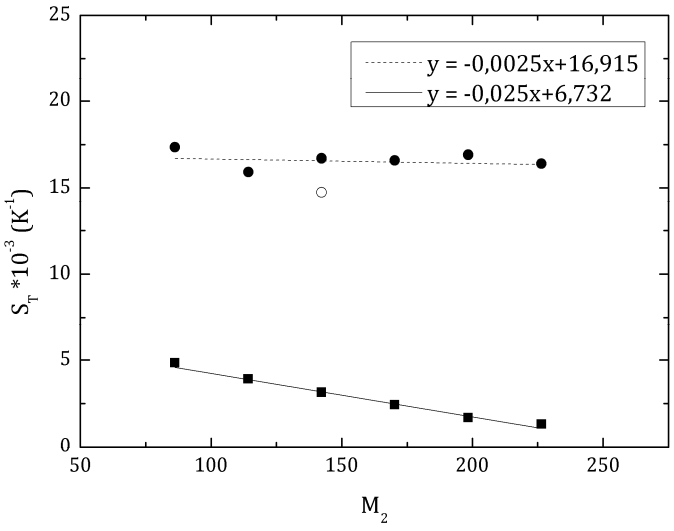

Figura 4.8. Coeficientes Soret en función de la masa molecular del n-alcano, para las series de Tol-nC$_i$ (cuadrados) y MN-nC$_i$ (círculos) a 25°C. El símbolo vacío representa el resultado publicado por Hartmann *et al.* [28].

Como se puede observar en la gráfica, los resultados para Tol-nC$_i$ se ajustan de forma lineal con pendiente negativa. Por tanto, los coeficientes Soret decrecen cuando la masa molecular del n-alcano aumenta. El comportamiento es muy similar al observado en mezclas de n-alcanos por Alonso de Mezquía *et al.* [30]. Este hecho indica la cuasi idealidad del comportamiento de la serie Tol-nC$_i$. Por el contrario, en el caso de las mezclas

de MN-*n*C_i esta relación es diferente. Como se puede observar, considerando el error experimental, el coeficiente Soret no depende de la masa molecular del n-alcano y podríamos decir que tiene un valor constante alrededor de $16{,}5 \cdot 10^{-3}$ K^{-1}. El comportamiento de este sistema se aleja de la idealidad de las mezclas binarias de n-alcanos.

En la Figura 4.8 también se presenta el resultado publicado por Hartmann *et al.* [28] para la mezcla MN-*n*C_{10}. Como se puede observar, el acuerdo es aceptable.

4.4. Conclusiones

Se han medido los coeficientes termodifusión de 77 mezclas binarias, y los coeficientes de difusión molecular y Soret de 13 mezclas binarias. Con ello se contribuye a la base de datos bibliográfica de resultados de mezclas binarias de hidrocarburos. Los resultados obtenidos para estas mezclas binarias se han publicado en el trabajo Apendice E y en el trabajo que se está preparando Apéndice J.

Se ha observado una clara influencia de la masa molecular, así como de la viscosidad, en los coeficientes de termodifusión. Además, se ha corroborado la no idealidad de las mezclas con anillos aromáticos y n-alcanos. La correlación cuantitativa desarrollada para predecir el coeficiente de termodifusión en mezclas binarias de n-alcanos [29] no es válida para las series de hidrocarburos analizadas durante este trabajo.

Además, se ha mostrado la linealidad en la relación del coeficiente de termodifusión de la mezcla diluida con respecto al inverso del producto de las masas moleculares de los componentes de la mezcla, siendo la pendiente de las dos series la misma. Estos resultados son acordes a las tendencias publicadas en la bibliografía para mezclas de polímero diluido y soluciones de n-alcanos en diferentes solventes y presentadas en modelos teóricos y simulaciones de RNEMD.

En el caso de la difusión molecular, se ha observado nuevamente la influencia de la viscosidad de la mezcla. En general se cumple para todas las mezclas analizadas, que al aumentar la viscosidad disminuye el coeficiente de difusión molecular.

En el caso del coeficiente Soret sin embargo, vuelven a aparecer discrepancias con respecto a las mezclas binarias de n-alcanos. Especialmente en el caso de la serie de MN-*n*C_i parece ser que el coeficiente S_T adquiere un valor constante para todas las mezclas de la serie a 0,50 de fracción másica.

5. BENCHMARK

Como se ha señalado en el capítulo de la introducción, en los últimos años el estudio del fenómeno de la termodifusión ha cobrado especial relevancia en mezclas ternarias. En la última década se han publicado varios trabajos aislados que proporcionan resultados en mezclas ternarias [34 - 36, 38, 40, 74, 75]. No obstante, estos resultados son limitados y no siempre son comparables, por lo que la dispersión es alta. Por ello, era necesario convocar y coordinar a todos los equipos experimentales que emplean diferentes técnicas y en diferentes condiciones para analizar un mismo sistema a fin de comparar y evaluar los resultados obtenidos. Esto permitiría subsanar las diferencias generando un sistema de referencia en lo que se refiere a mezclas ternarias. Con este propósito se ha desarrollado este primer *benchmark* en mezclas ternarias, en el marco del proyecto DCMIX, en el que se han comparado resultados obtenidos con diferentes técnicas tanto en condiciones terrestres como en condiciones de microgravedad. Estos últimos se han obtenido mediante la instalación *Selectable Optical Diagnostic Instrument* (SODI) a bordo de la Estación Espacial Internacional.

En octubre del 2013 se llevó a cabo un workshop del proyecto DCMIX en Mondragon Unibertsitatea en el que se decidió unificar los esfuerzos individuales para desarrollar este *benchmark* en mezclas ternarias. La mezcla elegida fue una de las propuestas en la primera fase del proyecto DCMIX: THN-IBB-*n*C_{12} a concentración másica de 0,80-0,10-0,10 y a 25°C. Tras realizar las investigaciones individuales, los resultados se pusieron en común durante el *11th International Meeting on Thermodiffusion* (IMT11) celebrado en Bayona (Francia) en junio de 2014. Los grupos que han participado en este trabajo son:

- El equipo del Prof. W. Köhler (WK), de la *Universität Bayreuth*, Alemania.
- El equipo de la Prof. V. Shevtsova (VS), de la *Université Libre de Bruxelles*, Bélgica.
- El equipo del Prof. S. Van Vaerenbergh (SVV), de la *Université Libre de Bruxelles*, Bélgica.
- El equipo del Prof. Z. Saghir (ZS), de la *Ryerson University*, Canada.
- El equipo de la Prof. T. Lyubimova (RAS) de la *Russian Academy of Science*, Rusia.
- El equipo del Prof. M. M. Bou-Ali (MBA) de Mondragon Goi Eskola Politeknikoa, España.

Tras analizar los resultados obtenidos mediante las diferentes técnicas, se ha publicado una colección de siete artículos en una edición especial de la revista *European Physical Journal E*. Uno de ellos es el resumen del trabajo [43] (Apéndice G) y los otros seis son el resultado de las investigaciones de cada equipo, detallando el procedimiento de análisis realizado de acuerdo con sus técnicas correspondientes [53, 76-80]. El artículo correspondiente al grupo de Mondragon Goi Eskola Politeknikoa puede encontrarse en el Apéndice H de esta memoria.

Durante todo este capítulo el componente 1 se refiere a THN, el componente 2 se refiere a IBB y el componente 3 se refiere a *n*C_{12}.

5.1. Técnicas experimentales

A continuación se describen las técnicas empleadas por cada equipo en condiciones terrestres y la técnica SODI empleada en condiciones de microgravedad.

5.1.1. Condiciones terrestres

El equipo de WK ha empleado la técnica *two-colour Optical Beam Deflection* (OBD) [37, 74] para determinar los coeficientes Soret y de termodifusión. En esta técnica se determinan los cambios de concentración ocasionados por un gradiente de temperatura en una célula de Soret. Para ello, se miden los gradientes de índice de refracción en la célula a dos longitudes de onda diferentes. En este caso se han empleado un láser azul de 450 nm y un láser rojo de 635 nm (Figura 5.1). Mediante los mismos se ha obtenido una matriz de factores de contraste con un número de condición de 50, que facilita enormemente la necesaria inversión de la matriz. Las amplitudes de concentración estacionarias se obtienen a partir de un ajuste numérico realizado a las señales de los dos haces. Finalmente, los coeficientes Soret se determinan a partir de los cambios de concentración obtenidos en el estado estacionario. Los coeficientes de termodifusión se determinan a partir de los cambios sufridos por los haces en el momento inicial del experimento, es decir, al aplicar el gradiente de temperatura.

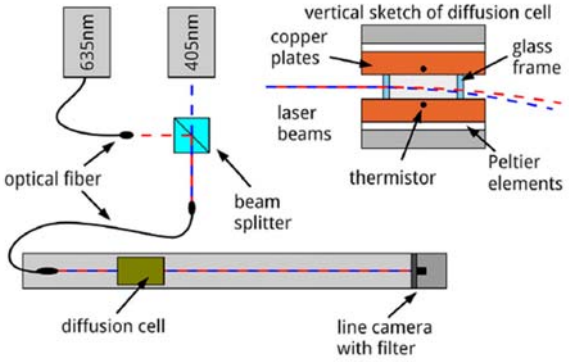

Figura 5.1. Esquema de la instalación Optical Beam Deflection (OBD) [76].

El equipo de VS ha empleado la técnica de *Optical Digital Interferometry* (ODI) [81] para determinar los coeficientes Soret y la técnica *Taylor Dispersion* (TDT) [38] para determinar los coeficientes de difusión molecular.

En la técnica ODI se utiliza un interferómetro Mach-Zehnder para examinar la separación en una célula Soret de una forma muy similar al experimento realizado en microgravedad. Se han empleado dos láseres de 670 y 925 nm de longitud de onda. Aunque la elección de las longitudes de onda no es óptima (el número de condición de la matriz se encuentra alrededor de 240 [82]), se hizo así intencionadamente para que fuera lo más parecido posible al instrumento SODI. Se han realizado experimentos independientes con diferentes fuentes de láser y se han repetido tres veces con cada láser. La técnica ODI permite realizar el seguimiento de la concentración durante todo el proceso de la termodifusión, proporcionando una gran cantidad de datos a los que se ajusta el modelo analítico completo del proceso de separación.

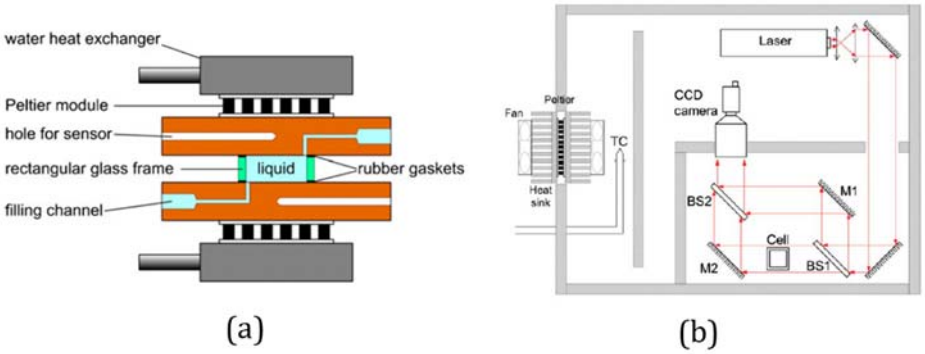

Figura 5.2. (a) Sección lateral de la célula de Soret. (b) Esquema general de la instalación *Optical Digital Interferometry* [81].

Para caracterizar la matriz de difusión mediante la técnica TDT (Figura 5.3) se han realizado pequeñas inyecciones de tres concentraciones diferentes en el flujo laminar de la solución portadora en un capilar largo y fino. Al final del capilar se monitoriza la variación de la concentración de las muestras inyectadas en función del tiempo. Para ello se emplea un refractómetro de alta sensibilidad diferencial que opera cerca del infrarrojo. La inyección de cada concentración particular se ha repetido 3-4 veces.

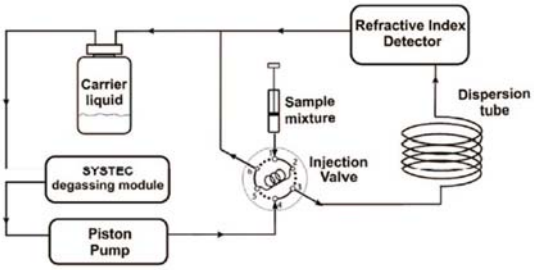

Figura 5.3. Instalación de la técnica *Taylor Dispersion Technique* [38].

El equipo de SVV ha empleado la técnica de *Open Ended Capillary* (OEC) [40] para determinar los coeficientes de difusión molecular. En esta técnica se genera un gradiente de concentración entre la solución contenida en tubos capilares y la solución contenida en el baño (Figura 5.4). El líquido contenido en los diferentes tubos se analiza en función del tiempo para medir su composición. Las mediciones de concentración se han realizado mediante ^{1}H-NMR. Los coeficientes de difusión molecular se determinan ajustando la evolución de la concentración. La precisión de los resultados obtenidos ha sido mejorada ajustando de manera simultánea los datos de dos experimentos independientes.

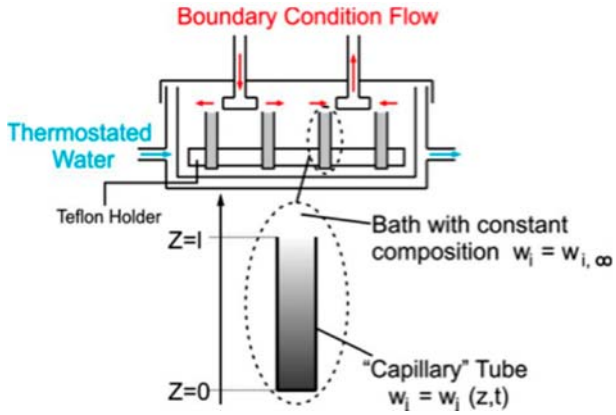

Figura 5.4. Esquema de la técnica *Open Ended Capillary* [40].

Por último, el grupo de MBA, ha empleado la técnica termogravitacional para determinar los coeficientes de termodifusión (TG) [56] y la técnica de *Sliding Symmetric Tubes* (SST) [36] para determinar los coeficientes de difusión molecular. Estas técnicas han sido ampliamente descritas en esta memoria, en las secciones 2.1 y 2.2 respectivamente.

En el caso de los coeficientes de termodifusión se han empleado las dos columnas termogravitacionales descritas anteriormente (STC y LTC) y en cada caso se ha repetido el ensayo tres veces. En el caso de los coeficientes de difusión molecular se han realizado cuatro experimentos, que combinados dos a dos, han permitido obtener cuatro series de resultados. Los coeficientes Soret se han determinado con los valores medios obtenidos para los coeficientes de termodifusión y difusión molecular.

5.1.2. Condiciones de microgravedad

Las medidas realizadas en condiciones de microgravedad se han llevado a cabo mediante la instalación SODI, que lleva trabajando con éxito a bordo de la Estación Espacial Internacional desde 2009 [83]. La configuración actual del dispositivo consta de dos módulos ópticos que disponen de interferómetros Mach-Zehnder, adecuados para monitorizar el índice de refracción en el interior de celdas transparentes [75, 84]. Uno de los módulos sostiene un interferómetro con una única longitud de onda, mientras que el otro presenta un interferómetro con dos longitudes de onda, de 670 y 935 nm. Este último módulo puede trasladarse lateralmente, lo que permite monitorizar diferentes células colocadas en la llamada matriz de células Figura 5.5. Mientras que la mayor parte de los aparatos están fijos en todos los experimentos, la matriz de células con las muestras líquidas puede cambiarse de un experimento a otro. El experimento DCMIX contiene una matriz de células que consiste en 5 células con mezclas ternarias y una célula con la mezcla binaria de referencia. La mezcla elegida en este *benchmark* es una de las cinco mezclas ternarias que se analizaron en el primer experimento DCMIX.

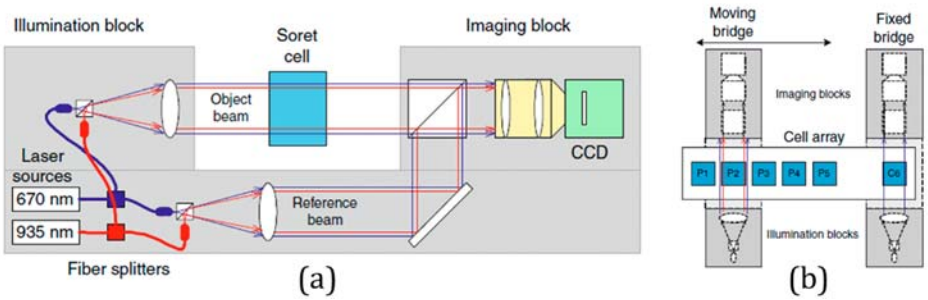

Figura 5.5. Esquema de la instalación SODI [84]. (a) Vista lateral del sistema óptico. (b) Vista superior del sistema óptico y el conjunto de celdas.

Los experimentos realizados en la instalación SODI han sido analizados por cuatro equipos independientemente para determinar los coeficientes Soret de la mezcla. En todos los casos se han empleado los mismos factores de contraste [82]. Los equipos que han determinado los coeficientes Soret en condiciones de microgravedad son:

- El equipo de VS [77].
- El equipo de SVV [78].
- El equipo de ZS [79].
- El equipo de RAS [80].

5.2. Coeficiente de termodifusión

En primer lugar se han medido las propiedades de la mezcla necesarias para determinar los coeficientes de termodifusión (densidad, coeficiente de expansión térmica y viscosidad dinámica) mediante la técnica termogravitacional. Así mismo, se han determinado los parámetros de calibración necesarios para calcular la concentración de cada componente en la mezcla, según se ha detallado en el apartado 3.2.3. En las Tabla 5.1 y Tabla 5.2 se muestran estos resultados [53].

Tabla 5.1. Densidad, coeficiente de expansión térmica y viscosidad dinámica de la mezcla ternaria THN-IBB-nC$_{12}$ a concentración másica de 0,80-0,10-0,10 y a 25°C.

ρ (kg/m^3)	α x 10^{-3} (K^{-1})	μ x 10^{-3} (Pa·s)
925,316	0,848	1,719

Tabla 5.2. Parámetros de calibración de la mezcla ternaria THN-IBB-nC$_{12}$ a concentración másica de 0,80-0,10-0,10 y a 25°C.

k_0 (kg/m^3)	k_1 (kg/m^3)	k_2 (kg/m^3)	k_0'	k_1'	k_2'
845,888	117,569	-142,028	1,48294	0,05497	-0,09042

Como se ha comentado, en el caso de la mezcla *benchmark* se ha determinado la variación de la concentración en estado estacionario, en función de la altura de la columna tanto en la STC como en la LTC (Figura 5.6). Además, en cada columna se han realizado tres experimentos con el fin de asegurar la repetibilidad de los resultados. Con las propiedades de la mezcla (Tabla 5.1) y la separación de la concentración en la columna, se

han determinado los coeficientes de termodifusión para los componentes 1 y 3, THN y nC$_{12}$ en este caso, mediante la ecuación (2.4).

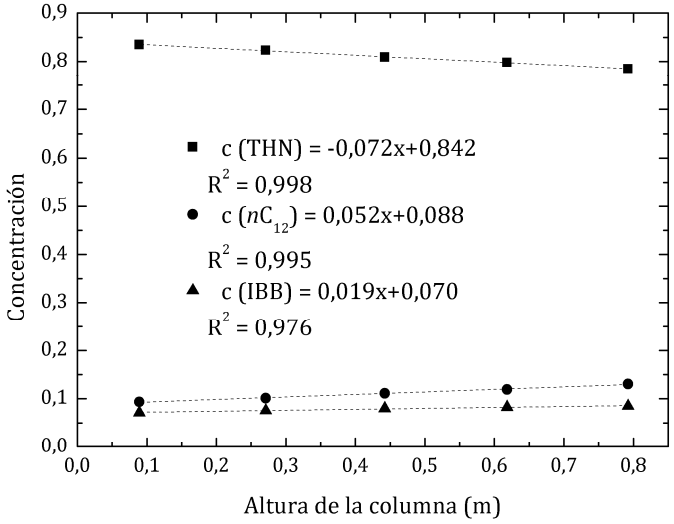

Figura 5.6. Variación de la concentración de cada componente en función de la altura de la columna LTC, para la mezcla THN-IBB-nC$_{12}$ a concentración de 0,80-0,10-0,10 y 25°C.

Los resultados obtenidos mediante ambas columnas se muestran en la Tabla 5.3 [53]. La desviación estándar entre los diferentes resultados es de 1,4% para el componente 1 y de 3,6% para el componente 3. Como se puede observar, esto representa una buena repetibilidad de los resultados obtenidos mediante la técnica termogravitacional. No obstante, el error experimental en la columna LTC es menor, gracias a su mayor sensibilidad en la determinación de la separación. Se ha tomado el valor medio de los seis experimentos como resultado propuesto para este trabajo de *benchmark*.

Tabla 5.3. Coeficientes de termodifusión correspondientes a los componentes 1 y 3, para la mezcla THN-IBB-nC$_{12}$ a concentración de 0,80-0,10-0,10 y 25°C, medidos mediante la técnica termogravitacional en las columnas STC y LTC.

	$D'_{T,1}$ x10^{-12} (m^2/sK)	$D'_{T,3}$ x10^{-12} (m^2/sK)
STC L_z = 500 mm	0,68 ± 0,03	-0,49 ± 0,01
	0,66 ± 0,05	-0,45 ± 0,07
	0,66 ± 0,03	-0,46 ± 0,03
LTC L_z = 980 mm	0,67 ± 0,04	-0,50 ± 0,03
	0,69 ± 0,03	-0,50 ± 0,03
	0,68 ± 0,04	-0,51 ± 0,03
Valores propuestos	0,67 ± 0,05	-0,49 ± 0,06

Los resultados correspondientes al componente 2, IBB en este caso, pueden calcularse directamente de la condición de que los tres coeficientes de termodifusión deben sumar cero.

Como se ha comentado en la introducción de este capítulo, los coeficientes de termodifusión de esta mezcla han sido determinados por otros dos grupos independientes. Por una parte, el grupo de la Prof. Shevtsova ha determinado los

coeficientes de termodifusión a partir de la combinación de los coeficientes Soret y de difusión molecular, medidos respectivamente mediante las técnicas ODI y TDT [77]. Por otra parte, el grupo del Prof. Köhler ha medido los coeficientes de termodifusión mediante la técnica OBD [76]. En la Tabla 5.4 se pueden observar los resultados propuestos por los tres grupos.

Tabla 5.4. Coeficientes de termodifusión para la mezcla THN-IBB-nC$_{12}$ a concentración de 0,80-0,10-0,10 y 25°C, medidos por tres grupos diferentes en condiciones terrestres.

	Técnica	$D'_{T,1}$ x10^{-12} (m^2/sK)	$D'_{T,3}$ x10^{-12} (m^2/sK)
Condiciones terrestres	ODI+TDT	0,69 ± 0,13	-0,48 ± 0,06
	OBD	0,72 ± 0,26	-0,50 ± 0,16
	TG	0,67 ± 0,05	-0,49 ± 0,06
	Media	0,68 ± 0,05	-0,48 ± 0,04

Como se puede observar el acuerdo entre los resultados medidos de manera independiente por los tres grupos es muy bueno, siendo la desviación estándar entre las medidas del 3,5% para el componente 1 y de 2,6% para el componente 3. Por ello, se ha decidido proponer la media ponderada de estos tres valores como valor *benchmark*. El factor de ponderación depende directamente del error experimental correspondiente a cada resultado. El error correspondiente a la media también se ha obtenido realizando una media ponderada de los tres resultados.

5.3. Coeficiente de difusión molecular

Como se ha descrito en la sección 2.2, para determinar los coeficientes de difusión molecular de una mezcla ternaria mediante la técnica SST es necesario realizar dos ensayos con concentraciones iniciales diferentes. Con el fin de analizar la repetibilidad de los resultados, en este caso se han realizado cuatro experimentos diferentes. Combinándolos dos a dos se han obtenido cuatro series de resultados. En la Tabla 5.5 se muestran las concentraciones iniciales correspondientes a cada componente en el tubo superior e inferior para los cuatro experimentos realizados. A partir de la variación de la concentración de los componentes en función del tiempo se determinan los coeficientes de difusión molecular.

Tabla 5.5. Concentraciones iniciales de los cuatro experimentos de difusión molecular realizados mediante la técnica SST para la mezcla THN-IBB-nC$_{12}$ a concentración de 0,80-0,10-0,10 y 25°C.

	Tubo inferior			Tubo superior		
	THN	IBB	nC$_{12}$	THN	IBB	nC$_{12}$
Exp. 1	0,84	0,08	0,08	0,76	0,12	0,12
Exp. 2	0,84	0,10	0,06	0,76	0,10	0,14
Exp. 3	0,85	0,07	0,08	0,75	0,13	0,12
Exp. 4	0,85	0,10	0,05	0,75	0,10	0,15

Como se puede observar, en los experimentos 1 y 3 se ha variado la concentración de los tres componentes entre el tubo superior e inferior. Sin embargo, en los experimentos 2

y 4 la concentración de IBB se ha mantenido constante entre ambos tubos. Para poder determinar los coeficientes de difusión molecular es necesario conocer la pendiente de la regresión lineal generada por la variación de la concentración en función de la raíz cuadrada del tiempo. En la Figura 5.7 se ha representado esta variación para los experimentos 3 y 4. Como se ha señalado en la sección 2.2, es importante identificar el tiempo de ensayo máximo para el cual la solución basada en la *error function* es válida. No obstante, en la publicación de la colección de los artículos del *benchmark* no se consideró este estudio. Por ello, en este capítulo se muestran nuevos resultados teniendo en cuenta este análisis.

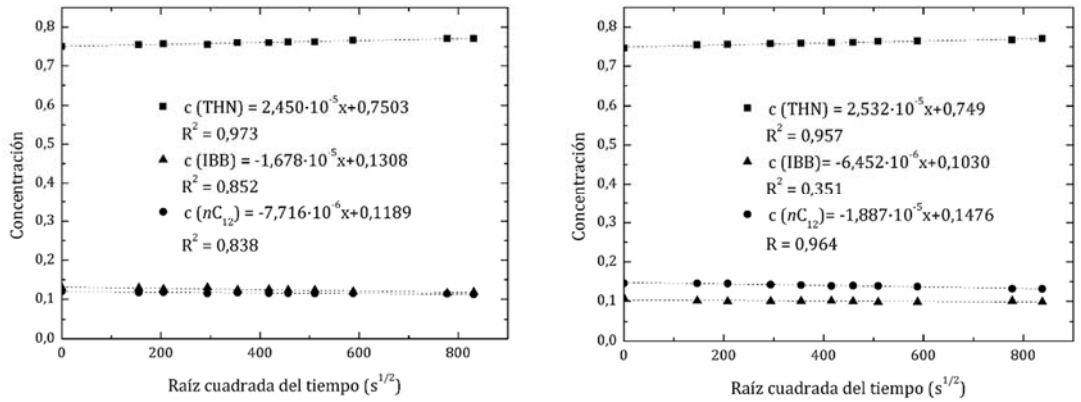

Figura 5.7. Variación de la concentración de los tres componentes de la mezcla en función de la raíz cuadrada del tiempo, en el tubo superior de la técnica SST, correspondientes a los experimentos 3 y 4 realizados para la mezcla THN-IBB-*n*C_{12} a concentración de 0,80-0,10-0,10 y 25°C.

Como se ha comentado anteriormente, en una mezcla ternaria se tiene una matriz de difusión de 2x2. Es decir, por cada matriz de difusión se tienen cuatro coeficientes de difusión molecular (dos puros y dos cruzados) y dos valores propios. Al contrario que en el caso de los coeficientes de termodifusión y Soret, no hay un coeficiente de difusión asignado a cada componente, si no que cada coeficiente representa las interacciones entre ellos. Por ello, hay que prestar especial atención al orden de los componentes en la mezcla, ya que los coeficientes de difusión determinados cambian. No obstante, los coeficientes pueden transformarse fácilmente de un orden a otro como se puede ver para el caso en el que se intercambian los componentes 2 y 3 [74]:

$$D_{11}^{*} = D_{11} - D_{12},$$

$$D_{12}^{*} = -D_{12},$$

$$D_{21}^{*} = D_{22} + D_{12} - D_{21} - D_{11},$$

$$D_{22}^{*} = D_{22} + D_{12}. \qquad (5.1)$$

En la Tabla 5.6 se presentan los resultados correspondientes a los coeficientes de difusión molecular y en la Tabla 5.7 los correspondientes a los valores propios de la matriz de difusión para las cuatro posibles combinaciones de experimentos.

Tabla 5.6. Coeficientes de difusión molecular medidos mediante la técnica SST para la mezcla THN-IBB-nC_{12} a concentración de 0,80-0,10-0,10 y 25°C.

Exp.	D_{11} x 10^{-10} (m^2/s)	D_{12} x 10^{-10} (m^2/s)	D_{21} x 10^{-10} (m^2/s)	D_{22} x 10^{-10} (m^2/s)
1-2	6,00 ± 1,00	-1,20 ± 0,20	-0,03 ± 0,01	7,00 ± 1,00
3-4	6,00 ± 1,00	-1,20 ± 0,20	-1,20 ± 0,20	7,00 ± 1,00
1-4	6,00 ± 1,00	0,08 ± 0,02	-1,50 ± 0,30	4,00 ± 0,80
2-3	6,00 ± 1,00	-2,10 ± 0,40	0,0014 ± 0,0003	9,00 ± 2,00
Media	6,00 ± 1,00	-1,10 ± 0,20	-0,70 ± 0,10	7,00 ± 1,00

Tabla 5.7. Valores propios de la matriz de difusión determinados mediante la técnica SST para la mezcla THN-IBB-nC_{12} a concentración de 0,80-0,10-0,10 y 25°C.

Exp.	$\hat{D}_1$ x10^{-10} (m^2/s)	$\hat{D}_2$ x10^{-10} (m^2/s)
1-2	7,0 ± 1,0	6,0 ± 1,0
3-4	5,0 ± 1,0	8,0 ± 2,0
1-4	4,1 ± 0,8	6,0 ± 1,0
2-3	6,0 ± 1,0	9,0 ± 2,0
Media	5,0 ± 1,0	8,0 ± 2,0

De acuerdo con los resultados, la mayor diferencia tras la consideración de los tiempos de ensayo se observa en el aumento del error experimental, directamente relacionado con el error de ajuste de la concentración en función de la raíz cuadrada del tiempo. Este aumento es debido a que en los tiempos iniciales de un experimento en la técnica SST se da una mayor dispersión de la concentración ocasionada por las posibles perturbaciones generadas al cambiar la posición de los tubos. Por ello, al reducir el tiempo de ensayo, aumenta el error de la regresión lineal. Lo que indica claramente la importancia de escoger el mayor tiempo de ensayo que permita emplear la solución basada en la *error function*.

Por otra parte, como se puede observar, la repetibilidad es buena en el caso de los valores propios y los coeficientes de difusión molecular puros. Sin embargo, en el caso de los coeficientes de difusión cruzados se aprecia una gran desviación entre los resultados de los diferentes ensayos, para los que se observan incluso cambios de signo. Aunque no tiene mucho sentido considerando las grandes desviaciones obtenidas, se ha calculado la media y se ha tomado la misma como un quinto caso de resultados. El propósito es analizar la fiabilidad y su efecto en los coeficientes Soret

En este trabajo de *benchmark* los coeficientes de difusión molecular han sido determinados por otros dos grupos en condiciones terrestres. Por una parte, el grupo de la Prof. Shevtsova ha medido los coeficientes de difusión molecular mediante la técnica TDT [77]. Por otra parte, el grupo del Prof. Van Vaerenbergh ha medido los coeficientes de difusión molecular mediante la técnica OEC [78]. En la Tabla 5.8 se presentan los resultados obtenidos por los tres grupos para los valores propios de la matriz de difusión. Seguidamente, en la Tabla 5.9 se muestran los resultados correspondientes a los coeficientes de difusión molecular. Los resultados aportados por los tres grupos y los valores *benchmark* se presentan tal cual aparecen publicados en el trabajo [43],

independientemente de si los decimales son significativos. Además, se incluyen los resultados actualizados en este trabajo tras la consideración de los tiempos de ensayo.

Tabla 5.8. Valores propios de la matriz de difusión para la mezcla THN-IBB-*n*C_{12} a concentración de 0,80-0,10-0,10 y 25°C, medidos por tres grupos diferentes en condiciones terrestres.

	Técnica	$\hat{D}_1$ x10^{-10} (m^2/s)	$\hat{D}_2$ x10^{-10} (m^2/s)
Condiciones terrestres	TDT	5,29 ± 0,09	7,30 ± 0,26
	OEC	5,50 ± 0,03	6,60 ± 0,03
	SST	5,43 ± 0,68	8,08 ± 1,02
	Media	5,48 ± 0,03	6,61 ± 0,03
	SST actualizado	5,00 ± 1,00	8,00 ± 2,00

Tabla 5.9. Coeficientes de difusión molecular para la mezcla THN-IBB-*n*C_{12} a concentración de 0,80-0,10-0,10 y 25°C, medidos por tres grupos diferentes en condiciones terrestres.

	Técnica	D_{11} x 10^{-10} (m^2/s)	D_{12}x 10^{-10} (m^2/s)	D_{21} x 10^{-10} (m^2/s)	D_{22}x 10^{-10} (m^2/s)
Condiciones terrestres	TDT	6,61 ± 0,10	-0,59 ± 0,54	-1,55 ± 0,10	5,98 ± 0,44
	OEC	5,50 ± 0,51	-0,99 ± 0,63	0,002 ± 0,03	6,60 ± 0,37
	SST	5,23 ± 0,66	-1,80 ± 0,23	0,39 ± 0,05	8,28 ± 1,00
	SST actualizado	6,00 ± 1,00	-1,10 ± 0,20	-0,70 ± 0,10	7,00 ± 1,00

Se ha observado un acuerdo razonable entre los valores propios obtenidos por los tres grupos, por lo que se ha calculado una media ponderada según el error experimental de cada resultado como valor *benchmark.* Además, como se puede observar en la Tabla 5.8, los resultados determinados en este trabajo coinciden con los valores publicados en el trabajo del *benchmark*.

Sin embargo, en el caso de los coeficientes de difusión molecular los resultados de los tres grupos no coinciden, encontrándose las mayores diferencias en los coeficientes de difusión cruzados. Se pueden observar incluso cambios de signo en el coeficiente D_{21}. Por ello, no se han dado valores *benchmark* para los coeficientes de difusión molecular.

Como se ha observado, la determinación de los coeficientes de difusión molecular en mezclas ternarias entraña problemas que aún están sin resolver. En esta sección se ha presentado un análisis más profundo de la determinación de los mismos mediante la técnica SST. Se ha mostrado cómo aunque los valores propios de la matriz de difusión se repitan, en los coeficientes de difusión pueden aparecer incluso cambios de signo. En la bibliografía se pueden encontrar trabajos en los que se muestran las complicaciones que surgen en la determinación de los coeficientes de difusión molecular mediante otras técnicas [37, 38, 57].

Esto lleva a pensar que puede haber más de una combinación de coeficientes de difusión que satisface la matriz. Por ello, resulta más fiable utilizar los valores propios de la matriz de difusión a la hora de comparar y validar los resultados.

5.4. Coeficiente Soret

Los coeficientes Soret se han determinado a partir de la combinación de los resultados correspondientes a los coeficientes de termodifusión y difusión molecular, mediante la ecuación (2.27). En el caso de los coeficientes de termodifusión, se ha empleado el valor medio presentado en la Tabla 5.3. En el caso de los coeficientes de difusión molecular, debido a los problemas de repetibilidad mostrados, se han empleado los resultados obtenidos en los cinco casos presentados en la Tabla 5.6. Por ello, en la siguiente Tabla 5.10 se muestran cinco casos de resultados para los coeficientes Soret correspondientes a la mezcla *benchmark*.

Al igual que para el coeficiente de termodifusión, en una mezcla ternaria hay tres coeficientes Soret, uno asociado a cada componente. En este caso se han determinado los coeficientes correspondientes a los componentes 1 y 3. El coeficiente del componente 2 se puede calcular directamente de la condición de que los tres coeficientes deben sumar cero. Debido a la modificación que han sufrido los coeficientes de difusión molecular al considerar los intervalos de ensayo, los coeficientes Soret también han sido modificados ligeramente con respecto a los publicados en [53].

Tabla 5.10. Coeficientes Soret calculados de manera indirecta para los cinco casos de coeficientes de difusión molecular, para la mezcla THN-IBB-*n*C_{12} a concentración de 0,80-0,10-0,10 y 25°C

$D'_{T,i}$	D_{ij}	$S'_{T,1}$ x 10^{-3} (K^{-1})	$S'_{T,3}$ x 10^{-3} (K^{-1})
Media	Exp. 1-2	1,1 ± 0,2	-0,9 ± 0,2
	Exp. 3-4	1,1 ± 0,2	-1,0 ± 0,2
	Exp. 1-4	1,1 ± 0,2	-1,0 ± 0,2
	Exp. 2-3	1,1 ± 0,2	-0,9 ± 0,2
	Media de D_{ij}	1,1 ± 0,2	-0,9 ± 0,2
Media propuesta		1,1 ± 0,2	-0,9 ± 0,2

Como se puede observar, para los cinco casos de coeficientes de difusión molecular se han obtenido los mismos valores de coeficientes Soret. Es decir, a pesar de la mala repetibilidad de los coeficientes de difusión molecular cruzados, su interacción en el cálculo del coeficiente Soret no parece tener una gran influencia. Esto refuerza la idea de que pueda haber varias combinaciones de coeficientes de difusión que satisfacen una misma matriz.

Dada la buena repetibilidad de los coeficientes Soret para los diferentes resultados de difusión molecular, se ha tomado la media como valor propuesto para esta mezcla.

Los coeficientes Soret correspondientes a la mezcla *benchmark* han sido medidos de forma directa y en condiciones terrestres por otros dos grupos. Por una parte, el grupo de la Prof. Shevtsova ha determinado los coeficientes Soret mediante la técnica ODI [77]. Por otra parte, el grupo del Prof. Köhler ha medido los coeficientes Soret mediante la técnica OBD [76]. En la Tabla 5.11 se pueden observar los resultados propuestos por los tres grupos y el valor *benchmark* tal cual aparecen publicados en el trabajo [43]. Además, se incluyen los resultados actualizados tras la consideración del tiempo de ensayo, que como se puede observar coinciden con los resultados publicados en el trabajo [43].

Tabla 5.11. Coeficientes Soret para la mezcla THN-IBB-*n*C_{12} a concentración de 0,80-0,10-0,10 y 25°C, medidos por tres grupos diferentes en condiciones terrestres.

	Técnica	$S'_{T,1}$ x10^{-3} (K^{-1})	$S'_{T,3}$ x10^{-3} (K^{-1})
Condiciones terrestres	ODI	1,04 ± 0,15	-0,94 ± 0,10
	OBD	1,20 ± 0,09	-0,86 ± 0,06
	TG+SST	1,19 ± 0,09	-0,91 ± 0,15
	Media	1,17 ± 0,06	-0,88 ± 0,05
	TG+SST actualizado	1,10 ± 0,20	-0,90 ± 0,20

Como se puede observar el acuerdo entre los resultados medidos de manera independiente por los tres grupos es muy bueno. Cabe destacar que se han obtenido resultados muy similares mediante tres métodos diferentes: dos técnicas de medición directa y la combinación de otras dos técnicas independientes.

Se ha propuesto la media ponderada de estos tres valores como valor *benchmark* en condiciones terrestres. El factor de ponderación depende directamente del error experimental correspondiente a cada resultado. El error correspondiente a la media también se ha obtenido realizando una media ponderada de los tres resultados.

En condiciones de microgravedad, como se ha comentado al inicio de esta sección, los experimentos correspondientes se realizaron mediante el instrumento SODI. No obstante, los resultados obtenidos han sido analizados por cuatro grupos de manera independiente para determinar los coeficientes Soret. En la Tabla 5.12 pueden observarse los resultados aportados por el grupo de la Prof. Lyubimova [80], el grupo del Prof. Saghir [79], el grupo de la Prof. Shevtsova [77] y el grupo del Prof. Van Vaerenbergh [78]. Estos resultados se presentan tal cual aparecen publicados en el trabajo [43], independientemente de si los decimales son significativos.

Tabla 5.12. Coeficientes Soret para la mezcla THN-IBB-*n*C_{12} a concentración de 0,80-0,10-0,10 y 25°C, determinados por cuatro grupos diferentes en condiciones de microgravedad.

	Técnica	$S'_{T,1}$ x10^{-3} (K^{-1})	$S'_{T,3}$ x10^{-3} (K^{-1})
Condiciones de microgravedad	RAS	1,40 ± 0,16	-0,83 ± 0,10
	ZS	1,37 ± 0,06	-0,57 ± 0,05
	VS	1,43 ± 0,21	-0,66 ± 0,07
	SVV	1,39 ± 0,25	-0,49 ± 0,08
	Media	1,38 ± 0,05	-0,61 ± 0,03

Como se puede observar, los resultados determinados en condiciones de microgravedad muestran un acuerdo aceptable. Las diferencias son mayores si los comparamos con los resultados medidos en condiciones terrestres, ya que se deberían obtener los mismos resultados independientemente de las condiciones de gravedad del experimento. No obstante, esta diferencia entre los dos grupos de resultados tiene una explicación lógica. El diseño del conjunto de células del instrumento SODI estaba sujeto una serie de condiciones extra (seguridad, viabilidad…) para poder operar a bordo de la Estación Espacial Internacional, que perjudican las características óptimas para la realización del experimento. Además, las diferencias de valores presentados en la Tabla 5.12 no son independientes, pues presentan una correlación lineal debida a las

propiedades específicas de la matriz de factores de contraste (el número de condición). Los detalles sobre esta discusión pueden encontrarse en los trabajos [76, 77, 80], en los que se realiza el análisis mediante métodos ópticos.

5.5. Conclusiones

Tal y como se ha comentado anteriormente es la primera vez que varios grupos experimentales se han puesto de acuerdo para analizar los coeficientes de termodifusión, difusión molecular y Soret de una mezcla ternaria. Los resultados obtenidos han mostrado un buen acuerdo en la mayoría de los casos, lo que supone un gran avance en el estudio del fenómeno de la termodifusión en mezclas líquidas multicomponentes. Se han presentado valores de referencia para los coeficientes de termodifusión (Tabla 5.4), los valores propios de la matriz de difusión (Tabla 5.8) y los coeficientes Soret, tanto en condiciones terrestres (Tabla 5.11) como de microgravedad (Tabla 5.12). Cabe destacar la buena coincidencia entre los resultados de los coeficientes Soret en condiciones terrestres, obtenidos tanto mediante dos técnicas diferentes de medición directa (ODI y OBD), como mediante la combinación de dos técnicas independientes (SST + TG).

Gracias a este trabajo pueden validarse las diferentes técnicas experimentales para el análisis de mezclas ternarias, entre ellas, las empleadas durante esta tesis: la técnica termogravitacional y la técnica *sliding symmetric tubes*.

Tras realizar un análisis más profundo de los tiempos de ensayo empleados en los experimentos de difusión molecular, se ha observado que era necesario ajustarlos para poder aplicar la solución analítica basada en la *error function*. Esto ha hecho que los resultados de difusión molecular, y por consiguiente los de Soret, varíen ligeramente con respecto a los publicados en el trabajo de *benchmark* [53]. La variación de los resultados no es significativa, aunque se consideran más correctos los valores mostrados en esta memoria.

Por otra parte, al comparar los resultados de difusión molecular se ha observado que aún hay cuestiones sin resolver en la determinación de los coeficientes de la matriz de difusión. No obstante, se ha mostrado que la mala repetibilidad en los coeficientes de difusión cruzados, no supone un efecto destacable sobre los coeficientes Soret calculados. Por ello, se ha considerado más consistente y fiable emplear los valores propios de la matriz de difusión para comparar los resultados obtenidos entre diferentes técnicas.

6. MEZCLAS TERNARIAS

Como ya se ha comentado anteriormente en esta memoria, el reto actual en la investigación de las propiedades de transporte en mezclas líquidas se encuentra en el estudio de mezclas ternarias. El mayor avance realizado en el campo experimental es el desarrollo del trabajo de *benchmark* descrito en el capítulo 5 de esta memoria. Gracias a ese trabajo en colaboración con diferentes equipos, se han podido validar las técnicas empleadas para la determinación de los coeficientes de transporte en mezclas ternarias. No obstante, como se ha mostrado, aún hay cierta incertidumbre en la determinación de los coeficientes de difusión molecular en mezclas ternarias.

Durante esta tesis doctoral se han analizado las mezclas ternarias correspondientes al proyecto DCMIX 1. Estas mezclas corresponden al sistema THN-IBB-*n*C_{12} analizado en el *benchmark*, a otras cinco concentraciones. Para estas cinco mezclas se han determinado los coeficientes de termodifusión, difusión molecular y Soret. Estos resultados y su análisis se han publicado en el trabajo presentado en el Apéndice I [85]. Además, se han determinado los coeficientes de termodifusión para ocho concentraciones de una nueva mezcla ternaria compuesta por MN-Tol-*n*C_{10}. La elección de este ternario se ha realizado con el fin de analizar otras mezclas de hidrocarburos, con forma molecular diferente (dos anillos, un anillo y una cadena) y considerando la densidad y el índice de refracción de los componentes puros. Los resultados obtenidos se publicarán en el trabajo en preparación mostrado en el Apéndice L. Todas las mezclas ternarias analizadas se presentan en la Tabla 6.1.

Tabla 6.1. Mezclas ternarias analizadas durante esta tesis

Sistema	c_1-c_2-c_3	Sistema	c_1-c_2-c_3
THN-IBB-*n*C_{12}	0,10-0,80-0,10	MN-Tol-*n*C_{10}	0,33-0,33-0,33
	0,10-0,10-0,80		0,10-0,10-0,80
	0,40-0,20-0,40		0,10-0,80-0,10
	0,45-0,10-0,45		0,20-0,20-0,60
	0,33-0,33-0,33		0,20-0,40-0,40
			0,20-0,60-0,20
			0,40-0,20-0,40
			0,40-0,40-0,20

6.1. Coeficiente de termodifusión

Los coeficientes de termodifusión de las mezclas ternarias analizadas en este trabajo se han medido mediante la técnica termogravitacional, con la columna LTC.

6.1.1. Mezcla THN-IBB-*n*C_{12}

Las propiedades termofísicas y los parámetros de calibración necesarios para determinar los coeficientes de termodifusión mediante la técnica termogravitacional se presentan en las Tablas 6.2 y 6.3. Estos datos fueron publicados por Blanco *et al.* [34] para la concentración equimásica y por Alonso de Mezquía *et al.* [56] (Apéndice F) para las demás concentraciones.

Tabla 6.2. Densidad, coeficiente de expansión térmica y viscosidad dinámica de las concentraciones analizadas de la mezcla ternaria THN-IBB-nC$_{12}$, a 25°C.

c_1-c_2-c_3	ρ (kg/m^3)	α x 10^{-3} (K^{-1})	μ x 10^{-3} (Pa·s)
0,10-0,10-0,80	771,994	0,954	1,314
0,45-0,10-0,45	841,822	0,900	1,440
0,40-0,20-0,40	842,524	0,905	1,354
0,33-0,33-0,33	843,541	0,914	1,295
0,10-0,80-0,10	847,553	0,947	1,053

Tabla 6.3. Parámetros de calibración para las concentraciones analizadas de la mezcla ternaria THN-IBB-nC$_{12}$, a 25°C.

c_1-c_2-c_3	k_0 (kg/m^3)	k_1 (kg/m^3)	k_2 (kg/m^3)	k_0'	k_1'	k_2'
0,10-0,10-0,80	838,380	89,227	-94,189	1,47635	0,04041	-0,05761
0,45-0,10-0,45	847,995	101,875	-115,505	1,48309	0,04672	-0,07131
0,40-0,20-0,40	848,077	102,365	-116,189	1,48292	0,04727	-0,07180
0,33-0,33-0,33	848,056	101,957	-115,443	1,48312	0,04728	-0,07159
0,10-0,80-0,10	849,052	105,245	-122,807	1,48380	0,04884	-0,07734

Como para la mezcla del *benchmark*, se ha determinado el coeficiente de termodifusión para los componentes 1 y 3 mediante la ecuación (2.4). Los resultados mostrados en la Tabla 6.4 son la media de al menos tres ensayos. La desviación estándar entre los ensayos es en todos los casos inferior al 4%.

Tabla 6.4. Coeficientes de termodifusión para los componentes 1 y 3 de la mezcla THN-IBB-nC$_{12}$ medidos mediante las columnas LTC y STC a 25°C

c_1-c_2-c_3	$D'_{T,1}$ x10^{-12} (m^2/sK)		Dif. %	$D'_{T,3}$ x10^{-12} (m^2/sK)		Dif. %
	LTC	STC		LTC	STC	
0,10-0,10-0,80	0.52±0.02	0.47±0.04[a]	9.61	-0.75±0.03	-0.75±0.03[a]	0.02
0,45-0,10-0,45	1.38±0.07	1.33±0.04[a]	3.62	-1.40±0.05	-1.44±0.02[a]	2.85
0,40-0,20-0,40	1.30±0.05	1.23±0.04[a]	5.38	-1.32±0.04	-1.33±0.02[a]	0.75
0,33-0,33-0,33	1.15±0.06	1.10±0.02[b]	4.34	-1.21±0.05	-1.23±0.02[b]	1.65
0,10-0,80-0,10	0.32±0.02	0.33±0.02[a]	3.12	-0.49±0.02	-0.45±0.03[a]	8.16

[a]Resultados publicados en Alonso de Mezquía *et al*. [56].

[b]Resultados publicados en Blanco *et al.* [34].

En el trabajo de Alonso de Mezquía *et al*. [56] se midieron los coeficientes de termodifusión de estas mismas mezclas pero empleando la columna STC. La mezcla de concentración equimásica también fue medida en la columna STC por Blanco *et al.* [34]. Estos resultados se muestran también en la Tabla 6.4.

Como se puede observar, los resultados obtenidos con ambas columnas son muy similares, tal y como se esperaba. A pesar de que algunos errores experimentales son menores en la columna STC, la repetibilidad de los resultados es mejor en la columna LTC. En algunos de los experimentos realizados con la columna STC fue necesario descartar uno de los puntos de concentración en función de la altura de la columna. Este hecho hace que

el error debido al ajuste de la regresión lineal sea menor. Además, fue necesario realizar un mayor número de repeticiones mediante la columna STC para obtener los resultados. En la columna LTC se evitan todos estos problemas de procedimiento experimental ya que gracias a su altura, la separación relativa de la mezcla es casi el doble que en la columna STC. Esta mayor sensibilidad es muy interesante para el caso de las mezclas ternarias, en las que la separación estacionaria es generalmente más pequeña que en las mezclas binarias. Por esta razón, después de este estudio se ha decidido emplear únicamente la columna LTC para analizar el coeficiente de termodifusión en las mezclas ternarias.

Por otra parte, se ha deducido una expresión de aproximación que permite calcular los coeficientes de termodifusión de cualquier concentración ternaria a partir de sus binarios correspondientes. En la Figura 6.1 se muestran los resultados experimentales de $D'_{T,1}$ con respecto a las concentraciones de los componentes 1 y 3, para las composiciones analizadas. La superficie se ha dibujado considerando las siguientes condiciones de contorno:

$$c_1 = 0 \quad \rightarrow \quad D'_{T,1} = 0\,,$$

$$c_1 = 1 \quad \rightarrow \quad D'_{T,1} = 0\,, \tag{6.1}$$

y las líneas de intersección de esta superficie con los planos c_3=0 y c_1+c_3=1 corresponden con los valores de D'_T de las mezclas binarias 1-2 y 1-3 respectivamente. Como se puede observar, las líneas de intersección de la superficie con los planos c_1 = *constante* son aproximadamente líneas rectas. Por tanto, se puede determinar $D'_{T,1}$ de forma orientativa, mediante la interpolación de cada valor de c_1 entre los valores limitantes del coeficiente de termodifusión del componente 1, correspondientes a las mezclas binarias c_3=0 y c_3=1-c_1 (Figura 6.1). Es decir, se puede escribir la siguiente expresión:

$$D'_{T,1} = D'_{T,1-2} + \frac{D'_{T,1-3} - D'_{T,1-2}}{(1-c_1)} c_3\,, \tag{6.2}$$

donde c_1 y c_3 son las concentraciones de los componentes 1y 3 en la mezcla ternaria y $D'_{T,1\text{-}2}$ y $D'_{T,1\text{-}3}$ son los coeficientes de termodifusión del componente 1 en las mezclas binarias formadas por los componentes 1-2 y 1-3 respectivamente.

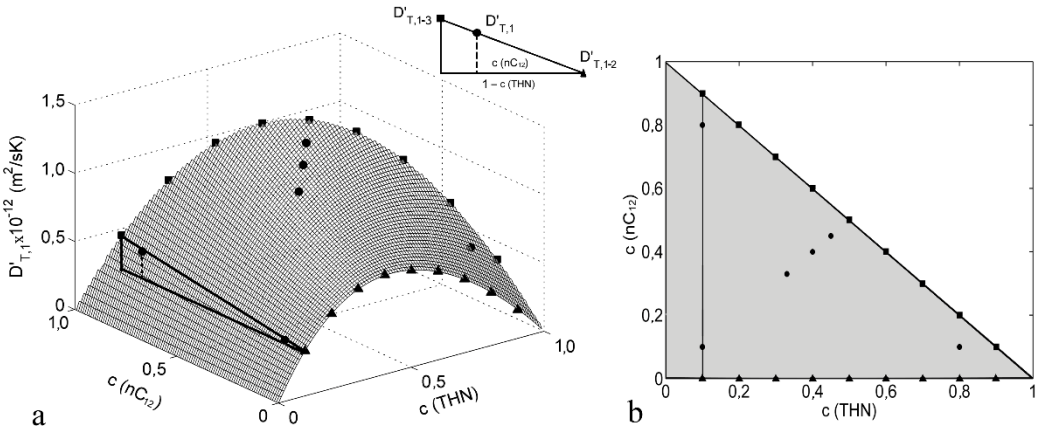

Figura 6.1. Coeficiente de termodifusión del componente 1 (THN) en función de las concentraciones másicas de los componentes 1 y 3 a 25°C. Los triángulos corresponden a la mezcla binaria THN-IBB ($D'_{T,1\text{-}2}$), los cuadrados corresponden a la mezcla binaria THN-*n*C$_{12}$ ($D'_{T,1\text{-}3}$) y los círculos corresponden a la mezcla ternaria. a) Vista en 3D. b) Vista superior.

De acuerdo con la definición dada en Bou-Ali *et al*. [43] para mezclas ternarias, en una mezcla binaria i-j:

$$D'_{T,i-j} = D_{T,i-j} c_i (1 - c_i), \tag{6.3}$$

y entonces la ecuación (6.2) puede escribirse como:

$$D'_{T,1} = D_{T,1-2} c_1 c_2 + D_{T,1-3} c_1 c_3 \tag{6.4}$$

donde c_1, c_2 y c_3 son las concentraciones de los componentes 1, 2 y 3 en la mezcla ternaria. Esta regla de combinación puede generalizarse para cualquier $D'_{T,i}$:

$$D'_{T,i} = D_{T,i-j} c_i c_j + D_{T,i-k} c_i c_k \tag{6.5}$$

Esta expresión es similar a la desarrollada por Larre *et al.* [86], pero en este caso los coeficientes de termodifusión de las mezclas binarias son los correspondientes a la concentración c_i.

Se han determinado los coeficientes de termodifusión para todas las concentraciones correspondientes a la mezcla ternaria THN-IBB-*n*C$_{12}$ analizadas en este capítulo y también para la concentración correspondiente al *benchmark*. En la Figura 6.2 se puede apreciar la comparación entre los coeficientes determinados experimentalmente y los calculados mediante la regla de combinación (6.5). En los resultados experimentales se ha incluido el resultado para la mezcla equimásica, determinado mediante la técnica OBD y publicado por Gebhardt y Köhler [37]. Para determinar los coeficientes de termodifusión de las mezclas binarias necesarias se han empleado los polinomios de aproximación propuestos por Gebhardt *et al.* en el trabajo[20].

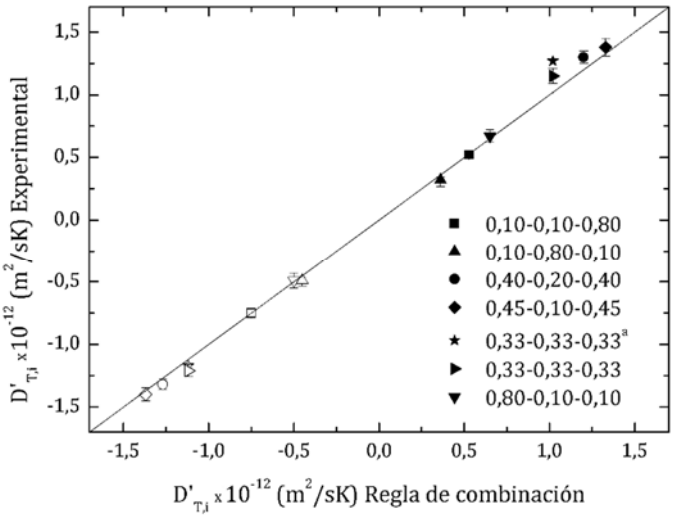

Figura 6.2. Comparación entre los coeficientes de termodifusión determinados mediante la regla de combinación (6.5) y experimentalmente mediante la columna LTC. [a]Resultado determinado mediante la técnica OBD en el trabajo [37]. Los símbolos rellenos corresponden al componente 1 y los símbolos vacíos corresponden al componente 3.

En la Figura 6.2, en primer lugar, se puede observar la comparación entre los valores experimentales medidos mediante la columna LTG y mediante la técnica OBD [37] para la concentración equimásica. Al igual que ocurría para la mezcla del *benchmark*, el acuerdo entre los resultados de estas dos técnicas es bueno. Por el momento no hay valores publicados para las demás concentraciones analizadas, por lo que no es posible comparar los demás resultados obtenidos mediante la técnica termogravitacional.

Por otra parte, como se puede observar, el acuerdo entre los valores experimentales y los calculados es muy convincente en todos los casos, siendo la mayor diferencia del 12%. Cabe destacar que los resultados obtenidos mediante la regla de combinación (6.5) dependen fuertemente a su vez de los polinomios de aproximación para mezclas binarias desarrollados por Gebhardt *et al.* en [20]. Por tanto, considerando los polinomios de aproximación publicados por Gebhardt *et al.* y esta regla de combinación, es posible determinar los coeficientes de termodifusión para cualquier composición de la mezcla ternaria THN-IBB-*n*C_{12}, a partir de los valores de concentración de los tres componentes en la mezcla ternaria.

En cuanto a la correlación presentada por Larre *et al.* [86], los resultados calculados también presentan un buen acuerdo con los resultados experimentales obtenidos mediante la columna LTC en este trabajo. Los resultados obtenidos mediante esta correlación se publicaron en el trabajo Alonso de Mezquía *et al*. [56] y en general presentan unas desviaciones ligeramente mayores que la regla de combinación (6.5) desarrollada en este trabajo.

6.1.2. Mezcla MN-Tol-*n*C_{10}

En las Tabla 6.5 se presentan la densidad, coeficiente de expansión térmica y viscosidad dinámica correspondientes a las ocho concentraciones de la mezcla MN-Tol-*n*C_{10} analizadas. Como se ha comentado anteriormente, estas propiedades son necesarias para determinar los coeficientes de termodifusión mediante la técnica termogravitacional.

Tabla 6.5. Densidad, coeficiente de expansión térmica y viscosidad dinámica de las concentraciones analizadas de la mezcla ternaria MN-Tol-*n*C_{10}, a 25°C.

c_1-c_2-c_3	ρ (kg/m^3)	α x 10^{-3} (K^{-1})	μ x 10^{-3} (Pa·s)
0,33-0,33-0,33	853,928	0,948	0,863
0,10-0,10-0,80	760,364	1,011	0,797
0,10-0,80-0,10	859,235	1,040	0,601
0,20-0,20-0,60	797,562	0,994	0,803
0,20-0,40-0,40	825,556	0,998	0,733
0,20-0,60-0,20	856,634	1,002	0,652
0,40-0,20-0,40	852,689	0,933	1,000
0,40-0,40-0,20	885,294	0,927	0,881

Seguidamente, en la Tabla 6.6 se muestran los parámetros de calibración de estas ocho mezclas analizadas. Estos parámetros permiten determinar la concentración de cada componente en una mezcla ternaria a partir de su densidad e índice de refracción, mediante las ecuaciones (3.5)-(3.7). Como se ha comentado en el apartado 3 de esta memoria, la calibración es un procedimiento especialmente delicado, ya que de ella depende la precisión de las mediciones de concentración. Por ello, y siempre, tras realizar cada calibración se verifican los ajustes mediante el análisis mezclas de concentración conocida.

Tabla 6.6. Parámetros de calibración para las concentraciones analizadas de la mezcla ternaria MN-Tol-*n*C_{10}, a 25°C.

c_1-c_2-c_3	k_0 (kg/m^3)	k_1 (kg/m^3)	k_2 (kg/m^3)	k_0'	k_1'	k_2'
0,33-0,33-0,33	859,389	139,791	-156,363	1,49368	0,10319	-0,10262
0,10-0,10-0,80	844,617	117,024	-119,877	1,48141	0,08785	-0,07311
0,10-0,80-0,10	862,120	139,761	-167,517	1,49372	0,10587	-0,10703
0,20-0,20-0,60	858,449	116,517	-139,869	1,49168	0,08672	-0,08749
0,20-0,40-0,40	858,663	131,649	-148,250	1,49162	0,09914	-0,09389
0,20-0,60-0,20	833,850	184,334	-70,703	1,44714	0,18153	0,05041
0,40-0,20-0,40	859,602	137,351	-154,621	1,49477	0,10274	-0,10385
0,40-0,40-0,20	860,876	146,227	-170,222	1,49305	0,11052	-0,11044

Los coeficientes de termodifusión correspondientes a las mezclas ternarias de este sistema se han medido únicamente mediante la columna LTC. En la Tabla 6.7 se muestran los resultados obtenidos para los coeficientes de los componentes 1 (MN) y 3 (*n*C_{10}). Los resultados que se muestran son la media de al menos tres experimentos en cada caso, entre los que la desviación típica es en general inferior al 3%. Como se ha comentado anteriormente, los coeficientes correspondientes al componente 2 (Tol) pueden determinarse directamente a partir de la condición de que los tres coeficientes de termodifusión deben sumar cero.

Tabla 6.7. Coeficientes de termodifusión determinado mediante la LTC, para las concentraciones analizadas de la mezcla ternaria MN-Tol-nC$_{10}$, a 25°C.

c_1-c_2-c_3	$D'_{T,1}$ x10^{-12} (m^2/sK)	$D'_{T,3}$ x10^{-12} (m^2/sK)
0,33-0,33-0,33	2,10 ± 0,10	-2,00 ± 0,10
0,10-0,10-0,80	0,95 ± 0,07	-1,26 ± 0,05
0,10-0,80-0,10	0,81 ± 0,05	-0,84 ± 0,05
0,20-0,20-0,60	1,80 ± 0,20	-2,00 ± 0,10
0,20-0,40-0,40	1,70 ± 0,10	-1,90 ± 0,10
0,20-0,60-0,20	2,10 ± 0,20	-1,10 ± 0,10
0,40-0,20-0,40	1,50 ± 0,10	-2,80 ± 0,10
0,40-0,40-0,20	2,10 ± 0,10	-1,50 ± 0,10

Con el fin de analizar el comportamiento de los coeficientes de termodifusión de este nuevo sistema ternario, se han comparado los resultados experimentales obtenidos en este trabajo con los determinados mediante la regla de combinación (6.5). Los coeficientes de las mezclas binarias necesarios se han determinado a partir de las aproximaciones lineales mostradas en las Figuras 4.1, 4.2 y 4.3. En la Figura 6.3 se puede observar que el acuerdo en este caso no es tan convincente como para la mezcla THN-IBB-nC$_{12}$. Aunque en la mayoría de los casos la precisión obtenida mediante la regla de combinación es aceptable, para algunos casos las desviaciones son considerables. Estas desviaciones pueden verse justificadas por la suma de las aproximaciones realizadas en mezclas binarias para la aplicación de la correlación (6.5).

En el caso de la correlación presentada por Larre *et al.* [86], las desviaciones entre los valores calculados y los experimentales son generalmente mayores que con respecto a la regla de combinación (6.5).

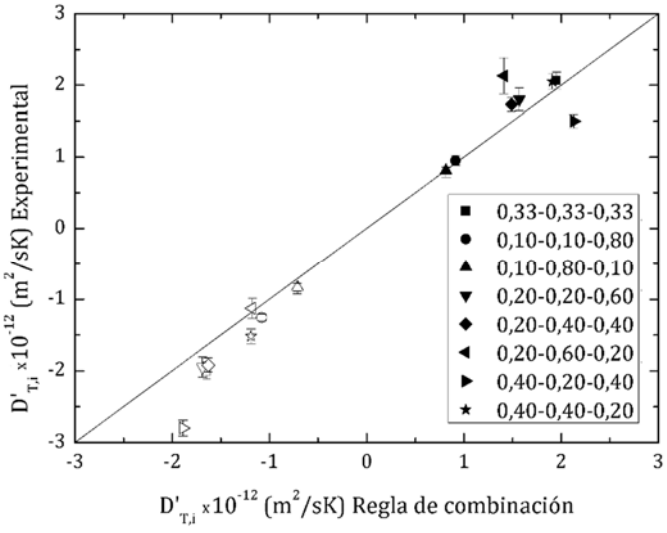

Figura 6.3. Comparación de los coeficientes de termodifusión medidos mediante la técnica termogravitacional y los determinados mediante la regla de combinación (6.5), para la mezcla MN-Tol-nC$_{10}$ a 25°C. Los puntos rellenos corresponden al componente 1 y los puntos vacíos al componente 3.

6.2. Coeficiente de difusión molecular

Se han determinado los coeficientes de difusión molecular para la mezcla THN-IBB-nC$_{12}$ a diferentes concentraciones, mediante la técnica SST y la ecuación basada en la *error function* (2.25). Para cada mezcla se ha analizado el tiempo de ensayo máximo para el cual se puede emplear esta ecuación y que además incluya el mayor número de puntos experimentales posible. Con estos criterios, se ha establecido que en general el número de puntos experimentales empleados quede limitado a un máximo de 196 horas de ensayo, para mezclas con coeficientes de difusión del mismo orden de magnitud que las analizadas en este trabajo y para diferencias de concentración inicial de c_i ± 5%.

En la Tabla 6.8 se muestran en primer lugar los resultados obtenidos para los autovalores de la matriz de difusión. Seguidamente, en la Tabla 6.9 se muestran los coeficientes de difusión molecular.

Tabla 6.8. Valores propios de la matriz de difusión para las mezclas de THN-IBB-nC$_{12}$, determinados mediante la técnica SST a 25°C.

c_1-c_2-c_3	$\hat{D}_1$ x10^{-10} (m^2/s)	$\hat{D}_2$ x10^{-10} (m^2/s)
0,10-0,10-0,80	9±1	11±2
0,45-0,10-0,45	7±1	7±1
0,40-0,20-0,40	4±1	7±2
0,33-0,33-0,33	5±1	10±3
0,10-0,80-0,10	9±2	12±3

Tabla 6.9. Coeficientes de difusión molecular para las mezclas de THN-IBB-nC$_{12}$, determinados mediante la técnica SST a 25°C.

c_1-c_2-c_3	D_{11} x 10^{-10} (m^2/s)	D_{12} x 10^{-10} (m^2/s)	D_{21} x 10^{-10} (m^2/s)	D_{22} x 10^{-10} (m^2/s)
0,10-0,10-0,80	10,00±1,00	-0,80±0,10	-1,50±0,20	10,00±1,00
0,45-0,10-0,45	7,00±1,00	0,32±0,06	-0,14±0,03	7,00±1,00
0,40-0,20-0,40	8,00±2,00	1,30±0,40	-1,30±0,40	4,00±1,00
0,33-0,33-0,33	8,00±2,00	-2,30±0,60	-2,00±0,50	6,00±2,00
0,10-0,80-0,10	10,00±3,00	-0,21±0,06	-1,70±0,40	7,00±2,00

Los resultados para la mezcla equimásica dados en las Tablas 6.8 y 6.9 no coinciden exactamente con los publicados en el trabajo Larrañaga *et al*. [36]. Esto es debido a que posteriormente a la publicación de ese trabajo se ha realizado un ajuste de los tiempos de ensayo empleados. Por ello, se está preparando un trabajo en el que se detalla el análisis de los tiempos de ensayo en la determinación de los coeficientes de difusión molecular mediante la técnica SST y se presentan los resultados actualizados para la mezcla equimásica (Apéndice K).

Hasta el momento en la bibliografía sólo existen resultados publicados para la composición equimásica, medidos mediante las técnica *Taylor dispersion* (TDT) y *Counter Flow Cell* (CFC) [38, 87] y mediante la técnica *Optical Beam Deflection* (OBD) [74]. En la siguiente Tabla 6.10 se muestra la comparación entre los coeficientes de difusión molecular determinados en este trabajo, y los resultados publicados en los trabajos [38, 74].

Tabla 6.10. Comparación de los coeficientes de difusión molecular publicados en la bibliografía para la mezcla THN-IBB-*n*C_{12} a concentración de 0,33-0,33-,033 y a 25°C.

Técnica	D_{11} x 10^{-10} (m^2/s)	D_{12} x 10^{-10} (m^2/s)	D_{21} x 10^{-10} (m^2/s)	D_{22} x 10^{-10} (m^2/s)
TDT [38]	10,31	0,33	-4,36	6,41
CFC [38]	11,61	0,32	-6,18	6,65
OBD[a] [74]	5,62	-5,91	1,08	12,18
SST	8,00±2,00	-2,30±0,60	-2,00±0,50	6,00±2,00

[a]Valores transformados mediante las ecuaciones (5.1) para que correspondan al mismo orden de componentes.

Como se puede observar, al igual que para la mezcla del *benchmark*, los resultados obtenidos mediante diferentes técnicas no muestran buen acuerdo. Especialmente en el caso de los coeficientes de difusión cruzados en los que se observan cambios incluso en el signo. Por ello, a continuación se muestra también la comparación de los valores propios de la matriz de difusión correspondientes a estas mismas mediciones (Tabla 6.11):

Tabla 6.11. Comparación de los valores propios de la matriz de difusión publicados en la bibliografía para la mezcla THN-IBB-*n*C_{12} a concentración de 0,33-0,33-,033 y a 25°C.

Técnica	$\hat{D}_1$ x10^{-10} (m^2/s)	$\hat{D}_2$ x10^{-10} (m^2/s)
TDT [38]	6,82	9,9
CFC [38]	7,09	11,17
OBD [74]	6,81	10,99
SST	5,00±1,00	10,00±3,00

En este caso se puede observar un acuerdo más aceptable de los resultados. Esto muestra una vez más que los valores propios resultan un parámetro más fiable y válido a la hora de comparar los resultados obtenidos mediante diferentes técnicas.

6.3. Coeficiente Soret

En este trabajo se han determinado los coeficientes de Soret para las mezclas de THN-IBB-*n*C_{12} a las diferentes concentraciones analizadas mediante la ecuación (2.27). Para ello se han empleado los coeficientes de termodifusión medidos mediante la LTC mostrados en la Tabla 6.4 y los coeficientes de difusión molecular mostrados en la Tabla 6.9. Los resultados obtenidos se muestran en la Tabla 6.12:

Tabla 6.12. Coeficientes Soret determinados para las mezclas de THN-IBB-*n*C_{12} a 25°C.

c_1-c_2-c_3	$S'_{T,1}$ x10^{-3} (K^{-1})	$S'_{T,3}$ x10^{-3} (K^{-1})
0,10-0,10-0,80	0,54 ± 0,07	-0,90 ±0,20
0,45-0,10-0,45	1,90 ±0,20	-2,00 ±0,30
0,40-0,20-0,40	1,50 ± 0,40	-2,10 ±0,60
0,33-0,33-0,33	1,60 ±0,40	-2,20 ±0,70
0,10-0,80-0,10	0,31 ± 0,06	-0,60 ± 0,20

Se ha observado que los coeficientes Soret siguen una tendencia muy similar a la de los coeficientes de termodifusión. Por ello, se ha establecido una regla de combinación

muy similar a la presentada en la ecuación (6.5) para determinar los coeficientes Soret de una mezcla ternaria a partir de los coeficientes correspondientes a las mezclas binarias:

$$S'_{T,i} = S_{T,i-j} c_i c_j + S_{T,i-k} c_i c_k \qquad (6.6)$$

En la Figura 6.4 se muestran los coeficientes Soret determinados mediante la ecuación (6.5) y los determinados a partir de los valores experimentales. También se incluyen los resultados más recientes para la composición equimásica determinados mediante la técnica OBD y publicados por Gebhardt y Köhler [37]. Los resultados de las mezclas binarias necesarios para aplicar la regla de combinación (6.6) han sido calculados empleando los polinomios de aproximación publicados por Gebhardt *et al* [20].

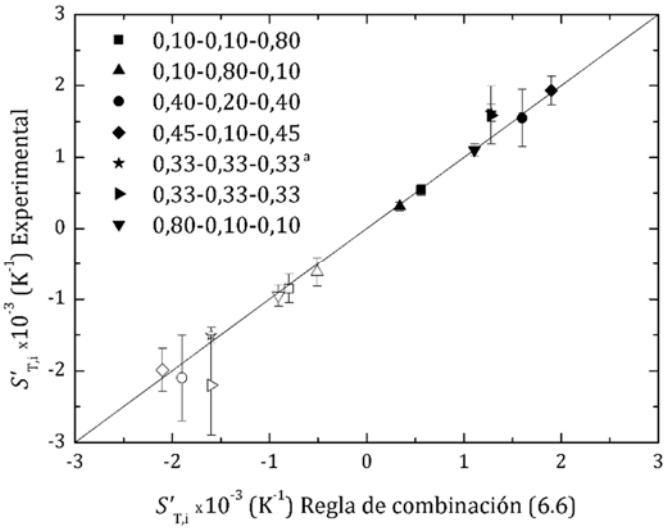

Figura 6.4. Comparación entre los coeficientes Soret determinados experimentalmente y mediante la regla de combinación (6.6). [a]Resultado determinado mediante la técnica OBD en el trabajo [37]. Los símbolos rellenos corresponden al componente 1 y los símbolos vacíos corresponden al componente 3.

En primer lugar, se puede observar que los resultados experimentales para la composición equimásica obtenidos en este trabajo y los publicados en el trabajo [37] muestran un buen acuerdo. Además, también se muestra que los resultados experimentales muestran en general un buen acuerdo con respecto a los determinados mediante la regla de combinación (6.6). Especialmente si se tiene en cuenta que los coeficientes para mezclas binarias empleados en la correlación han sido igualmente calculados mediante los polinomios de aproximación publicados por Gebhardt *et al* [20]. En definitiva, es posible calcular de una manera bastante aproximada los coeficientes Soret para la mezcla ternaria THN-IBB-*n*C_{12} a cualquier concentración, a partir de los valores de concentración de cada componente.

6.4. Conclusiones

Se han determinado las propiedades termofísicas y los coeficientes de termodifusión de 13 mezclas correspondientes a dos sistemas ternarios, mediante la nueva columna LTC.

Con la mezcla THN-IBB-nC$_{12}$ se ha mostrado la comparación entre esta nueva columna y la STC, utilizada anteriormente tanto en la determinación de mezclas binarias como ternarias. Los problemas en el procedimiento experimental que surgían en la columna STC al analizar mezclas ternarias, impulsaron el diseño y construcción de la nueva LTC, que tiene la misma anchura de gap pero prácticamente el doble de altura. Se ha comprobado cómo esta doble altura le otorga una mayor sensibilidad en la determinación de la separación relativa a la altura de la columna, que se traduce en un menor error experimental considerando las cinco tomas a lo largo de la altura de la columna.

Además, se ha desarrollado una regla de combinación que permite determinar los coeficientes de termodifusión de la mezcla ternaria THN-IBB-nC$_{12}$ a cualquier concentración. Unida a los polinomios de aproximación publicados por Gebhardt *et al* [20], es posible reproducir de manera convincente los coeficientes de termodifusión para cualquier concentración de la mezcla ternaria a partir de los valores de concentración.

A su vez, se han determinado los coeficientes de termodifusión de ocho concentraciones de la mezcla ternaria MN-Tol-nC$_{10}$. Para ello, también se han medido la densidad, viscosidad dinámica y coeficiente de expansión térmica, y se han realizado las calibraciones de las mezclas correspondientes. Las correlaciones cuantitativas para predecir los coeficientes de termodifusión en mezclas ternarias han mostrado, en general, un acuerdo aceptable con los resultados experimentales presentados. El mejor acuerdo se ha obtenido con la regla de combinación (6.5) presentada en este trabajo.

En cuanto al coeficiente de difusión molecular, se ha determinado mediante la técnica SST para las cinco concentraciones correspondientes a la mezcla THN-IBB-nC$_{12}$. Además, se ha corroborado la importancia del tiempo de ensayo en el método experimental empleado en este trabajo. Como se ha descrito en el apartado 2.2 de esta memoria, hay que operar en el determinado tiempo intermedio. Es decir, el tiempo ha de ser suficientemente corto como para poder emplear la ecuación basada en la *error function* pero también lo suficientemente largo como para que las perturbaciones que aparecen al cambiar de posición los tubos, no afecten a los resultados.

Por último, se han determinado los coeficientes Soret de las cinco concentraciones analizadas de la mezcla THN-IBB-nC$_{12}$. A día de hoy sólo se ha podido comparar el resultado correspondiente a la mezcla equimásica con los resultados publicados por Gebhardt y Köhler [37], mostrando un buen acuerdo.

Además se ha desarrollado una regla de combinación para determinar los coeficientes Soret muy similar a la propuesta para los coeficientes de termodifusión. Por tanto, de igual forma es posible determinar los coeficientes Soret de la mezcla ternaria a partir de los coeficientes Soret de las mezclas binarias correspondientes, que a su vez se pueden determinar a partir de los polinomios de aproximación publicados por Gebhardt *et al.* [20]. Por tanto, con estas dos aproximaciones es posible determinar los coeficientes Soret de la mezcla ternaria THN-IBB-nC$_{12}$. a cualquier concentración, a partir de los valores de concentración.

7. CONCLUSIONES

**********CASTELLANO**********

En este capítulo se recogen las conclusiones generales de esta tesis doctoral, de acuerdo con los objetivos planteados.

Los coeficientes de termodifusión en mezclas ternarias se han determinado mediante la técnica termogravitacional.

Cabe destacar que se ha desarrollado una nueva metodología para determinar experimentalmente los coeficientes de difusión molecular en mezclas ternarias, mediante la técnica SST. Además, esta metodología ha sido analizada profundamente para corroborar los límites de validez de la misma en función del tiempo de ensayo.

La determinación de los coeficientes de difusión molecular y termodifusión en mezclas ternarias ha permitido a su vez determinar los coeficientes Soret en estas mezclas. Así pues, se han determinado los coeficientes de difusión molecular, termodifusión y Soret de las seis mezclas ternarias correspondientes al proyecto DCMIX1.

Bajo el paraguas del proyecto DCMIX1 se ha llevado a cabo el primer *benchmark* en mezclas ternarias, en el que han participado 6 grupos a escala internacional. En él se han analizado los coeficientes de transporte en la mezcla THN-IBB-nC$_{12}$ a concentración de 0,80-0,10-0,10 y a 25°C, tanto en condiciones terrestres como de microgravedad. Este trabajo supone uno de los mayores avances de la última década en el estudio del fenómeno de la termodifusión en mezclas líquidas. Ha permitido contrastar y validar las técnicas experimentales de cada laboratorio, entre ellas, las técnicas y metodología empleadas en esta tesis. A su vez, se han establecido unos valores para la mezcla analizada que servirán como referencia para futuros trabajos en mezclas ternarias. No obstante, se ha observado que en el caso de la difusión molecular, aún hay problemas sin resolver, por lo que los valores propios de la matriz de difusión han demostrado ser más fiables y robustos al comparar los resultados de las diferentes técnicas.

Además, se han medido los coeficientes de termodifusión de una nueva mezcla ternaria formada por MN-Tol-nC$_{10}$, a ocho concentraciones diferentes.

El análisis de los coeficientes de termodifusión en estas dos mezclas ternarias ha permitido desarrollar una regla de combinación para predecir los coeficientes de termodifusión en mezclas ternarias, a partir de los coeficientes de termodifusión en las mezclas binarias correspondientes.

Por otra parte, en cuanto al estudio de mezclas binarias, se han analizado los coeficientes de termodifusión de 13 sistemas a diferentes concentraciones, haciendo un total de 77 mezclas binarias. Además, se han determinado los coeficientes de difusión molecular y Soret para las concentraciones equimásicas de estos 13 sistemas. A partir de los resultados obtenidos se han analizado las influencias de las propiedades de las mezclas como masa molecular o viscosidad.

Con los resultados experimentales obtenidos para mezclas binarias y ternarias se ha contribuido a completar la base de datos experimentales de la bibliografía, que permitirá continuar profundizando en la compresión y análisis de los fenómenos de transporte.

Los resultados obtenidos a lo largo de esta tesis han sido publicados en revistas indexadas, así como en varios congresos tanto nacionales como internacionales. En los apéndices se pueden encontrar los artículos publicados, así como los trabajos que se

encuentran en preparación. En los siguientes subapartados se detallan las referencias correspondientes.

**********ENGLISH**********

In this chapter are summarized the general conclusions of this doctoral thesis, according to the proposed objectives.

The thermodiffusion coefficients in ternary mixtures have been determined by the thermogravitational technique.

It is worth noting that we have developed a new methodology to experimentally determine the molecular diffusion coefficients in ternary mixtures by the SST technique. In addition, we have deeply analysed this methodology in order to check its validity limits in function of testing time.

The determination of the molecular diffusion and thermodiffusion coefficients in ternary mixtures has enable the determination of the Soret coefficients in these mixtures. Therefore, we have determined the molecular diffusion, thermodiffusion and Soret coefficients of the six ternary mixtures related to the project DCMIX1.

In the framework of the project DCMIX1 we have conducted the first benchmark in ternary mixtures, in which six teams have taken part. In this benchmark work we have analysed the transport coefficients of the mixture THN-IBB-nC$_{12}$ at mass fraction of 0.80-0.10-0.10 and at 25°C, both in microgravity and ground conditions. This work has come as one of the greatest breakthroughs of the last decade in the research of the thermodiffusion phenomenon in liquid mixtures. It has helped to check and validate the experimental techniques of each laboratory, among them, the techniques and methodology employed in the work of this thesis. At the same time, we have established benchmark values for the coefficients of the analysed mixture which will serve as reference for future works about ternary mixtures. However, in the case of the molecular diffusion, we have observed that there are still some uncertainties. Therefore, the eigenvalues of the diffusion matrix have proved to be more reliable and robust to compare the results obtained by different techniques.

In addition, we have measured the thermodiffusion coefficients of a new ternary mixture composed by MN-Tol-nC$_{10}$, at eight different compositions.

The analysis of the thermodiffusion coefficients of these two ternary mixtures has resulted in the development of a new combination rule to predict the thermodiffusion coefficients in ternary mixtures, from the thermodiffusion coefficients of the corresponding binaries.

On the other hand, regarding to the study of binary mixtures, we have analysed the thermodiffusion coefficients of 13 systems at different concentrations, making a total of 77 binary mixtures. Additionally, we have determined the molecular diffusion and Soret coefficients of the 13 systems at mass fraction of 0.50. From the obtained results we have analysed the influences of different properties of the mixture, such as molecular weight or viscosity.

With the results obtained in this work for binary and ternary mixtures we contribute to the experimental database of the literature, which will help to further deepen the understanding and analysis of the transport phenomena.

The results obtained during this doctoral thesis have been published in journals, as well as in several conferences both national and international. The published papers can be found in the appendices of this document. Hereafter the corresponding references are given.

7.1. Published papers

The following papers have been published in journals:

- M. Larrañaga, M.M. Bou-Ali, D. Soler, M. Martinez-Agirre, A. Mialdun, V. Shevtsova, Remarks on the analysis method for determining diffusion coefficient in ternary mixtures, *C. R. Mecanique*, 341, 356-364, **2013**.

- M. Larrañaga, D. A. S. Rees, M.M. Bou-Ali, Determination of the molecular diffusion coefficients in ternary mixtures by the Sliding Symmetric Tubes technique, *J. Chem. Phys.* 140, 054201, **2014**.

- M. Larrañaga, M. M. Bou-Ali, E. Lapeira, C. Santamaria, J.A. Madariaga, Effect of thermophysical properties and morphology of the molecules on thermodiffusion coefficient of binary mixtures, *Microgravity Sci. and Technol.*, 26, 29-35, **2014**.

- D. Alonso de Mezquía, M. Larrañaga, M. M. Bou-Ali, J. A. Madariaga, C. Santamaria, J. K. Platten, Contribution to thermodiffusion coefficient measurements in DCMIX project, *Int. J. Thermal Sci*. 92, 14-16, **2015**.

- M. Larrañaga, M. M. Bou-Ali, D. Alonso de Mezquía, D.A.S. Rees, J. A. Madariaga, C. Santamaria, J. K. Platten, Contribution to the benchmark for ternary mixtures: Determination of Soret coefficients by the thermogravitational and the sliding symmetric tubes techniques, *Eur. Phys. J. E*, 38: 28, **2015**.

- M. M. Bou-Ali, A. Ahadi, D. Alonso de Mezquía, Q. Galand, M. Gebhardt, O. Khlybov, W. Köhler, M. Larrañaga, J.C. Legros, T. Lyubimova, A. Mialdun, I. Ryzhkov, M.Z. Saghir, V. Shevtsova, S. Van Vaerenbergh, Benchmark values for the Soret, thermodiffusion and molecular diffusion coefficients of the ternary mixture tetralin+isobutylbenzene+n-dodecane with 0.8-0.1-0.1 mass fraction, *Eur. Phys. J. E*, 38: 30, **2015**.

- M. Larrañaga, M. M. Bou-Ali, I. Lizarraga, J.A. Madariaga, C. Santamaria, Soret coefficients of the ternary mixture 1,2,3,4-tetrahydronaphtalene +isobutylbenzene +n-dodecane, *J. Chem. Phys*. Accepted, **2015**

In addition, during these years we have taken part in the following works:

- D. Alonso de Mezquia, M.M. Bou-Ali, M. Larrañaga, J.A. Madariaga, C. Santamaria, Determination of Molecular Diffusion Coefficient in n-Alkane Binary Mixtures: Empirical Correlations, *J. Phys. Chem. B*, 116 (9), 2814-2819, **2012**.

- P. Naumann, A. Martin, H. Kriegs, M. Larrañaga, M.M. Bou-Ali and S. Wiegand, Development of a Thermogravitational micro-Column with an Interferometric Contactless Detection System, *J. Phys. Chem. B*, 116(47), 13889-13897, **2012.**

7.1.1. Papers under preparation

The following journal papers are under preparation. In the appendices can be found the abstracts of these works.

- M. Larrañaga, M. M. Bou-Ali, E. Lapeira, I. Lizarraga, J. A. Madariaga, C. Santamaria, Thermodiffusion, molecular diffusion and Soret coefficients of aromatic+n-alkane binary mixtures.

- M. Larrañaga, M. Gebhardt, T. Triller, W. Köhler, J. C. Legros, A. Mialdun, V. Shevtsova, M. M. Bou-Ali, Analysis of the molecular diffusion coefficients in ternary mixtures by three different techniques.
- M. Larrañaga, M. M. Bou-Ali, E. Lapeira, I. Lizarraga, J. A. Madariaga, C. Santamaria, Thermodiffusion coefficient measurements of the ternary mixture 1-Mthylnaphtalene-Toluene-nDecane.

7.2. Conference communications

During this doctoral thesis the following works have been presented in several national and international conferences:

- M. Larrañaga, M.M. Bou-Ali, E. Lapeira, C. J. Santamaria, J.A. Madariaga and J.K. Platten, Thermodiffusion coefficient in toluene-n-alkane binary mixtures, *10th International Meeting on Thermodiffusion (IMT10)*, Bruselas (Bélgica), **2012,** Comunicación oral.

- M. Larrañaga, M.M. Bou-Ali, D. Soler, M. Martinez, A. Mialdun, V. Shevtsova, Remarks on the analysis method for determining the diffusion coefficient in ternary mixtures, *10th International Meeting on Thermodiffusion (IMT10)*, Bruselas (Bélgica), **2012,** Comunicación escrita.

- M. Larrañaga, M.M. Bou-Ali, D. Alonso de Mezquia, E. Lapeira, J.A. Madariaga, C. Santamaria and J.K. Platten, Quantitative correlations for the prediction of the transport coefficients in liquid mixtures, *11eme Congres de Mecanique*, Agadir (Marruecos), **2013,** Comunicación escrita.

- M. Larrañaga, M.M. Bou-Ali, A. Mialdun, V. Shevtsova, The impact of the different fitting methods on the experimental determination of the molecular diffusion coefficients in ternary mixtures, *11eme Congres de Mecanique*, Agadir (Marruecos), **2013,** Comunicación oral.

- M. Larrañaga, M.M. Bou-Ali, E. Lapeira, J.A. Madariaga, C. Santamaria, Effect of thermophysical properties and morphology of the molecules in thermodiffusion coefficient of alkane-alkane and alkane-aromatic binary mixtures, *ELGRA Biennial Symposium and General Assembly*, Ciudad Vaticano (Vaticano), **2013,** Comunicación oral.

- M. Larrañaga, D. A. S. Rees, M. M. Bou-Ali, D. Alonso de Mezquía, J. K. Platten, J. A. Madariaga, C. Santamaria, Thermodiffusion, molecular diffusion and Soret coefficients for DCMIX1 ternary mixtures, *11th International Meeting on Thermodiffusion (IMT11)*, Bayona (Francia), **2014**, Comunicación oral.

- M. M. Bou-Ali, A. Ahadi, D. Alonso de Mezquía, Q. Galand, M. Gebhardt, O. Khlybov, W. Köhler, M. Larrañaga, J.C. Legros, T. Lyubimova, A. Mialdun, I. Ryzhkov, M.Z. Saghir, V. Shevtsova, S. Van Vaerenbergh, Benchmark DCMIX1: Soret, thermodiffusion and molecular diffusion coefficients of the ternary mixture THN-IBB-nC$_{12}$, *11th International Meeting on Thermodiffusion (IMT11)*, Bayona (Francia), **2014**, Comunicación oral y escrita.

- M. Larrañaga, D. Alonso de Mezquía, M. M. Bou-Ali, J. A. Madariaga, C. Santamaria, Quantitative correlations for the predictions of thermodiffusion, molecular diffusion and soret coefficients in n-alkane binary mixtures, *11th International Meeting on Thermodiffusion (IMT11)*, Bayona (Francia), **2014**, Comunicación escrita.

- M. Larrañaga, M. M. Bou-Ali, D. A. S. Rees, A. Martin, Determination of Soret coefficients in binary mixtures by a flow cell, *11th International Meeting on Thermodiffusion (IMT11)*, Bayona (Francia), **2014**, Comunicación escrita.

- M. Larrañaga, M. M. Bou-Ali, E. Lapeira, J. A. Madariaga, C. Santamaria, Determination of thermodiffusion, molecular diffusion and Soret coefficients in binary mixtures, *11th International Meeting on Thermodiffusion (IMT11)*, Bayona (Francia), **2014**, Comunicación escrita.

- M. Larrañaga, E. Lapeira, M. M. Bou-Ali, J. A. Madariaga, C. Santamaría, Nahasketa ternarioen propietate termofisikoak eta garraio propietateak, *II. Materialen Zientzia eta Teknologiako kongresua*, Donostia (Guipúzcoa), **2014**, Comunicación oral.

- M. Larrañaga, E. Lapeira, M. M. Bou-Ali, J. A. Madariaga, C. Santamaría, Determination of thermodiffusion, molecular diffusion and Soret coefficients in ternary mixtures, *20th European Conference on Thermophysical properties (ECTP20)*, Oporto (Portugal), **2014**, Comunicación oral.

- M. Larrañaga, M. M. Bou-Ali, D. Alonso de Mezquía, D. A. S. Rees, J. A. Madariaga, C. Santamaría, Determinación de los coeficientes de transporte en mezclas ternarias, *XIV Encuentro Inter-Bienal del Grupo Especializado de Termodinámica (GET-TERMO2014)*, Baiona (Pontevedra), **2014**, Comunicación oral.

- M. Larrañaga, M. M. Bou-Ali, D. Alonso de Mezquía, E. Lapeira, J. A. Madariaga, C. Santamaría, Correlaciones cuantitativas para la predicción de los coeficientes de transporte en mezclas líquidas, *XIV Encuentro Inter-Bienal del Grupo Especializado de Termodinámica (GET-TERMO2014)*, Baiona (Pontevedra), **2014**, Comunicación escrita.

- M. M. Bou-Ali, A. Ahadi, D. Alonso de Mezquía, Q. Galand, M. Gebhardt, O. Khlybov, W. Köhler, M. Larrañaga, J.C. Legros, T. Lyubimova, A. Mialdun, I. Ryzhkov, M.Z. Saghir, V. Shevtsova, S. Van Vaerenbergh, Benchmark DCMIX1: determinación de los coeficientes de termodifusión, difusión molecular y Soret de la mezcla ternaria THN-IBB-*n*C_{12}, *XIV Encuentro Inter-Bienal del Grupo Especializado de Termodinámica (GET-TERMO2014)*, Baiona (Pontevedra), **2014**, Comunicación escrita.

- M. Larrañaga, M. M. Bou-Ali, J. A. Madariaga, C. Santamaría, Determination of the transport coefficients of the DCMIX1 ternary mixtures, *12éme Congres de Mecanique*, Casablanca (Marruecos), **2015**, Comunicación oral.

- M. M. Bou-Ali, A. Ahadi, D. Alonso de Mezquía, Q. Galand, M. Gebhardt, O. Khlybov, W. Köhler, M. Larrañaga, J.C. Legros, T. Lyubimova, A. Mialdun, I. Ryzhkov, M.Z. Saghir, V. Shevtsova, S. Van Vaerenbergh, Benchmark DCMIX1: Soret, thermodiffusion and molecular diffusion coefficients of the ternary mixture THN-IBB-*n*C_{12}, *12éme Congres de Mecanique*, Casablanca (Marruecos), **2015**, Comunicación oral.

- M. Larrañaga, E. Lapeira, M. M. Bou-Ali, J. A. Madariaga, C. Santamaría, Garraio propietateak nahasketa hirutarretan, *IkerGazte 2015*, Durango (Bizkaia), **2015**, Comunicación oral.

- M. Larrañaga, M. Gebhardt, T. Triller, W. Köhler, J. C. Legros, A. Mialdun, V. Shevtsova, M. M. Bou-Ali, Analysis of the molecular diffusion coefficients in ternary mixtures by three different techniques, *ELGRA Biennial Symposium and General Assembly*, Corfu (Grecia), **2015**, Comunicación escrita.

- M. M. Bou-Ali, A. Ahadi, D. Alonso de Mezquía, Q. Galand, M. Gebhardt, O. Khlybov, W. Köhler, M. Larrañaga, J.C. Legros, T. Lyubimova, A. Mialdun, I. Ryzhkov, M.Z. Saghir, V. Shevtsova, S. Van Vaerenbergh, Benchmark DCMIX1: Soret, thermodiffusion and molecular diffusion coefficients of the ternary mixture THN-IBB-*n*C_{12}, *ELGRA Biennial Symposium and General Assembly*, Corfu (Grecia), **2015**, Comunicación escrita.

Additionally, it has been taken part in the following conference communications:

- D. Alonso de Mezquia, M.M. Bou-Ali, J.A. Madariaga, C. Santamaria, P. Urteaga and M. Larrañaga, Determination of Thermal Diffusion and Molecular Diffusion Coefficients in n-Alkane Binary Mixtures, *European Conference on Thermophysical Properties (ECTP19)*, Tesalónica (Grecia), **2011**, Comunicación oral.

- D. Alonso de Mezquia, M.M. Bou-Ali, J.A. Madariaga, C. Santamaría, P. Urteaga and M. Larrañaga, Thermodiffusion and Molecular Diffusion Coefficient values for n-Alkane binary mixtures at 25°C, *Joint European Thermodynamics Conference (JECT11)*, Cheminitz (Alemania), **2011**, Comunicación escrita.

- D. Alonso de Mezquia, M.M. Bou-Ali, M. Larrañaga, J.A. Madariaga, C. Santamaria, Experimental and Analytical Determination of Molecular Diffusion Coefficient in alkane binary mixtures at 50 wt%, *6th International Conference on Thermal Engineering: Theory and Applications (ICTEA 2012)*, Estambul (Turquía), **2012**, Comunicación oral.

- P. Naumann, H. Kriegs, S. Wiegand, A. Martin, M. Larrañaga, and M.M. Bou-Ali, Development of an interferometric contactless detection system for a micro-thermogravitational column with transparent windows, *10th International Meeting on Thermodiffusion (IMT10)*, Bruselas (Bélgica), **2012,** Comunicación oral.

- D. Alonso de Mezquia, M.M. Bou-Ali, M. Larrañaga, J.A. Madariaga, C. Santamaria, Determination of the Molecular Diffusion coefficient in binary n-Alkane Mixtures, *10th International Meeting on Thermodiffusion (IMT10)*, Bruselas (Bélgica), **2012,** Comunicación escrita.

7.3. Patents

K. del Teso, M. M. Bou-Ali, A. Martin, M. Larrañaga, Fantoma de sangre, nº patente: 201430037.

7.4. Prizes

First prize to the best poster for the work: *Quantitative correlations for the prediction of the transport coefficients in liquid mixtures* in the 11eme Congres de Mecanique, Agadir (Marruecos), 2013.

7.5. Stays at foreign centres

Three-month stay in the Mechanical Engineering department of the University of Bath (United Kingdom), to work in collaboration with Prof. D. Andrew S. Rees in the

determination of the molecular diffusion coefficients of ternary mixtures (01-03-2013 a 30-05-2013).

8. REFERENCIAS BIBLIOGRÁFICAS

[1] F. Capuano, L. Paduano, G. D'Errico, G. Mangiapia and R. Sartorio. Diffusion in ternary aqueous systems containing human serum albumin and precipitants of different classes. *Phis. Chem. Chem. Phys.*, 13 (8), 3319-3327, 2011.

[2] G. R. Longhurst. Soret effect and its implications for fusion reactors. *J. Nucl. Mater.*, 131 (1), 61-69, 1985.

[3] A. E. Fick. Üeber diffusion. *Annalen del Physik*, 94, 59-86, 1855.

[4] C. Ludwig. Diffusion zwischen ungleich erwärmten orten gleich zusammengesetzter lösungen. *Sitz. Ber. Akad. Wiss. Wien Math.-Naturw. Kl.*, 20, 539, 1856.

[5] C. Soret. Au point de vue de sa concentration une dissolution saline primitevement homogéne don't deux parties sont portées a des temperatures différentes. *Archives des Sciences Physiques et Naturelles de Geneve*, 2, 48-61, 1879.

[6] C. Soret. Influence de la tempèrature sur la distribution des sels dans leurs solutions. *C R Academie Scientifique*, 91 (5), 289-290, 1880.

[7] K. Clusius and G. Dickel. Kurze originalmitteilungen (new process for separation of gas mixtures and isotopes). *Naturwissenschaften*, 26, 546, 1938.

[8] A. Martin, M. M. Bou-Ali, H. Barrutia and D. Alonso de Mezquia. Microfluidic separation process by the soret effect in biological fluids. *C. R. Mecanique*, 339, 342-348, 2011.

[9] D. E. Rosner. Thermal (soret) diffusion effects on interfacial mass transport rate. *PCH Physicochemical Hydrodynamics*, 1, 159-185, 1978.

[10] J. Schott. Thermal diffusion and magmatic differentiation: a new look and an old problem. *Bulletin Mineralogie*, 106, 247, 1983.

[11] R. Piazza and A. Parola. Thermophoresis in colloidal suspensions. *J. Phys.: Condens. Matter*, 20 (15), 153102, 2008.

[12] S. Duhr, S. Arduini and D. Braun. Thermophoresis of dna determined by microfluidic fluorescence. *Eur. Phys. J. E*, 15 (3): 277-286, 2004.

[13] D. Braun and A. Libchaber. Thermal force approach to molecular evolution. *Institute of Physics Publishing*, Phys. Biol. 1, 1-8, 2004.

[14] P. Baaske, F. M. Weinert, S. Duhr, K. H. Lemke, M. J. Russell and D. Braun. Extreme accumulation of nucleorides in simulated hydrothermal pore systems. *Proc. Natl. Acad. Sci. USA*, 104 (22), 9346-9351, 2007.

[15] F. Montel. Importance de la Thermodiffusion en exploration et production pétroliéres. *Entropie*, 184, 86-93, 1994.

[16] K. Ghorayeb, A. Firoozabadi and T. Anraku. Interpretation of the unusual fluid distribution in the yufutsu gas-condensate field. *SPE Journal*, 8 (2), 114-123, 2003.

[17] M. Touzet, G. Galliero, V. Lazzeri, M. Z. Saghir, F. Montel and J. C. Legros. Thermodiffusion: from microgravity experiments to the initial state of petroleum reservoirs. *C. R. Mecanique*, 339, 318-323, 2011.

[18] F. Montel, J. Bickert, A. Legisquet and G. Galliero. Initial state of petroleum reservoirs: A comprehensive approach. *J. Petrol. Sci. Eng.*, 58, 391-402, 2007.

[19] P. Blanco, P. Polyakov, M. M. Bou-Ali and S. Wiegand. Thermal diffusion and molecular diffusion values for some alkane mixtures: a comparison between thermogravitational column and thermal diffusion forced Rayleigh scattering. *J. Phys. Chem. B*, 112 (28), 8340-8345, 2008.

[20] M. Gebhardt, W. Köhler, A. Mialdun, V. Yasnou and V. Shevtsova. Diffusion, thermal diffusion and soret coefficients and optical contrast factors of the binary mixtures of dodecane, isobutylbenzene and 1,2,3,4-tetrahydronaphthalene. *J. Chem. Phys.*, 138, 114503, 2013.

[21] A. Leahy-Dios and A. Firoozabadi. Molecular and thermal diffusion coefficients of alkane-alkane and alkane-aromatic binary mixtures: Effect of shape and size of molecules. *J. Phys. Chem. B*, 111 (1), 191-198, 2007.

[22] D. Alonso de Mezquia, M. M. Bou-Ali, M. Larrañaga, J. A. Madariaga and C. Santamaria. Determination of molecular diffusion coefficient in n-alkane binary mixtures: Empirical correlations. *J. Phys. Chem. B*, 116 (9), 2814-2819, 2012.

[23] A. A. Alizadeh and W. A. Wakeham. Mutual diffusion coefficients for binary mixtures of normal alkanes. *Int. J. Thermophys.*, 3 (4), 307-323, 1982.

[24] P. Blanco, M. M. Bou-Ali, J. K. Platten, P. Urteaga, J. A. Madariaga and C. Santamaria. Determination of thermal diffusion coefficient in equimolar n-alkane mixtures: empirical correlations. *J. Chem. Phys.*, 129 (17), 174504, 2008.

[25] A. Abbasi, M. Z. Saghir and M. Kawaji. A new proposed approach to estimate the Thermodiffusion coefficients for linear chain hydrocarbon binary mixtures. *J. Chem. Phys.*, 131 (1), 014502, 2009.

[26] G. Galliero, B. Duguay, J. P. Caltagirone and F. Montel. Thermal diffusion sensitivity to the molecular parameters of a binary equimolar mixture, a non-equilibrium molecular dynamics approach. *Fluid Phase Equilibr.*, 208, 171-188, 2003.

[27] S. Hartmann, G. Wittko, W. Köhler, K. I. Morozov, K. Albers and G. Sadowski. Thermophobicity of liquids: heats of transport in mixtures as pure component properties. *Phys. Rev. Let.*, 109 (6), 065901, 2012.

[28] S. Hartmann, G. Wittko, F. Schock, W. Gross, F. Lindner, W. Köhler and K. I. Morozov. Thermophobicity of liquids: Heats of transport in mixtures as pure component poperties: The case of arbitrary concentration. *J. Chem. Phys.*, 141 (13), 134503, 2014.

[29] J. A. Madariaga, C. Santamaria, M. M. Bou-Ali, P. Urteaga and D. Alonso de Mezquia. Measurement of thermodiffusion coefficient in n-alkane binary mixtures: composition dependence. *J. Phys. Chem. B*, 114 (20), 6937-6942, 2010.

[30] D. Alonso de Mezquia, M. M. Bou-Ali, J. A. Madariaga and C. Santamaria. Mass effect on the soret coefficient in n-alkane mixtures. *J. Chem. Phys.,* 140 (8), 084503, 2014.

[31] A. Leahy-Dios, L. Zhuo and A. Firoozabadi. New thermal diffusion coefficient measurements for hydrocarbon binary mixtures: viscosity and composition dependency. *J. Phys. Chem. B*, 112, 6442-6447, 2008.

[32] K. Ghorayeb and A. Firoozabadi. Molecular, pressure and thermal diffusion in nonideal multicomponent mixtures. *AlChE*, 46, 883-891, 2000.

[33] L. J. T. M. Kempers. A thermodynamic theory of the soret effect in a multicomponent liquid. *J. Chem. Phys.*, 90 (11), 6541-6548, 1989.

[34] P. Blanco, M. M. Bou-Ali, J. K. Platten, D. Alonso de Mezquia, J. A. Madariaga and C. Santamaria. Thermodiffusion coefficients of binary and ternary hydrocarbon mixtures. *J. Chem. Phys.*, 132 (11), 114506, 2010.

[35] A. Leahy-Dios, M. M. Bou-Ali, J. K. Platten and A. Firoozabadi. Measurements of molecular and thermal diffusion coefficients in ternary mixtures. *J. Chem. Phys.*, 122 (23), 234502, 2005.

[36] M. Larrañaga, D. A. S. Rees and M. M. Bou-Ali. Determination of the molecular diffusion coefficients in ternary mixtures by the sliding symmetric tubes technique. *J. Chem. Phys.*, 140 (5), 054201, 2014.

[37] M. Gebhardt and W. Köhler. What can be learned from optical two-color diffusion and Thermodiffusion experiments on ternary fluid mixtures? *J. Chem. Phys.*, 142 (8), 084506, 2015.

[38] A. Mialdun, V. Sechenyh, J. C. Legros, J. M. Ortiz de Zarate and V. Shevtsova. Investigation of fickian diffusion in the ternary mixture of 1,2,3,4-tetrahydronaphthalene, isobutylbenzene and dodecane. *J. Chem. Phys.*, 139 (19), 104903, 2013.

[39] C. I.A.V. Santos, M. A. Esteso, V. M. M. Lobo and A. C. F. Ribeiro. Multicomponent diffusion in (cyclodextrin-drug + salt + water) systems: 2-Hydroxypropyl–Cyclodextrin (HP-CD) + KCl + theophylline + water, and -cyclodextrin (CD) + KCl + theophylline + water. *J. Chem. Thermodyn.*, 59, 139-143, 2013.

[40] Q. Galand, S. Van Vaerenbergh and F. Montel. Measurement of diffusion coefficients in binary and ternary mixtures by the open ended capillary technique. *Energy and Fuels*, 22 (2), 770-774, 2008.

[41] X. Liu, A. Martin-Calvo, E. McGarrity, S. K. Schnell, S. Calero, J. M. Simon, D. Bedeaux, S. Kjelstrup, A. Bardow and T. J. H. Vlugt. Fick diffusion coefficients in ternary liquid systems from equilibrium molecular dynamics simulations. *Industrial and Engineering Chemistry Research*, 51 (30), 10247-10258, 2012.

[42] H. A. Tello Alonso, A. C. Rubiolo and S. E. Zorrilla. Prediction of the diffusion coefficients in multicomponent liquid refrigerant solutions. *J. Food Eng.*, 109, 490-495, 2012.

[43] M. M. Bou-Ali, A. Ahadi, D. Alonso de Mezquia, Q. Galand, M. Gebhardt, O. Khlybov, W. Köhler, M. Larrañaga, J.C. Legros, T. Lyubimova, A. Mialdun, I. Ryzhkov, M.Z. Saghir, V. Shevtsova and S. Van Vaerenbergh. Benchmark values for the Soret, thermodiffusion and molecular diffusion coefficients of the ternary mixture tetralin+isobutylbenzene+n-dodecane with 0.8-0.1-0.1 mass fraction. *Eur. Phys. J. E*, 38: 30, 2015.

[44] *El País*. On line [Consulta: 29 octubre 2014]. http://internacional.elpais.com /internacional/2014/10/29/actualidad/1414538303_720082.html.

[45] J. K. Platten, M. M. Bou-Ali and J. F. Dutrieux. Enhanced molecular separation in inclined thermogravitational columns. *J. Phys. Chem. B*, 107, 11763-11767, 2002.

[47] M. M. Bou-Ali, O. Ecenarro, J. A. Madariaga, C. Santamaria and J. J. Valencia. Thermogravitational measurement of the soret coefficient of liquid mixtures. *J. Phys-Condens. Mat.*, 10, 3321-3331, 1998.

[48] W. H. Furry, R. Clark Jones and L. Onsager. On the theory of isotope separation by thermal diffusion. *Phys. Rev. E*, 55, 1083-1095, 1939.

[49] S. D. Majumdar. The theory of the separation of isotopes by thermal diffusion. *Phys. Rev. E*, 81, 844-848, 1951.

[50] J. J. Valencia, M. M. Bou-Ali, O. Ecenarro, J. A. Madariaga and C. Santamaria. Validity limits of the fjo thermogravitational column theory. In W. Köhler and S. Wiegand, editors, *Thermal Nonequilibrium Phenomena in Fluid Mixtures*, 233-249. Springer Berlin/Heidelberg, 2002.

[51] J. A. Madariaga, C. Santamaria, H. Barrutia, M. M. Bou-Ali, O. Ecenarro and J. J. Valencia. Validity limits of the fjo thermogravitational column theory: experimental and numerical analysis. *C. R. Mecanique*, 339, 292-296, 2011.

[52] A. Mialdun, V. Yasnou, V. Shevtsova, A. Königer, W. Köhler, D. Alonso de Mezquia and M. M. Bou-Ali. A comprehensive study of diffusion, thermodiffusion and soret coefficients of wáter-isopropanol mixtures. *J. Chem. Phys.*, 136, 244512, 2012.

[53] M. Larrañaga, M. M. Bou-Ali, D. Alonso de Mezquia, D.A.S. Rees, J. A. Madariaga, C. Santamaria and J. K. Platten. Contribution to the benchmark for ternary mixtures: Determination of Soret coefficients by the thermogravitational and the sliding symmetric tubes techniques. *Eur. Phys. J. E*, 38: 28, 2015.

[54] J. K. Platten, M. M. Bou-Ali, P. Costeséque, J. F. Dutrieux, W. Köhler, C. Leppla, S. Wiegand and G. Wittko. Benmchmark values for the soret, thermal diffusion and diffusion coefficients of three binary organic liquid mixtures. *Philos. Mag*, 83, 1965-1971, 2003.

[55] M. M. Bou-Ali and J. K. Platten. Metrology of the thermodiffusion coefficients in a ternary system. *J. Non-Equil. Thermody.*, 30 (4), 385-399, 2005.

[56] D. Alonso de Mezquia, M. Larrañaga, M. M. Bou-Ali, J. A. Madariaga, C. Santamaria and J. K. Platten. Contribution to thermodiffusion coefficient measurements in DCMIX project. *Int. J. Thermal Sci*., 92, 14-16, 2015.

[57] M. Larrañaga, M.M. Bou-Ali, D. Soler, M. Martinez-Agirre, A. Mialdun and V. Shevtsova. Remarks on the analysis method for determining diffusion coefficient in ternary mixtures. *C. R. Mecanique*, 341, 356-364, 2013.

[58] H. S. Carslaw and J. C. Jaeger. *Conduction of Heat in Solids*, page 50. Clarendon Press, Oxford, 1959.

[59] A. Mialdun and V. Shevtsova. Communication: New approach for analysis of thermodiffusion coefficients in ternary mixrures. *J. Chem. Phys.*, 138, 161102, 2013.

[60] M. J. Sawicka and J. A. Soroka. Application of the calibration surfaces method in quantitative analysis of water-ethanol-methanol mixture. *Cent. Eur. J. Chem.*, 11 (7), 1239—1247, 2013.

[61] J. K. G. Dhont, S. Wiegand, S. Duhr and D. Braun. Thermodiffusion of charged colloids: single-particle diffusion. *Langmuir*, 23 (4), 1674-1683, 2007.

[62] M. Klein and S. Wiegand. The Soret effect of mono-, di- and tri-glycols in ethanol. *Phys. Chem. Chem. Phys.*, 13 (15), 7090-7094, 2011.

[63] S. Wiegand, H. Ning and H. Kriegs. Thermal diffusion forced Rayleigh scattering setup optimized for aqueous mixtures. *J. Phys. Chem. B*, 111 (51), 14169-14174, 2007.

[64] S. Pan, M. Z. Saghir, M. Kawaji, C. G. Jiang and Y. Yan. Theoretical approach to evaluate thermodiffusion in aqueous alkanol solutions. *J. Chem. Phys.*, 126 (1), 014502, 2007.

[65] S. Hartmann, W. Köhler and K. I. Morozov. The isotope soret effect in molecular liquids: a quantum effect at room temperatures. *Soft Matter*, 8 (5), 1355-1360, 2012.

[66] S. Villain-Guillot and A. Würger. Thermal diffusion in a binary liquid due to rectified molecular fluctuations. *Phys. Rev. E*, 83 (3), 030501, 2011.

[67] D. Alonso de Mezquia, Z. Wang, E. Lapeira, M. Klein, S. Wiegand and M. M. Bou-Ali. Thermodiffusion, molecular diffusion and soret coefficient of binary and ternary mixtures of n-hexane, n-dodecane and toluene. *Eur. Phys. J. E.*, 37: 11, 2014.

[68] P. Polyakov and S. Wiegand. Experimental study of the thermal diffusion behavior of mixtures consisting of simple and chain-like molecules using thermal diffusion forced Rayleigh scattering method. In M. M. Bou-Ali and J. K. Platten, editors, *Thermodiffusion: basics and applications (IMT7)*, 399-407, Mondragon 2006.

[69] J. Rauch and W. Köhler. On the molar mass dependence of the thermal diffusion coefficient of polymer solutions. *Macromolecules*, 38 (9), 3571-3573, 2005.

[70] D. Stadelmaier and W. Köhler. Thermal diffusion of dilute polymer solutions: the role of chain flexibility and the effective segment size. *Macromolecules*, 42 (22), 9147-9152, 2009.

[71] A. Würger. Thermophoresis in colloidal suspensions driven by marangoni forces. *Phys. Rev. Let.*, 98 (13), 2007.

[72] A. Würger. Molecular-weight dependent thermal diffusion in dilute polymer solutions. *Phys. Rev. Let.*, 102 (7), 2009.

[73] M. Zhang and F. Müller-Plathe. The soret effect in dilute polymer solutions: Influence of chain length, chain stiffness, and solvent quality. *J. Chem. Phys.*, 125 (12), 124903, 2006.

[74] A. Königer, H. Wunderlich and W. Köhler. Measurement of diffusion and thermal diffusion in ternary fluid mixtures using a two-color optical beam deflection technique. *J. Chem. Phys.*, 132, 174506, 2010.

[75] A. Ahadi, S. Van Vaerenbergh and M. Z. Saghir. Measurement of the soret coefficients for a ternary hydrocarbon mixture in low gravity environment. *J. Chem. Phys.*, 138, 204201, 2013.

[76] M. Gebhardt and W. Köhler. Contribution to the benchmark for ternary mixtures: measurement of the soret and thermodiffusion coefficients of tetralin+isobutylbenzene+n-dodecane at a composition of (0.8/0.1/0.1) mass fractions by two-color optical beam delfection. *Eur. Phys. J. E*, 38: 24, 2015.

[77] A. Mialdun, J.-C. Legros, V. Yasnou, V. Sechenyh and V. Shevtsova. Contribution to the benchmark for ternary mixtures: measurement of the soret, diffusion and thermodiffusion coefficients in the ternary mixture THN/IBB/nC_{12} with 0.8/0.1/0.1 mass fractions in ground and orbital laboratories. *Eur. Phys. J. E*, 38: 27, 2015.

[78] Q. Galand and S. Van Vaerenbergh. Contribution to the benchmark for ternary mixtures: measurement of diffusion and soret coefficients of ternary system tetrahydronaphthalene+isobutylbenzene+n-dodecane with mass fractions 80-10-10 at 25°C. *Eur. Phys. J. E*, 38: 26, 2015.

[79] A. Ahadi and M.Z. Saghir. Contribution to the benchmark for ternary mixtures: transient analysis in microgravity conditions. *Eur. Phys. J. E*, 38: 25, 2015.

[80] A. Khlybov, I.I. Ryzhkov and T. P. Lyubimova, Contribution to the benchmark for ternary mixtures: measurement of diffusion and soret coefficients in 1,2,3,4-tetrahydronaphthalene, isobutylbenzene and dodecane onboard the ISS. *Eur. Phys. J. E*, 38: 29, 2015.

[81] A. Mialdun and V. Shevtsova. Measurement of the soret and diffusion coefficients for benchmark binary mixtures by means of digital interferometry. *J. Chem. Phys.*, 134, 044524, 2011.

[82] V. Sechenyh, J. C. Legros and V. Shevtsova. Optical properties of binary and ternary liquid mixtures containing tetralin, isobutylbenzene and dodecane. *J. Chem Thermod.*, 62, 64-68, 2013.

[83] S. Mazzoni, V. Shevtsova, A. Mialdun, D. Melnikov, Y. Gaponenko, T Liubimova and M. Z. Saghir. Vibrating liquids in space. *Europhysics news*, 41 (6), 14-16, 2010.

[84] A. Mialdun, C. Minetti, Y. Gaponenko, V. Shevtsova and F. Dubois. Analysis of the thermal performance of SODI instrument for DCMIX configuration. *Microgravity Sci. Technol.*, 25, 83-94, 2013.

[85] M. Larrañaga, M. M. Bou-Ali, I. Lizarraga, J.A. Madariaga and C. Santamaria. Soret coefficients of the ternary mixture 1,2,3,4-tetrahydronaphthalene +isobutylbenzene +n-dodecane, *J. Chem. Phys.*, 143, Accepted, 2015.

[86] J. P. Larre, J. K. Platten and G. Chavepeyer. Soret effects in ternary systems heated from below. *Int. J. Heat Mass Transfer*, 40 (3), 545-555, 1997.

[87] A. Mialdun, V. Yasnou and V. Shevtsova. Measurement of isothermal diffusion coefficients in ternary mixtures using counter flow diffusion cell. *C. R. Mecanique*, 341, 462-468, 2013.

APÉNDICES

A. Determination of molecular diffusion coefficient in n-alkane binary mixtures: empirical correlations.

THE JOURNAL OF PHYSICAL CHEMISTRY B

Article

pubs.acs.org/JPCB

Determination of Molecular Diffusion Coefficient in *n*-Alkane Binary Mixtures: Empirical Correlations

D. Alonso De Mezquia,[†] M. Mounir Bou-Ali,*[,†] M. Larrañaga,[†] J. A. Madariaga,[‡] and C. Santamaría[‡]

[†]Mechanical and Manufacturing Department, Engineering Faculty, Mondragon Unibertsitatea, Loramendi 4 Apdo. 23, 20500 Mondragon, Spain

[‡]Department of Applied Physics II, University of Basque Country, Apdo. 644, 48080 Bilbao, Spain

ABSTRACT: In this work we have measured the molecular diffusion coefficient of the *n*-alkane binary series nC_i-nC_6, nC_i-nC_{10}, and nC_i-nC_{12} at 298 K and 1 atm and a mass fraction of 0.5 by using the so-called sliding symmetric tubes technique. The results show that the diffusion coefficient at this concentration is proportional to the inverse viscosity of the mixture. In addition, we have also measured the diffusion coefficient of the systems nC_{12}-nC_6, nC_{12}-nC_7, and nC_{12}-nC_8 as a function of concentration. From the data obtained, it is shown that the diffusion coefficient of the n-alkane binary mixtures at any concentration can be calculated from the molecular weight of the components and the dynamic viscosity of the corresponding mixture at 50% mass fraction.

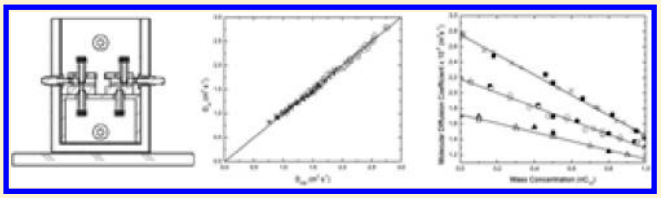

I. INTRODUCTION

A concentration gradient within a mixture results in a mass transport of its components from the zones of a higher concentration to those of a lower concentration. This phenomenon, known as molecular diffusion, has generated great interest since its discovery in the nineteenth century when, first in gases and later on in liquids, it was studied with the aim of understanding the atom's behavior.

It was in 1855 when Fick[1] established the first quantitative relation for the molecular diffusion phenomenon, known nowadays as Fick's law. Since then, interest in this transport property has increased, discovering a great number of fields in which the molecular diffusion coefficient has a huge influence, such as medicine or phisiology.[2]

As a consequence of this interest, there have appeared a great number of apparatus designed for the determination of the molecular diffusion coefficient. There are, for example, techniques that employ the principle of Taylor dispersion[3] or other techniques such as open ended capillary (OEC)[4] or thermal diffusion forced Rayleigh scattering (TDFRS)[5] developed for the study of the molecular diffusion coefficient in liquid mixtures. The different techniques used for the determination of the molecular diffusion coefficient can be found elsewhere.[2,6−9]

Some of these techniques, such as the OEC, have already been satisfactorily used in several studies earlier.[4,10] With the aim of correcting some of the limitations of this technique, the sliding symmetric tubes (SST) technique has been developed. This new technique takes out perturbations that appeared in the OEC technique, especially in aspects such as evaporations or manipulation of the apparatus, reducing, at the same time, the liquid quantity needed to carry out a measurement. In this work a complete description of the SST technique will be done, including the improvements obtained compared with the OEC technique, and the validation process used to validate this new technique.

On the other hand, nowadays, there exist several models developed for the estimation of the molecular diffusion coefficient.[11,12] In order to check the validity of these models, it is necessary to compare the theoretical values obtained with the experimental ones. On some occasions, the procedure that checks these models requires a huge number of experimental values, which, at the same time, requires a great experimental effort. In this work, a new correlation, which is capable of predicting the molecular diffusion coefficient in normal alkane binary mixtures, is presented. The use of this correlation may help in the development of new theories or could be useful in verifying the existing ones.

This article is organized as follows: In section II, the SST technique is presented, and a complete description of the experimental installation and its analytical resolution is done. In this section, the process used to validate the technique is also included. In section III, the results obtained in the measurement of the molecular diffusion coefficient in several normal alkane mixtures are presented, to continue with the discussion and the development of new correlations for the prediction of the molecular diffusion coefficient (D_{12}) in normal alkane mixtures. In section IV, the conclusions obtained are based on the study carried out in this work.

II. SST TECHNIQUE

A. SST Technique Description. The SST technique consists of several sets of two identical vertical tubes. Each set has two positions: "faced tubes" (Figure 1a), in which the

Received: October 13, 2011
Revised: January 12, 2012
Published: January 20, 2012

dx.doi.org/10.1021/jp209838m | *J. Phys. Chem. B* 2012, 116, 2814−2819

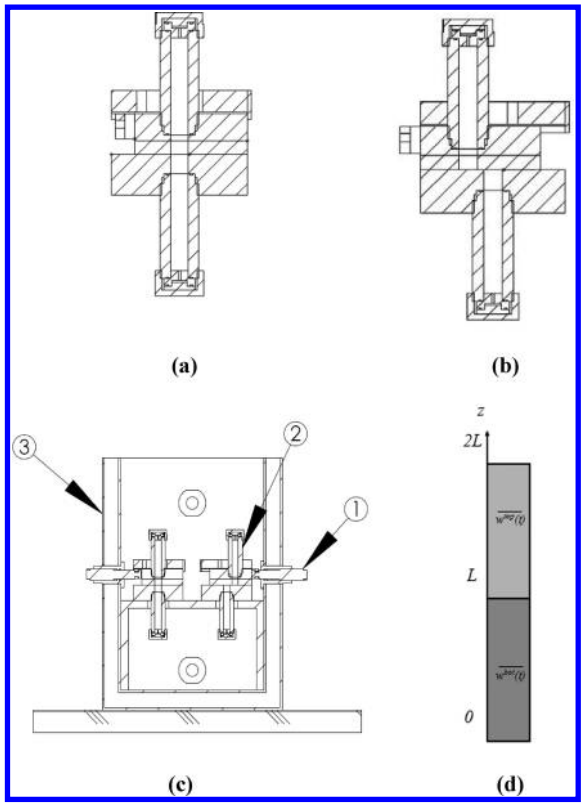

Figure 1. (a) Scheme of the sets of the SST technique on "faced tubes" configuration. (b) Scheme of the sets of the SST technique on "separated tubes" configuration. (c) Scheme of the SST sets (2) inside the water bath (3) in both their configurations: "faced tubes" position (left) and "separated tubes" position (right) and the screws (1) used to make the tubes slide. (d) Scheme of SST technique. $\overline{w^{top}}(t)$ and $\overline{w^{bot}}(t)$ are the mass fractions of component i in the top and bottom recipient, respectively.

mass transfer between both tubes is permitted, and "separated tubes" (Figure 1b). In this position, the content of the tubes is isolated. At the beginning of an experiment, the studied mixture with a slight difference of mass fraction of its components is introduced in each of the tubes. The mixture with a higher mass fraction of the denser component is introduced in the bottom tube, and the upper tube is filled with the mixture with a less concentration of the denser component so that the convective instability is avoided.

The SST technique introduces some improvements compared with the OEC technique on which it is based. For example, since the mixture is contained inside closed tubes, evaporations are eliminated, which gives the advantage of using this technique with volatile mixtures without reducing its efficiency. Another fact that has been improved has been the mixture quantity needed to carry out an essay. The OEC technique requires a huge quantity of mixture (400 cm^3 approximately). This quantity is highly reduced in the SST technique, as it only needs around 100 cm^3 of mixture in each experiment. One more improvement has been done related to the setup handling. In the OEC technique, whenever it is needed to analyze the experiment evolution, it is necessary to manipulate the setup. This fact affects the results of the experiment, which are highly influenced by the experimenter's expertise. However, in the SST technique, thanks to its design, all of these influences have been eliminated.

B. Analytical Solution. Assuming Fick's second law in one dimension (z: vertical direction), the following can be written:

$$\frac{\partial w}{\partial t} = D_{12}\frac{\partial^2 w}{\partial z^2} \tag{1}$$

where D_{12} is the molecular diffusion coefficient, which is considered constant for small mass fraction (w) changes. The formulation can be implemented as can be seen in Figure 1d considering the following boundary conditions:

$$w(z, 0) = \begin{cases} w^{bot} & 0 \le z < L \\ w^{top} & L < z \le 2L \end{cases} \tag{2}$$

$$\frac{\partial w(z, t)}{\partial t} = 0 \text{ at } z = 0,\ 2L \text{ and } t > 0 \tag{3}$$

where w^{bot} and w^{top} are the mass fractions of the bottom and upper tube, respectively, and L is the tube length. Solving eqs 1−3, we have

$$w(z, t) = \frac{w^{top} + w^{bot}}{2} - \frac{2(w^{top} - w^{bot})}{\pi} \sum_{n=0}^{\infty} \frac{(-1)^n e^{\phi} \cos\left(\frac{2n+1}{2}\pi\frac{z}{L}\right)}{2n+1} \tag{4}$$

where $\varphi = -((2n + 1)/2)^2(\pi/L)^2 D_{12}t)$. Therefore, at the middle point between both the tubes, we have

$$w(L, t) = \frac{w^{top} + w^{bot}}{2} \tag{5}$$

The change of mass fraction in each tube in function of time can be obtained using the following equations:

$$\overline{w^{top}(t)} = \frac{1}{L}\int_{L}^{2L} w(z, t)\, dz = \frac{w^{top} + w^{bot}}{2} + \frac{4(w^{top} - w^{bot})}{\pi^2} \sum_{n=0}^{\infty} \frac{e^{\phi}}{(2n+1)^2} \tag{6}$$

$$\overline{w^{bot}(t)} = \frac{1}{L}\int_{0}^{L} w(z, t)\, dz = \frac{w^{top} + w^{bot}}{2} - \frac{4(w^{top} - w^{bot})}{\pi^2} \sum_{n=0}^{\infty} \frac{e^{\phi}}{(2n+1)^2} \tag{7}$$

where $\overline{w^{top}}$ and $\overline{w^{bot}}$ are the mean mass fractions in the upper and bottom tube, respectively. The solution of the inverse problem posed by eqs 6 and 7 to obtain the molecular diffusion coefficient (D_{12}) is solved by the least-squares method using *Matlab* software. Solving expressions 6 and 7 when $n = 0$, an initial guess of the molecular diffusion coefficient D_{12} is obtained. This initial value is then used for obtaining the D_{12} coefficient iterating the eqs 10 times and using terms on the summation up to $n = 1000$. The more experimental points used, the more accurate the estimated value of the molecular

dx.doi.org/10.1021/jp209838m | J. Phys. Chem. B 2012, 116, 2814−2819

diffusion coefficient. Typically up to 11 points are used in each experiment. This tactic allows the use of experimental points from the very beginning of the experiment, which does not happen in other similar techniques that require some initial experimental time before beginning the analysis of experimental data.[3,8]

C. Equipment and Procedure. We have used the SST equipment designed and constructed in Mondragon Goi Eskola Politeknikoa and described elsewhere.[13−15] The two tubes with which each set of the device is provided have the same dimensions (length of 60 ± 0.01 mm and diameter of 9 ± 0.01 mm).

The experimental procedure starts with the preparation of two mixtures of 50 cm^3 with a mass fraction difference (±4−6 wt %) so that the mean concentration of both mixtures corresponds with the one of the mixture to be studied. The tubes of several sets (typically 10) in their "separated tubes" position are filled with the mixtures, next introducing the sets in the water bath (Figure 1d) so that the mixture obtains the working temperature (T = 298 K). The temperature of the water in this bath is controlled by a thermostatic bath, which has a temperature control of 0.1 K. In order to make sure that the studied mixture is in the working temperature, the sets in their "separated tubes" configuration are introduced in the bath no less than 48 h before the beginning of the experiment.

Once the mixture has reached the working temperature, all the sets in the bath are changed to their "faced tubes" configuration, starting the diffusion process in this manner. With the aim of making this transition, the bath has some external screws (Figure 1c) that make sliding of the tubes possible in a controlled way.

In determined time intervals, the position of the sets is changed one by one using the screws back to the "separated tubes position." The time intervals in which the set's positions are changed are between 6, 12, or 24 h, depending on the speed at which sensitive concentration changes occur in the tubes. After stopping the mass transfer process between the tubes, the sets are extracted from the bath, and the concentration in each of them is analyzed. This allows obtaining the concentration change in the tubes in function of time.

The SST technique was validated[13,14] using five binary mixtures: the three binary mixtures composed of pairwise combinations of tetrahydronaphtalene, normal dodecane, and isobutylbenzene at 298 K and 50 wt % of each component used in a benchmark test[16] to compare various experimental techniques and the binary mixtures: water−ethanol at 298 K and 60.88 wt % water and toluene-n hexane at 298 K and 51.67 wt % toluene, which have been widely studied in the literature.[17−20] The experimental test was repeated at least twice. The reproducibility of the experimental results of the SST technique is within 3% of deviation. In general, the differences with published data are, on an average, below 3%.

The determination of the mass fraction of a mixture is essential to determine molecular diffusion coefficients. In binary mixtures, the mass fraction is related to one physical property of the mixture (the density in this experimental study). An Anton Paar DMA 5000 vibrating quartz U-tube densimeter having an accuracy of $\pm 5 \times 10^{-6}$ g/cm^3 is used to determine the density of the mixture. Since we are working with small mass fraction differences, it can be supposed that

$$\rho = aw_i \tag{8}$$

where ρ is the density of the mixture, w_i is the mass fraction of component i in the binary mixture, and a is a constant parameter. To determine the constant parameter, a, five mixtures of known concentration are prepared by weighing and then, the density of each mixture is measured. Thus, we

Table 1. Values of Viscosity (μ) and Molecular Diffusion Coefficient (D_{12}) for the nC_6-nC_i, nC_{10}-nC_i, and nC_{12}-nC_i Series at 50 wt % and 298 K[a]

system	μ mPa s	D_{12} 10^{-9} m^2 s^{-1}	$(\overline{D_{12}})_{cc}10^{-9}$ m^2 s^{-1}	δ (%)
		set 1: nC_i-nC_6		
nC_{10}-nC_6	0.4704	2.53	2.51	0.8
nC_{11}-nC_6	0.5312	2.27	2.22	2.1
nC_{12}-nC_6	0.5581	2.09	2.11	−1.2
nC_{13}-nC_6	0.6103	1.96	1.93	1.4
nC_{14}-nC_6	0.6556	1.76	1.80	−2.3
nC_{15}-nC_6	0.6938	1.62	1.68	−3.7
nC_{16}-nC_6	0.7446	1.54	1.58	−2.6
nC_{17}-nC_6	0.7737	1.46	1.52	−4.1
nC_{18}-nC_6	0.8265	1.39	1.43	−2.9
		set 1: nC_i-nC_{10}		
nC_5-nC_{10}	0.3993	3.03	2.96	2.3
nC_6-nC_{10}	0.4704	2.54	2.51	1.2
nC_7-nC_{10}	0.5633	2.09	2.09	−0.0
nC_{14}-nC_{10}	1.2929	0.913	0.915	−0.2
$nC1_5$-nC_{10}	1.3972	0.819	0.845	−3.1
nC_{16}-nC_{10}	1.5150	0.756	0.779	−3.0
nC_{17}-nC_{10}	1.6337	0.702	0.722	−2.8
nC_{18}-nC_{10}	1.7780	0.656	0.664	−1.2
		set 1: nC_i-nC_{12}		
nC_5-nC_{12}	0.4551	2.57	2.59	−0.9
nC_6-nC_{12}	0.5581	2.09	2.11	−1.2
nC_7-nC_{12}	0.6823	1.70	1.73	−1.7
nC_8-nC_{12}	0.8071	1.49	1.46	1.9
nC_9-nC_{12}	0.9452	1.24	1.25	−0.8
nC_{16}-nC_{12}	2.0335	0.589	0.580	1.5
nC_{17}-nC_{12}	2.2323	0.547	0.529	3.2
nC_{18}-nC_{12}	2.3945	0.503	0.493	2.0

[a] $(\overline{D_{12}})_{cc}$ is the diffusion coefficient calculated from eq 9, and δ is the relative deviation between D_{12} and D_{cc}.

Table 2. Diffusion Coefficient (D_{12}) in the nC_{12}-nC_6, nC_{12}-nC_7, and nC_{12}-nC_8 Systems for Different Mass Fractions of nC_{12} (w_1) at 298 K[a]

mixture	w_1	D_{12} 10^{-9} m^2 s^{-1}	$(D_{12})_{cc}$ 10^{-9} m^2 s^{-1}	δ (%)
nC_{12}-nC_6	0.18	2.48	2.55	−3.0
	0.46	2.24	2.17	3.1
	0.50	2.13	2.11	0.7
	0.66	1.93	1.88	2.2
	0.82	1.72	1.67	2.9
	0.95	1.51	1.49	1.0
nC_{12}-nC_7	0.16	2.09	2.04	2.6
	0.42	1.84	1.80	2.2
	0.50	1.70	1.73	−1.7
	0.63	1.64	1.61	1.6
	0.80	1.48	1.46	1.2
	0.94	1.37	1.33	2.9
nC_{12}-nC_8	0.10	1.70	1.69	0.6
	0.40	1.56	1.52	2.5
	0.50	1.49	1.46	2.0
	0.80	1.25	1.28	−2.4

[a] $(D_{12})_{cc}$ is the diffusion coefficient calculated from eq 19, and δ is the relative deviation between calculated and measured diffusion coefficient.

dx.doi.org/10.1021/jp209838m | J. Phys. Chem. B 2012, 116, 2814−2819

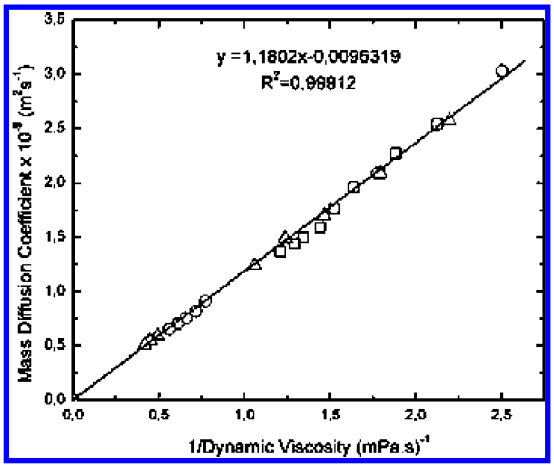

Figure 2. Diffusion coefficient as a function of the inverse of the dynamic viscosity for the systems nC_6-nC_i (□), nC_{10}-nC_i (○), and nC_{12}-nC_i (Δ), at 50 wt % and 298 K.

determined the mass fraction with a deviation around wt % ± 0.01.

The dynamic viscosity (μ) of the studied mixtures has been measured with an Anton Paar AMVn falling ball Micro-viscosimeter with reproducibility better than 0.1%. All the measurements were done at 298 K.

III. RESULTS AND DISCUSSION

A. Studied Mixtures. All of the products used in this study were purchased from Merck with a purity better than 99%. The studied mixtures have been prepared by weight using a Gram VXI-310 digital scale with a precision of 0.001 g. and introducing first the less volatile component and then the corresponding amount of the second component; the mixture is finally shaken to ensure homogeneity. After the preparation, the density of the mixture was measured to confirm that the composition deduced from the calibration curve coincides with the prepared one. This was always the case.

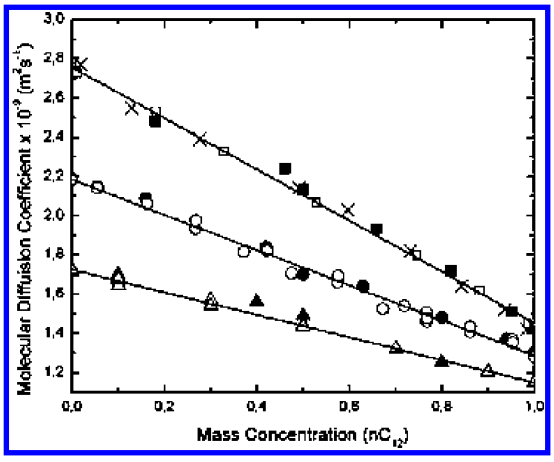

Figure 3. Diffusion coefficient as a function of the mass fraction of the denser component (nC_{12}) for the mixtures, nC_{12}-nC_6, nC_{12}-nC_7, and nC_{12}-nC_8 at 298 K. ■, nC_{12}-nC_6 this work; □, nC_{12}-nC_6 ref 22; ×, nC_{12}-nC_6 ref 24; ●, nC_{12}-nC_7 this work; ○, nC_{12}-nC_7 ref 23; ▲, nC_{12}-nC_8 this work; Δ, nC_{12}-nC_8 ref 21. The continuous lines represent a linear fit to the data.

In this study, 25 mixtures at 50 wt % have been prepared corresponding to the *n*-alkane series

$$nC_6 - nC_i \; i = 10, 11, 12, 13, 14, 15, 16, 17, 18$$

$$nC_{10} - nC_i \; i = 5, 6, 7, 14, 15, 16, 17, 18$$

Table 3. Values of the Limiting Diffusion Coefficient (D_1^0 and D_2^0) Taken from Refs 3 and 23[a]

system	D_1^0	D_2^0	D_1^0/D_2^0	M_1/M_2	δ(%)
nC_{16}-nC_6	2.21	0.85	2.60	2.62	0.7
nC_{12}-nC_6	2.74	1.42	1.93	1.97	2.5
nC_{12}-nC_7	2.19	1.30	1.69	1.70	0.6
nC_{12}-nC_8	1.71	1.15	1.49	1.49	0.0
nC_{16}-nC_{12}	0.67	0.49	1.36	1.33	−2.2
nC_7-nC_8	2.80[b]	2.43[b]	1.15	1.14	−1.7

[a] M_1 and M_2 are the molecular masses of the components, and δ is the relative deviation between the ratios D_1^0/D_2^0 and M_1/M_2. [b] Interpolated from ref 3.

$$nC_{12} - nC_i \; i = 5, 6, 7, 8, 9, 16, 17, 18$$

The measured values at 298 K for dynamic viscosity (μ) and mass diffusion coefficients for these mixtures are summarized in Table 1.

In addition, this study has been completed measuring the molecular diffusion coefficient of the systems nC_{12}-nC_6, nC_{12}-nC_7, and nC_{12}-nC_8 at 298 K at different concentrations. For this end, the following mixtures were prepared:

$$nC_{12} - nC_6 \; w_1 = 0.18, 0.46, 0.50, 0.66, 0.82, 0.95.$$

$$nC_{12} - nC_7 \; w_1 = 0.16, 0.42, 0.50, 0.63, 0.80, 0.94.$$

$$nC_{12} - nC_8 \; w_1 = 0.10, 0.40, 0.50, 0.80.$$

where w_1 is the mass fraction of dodecane.

In Table 2, the measured values of the diffusion coefficients of these systems at the concentrations considered are shown.

These systems were chosen, as hydrocarbon mixtures are quite regular in their properties. It was hoped that at least some general and useful empirical relationship would be found.

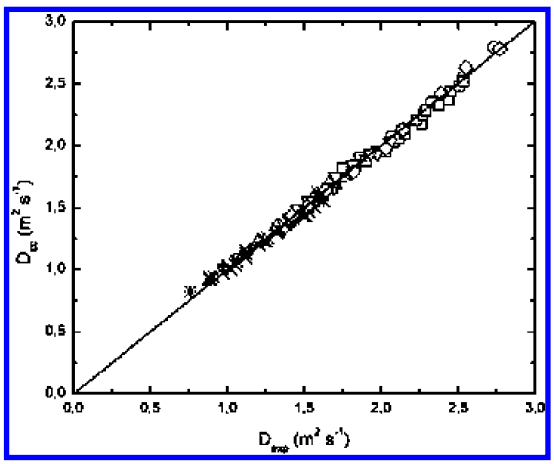

Figure 4. Experimental diffusion coefficient versus calculated from eq 19 diffusion coefficient. ×, nC_{10}-nC_7 ref 23; ○, nC_{12}-nC_6 ref 22; ◊, nC_{12}-nC_6 ref 24; ∇, nC_{12}-nC_7 ref 23; Δ, nC_{12}-nC_8 ref 21; +, nC_{14}-nC_7 ref 23; ×, nC_{14}-nC_8 ref 23; *, nC_{16}-nC_7 ref 22.

dx.doi.org/10.1021/jp209838m | J. Phys. Chem. B 2012, 116, 2814–2819

B. Correlation between Diffusion and Viscosity. In what follows, we shall analyze the relation between the diffusion coefficient and the dynamic viscosity for mixtures at a mass fraction equal to 50 wt % (equimass mixtures).

In Figure 2, the values of D_{12} as a function of the inverse of dynamic viscosity for the equimass mixtures in Table 1 are represented. As can be seen, the data fit well to a straight line, which passes through the origin and, thus, the following linear relation can be written:

$$\overline{D_{12}} = k\frac{1}{\bar{\mu}} \tag{9}$$

where $\overline{D_{12}}$ and $\bar{\mu}$ are the diffusion coefficient and the dynamic viscosity at $w_1 = 0.5$, respectively. The proportionality constant k is $k = 1.18 \times 10^{-12}$ kg m/s^2.

In Table 1, the values of $\overline{D_{12}}$ calculated using eq 9 for each mixture are also shown and in the last column, the relative deviations with the measured values are given. As can be seen, these deviations are smaller than 3% in all the cases. Thus, we can conclude that the product $\overline{D_{12}}\mu$ for equimass mixtures is a universal constant for *n*-alkane mixtures.

D. Dependence of the Diffusion Coefficient with Composition. According to Darken equation for thermodynamic ideal mixtures, the diffusion coefficient should be a linear function of the molar fraction. However, as was suggested in an earlier work by van Geet and Adamson,[21] the diffusion coefficient in n-alkane mixtures is linear with the mass fraction but not with the mole fraction. To closely analyze the diffusion composition dependence we have measured the diffusion coefficient as a function of composition for the three systems: nC_{12}-nC_6, nC_{12}-nC_7, and nC_{12}-nC_8. The results obtained appear in Table 2. In Figure 3, these data as a function of the mass fraction of the heavier component, w_1, are plotted. As can be seen, the ordinary diffusion coefficient is for each system a linear function of the mass fraction and decreases with the concentration of the heavier component. In this figure, the diffusion data in the literature for the systems considered[21−24] are also shown. These data coincide with our measurements within the experimental error.

Thus, the dependence of D_{12} with composition can be written as follows:

$$D_{12} = w_2 D_1^0 + w_1 D_2^0 \tag{10}$$

where w_1 and w_2 are the mass fraction of heavier and lighter components, respectively, and D_1^0 and D_2^0 are the limiting diffusion coefficients defined by

$$D_1^0 = \lim_{w_1 \to 0} D_{12} \tag{11}$$

$$D_2^0 = \lim_{w_2 \to 0} D_{12} \tag{12}$$

In Table 3, the values of D_1^0 and D_2^0 for some selected mixtures reported in the literature[3,23] covering a large range of mass ratio for liquid n-alkanes are given. As can be seen in this table, the ratio D_1^0/D_2^0 is always close to the ratio of the molecular masses M_1/M_2 of the two alkanes involved. Thus, we have

$$\frac{D_1^0}{D_2^0} = \frac{M_1}{M_2} \tag{13}$$

Introducing eq 13 in eq 10, one obtains

$$D_{12} = D_1^0\left(w_2 + \frac{M_2}{M_1}w_1\right) \tag{14}$$

For $w_1 = w_2 = 0.5$, the corresponding diffusion coefficient $\overline{D_{12}}$ will be

$$\overline{D_{12}} = \frac{D_1^0}{2}\left(\frac{M_1 + M_2}{M_1}\right) \tag{15}$$

and then, eq 14 in terms of $\overline{D_{12}}$ can be written as

$$D_{12} = 2\overline{D_{12}}\left(\frac{M_1 w_2 + M_2 w_1}{M_1 + M_2}\right) \tag{16}$$

In particular, the infinite dilution values D_1^0 and D_2^0 will be

$$D_1^0 = 2\overline{D_{12}}\frac{M_1}{M_1 + M_2} \tag{17}$$

$$D_2^0 = 2\overline{D_{12}}\frac{M_2}{M_1 + M_2} \tag{18}$$

Finally, using eq 9, the diffusion coefficient can be written as

$$D_{12} = \frac{2k}{\bar{\mu}}\left(\frac{M_1 w_2 + M_2 w_1}{M_1 + M_2}\right) \tag{19}$$

where $k = 1.18 \times 10^{-12}$ kg m/s^2.

Equation 16 allows determining D_{12} from $\overline{D_{12}}$ measurements, which, in turn, can be calculated using eq 9 from viscosity measurements.

To confirm the validity of this correlation, we have determined the values of D_{12} from eq 19 for the mixtures given in Table 2. As shown in the last column of this table, the relative deviations between these values and the experimental ones are inferior to the experimental error.

As an additional test of eq 19, we have taken the experimental D_{12} values as a function of concentration reported in the literature[21−24] for different *n*-alkane systems. In Figure 4, the values of D_{12} calculated using eq 19 are plotted against the corresponding experimental ones. As seen here, all data lie on a straight line through the origin with slope unity.

From what has been just mentioned, we can conclude that the diffusion coefficient of *n*-alkane mixtures at any concentration can be calculated from the data of dynamic viscosity for equimass mixtures.

IV. CONCLUSIONS

In this work, the diffusion coefficient of several *n*-alkane mixtures at 50 wt % has been measured by using the SST technique. From the results obtained, it is shown that the product of the diffusion coefficient and the dynamic viscosity for these mixtures is a universal constant independent of the alkane involved.

In addition, the diffusion coefficient of the systems nC_{12}-nC_6, nC_{12}-nC_7, and nC_{12}-nC_8 in the whole concentration range has also been measured. We have obtained for each system a linear correlation between the diffusion coefficient and the mass fraction. This correlation allows determining the diffusion coefficient at any concentration from the molecular weight of the components of a mixture and the dynamic viscosity of the mixture at 50 wt %.

dx.doi.org/10.1021/jp209838m | J. Phys. Chem. B 2012, 116, 2814−2819

AUTHOR INFORMATION

Corresponding Author

*E-mail: mbouali@mondragon.edu.

Notes

The authors declare no competing financial interest.

ACKNOWLEDGMENTS

This article presents results that were partly obtained in the framework of the following projects: GOVSORET3 (PI2011-22), MIBIO, and Research Groups (IT557-10) of Basque Government and DCMIX from the European Space Agency.

REFERENCES

(1) Fick, A. *Poggendorff's Ann. Phys.* **1855**, *94*, 59.
(2) Cussler, E. *Diffusion Mass Transfer in Fluid Systems*; Cambridge Univesity Press: New York, 1997.
(3) Alizadeh, A. A.; Wakeham, W. A. *Int. J. Themophys.* **1982**, *3* (4), 307.
(4) Dutrieux, J.; Platten, J. K.; Chavepeyer, G.; Bou-Ali, M. M. *J. Phys. Chem. B* **2002**, *106*, 6104.
(5) Wiegand, S.; Köhler, W. *Thermal Nonequilib. Phenom. Fluid Mixt.*; Springer: Berlin, 2002; pp 36−43.
(6) Taylor, R.; Krishna, R. *Multicomponent mass transfer*; John Wiley & Sons Inc.: New York, 1993.
(7) Cussler, E. *Multicomponent diffusion*; Elsevier Scientific Publishing Company: Amsterdam, 1976.
(8) Rutten, P. W. M. *Diffusion in liquids*; Delft University Press: Delft, 1992.
(9) Tyrrell, J. V. Harris, K. R. *Diffusion in liquids*; Butterworth & Co., Ltd.: London, 1984.
(10) Leahy-Dios, A.; Bou-Ali, M. M.; Platten, J. K.; Firoozabadi, A. *J. Chem. Phys.* **2005**, *122*, 234502.
(11) Ghorayeb, K.; Firoozabadi, A. *AIChE J.* **2000**, *46*, 883−891.
(12) Polyakov, P.; Müller-Plathe, F.; Wiegand, S. *J. Phys. Chem. B* **2008**, *112*, 14999.
(13) Blanco P.; Bou-Ali M. M.; Urteaga P.; Alonso de Mezquia D.; Platten J. K. Sliding Symmetric Tubes: new technique for the molecular diffusion coefficients determination of liquid mixtures. 18th European Conference on Thermophysical Properties, Pau, France, 2008.
(14) Alonso de Mezquia D.; Blanco, P.; Bou-Ali M. M.; Zebib A. New Technique for Measuring the Molecular Diffusion Coefficients of Binary Liquid Mixtures. *European Thermodynamics Seminar EUROTHERM* 84, Namur, Belgium, **2009**.
(15) Blanco P., Bou-Ali M. M., Urteaga P.; *Tubos Simétricos Deslizantes*, Patente P200700132/2, 2008.
(16) Platten, J. K.; Bou-Ali, M. M.; Costesèque, P.; Dutrieux, J.; Köhler, W.; Leppla, C.; Wiegand, S.; Wittko, G. *Philos. Mag.* **2003**, *83*, 1965.
(17) Leahy-Dios, A.; Firoozabadi, A. *J. Phys. Chem. B* **2007**, *111*, 191.
(18) Zhang, K. J.; Briggs, M. E.; Gammon, R. W.; Sengers, J. V. *J. Chem. Phys.* **1996**, *104*, 6881.
(19) Kolodner, P.; Williams, H.; Moe, C. *J. Chem. Phys.* **1988**, *88*, 6512.
(20) Köhler, W.; Müller, B. *J. Chem. Phys.* **1995**, *103*, 4367.
(21) Van Geet, L. A.; Adamson, W. A. *J. Phys. Chem.* **1964**, *68* (2), 238.
(22) Bidlack, D. L.; Anderson, D. K. *J. Phys. Chem.* **1964**, *68*, 3790.
(23) Lo, H. Y. *Chem. Eng. Data Ser.* **1974**, *19* (3), 236−241.
(24) Shieh, J. J. C.; Lyons, P. A. *J. Phys. Chem.* **1969**, *73*, 3258.

B. Development of a thermogravitational micro-column with an interferometric contactless detection system.

THE JOURNAL OF PHYSICAL CHEMISTRY B

Article

pubs.acs.org/JPCB

Development of a Thermogravitational Microcolumn with an Interferometric Contactless Detection System

Philipp Naumann,[†] Alain Martin,[‡] Hartmut Kriegs,[†] Miren Larrañaga,[‡] M. Mounir Bou-Ali,*[,‡] and Simone Wiegand*[,†]

[†]Research Center Juelich, ICS-3 Soft Condensed Matter, 52425 Jülich, Germany

[‡]MGEP Mondragon Goi Eskola Politeknikoa, Mechanical and Manufacturing Department, Loramendi 4, Apdo. 23, 20500, Mondragon, Spain

ABSTRACT: We present a new type of thermogravitational (TG) column, a so-called TG microcolumn with transparent windows and a very small sample volume of less than 50 μL. The TG microcolumn has a planar geometry with a thickness of 0.523 ± 0.004 mm, a height of 30 mm, and a width of 3 mm. The concentration difference between two points at different heights is measured with an interferometer using active phase control. From the concentration difference we can determine the thermal diffusion coefficient, D_T, using the refractive index variation with concentration, which has to be determined independently. We studied the three binary mixtures of dodecane, isobutylbenzene, and 1,2,3,4-tetrahydronaphthalene with a concentration of 50 wt % at a temperature of 298 K. The thermal diffusion coefficients agree within a few percent with the proposed benchmark values. In addition we investigated also the binary mixture toluene/*n*-hexane and compare the results with literature values. For the investigated mixtures the typical measurement times were between 30 min and 2 h with an applied temperature difference of ΔT = 6 K.

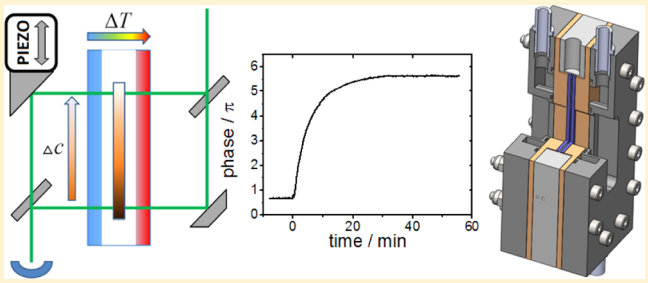

INTRODUCTION

One classical method to study the thermal diffusion or thermodiffusion behavior of binary and multicomponent mixtures is the use of a thermogravitational column (TG).[1] Here, a vertical concentration profile develops due to a combination of thermal diffusion and convection. By combining these two effects, the separation ratio increases compared to a method only relying on the thermal diffusion process.[2] To make a precise measurement possible, the experiment needs to be designed carefully to avoid turbulence. The basic principle was first introduced by Clusius and Dickel[3] and has been evolved into different types of columns. Several designs of TG columns, such as annular TGs[1] and vertical parallelepipedic columns with velocity amplitude determination by laser Doppler velocimetry[4] have been successfully validated in a benchmark with other groups and methods. Nowadays, in conventional TGs a fairly large sample volume of 25 mL and more is required,[5] and small samples of the mixture, typically 1.5 mL, are extracted at different heights from the column after the steady state is reached.[6] These samples are analyzed to determine the composition and thus the separation ratio. For ternary mixtures, two additional properties should be determined (such as density and refractive index) in order to deduce the thermal diffusion coefficients.[7,8] With classical TGs an investigation of expensive substances such as biological systems is often not possible due to the relatively large sample volume which is required to measure the refractive index and density from extracted samples with sufficient accuracy. Therefore, we developed a TG microcolumn with a contactless optical detection system, which works as Mach−Zehnder interferometer. The sample volume is less than 50 μL, so that the investigation of expensive substances or substances which cannot be obtained in large quantities is feasible. Another advantage of the method is the continuous analysis of the concentration profile by measuring the phase difference between two different heights. The possibility to determine the gap width of the microcolumn experimentally once it is mounted is one of the big advantages of our new microcolumn, because the precise knowledge of the width is crucial as the determined thermal diffusion coefficient is proportional to the fourth power of the gap width (eq 5) when calculated from the concentration difference. By use of our optical method, D_T can directly be determined from the phase difference $\Delta\phi$ instead of the measured concentration differences as in conventional TG setups. In the resulting working equation for D_T, the exponent of the gap width reduces to three (eq 6). Therefore, we are less dependent on the precision of fabrication. To validate the new setup, we investigated three binary mixtures of dodecane (DD), isobutylbenzene (IBB), and 1,2,3,4-tetrahydronaphthalene (THN) for a concentration of 50 wt % at a mean temperature of 298 K, which had been used in a benchmark.[9−11] Beside the benchmark systems we investigated also the mixture toluene

Received: June 14, 2012
Revised: November 5, 2012
Published: November 6, 2012

   dx.doi.org/10.1021/jp3098473 | *J. Phys. Chem. B* 2012, 116, 13889−13897

(TOL)/*n*-hexane (HEX) at 298 K and 50 wt %. This organic mixture has been studied by various groups[12−14] with convective and convective-free methods. In the following we discuss the design, construction, and operation of the microcolumn and the interferometer plus its stability. In the appendix we look into some technical details such as the instant when the temperature gradient is applied and the interferometer is disturbed by temperature inhomogeneities within and close to the column.

EXPERIMENTAL SETUP

Materials. We investigated the three binary mixtures consisting of DD (Aldrich, purity 99%), IBB (Aldrich, purity 99%), and THN (Aldrich, purity 99%) at a mean temperature of 298 K. Additionally, we studied also the binary mixture toluene (Aldrich, purity 99%) and *n*-hexane (Aldrich, purity 99%). All chemicals were used without further purification. The investigated mixtures contained 50 wt % of each component. Each sample has been investigated at least five times.

Design and Construction of the TG Microcolumn. The TG microcolumn is composed of two sapphire windows, which are transparent in the visible range of light and have a high thermal conductivity of 34 W/mK at room temperature.[15] The transparency makes it possible to check the cell by eye for defects such as bubbles or dirt. To avoid a distortion of the phase front the material has been cut in the *c* plane (0001). As a thermally insulating gap material we used an advanced polymer material, polyetheretherketone (PEEK), with a very low thermal conductivity of 0.25W/mK,[16] with good chemical resistance and a very low thermal expansion coefficient (50×10^{-6} K^{-1}).[17] Figure 1 shows a sketch of the cell. It consists of

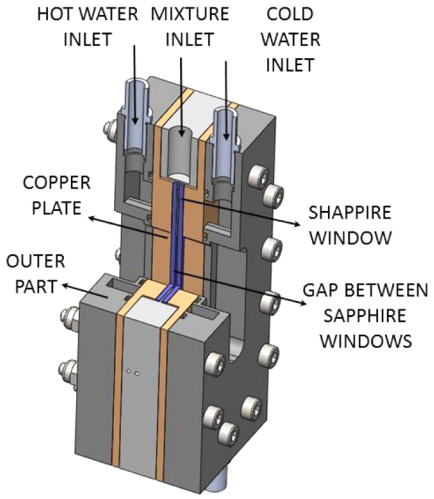

Figure 1. A sketch of the composed microcolumn with a cut in the upper part.

two outer parts made of stainless steel with channels for the thermostated water. For better temperature homogeneity two copper plates in good thermal contact with the two sapphire windows are inserted.

The prepared solutions were slowly inserted from below into the TG microcolumn through two bores in the PEEK part by means of a syringe carefully avoiding bubbles. Once the cell was filled, it was closed by Teflon stoppers to avoid evaporation of the mixture.

On each side a thin channel with a length of 14.5 mm and a width of 250 μm is used to fill the gap. These inlets form dead volumes, which influence the concentration difference between the top and the bottom of the gravitational column and will be discussed in the Numerical Simulation section. The dimensions of the TG microcolumn have been mainly determined by the limits of validity of the Furry−Jones−Onsager (FJO) theory,[18] the limitations on the machining process and experimental conditions such as a sufficient separation ratio and equilibration times in the order of several hours for the systems under investigation.[19] These considerations led to a gap width L_x = 500 μm, a cell height L_{total} = 30 mm, and a width of L_y = 3 mm, so that the aspect ratio is L_{total}/L_x = 60.

Design and Construction of the Interferometer. Figure 2 shows a sketch of the interferometer built around the TG

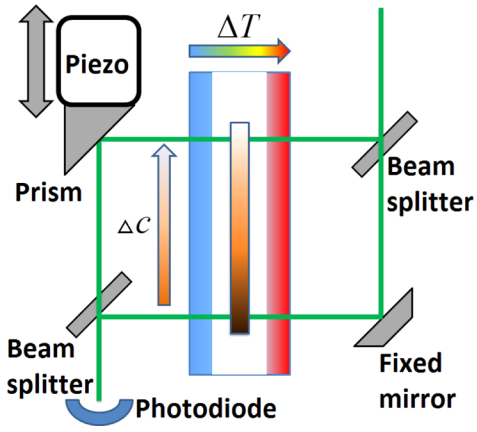

Figure 2. Schematic sketch of the interferometer probing the concentration difference at two different heights of the TG microcolumn with a horizontal temperature gradient. The concentration difference results in a phase shift $\Delta\phi$ of the intensity signal determined by a 2π scan of the prism mounted on the piezo stack.

microcolumn. The microcolumn is mounted inside the interferometer which is built up vertically, splitting the source beam in two parallel beams which probe the TG microcolumn at different heights. The positioning of the cell and the beams is done in a way that one beam passes at the lower end of the window and the other at the upper end. Typically the vertical distance of the two beams is adjusted to 22 mm. To measure at other height differences the vertical position of one of the probing beams can be shifted by moving the two opposing optical elements up- or downward. A He−Ne laser (Melles Griot) with a nominal power of 1 mW and a beam width of 1 mm, operating at 543 nm, is used as a beam source. The typical power at the photodiode (Hamamatsu S2386−8K, active diameter 5.8 mm) is 0.25 mW. Thermostated water from two thermostats (Lauda RE-306) flows through two stainless steel plates mounted at the two sides of the TG microcolumn. To achieve homogeneous starting conditions and to determine the initial phase, the water of both thermostats is mixed and both sides are kept at the same temperature. At time t_0 the temperature gradient is applied by separating the flow from both thermostats.

We use a mirror mounted on a piezo stack (PI P-840-10) to control the phase position while measuring. The piezo is ramped with a step rate of 10 kHz so that we determine the phase from a full 2π scan 2 times per second. This will yield precise knowledge of the initial and final phase positions,

dx.doi.org/10.1021/jp3098473 | J. Phys. Chem. B 2012, 116, 13889−13897

making the determination of the absolute phase shift more exact than measuring only the intensity. The piezo and the recording of the phase shifts (π) are controlled by a computer equipped with an interface card (NI PCI-6014).

The beam width of 1 mm is quite broad compared to the distance between the two probing beams, and the question is whether this will influence the measurements. We can do the following *Gedankenexperiment* by splitting artifically an arbitrary narrow laser beam in one center beam and two *edge beams*, one below and one above the center beam. The vertical concentration profile in the cell is linear, so that the phases of the *edge beams* are shifted by the same amount but in different directions. The resulting *interfering beams* show equal phase shifts stemming from the center and the edges. The relative large area of the photodiode averages over the *beams* recording the same phase as the *center beam* with a slightly lower contrast. Because of the fact that we determine the concentration change by measuring the phase difference, the influence on the measurement should be small as long as the concentration profile is linear over the beam width. In our case the concentration profile is even linear over the entire cell height so there is no influence on the measured phase.

Interferometric Measurement. In an interferometer the intensity varies when the relative phase between the two beams changes. In a simple analysis the phase change can be measured by counting the number of minima and maxima of the varying intensity. To achieve a higher resolution than π the current intensity can be compared to the intensity extrema. This simple method relies on the intensity stability. Therefore, we added an active phase control to our interferometer to achieve a higher precision and reliability. We change the optical path length of one of the beams with a mirror mounted on a piezo and record the modulated intensity (c.f. Figure 3). The resulting intensity

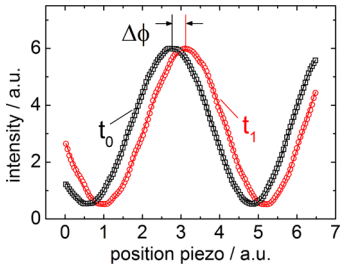

Figure 3. Sketch of the active phase control mechanism. Two intensity scans recorded at two different times t_0 and t_1 (squares and circles) and the fitted sinusoidal curves. The phase shift $\Delta\phi$ is caused by concentration changes.

is fitted to a sinusoidal function which gives a phase value. The curves shown in Figure 3 correspond to the starting time t_0 and a later time t_1. Because of a relative phase shift between the two beams, the signal at t_1 is shifted by $\Delta\phi$ to the right. This full 2π scan takes less than 1 s and is therefore much faster than the expected concentration changes in the microcolumn. We can analyze the phase change by using the forward and the backward movement of the piezo. Both scans give the same phase behavior except for a constant offset caused by the known hysteresis effect of piezos. The interferometer with active phase control is less sensitive to intensity fluctuations caused by mechanical disturbances, and we do not need the reference information about the actual intensity extrema to be measured in advance.

Characterization of the Cell. The gap width of the microcolumn has been determined with a microscope setup, focusing a probing beam onto the surface and detecting the reflected signal. The objective used (10× Mitutoyo) has a long working distance of 33.8 mm and a very small focus depth of 3.58 μm. A principle sketch of the setup is shown in Figure 4a. When the beam is focused on an interface, the reflected beam forms a sharp focused spot and the intensity is on its local maximum. We record the focus shift from the first window-cell interface to the second via an elevator stage. The precision of the height reading is better than 0.5 μm. With this method we determined the average cell thickness to be 523 μm with an uncertainty of 4 μm. The roughness of the inner walls is smaller than the uncertainty.

THEORETICAL APPROACHES

Determination of the Phase Shift due to Concentration. As sketched in Figure 2 we are probing the relative phase difference along the TG microcolumn at two different heights. The phase ϕ between the two beams corresponds to their optical path lengths s_{top} and s_{bottom} inside the column gap via

$$\phi = k(s_{top} - s_{bottom}) \tag{1}$$

with the wave vector $k = (2\pi)/\lambda$ and λ, the wavelength of the laser, assuming a perfectly frequency stable laser. A change in the optical path lengths, Δs_{top} and Δs_{bottom} at the top and bottom, respectively, leads to a change in the phase $\Delta\phi$

$$\Delta\phi = k(\Delta s_{top} - \Delta s_{bottom}) \tag{2}$$

We assume here that the change in refractive index along the column in vertical direction depends only on the concentration difference between top and bottom beam positions. Supported by the simulations we suppose that the temperature changes linearly over the gap). Therefore, the mean temperature is in the middle of the gap, and it is a constant as function of the height. Looking at the horizontal variation of the refractive index we have on the warm side a slightly lower refractive index compared to the middle and at the cold side a slightly higher refractive index compared to the middle. Because of the linearity of the temperature the averaged refractive index probed by the laser beam corresponds to the value in the middle, which is constant over the height of the cell. Therefore we consider that all observed changes in the refractive index are due to concentration changes. Since the change of the optical path results from the change in refractive indices, Δn_{top} and Δn_{bottom} at the top and bottom, respectively, one can write

$$\Delta\phi = kL_x(\Delta n_{top} - \Delta n_{bottom}) = kL_x\Delta n \tag{3}$$

$$\Leftrightarrow \Delta n = \Delta\phi(kL_x)^{-1}$$

with the gap width L_x and the refractive index difference Δn between top and bottom. Additionally, we neglect the phase changes between the top and bottom beam caused by refractive index change and thermal expansion of the sapphire windows (c.f. Figure 1) and the air around the cell due to the temperature gradient, since both beams are affected in the same way. Dividing both sides of (eq 2) by Δc and replacing $\Delta n/\Delta c$ with $(\partial n/\partial c)_{p,T}$, we obtain an expression for Δc

$$\Delta c = \frac{1}{kL_x}\left(\frac{\partial n}{\partial c}\right)^{-1}_{p,T}\Delta\phi \tag{4}$$

dx.doi.org/10.1021/jp3098473 | J. Phys. Chem. B 2012, 116, 13889−13897

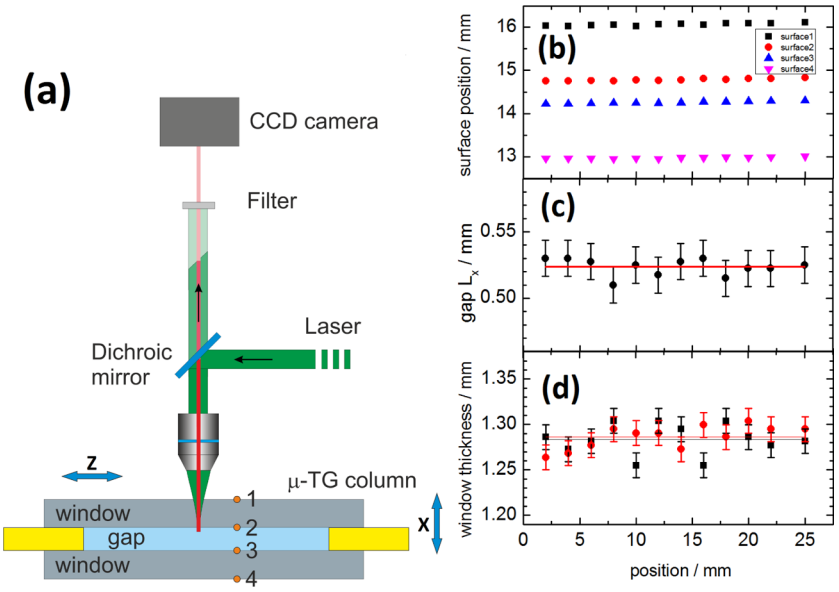

Figure 4. Optical tweezers setup to determine the position of the sapphire surfaces. The cell can be moved in the *x*- and *z*-directions on a micrometer stage. (b) Position of the different surfaces along the cell. (c) The calculated gap width and the width of the (d) sapphire windows as function of the cell height.

The refractive index increment $(\partial n/\partial c)_{p,T}$ can be determined independently. Furthermore, we would like to point out that due to continuous observation of $\Delta\phi$ also phase differences larger than 2π can be detected.

Determination of the Concentration Change. We use the FJO theory[18,20] to calculate the concentration difference at the steady state at two points separated by L_z to

$$\Delta c = 504\frac{\nu}{\alpha g}D_T c_0(1 - c_0)\frac{L_z}{L_x^4} \tag{5}$$

where c_0 is the initial mass fraction concentration of the reference component, ν is the kinematic viscosity, α is the thermal expansion coefficient, L_z is the vertical distance between the probing laser beams (22 mm), D_T the thermal diffusion coefficient, and g the gravity acceleration. In the derivation it is used that the initial concentration c_0 changes only slightly, so that D_T and also D can still be treated as a constant. This assumption might break down, if large concentration changes occur. Combining eqs 4 and 5 gives the thermal diffusion coefficient

$$D_T = \frac{1}{504}\frac{\alpha g}{k\nu}\frac{1}{c_0(1 - c_0)}\frac{L_x^3}{L_z}\left(\frac{\partial n}{\partial c}\right)_{p,T}^{-1}\Delta\phi \tag{6}$$

Because of the fact that we do have a method which measures the phase continuously, we might also look at the temporal behavior of the transient concentration difference. This is given by[21]

$$\Delta c = \Delta c_\infty(1 - ae^{-t/t_r}) \tag{7}$$

It needs to be pointed out that eq 7 is only satisfied for times t larger than one-third of the relaxation time t_r because it corresponds only to the first term of an infinite series. Another shortcoming of eq 7 is that an ideal infinitely sharp switching of the temperature gradient is assumed, which practically cannot be achieved. In the future we will develop an experimental procedure to obtain the molecular diffusion coefficient from the transient signal.

NUMERICAL SIMULATIONS

Numerical Validation of the TG Microcolumn. To validate the proposed geometry for the TG microcolumn, a numerical study using ANSYS-Fluent software[22] is made. The simulations are performed using a finite volume (illustrated in Figure 5) method in 3D (FVM) based on fluid flow solutions under the assumption of an incompressible fluid and laminar flow under atmospheric pressure.

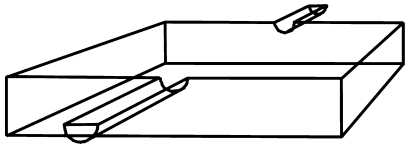

Figure 5. A sketch of the cell volume including the considered dead volumes, which are used for filling the microcolumn.

The model covers the Fickian mass, the thermal diffusion, and the Navier–Stokes equation, whereas the density changes in the fluid with concentration and temperature are covered by the Boussinesq approximation[23]

$$\rho = \rho_0(1 - \alpha(T - T_0) + \beta(c - c_0)) \tag{8}$$

where ρ is the local density of the mixture, ρ_0 is the density of the homogeneous mixture, T_0 is the mean temperature, $\alpha = -(1/\rho)(\partial\rho/\partial T)_{p,c}$ is the thermal expansion coefficient and $\beta = +(1/\rho)(\partial\rho/\partial c)_{p,T}$ is the mass expansion coefficient. The value of the mass and thermal expansion coefficient are experimentally determined.[24] We used no-slip boundary conditions and applied a constant temperature gradient of 5 K perpendicular to the gravity field.

The governing equations are solved using a pressure-based implicit simple velocity-pressure coupling scheme with a double-precision module. The second-order numerical discretization scheme is used for pressure, density, momentum, and mass flux to avoid numerical instabilities. The iterative convergence criteria is set to 10^{-9} for all solution variables.

dx.doi.org/10.1021/jp3098473 | J. Phys. Chem. B 2012, 116, 13889–13897

For the preprocessing of the geometry Gambit[25] is used, where the geometry of the gap (523 μm × 3 mm ×30 mm) was defined. This 3D computational domain consists of nonuniformly spaced hexahedral mesh cells. A very fine mesh resolution was used with 720 000 hexahedral cells to have a realistic representation of the concentration gradients.

Simulation Results. For the numerical validation of the microcolumn, the TG effect in the steady state is analyzed using a reference mixture TOL/HEX at a mass fraction of 0.5167 and at T = 298 K. Table 1 lists the parameters for the TOL/HEX mixture. Köhler and Müller measured only at T = 296 K and higher temperatures so that D_T and D at T = 298 K have been obtained by linear interpolation.[12]

Table 1. Experimental Density, ρ_0, Dynamic Viscosity, μ, Mass Expansion Coefficient, β, and the Thermal Diffusion Coefficient, D_T, for the Mixture TOL/HEX with a Mass Fraction of 0.5167 at T = 298 K Used in the Numerical Simulation

ρ_0/kg/m^3	μ/Pa·s	α/K^{-1}	β	$D_T/10^{-12}$ m^2/sK	$D/10^{-9}$m^2/s
748.19	3.861	1.23	0.275	13.7 [ref 13]	2.78 [ref 13]
				13.2 [ref 14]	2.85 [ref 12]
				14.0 [ref 12]	

For the TOL/HEX mixture with c_0 = 0.5167 the steady state temperature, velocity, and concentration profiles obtained from numeric simulations are shown in Figure 6 and Figure 7. Figure 7a shows the temperature profile within the gap which decays linearly from the warm to the cold side. Figures 6 and 7b show the velocity and the toluene concentration profiles inside the gap at the midheight of the microcolumn at 15 mm. The velocity (c.f. Figure 7b) has a cubical profile while the concentration profile (c.f. Figure 6) has to be described by a polynomial of the fifth order. Figure 7c show the distribution of the concentration referring to the densest component (TOL) in the stationary state. Along the microcolumn the results show an increase in the concentration of the densest component (TOL) in the lower and of the lightest component (HEX) in the upper parts of the column. The profiles obtained in the microcolumn are those predicted by the TG theory.[26,27]

Table 2 summarizes the results of numerical simulation and compares the concentration difference and the thermal diffusion coefficient in the steady state with the experimental values. The simulation results agree within a few percent with the experimental values and the mean experimental value agrees within 1%. The excellent agreement between the simulation results and the experimental values shows that the design fulfills the conditions of the FJO theory.

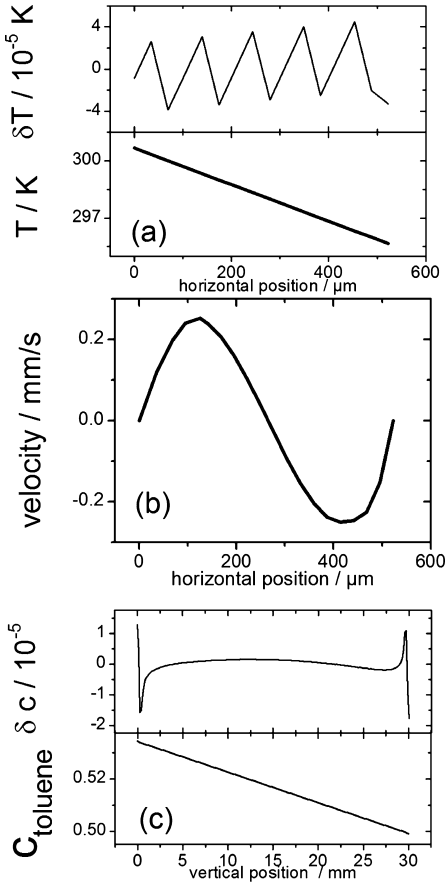

Figure 7. Numerical simulation results for the binary mixture TOL/HEX at the stationary state. (a) Temperature profile within the microcolumn gap. The upper part shows the deviations from a linear fit. (b) Velocity profile within de microcolumn gap at a height of 15 mm. (c) The vertical concentration distribution profile of the TOL mass fraction in the middle of the gap along the microcolumn. The upper part shows again the deviations from a linear fit.

Additionally, we analyzed numerically the effect on the concentration difference probably caused by dead volumes at the inlet and outlet. The considered dead volumes are in the order of 3.625 μL stemming from two channels with a diameter of 250 μm and 14.5 mm in length. Figure 5 shows the model used. As shown in Table 3, the obtained concentration difference from the simulation Δc_{fluent} agrees within 1% with

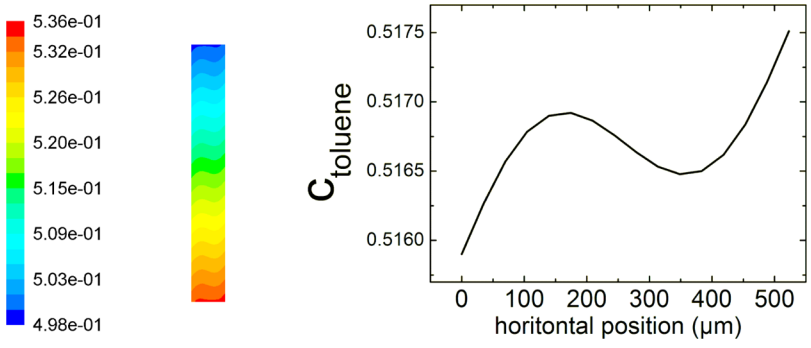

Figure 6. Numerical simulation results of the toluene mass fraction profile in the binary mixture TOL/HEX. The left figure shows the profile over the entire height of the microcolumn. The right figure is a plot of the concentration profile at a height of 15 mm at the stationary state.

dx.doi.org/10.1021/jp3098473 | J. Phys. Chem. B 2012, 116, 13889−13897

Table 2. Comparison between Experimental and Numerical Simulation Results of the Stationary Separation under the TG Effect for the New Design of the Microcolumn for the Mixture TOL/HEX with a Mass Fraction of 0.5167[a]

L_z/ mm	Δc (eq 5)	Δc_{fluent}	dev/ %	$D_{T_{exp}}$/ 10^{-12} m^2/sK	$D_{T_{fluent}}$/ 10^{-12} m^2/sK	dev/ %
30	0.0295	0.0297	<1	13.63	13.74	<1
22	0.0216	0.0218	<1	13.63	13.76	<1

[a] D_T is the average of the individual literature values listed in Table 1.

the calculated concentration difference Δc (eq5). The determined thermal diffusion coefficients for TOL/HEX, THN/IBB, IBB/DD, and THN/DD mixtures at a mass fraction of 50% at T = 298 K agree also within a few percent with the simulation results obtained for a gap of 523 μm including the dead volume effect.

RESULTS AND DISCUSSION

Figure 8 shows a typical time development of the phase for the system TOL/HEX and THN/DD at an average temperature of T = 298 K and a temperature difference of ΔT = 6 K over the gap of the cell. At time t = 0 the temperature gradient is applied while at earlier times both sides of the cell are kept at an average mixing temperature, T_{mix}, which leads to a constant phase after some settling time of the order of an hour. Once the temperature gradient is applied, the phase shows an exponential increase until it reaches a plateau value. The phase difference is determined by the difference of the plateau value in the steady state and the phase at the baseline before switching on the temperature gradient. In all our experiments this phase change in the jump was of the order of 0.2 π, and its origin will be discussed in the Appendix. The so-determined phase difference is used in eq 6 to calculate the thermal diffusion coefficient, D_T. The obtained values for the four systems are listed in Table 4 and shown in Figure 9 in comparison with literature values. For most of the systems the deviations are below or around 6%. The absolute uncertainty was below 0.6 × 10^{-12} m^2 s^{-1} K^{-1}. With this new TG microcolumn design in combination with the interferometric detection with one wavelength we surrender a strong point of the TGs, namely, the investigation of ternary mixtures. In addition we employ very small sample volume of less than 50 μL, with similar measurement times compared to the conventional TGs of 30 min up to 2 h for the investigated mixtures. Both the design and the measurement system developed in this work for the new TG microcolumn installation is well suited for biological systems. The transparent windows of the TG microcolumn have several advantages. First, a precise determination of the gap width over the entire height of the TG microcolumn is possible. This is especially important, because the thermal diffusion coefficient, D_T depends on the gap width to the power of three (c.f., eq 6) for our optical system. So far we have only studied organic mixtures, but the setup should also work for aqueous solutions. Because of the higher surface tension of water, special care needs to be taken in order to avoid air bubbles in the cell. Another nice feature of the TG microcolumn is that we can monitor the concentration change as function of time. In principle it should therefore also be possible to determine the diffusion constant D in the same setup. In the present design, however, we were not able to obtain sufficiently accurate values for D. The largest problem is the uncertainty in ΔT, which needs to be obtained at the inside of the sapphire windows. We hope that we can analyze in the near future the time dependence of the concentration to obtain also the Soret

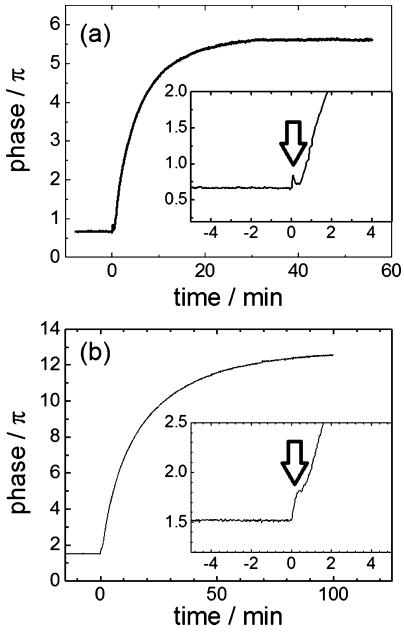

Figure 8. (a) Typical experimental results for phase shift between top and bottom for the mixture TOL/HEX and (b) THN/DD with a mass weight fraction of 50% as function of time. The time base has been chosen in such a way that at time zero the temperature gradient has been enabled. The inset shows the phase close to the turn-on time. The origin of the fast jump in the signal will be discussed in detail in the Appendix.

Table 4. Thermal Diffusion Coefficients Determined for Four Binary Mixtures with 50 wt %[a]

mixture	D_T/(this work) 10^{-12} m^2/sK	D_T/(literature) 10^{-12} m^2/sK	dev/ %
TOL-HEX	13.0 ± 0.35	13.6 [avg]	−0.44
THN-DD	5.87 ± 0.23	5.9 [ref 9]	−0.50
THN-IBB	2.63 ± 0.01	2.8 [ref 9]	−6.07
IBB-DD	3.91 ± 0.15	3.7 [ref 9]	+5.68

[a] All measurements have been performed at 298 K. The error is the variance of the mean from five individual measurements.

Table 3. Experimental and Numerical Results for the Investigated Binary Mixtures at T = 298 K and a Mass Fraction of c = 0.5[a]

mixture	Δc (eq 5), L_z = 22 mm	Δc_{fluent}, L_z = 22 mm	dev/%	$D_{T_{exp}}/10^{-12}$ m^2/sK	$D_{T_{sim}}/10^{-12}$ m^2/sK	dev/%
TOL-HEX	0.0213	0.0214	0.47	13.6 [avg, ref 12−14]	13.56	−0.29
THN-DD	0.0451	0.0453	0.44	5.90 [ref 9]	5.93	0.50
THN-IBB	0.0180	0.0177	−1.66	2.80 [ref 9]	2.78	−0.71
IBB-DD	0.0207	0.0206	−0.48	3.70 [ref 9]	3.68	−0.54

[a] In all simulations the dead volume caused by the inlet and the outlet has been considered.

dx.doi.org/10.1021/jp3098473 | J. Phys. Chem. B 2012, 116, 13889−13897

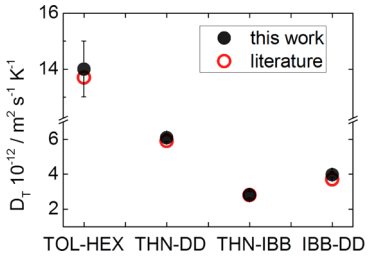

Figure 9. The thermal diffusion coefficient, D_T, for the four studied systems in comparison with literature values. The largest absolute deviations are found for the system TOL/HEX, while the largest relative deviation of around 6% is found for the system THN-IBB.

coefficient, S_T, but this might also require a more sophisticated model for the data analysis.

Compared to other optical detection methods such as thermal diffusion forced Rayleigh scattering (TDFRS)[28,29] or beam deflection (BD)[10,30] the sample volume of 50 μL is very small. The equilibration times are comparable with BD but much slower than in the TDFRS experiments. One drawback of the method is that we are not capable to determine also the diffusion coefficient D using eq 7, because the experimental data show systematic deviations from a simple exponential function. The operating expenses are much lower than in the case of the TDFRS and comparable with the BD. This method might open up other possibilities by combining it with a microscope and fluorescent detection methods. This new method will also be useful for further benchmark campaigns as a convective method in combination with optical detection.

In conclusion we can state that the TG microcolumn is a nice compact device which allows reliable, contactless measurements of the thermal diffusion coefficient, D_T. The typical deviations from the literature values found are in the order of 5% (c.f., Table 4), which is comparable with the deviation found in the benchmark.[9]

APPENDIX

As mentioned in the Results and Discussion section we observe always a fast phase jump shortly after switching on the temperature gradient. In the following section we will discuss this issue and will relate it to a slight asymmetry in the formation of the temperature gradient.

Characterization of the Temperature Switching

Before the measurement starts, we mix the water of the two thermostats, which are kept at different temperatures T_{cold} and T_{warm}. We adjust the flows of the two thermostats so that the temperature of the mixed water corresponds to the average of the two temperatures $T_{mean} = 0.5(T_{cold} + T_{warm})$. Practically, small deviations of the order of $\Delta T = 0.1$ K are detected. This leads to a small temperature difference to the mean temperature, T_{mean}, of the cell prior the temperature gradient and causes a small horizontal asymmetry in the $(\partial n/\partial T)_{p,T}$ contributions. If the thickness of the gap and the windows between top and bottom are equal, this affects top and bottom in the same way, so that changes in the phases should cancel.

Figure 10 shows the temperatures on the cold and warm sides as a function of time after the temperature gradient has been switched on. The temperatures have been measured with an infrared camera (FLIR T400) at the surface of the sapphire windows, which has been covered with a 100-μm Teflon foil to avoid reflections. Because of the insulation of the Teflon foil the temperature reading will be a bit lower compared to the

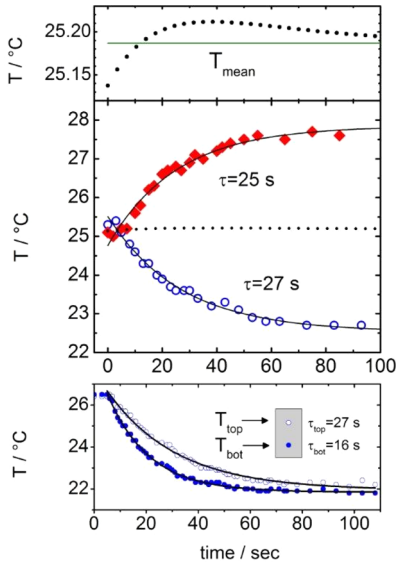

Figure 10. Top: temperature at the outside of the sapphire windows at the two sides (warm side, filled diamonds; cold side, open circles) of the TG microcolumn filled with toluene as function of time measured by means of an infrared camera. The upper graph shows that due to different time constants for the warm and the cold side there is a small overshot in the mean temperature (small dots) as function of time. Bottom: development of the temperature at the bottom and at the top of the cell measured at the covered metal surface. The temperature equilibrates at the bottom of the cell much faster than at the top, so that for a short time a vertical temperature gradient in the order of 0.2−0.3 K is established. The solid lines are exponential fits with time constants given in the graph.

temperature at the outside of the sapphire window, but this will affect both sides in the same way. Also the surrounding metal parts have been taped to prevent reflections at the metal surfaces, which could influence the temperature reading. Figure 10 shows the time development of the temperatures on the warm and cold side, which can be described by an exponential increase and decrease, respectively. Typical time constants of an exponential fit to reach the final values T_{cold} and T_{warm} are 27 and 25 s, respectively, indicating that heating is slightly faster than cooling. This leads as in the upper graph of Figure 10 shown to a slight overshot of the average temperature, T_{mean}. But this effect will also influence the top and the bottom in the same way so that those contributions cancel.

By thermal analysis with the infrared camera, we have seen that during the initial state of applying the temperature gradient the temperature propagates from the bottom to the top, which means that the final temperature at the bottom is reached earlier compared to the top. The lower graph of Figure 10 shows the temperature at the top and bottom measured at the metal surface of the cell. Because of the small window of a width of 3 mm we were not able to obtain reliable measurements at two different height positions directly at the sapphire windows. As seen in the figure the time constants between top and bottom differ substantially. Typical exponential time constants at the bottom and at the top of the cell are 16 and 27 s, respectively. This is indeed a problem of the present setup and leads to phase shift between the bottom and the top present in the beginning of the experimental phase curves. This difficulty can be solved by using a cross-flow in the microcolumn similar to the circulating

dx.doi.org/10.1021/jp3098473 | J. Phys. Chem. B 2012, 116, 13889−13897

water loops used by Zhang et al.[13] or by imaging the phase profile over the entire height.

Stability and Response of the Interferometer

The precision of the setup depends strongly on the stability of the interferometer. The drift should be very small over the measurement time. A typical measurement time is of the order of 30 minutes to 2 h depending on the system. A small drift has little influence and can be subtracted from the measured signal. To achieve a very small drift, we have to insulate the laser beam paths from temperature changes by insulating the cell and the tubes. This will reduce the effect but not cancel it out completely. The interferometer mirrors are mounted on vertical pillars. Care needs to be taken to have stable temperature conditions taking into account heat sources and fluctuations.

A typical example for the time dependence of pure THN is shown in Figure 11b. At short times when no temperature gradient is applied, we observe a constant drift of the phase. After 10 minutes a temperature gradient is applied, and the phase changes rapidly within a minute and approaches then a constant drift rate. When the temperature gradient is switched off, we observe the reverse behavior. A similar jump occurs also in the empty cell and during the regular measurements and is always in the order of 0.2π. Therefore, we assume that it is related to an asymmetry in the setup, but the reason is not fully understood. In the last section we discussed a small vertical temperature gradient and the temporal change of the mean temperature in Figure 11b and the top portion of Figure 10, respectively. The maximal temperature difference between top an bottom is of the order of 0.2−0.3 K; with a typical $(\partial n/\partial T)_{p,c} = 5 \times 10^{-4}$ K^{-1}, we obtain a phase shift of the order of 0.2π−0.3π, which corresponds to the typical observed values of 0.2π. On the other hand it is also possible that the two beams are slightly deflected leading to a shift of the interference pattern, which results then into an intensity change. We want to clarify this issue in the future by comparing different microcolumns.

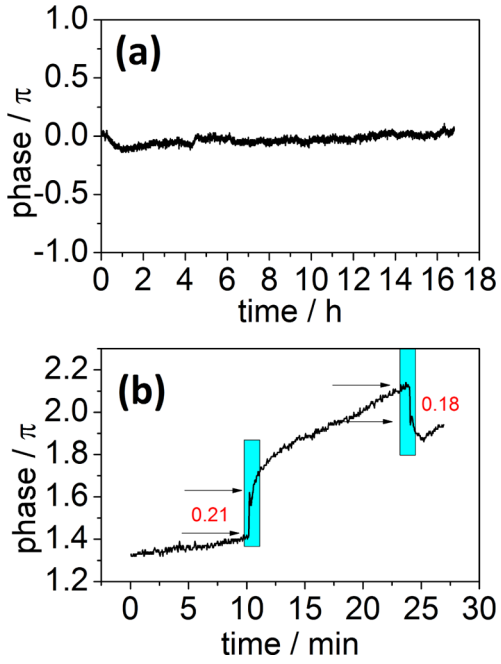

Figure 11. (a) Phase drift as function of time. After equilibration within the first hour, the phase drifts with a rate 0.0064 π/h. This corresponds to a drift of less than 0.02 π for a measurement time of 3 h, which results for IBB/THN, the system with the weakest measurement signal, in a relative error of 1%. (b) Phase response in pure THN, when the temperature gradient is switched on and off, respectively.

AUTHOR INFORMATION

Corresponding Author

*E-mail: mbouali@mondragon.edu (M.M.B.-A.); s.wiegand@fz-juelich.de (S.W.).

Notes

The authors declare no competing financial interest.

ACKNOWLEDGMENTS

We thank Jan Dhont for his constant interest and many helpful discussions. Special thanks to Axel Ackens, who lended the infrared camera to us. We thank also Christoph July and Peter Lang for the use of their tweezers setup for the determination of the cell thickness and we show our gratitude to Michael Klein for a first outline of the interferometer. The Jülich group acknowledges financial support due to the DAAD PPP program and the Deutsche Forschungsgemeinschaft Grant Wi 1684. The MGEP group thanks the TEDIBIO integrated action project (No. DE 2009-0024) and LOCUS2 (No. BIO2011-30535-C04-04) project from the Spanish Goverment, as well as the GOVSORET3 (No. PI2011-22), MIDIAG project, and the project of Fluids Mechanics Groups (IT557-10) of the Basque Country Government.

REFERENCES

(1) Bou-Ali, M. M.; Valencia, J. J.; Madariaga, J. A.; Santamaria, C.; Ecenarro, O.; Dutrieux, J. F. *Philos. Mag.* **2003**, *83*, 2011−2015.

(2) Platten, J. K.; Bou-Ali, M. M.; Dutrieux, J. F. *J. Phys. Chem. B* **2003**, *107*, 11763−11767.

(3) Clusius, K.; Dickel, G. *Naturwissenschaften* **1938**, *26*, 546−546.

(4) Platten, J. K.; Bou-Ali, M. M.; Dutrieux, J. F. *Philos. Mag.* **2003**, *83*, 2001−2010.

(5) Blanco, P.; Bou-Ali, M. M.; Platten, J. K.; de Mezquia, D. A.; Madariaga, J. A.; Santamaria, C. *J. Chem. Phys.* **2010**, *132*, 114506 1−6.

(6) Dutrieux, J. F.; Platten, J. K.; Chavepeyer, G.; Bou-Ali, M. M. *J. Phys. Chem. B* **2002**, *106*, 6104−6114.

(7) Bou-Ali, M.; Platten, J. K. *J. Non-Equil. Thermody.* **2005**, *30*, 385−399.

(8) Leahy-Dios, A.; Bou-Ali, M. M.; Platten, J. K.; Firoozabadi, A. *J. Chem. Phys.* **2005**, *122*, 234502 1−12.

(9) Platten, J. K.; Bou-Ali, M. M.; Costeseque, P.; Dutrieux, J. F.; Köhler, W.; Leppla, C.; Wiegand, S.; Wittko, G. *Philos. Mag.* **2003**, *83*, 1965−1971.

(10) Königer, A.; Meier, B.; Köhler, W. *Philos. Mag.* **2009**, *89*, 907−923.

(11) Mialduna, A.; Shevtsova, V. *J. Chem. Phys.* **2011**, *134*, 044524 1−12.

(12) Köhler, W.; Müller, B. *J. Chem. Phys.* **1995**, *103*, 4367−4370.

(13) Zhang, K. J.; Briggs, M. E.; Gammon, R. W.; Sengers, J. V. *J. Chem. Phys.* **1996**, *104*, 6881−6892.

(14) Bou-Ali, M. M.; Ecenarro, O.; Madariaga, J. A.; Santamaria, C. M.; Valencia, J. J. *J. Phys.: Condens. Matter* **1998**, *10*, 3321−3331.

(15) Burghartz, S.; Schulz, B. *J. Nucl. Mater.* **1994**, *212*, 1065−1068.

(16) Choy, C. L.; Kwok, K. W.; Leung, W. P.; Lau, F. P. *J. Polym. Sci., Part B: Polym. Phys.* **1994**, *32*, 1389−1397.

(17) Choy, C. L.; Leung, W. P. *J. Polym. Sci., Part B: Polym. Phys.* **1990**, *28*, 1965−1977.

(18) Furry, W. H.; Jones, R. C.; Onsager, L. *Phys. Rev.* **1939**, *55*, 1083−1095.

(19) Martin, A.; Bou-Ali, M. M.; Gandarias, E.; Aristimuño, P.; Wiegand, S. EP12382015, Europe, 2012.

(20) Majumdar, S. D. *Phys. Rev.* **1951**, *81*, 844−848.
(21) Valencia, J. J.; Bou-Ali, M. M.; Platten, J. K.; Ecenarro, O.; Madariaga, J. M.; Santamaria, C. M. *J. Non-Equil. Thermody.* **2007**, *32*, 299−307.
(22) *Ansys Inc*; Ansys-Fluent 13.0, Lebanon, USA, 2010.
(23) Platten, J. K.; Chavepeyer, G. *Int. J. Heat Mass Transf.* **1976**, *19*, 27−32.
(24) Blanco, P.; Bou-Ali, M. M.; Platten, J. K.; Urteaga, P.; Madariaga, J. A.; Santamaria, C. *J. Chem. Phys.* **2008**, *129* (174504), 1−6.
(25) *Ansys Inc*; Gambit 2.4.6, Lebanon, USA, 2010.
(26) Valencia, J.; Bou-Ali, M. M.; Ecenarro, O.; Madariaga, J. A.; Santamaria, C. M. *Thermal Nonequilibrium Phenomena in Fluid Mixtures* **2002**, *584*, 233−249.
(27) Madariaga, J. A.; Santamaria, C.; Barrutia, H.; Bou-Ali, M. M.; Ecenarro, O.; Valencia, J. J. *Cr. Mecanique* **2011**, *339*, 292−296.
(28) Köhler, W.; Rossmanith, P. *J. Phys. Chem.* **1995**, *99*, 5838−5847.
(29) Wiegand, S.; Ning, H.; Kriegs, H. *J. Phys. Chem. B* **2007**, *111*, 14169−14174.
(30) Kolodner, P.; Williams, H.; Moe, C. *J. Chem. Phys.* **1988**, *88*, 6512−6524.

C. Remarks on the analysis method for determining diffusion coefficient in ternary mixtures.

C. R. Mecanique 341 (2013) 356–364

Contents lists available at SciVerse ScienceDirect

Comptes Rendus Mecanique

www.sciencedirect.com

10th International Meeting on Thermodiffusion

Remarks on the analysis method for determining diffusion coefficient in ternary mixtures

Miren Larrañaga [a], M. Mounir Bou-Ali [a,*], Daniel Soler [a], Manex Martinez-Agirre [a], Aliaksandr Mialdun [b], Valentina Shevtsova [b,*]

[a] MGEP Mondragon Goi Eskola Politeknikoa, Mechanical and Industrial Manufacturing Department, Loramendi 4, Apdo. 23, 20500 Mondragon, Spain
[b] MRC, ULB, EP – CP165/62, Dept. Chemical Physics, B1050, Brussels, Belgium

ARTICLE INFO

Article history:
Available online 27 February 2013

Keywords:
Molecular diffusion
Ternary mixture
Sliding Symmetric Tubes
Fitting procedure

ABSTRACT

The objective of this work is the determination of diagonal and cross-diagonal molecular diffusion coefficients in a ternary mixture, using the 'Sliding Symmetric Tubes' (SST) technique. The analyzed mixture consists of two aromatics and one normal alkane (tetrahydronaphthalene–dodecane–isobutylbenzene) with an equal mass fraction for all components (1:1:1) at 25 °C. The analytical solution corresponding to the SST technique has been successfully derived. The different fitting procedures were utilized by two scientific teams to subtract diffusion coefficients from the experimentally measured time-dependent concentration field. None of the attempts provided reliable results for the data from a single experiment. The "simplex"-based methods display reasonable results assuming that cross-diagonal coefficients are close to zero, i.e. quasi-binary and diluted mixtures. The results obtained by "trust region method" are satisfactory if the initial guess is good. To achieve better results, it is necessary to increase the number of experimental data.

1. Introduction

A concentration gradient within a liquid mixture generates a transport of matter from the zones of higher concentration, to the ones of lower concentration. This phenomenon is known as molecular diffusion and it has generated a big interest since its discovery in the nineteenth century, when it was studied in order to understand the atom's behavior. In 1855 Fick [1] established the first quantitative relation for the molecular diffusion phenomenon, known as Fick's law. Since then, the interest on this phenomenon has increased, discovering the influence it has in many fields, such as medicine or physiology [2].

Due to this interest, a lot of new experimental techniques designed for the determination of the molecular diffusion coefficient have been developed. These are, for example, techniques that employ the Taylor dispersion principle [3], or Open Ended Capillary technique (OEC) [4] or Thermal Forced Rayleigh Scattering (TDFRS) [5]. Other different techniques used for the determination of the molecular diffusion coefficient can be found in the literature [2,6–9]. The Sliding Symmetric Tubes technique was developed in order to make up for some limitations of the OEC technique, such as the problem of the evaporations or the volume of fluid needed for each experiment [10].

Molecular diffusion in multicomponent mixtures has a very important role in a lot of natural and industrial processes. However, although there are plenty of experimental data in binary mixtures, in the case of multicomponent mixtures the

* Corresponding authors.
E-mail addresses: mbouali@mondragon.edu (M.M. Bou-Ali), vshev@ulb.ac.be (V. Shevtsova).

1631-0721/$ – see front matter
http://dx.doi.org/10.1016/j.crme.2013.01.008

available information, both theoretical and experimental, is limited [11]. The existence of cross-diagonal diffusion coefficients makes their determination difficult already in ternary mixtures.

The main objective of this work is to analyze the results obtained by different fitting procedures done in order to determinate the diagonal and cross-diagonal molecular diffusion coefficients from the measurements of a concentration variation with time by the SST technique.

This article is organized as follows: in Section 2, the SST technique is presented; the details of the elaboration of the analytical solution for ternary mixtures and the description of the experimental method are given. In Section 3, the experimental results are analyzed and, particularly, the dependence of the determined molecular diffusion coefficients D_{ij} $(i, j = 1, 2)$ on fitting procedure is discussed. Finally, conclusions are drawn in Section 4.

2. Sliding Symmetric Tubes technique

2.1. Technique description

In the SST technique, several sets of two identical vertical tubes can be used. Each set has two positions: 'faced tubes' and 'separated tubes' [12]. In 'faced tubes' position the mixture of both tubes is in contact, allowing the transport of matter; whereas in 'separated tubes' position, the transport of matter is stopped. At the beginning of the experiment, the studied mixture is introduced in each tube, with a slight concentration difference. The denser mixture is introduced in the bottom tube, and the upper tube is filled with the less dense mixture in order to avoid the convective instability.

This technique was validated in previous works, [13], using 5 binary mixtures: the three binary mixtures composed by 1,2,3,4-tetrahydronaphthalene (THN), dodecane (*n*C12), and isobutylbenzene (IBB) at 25 °C and 50 wt%, used in a benchmark test [14], and the binary mixtures: water/ethanol at 25 °C and 60.88 wt% water and toluene/*n*-hexane at 25 °C and 51.67 wt% toluene, which have been extensively studied in the literature [15–19]. In general, the differences with the published data are below 3%.

2.2. Analytical solution

Assuming Fick's second law in one dimension (z: vertical direction), the following system of equations for a ternary mixture is obtained, where the corresponding matrix to the diagonal and cross-diagonal molecular diffusion coefficients appears.

$$\frac{\partial}{\partial t}\begin{Bmatrix} w_1 \\ w_2 \end{Bmatrix} = \begin{bmatrix} D_{11} & D_{12} \\ D_{21} & D_{22} \end{bmatrix} \cdot \frac{\partial^2}{\partial z^2}\begin{Bmatrix} w_1 \\ w_2 \end{Bmatrix} \rightarrow \begin{cases} \frac{\partial w_1}{\partial t} = D_{11} \cdot \frac{\partial^2 w_1}{\partial z^2} + D_{12} \cdot \frac{\partial^2 w_2}{\partial z^2} \\ \frac{\partial w_2}{\partial t} = D_{21} \cdot \frac{\partial^2 w_1}{\partial z^2} + D_{22} \cdot \frac{\partial^2 w_2}{\partial z^2} \end{cases} \tag{1}$$

where w_1 and w_2 are the concentrations of the component 1 and the component 2, respectively, and D_{11}, D_{22}, D_{12}, and D_{21} are the diagonal and cross-diagonal molecular diffusion coefficients.

The boundary conditions in this case are:

$$\overline{w}(z, 0) = f(z) = \begin{cases} w_i^{\text{bot}} & 0 \leqslant z < L \\ w_i^{\text{up}} & L < z \leqslant 2L \end{cases} \tag{2}$$

$$\left.\frac{\partial w_i}{\partial z}\right|_{z=0,2L} = 0 \quad \forall t \tag{3}$$

where w_i^{up} and w_i^{bot} are the initial mass fractions in the upper and the bottom tubes, respectively.

As has been done in the case of the OEC technique [20], the system (1) can be solved diagonalizing the diffusion matrix $\overline{\overline{D}}$ in order to uncouple the system into two equations. In this case, obtained eigenvalues and eigenvectors matrix are given by:

$$\lambda_1 = \frac{D_{11} + D_{22} + \sqrt{(D_{11} - D_{22})^2 + 4 \cdot D_{12} \cdot D_{21}}}{2} \tag{4}$$

$$\lambda_2 = \frac{D_{11} + D_{22} - \sqrt{(D_{11} - D_{22})^2 + 4 \cdot D_{12} \cdot D_{21}}}{2} \tag{5}$$

$$\overline{\overline{P}} = \begin{bmatrix} 1 & \frac{D_{12}}{\lambda_2 - D_{11}} \\ \frac{\lambda_1 - D_{11}}{D_{12}} & 1 \end{bmatrix} \tag{6}$$

The diagonalization allows us to define a new concentration variable:

$$\overline{\phi} = \overline{\overline{P}}^{-1} \cdot \overline{w} \tag{7}$$

It results in a new problem where the equations are uncoupled and where there are new initial and boundary conditions:

$$\begin{Bmatrix} \frac{\partial \phi_1}{\partial t} \\ \frac{\partial \phi_2}{\partial t} \end{Bmatrix} = [D_d] \cdot \begin{Bmatrix} \frac{\partial^2 \phi_1}{\partial z^2} \\ \frac{\partial^2 \phi_2}{\partial z^2} \end{Bmatrix} \tag{8}$$

$$\overline{\phi}_i(z,0) = \begin{cases} \overline{\overline{P}}^{-1} \cdot \overline{w_l^{\text{bot}}} & 0 < z < L \\ \overline{\overline{P}}^{-1} \cdot \overline{w_l^{\text{up}}} & L < z < 2L \end{cases} \tag{9}$$

$$\left.\frac{\partial \overline{\phi}_i}{\partial z}\right|_{z=0,2L} = 0 \quad \forall t \tag{10}$$

The equations solved by the separation of variables method, as it was done in the case of binary mixtures [12], yield to the following equations for the mean concentration of the component 1 and the component 2, in the upper tube and the bottom tube ($\emptyset_i^{\text{up/bot}}|_{\text{m}}$):

$$\emptyset_1^{\text{bot}}|_{\text{m}}(t) - \frac{\phi_{1i}^{\text{bot}} + \phi_{1i}^{\text{up}}}{2} = \frac{4}{\pi^2} \cdot \left(\phi_{1i}^{\text{bot}} - \phi_{1i}^{\text{up}}\right) \cdot \sum_{n=0}^{\infty} \frac{e^{-(n+\frac{1}{2})^2 \cdot \frac{\pi^2}{L^2} \cdot \lambda_1 \cdot t}}{(2n+1)^2} \tag{11}$$

$$\emptyset_1^{\text{up}}|_{\text{m}}(t) - \frac{\phi_{1i}^{\text{bot}} + \phi_{1i}^{\text{up}}}{2} = \frac{4}{\pi^2} \cdot \left(\phi_{1i}^{\text{up}} - \phi_{1i}^{\text{bot}}\right) \cdot \sum_{n=0}^{\infty} \frac{e^{-(n+\frac{1}{2})^2 \cdot \frac{\pi^2}{L^2} \cdot \lambda_1 \cdot t}}{(2n+1)^2} \tag{12}$$

$$\emptyset_2^{\text{bot}}|_{\text{m}}(t) - \frac{\phi_{2i}^{\text{bot}} + \phi_{2i}^{\text{up}}}{2} = \frac{4}{\pi^2} \cdot \left(\phi_{2i}^{\text{bot}} - \phi_{2i}^{\text{up}}\right) \cdot \sum_{n=0}^{\infty} \frac{e^{-(n+\frac{1}{2})^2 \cdot \frac{\pi^2}{L^2} \cdot \lambda_2 \cdot t}}{(2n+1)^2} \tag{13}$$

$$\emptyset_2^{\text{up}}|_{\text{m}}(t) - \frac{\phi_{2i}^{\text{bot}} + \phi_{2i}^{\text{up}}}{2} = \frac{4}{\pi^2} \cdot \left(\phi_{2i}^{\text{up}} - \phi_{2i}^{\text{bot}}\right) \cdot \sum_{n=0}^{\infty} \frac{e^{-(n+\frac{1}{2})^2 \cdot \frac{\pi^2}{L^2} \cdot \lambda_2 \cdot t}}{(2n+1)^2} \tag{14}$$

In order to check the obtained equations, the transition from the ternary to binary mixture is applied in Eqs. (13), (14). For that, it is taken into account that in the case of binary mixtures, the concentration of only one of the components is considered, and there exists only one molecular diffusion coefficient D.

$$D_{11} = D_{22} = D \tag{15}$$

$$D_{12} = D_{21} = 0 \tag{16}$$

The eigenvalues (4) and (5) of the matrix are as follows:

$$\lambda_1 = \frac{D + D + 0}{2} = D \tag{17}$$

$$\lambda_2 = \frac{D + D - 0}{2} = D \tag{18}$$

Substituting these values in Eqs. (11)–(14), the following expressions are obtained:

$$w_l^{\text{bot}}|_{\text{m}}(t) - \frac{w_i^{\text{bot}} + w_i^{\text{up}}}{2} = \frac{4}{\pi^2} \cdot \left(w_i^{\text{bot}} - w_i^{\text{up}}\right) \cdot \sum_{n=0}^{\infty} \frac{e^{-(n+\frac{1}{2})^2 \cdot \frac{\pi^2}{L^2} \cdot D \cdot t}}{(2n+1)^2} \tag{19}$$

$$w_l^{\text{up}}|_{\text{m}}(t) - \frac{w_i^{\text{bot}} + w_i^{\text{up}}}{2} = \frac{4}{\pi^2} \cdot \left(w_i^{\text{up}} - w_i^{\text{bot}}\right) \cdot \sum_{n=0}^{\infty} \frac{e^{-(n+\frac{1}{2})^2 \cdot \frac{\pi^2}{L^2} \cdot D \cdot t}}{(2n+1)^2} \tag{20}$$

The obtained solution is the same as the one in the case of binary mixtures [12], so it can be corroborated that the solution calculated is correct.

Moreover, it should be added that there are some restrictions [11] that diagonal and cross-diagonal molecular diffusion coefficients must satisfy, and which can also be used for validation of the obtained results [11]. According to Taylor and Krishna [6], the restrictions are the following:

The diagonal diffusion coefficients are positive:

$$D_{11} > 0$$

$$D_{22} > 0 \tag{21}$$

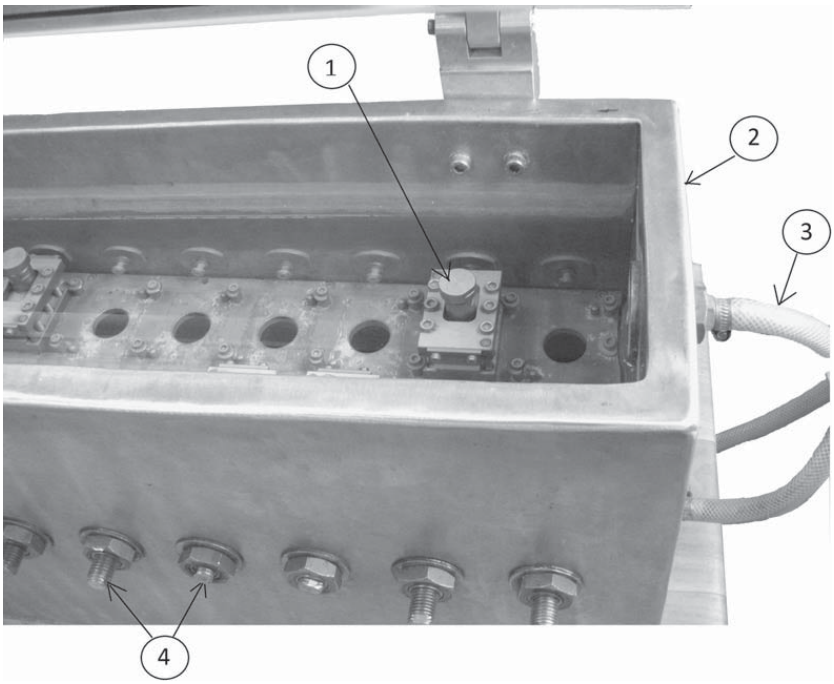

Fig. 1. Installation of the SST technique. (1) Sets of the SST technique; (2) water bath; (3) water circuit for temperature control; (4) screws used to make the tubes slide from one position to the other.

The determinant $\overline{\overline{D}}$ of the diffusion matrix is positive:

$$D_{11}D_{22} - D_{12}D_{21} > 0 \tag{22}$$

The eigenvalues (4) and (5) are real:

$$(D_{11} - D_{22})^2 + 4 \cdot D_{12} \cdot D_{21} \geqslant 0 \tag{23}$$

2.3. Equipment and procedure

The SST equipment, designed and constructed in Mondragon Goi Eskola Politeknikoa has been used to determine the molecular diffusion coefficient [10].

In an experimental run, 10 sets of tubes are filled and put in the 'separated tubes' position. Then, all the sets are placed in the water bath, described in Fig. 1, so that the mixtures are maintained at the working temperature during all the experiment. The temperature of the water in the bath is controlled by a thermostatic bath with a temperature control of 0.1 °C. To ensure that the mixture is at the working temperature, the sets are placed in the water bath 48 hours prior to the experiment in the 'separated tubes' configuration.

Once the mixture has reached the working temperature, all the sets are changed to 'faced tubes' position by the external screws. Since this moment, at prescribed time intervals, each set is changed to 'separated tubes' position. After stopping the molecular diffusion process, the concentration of each tube is analyzed. Therefore, at the end of the experiment, the variation of the mean concentration with time in each tube is obtained.

To determine the concentration in each point, the density and the refractive index of the mixture were measured by an *Anton Paar DMA 5000* vibrating quartz U-tube densimeter with an accuracy of 5×10^{-6} g/cm^3 and by an *Anton Paar RXA* 156 refractometer with an accuracy of 2×10^{-5} nD, respectively. From the density and the refractive index, the concentration of each component is obtained by these equations:

$$w_1 = \frac{c'(\rho - a) - c(n_D - a')}{bc' - b'c} \tag{24}$$

$$w_2 = \frac{b(n_D - a') - b'(\rho - a)}{bc' - b'c} \tag{25}$$

$$w_3 = 1 - w_1 - w_2 \tag{26}$$

where ρ and n_D are the density and refractive index, respectively, and a, a', b, b', c and c' are the calibration parameters obtained for each mixture. Those parameters were obtained from calibration planes. In order to create these planes (Fig. 2), 25 mixtures with concentrations around the studied one were analyzed.

Measurements of density and refractive index allow us to determine the parameters which define the calibration planes. In the case of the mixture analyzed in this work, the calibration parameters were those shown in Table 1.

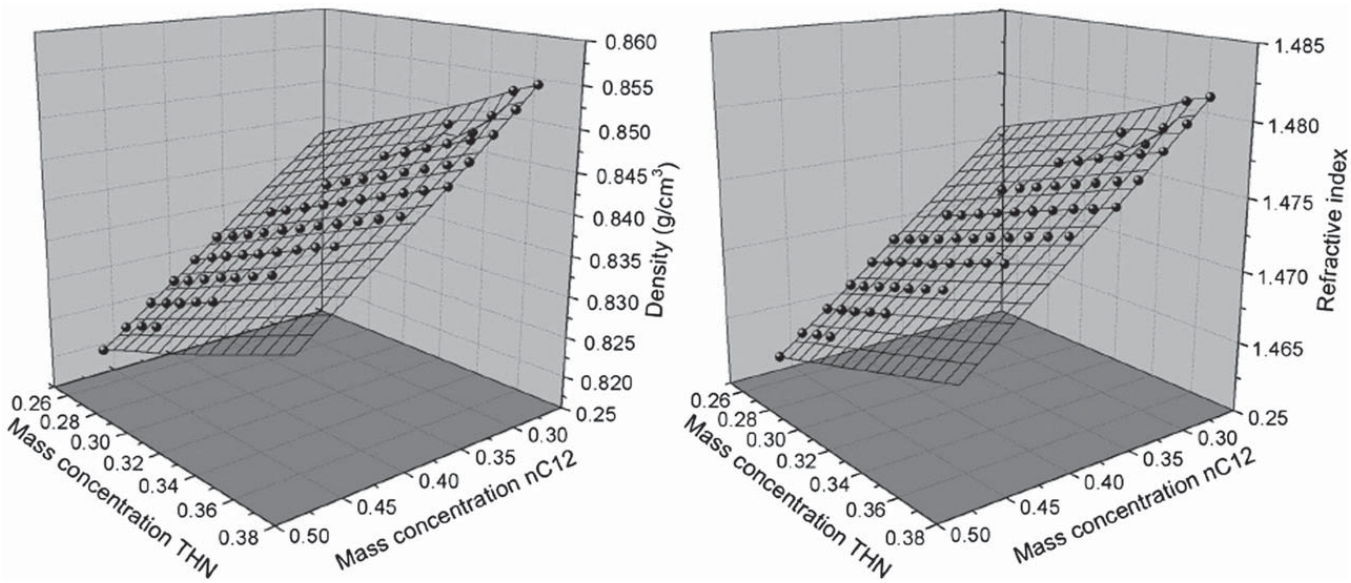

Fig. 2. Calibration planes for THN–*n*C12–IBB mixture around the point with mass fraction (1:1:1) at 25 °C.

Table 1
Calibration parameters for THN–*n*C12–IBB mixture with mass fraction of (1:1:1), and at 25 °C.

a	0.848055	a'	1.483118
b	0.101957	b'	0.047281
c	−0.115442	c'	−0.071592

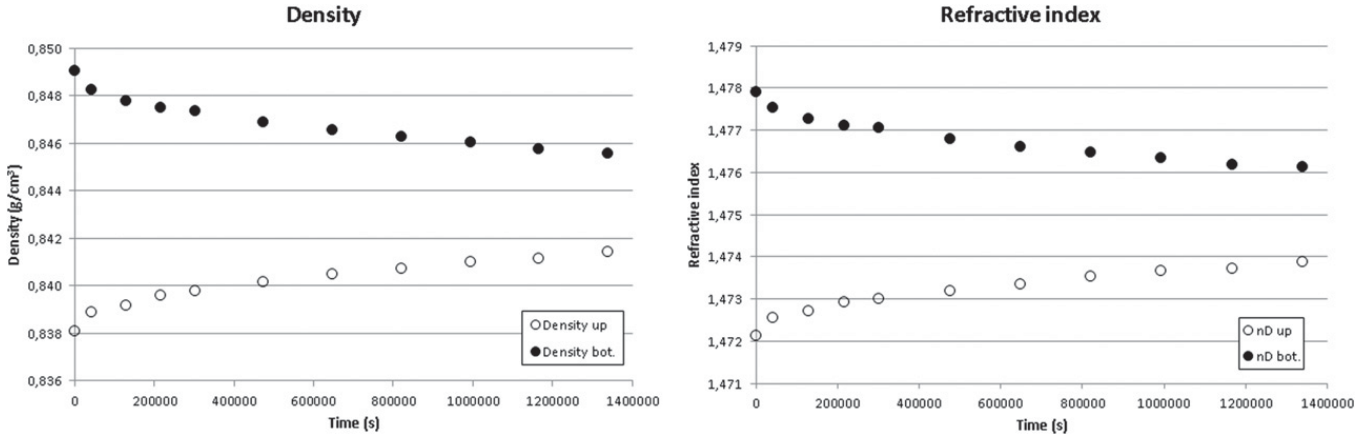

Fig. 3. Density and refractive index variation in the upper and the bottom tubes for THN–*n*C12–IBB mixture with mass fraction of (1:1:1) at 25 °C.

3. Results and discussion

3.1. Experimental results

The mixture used in this study was formed by THN, *n*C12 and IBB at 1/3 mass fraction of each component. All the components were purchased from Merck with purity better than 99% in the case of *n*C12 and better than 98% in the case of THN and IBB. The studied mixtures were prepared by weight using a *Gram VXI-310* digital scale with a precision of 1×10^{-4} g, introducing them in decreasing order of volatility. After the preparation, density and refractive index were measured in order to confirm, using the calibration, that the mixture had the intended composition.

During this study, THN was taken as component 1 and *n*C12 was taken as component 2. The mass fraction of the third component, IBB, is obtained from Eq. (26). The variations of density and refractive index with respect to time were determined and the corresponding results for the components 1 and 2 in the upper and bottom tubes are shown in Fig. 3.

Using Eqs. (24) and (25) and the experimental data, the variation of the concentration of each component with time was determined, see Fig. 4.

The initial concentrations of each component in this experiment are displayed in Table 2.

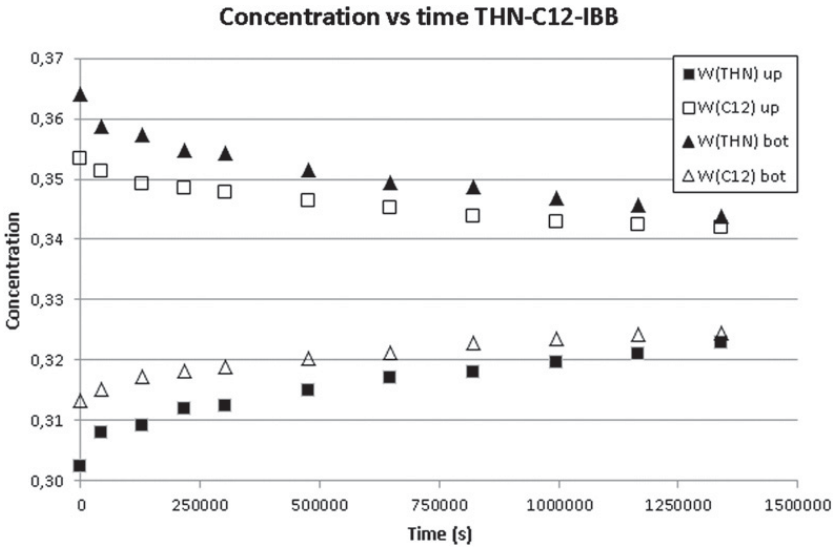

Fig. 4. Variation of the concentration of the components 1 and 2 with time, for THN–*n*C12–IBB mixture with mass fraction of (1:1:1) at 25 °C.

Table 2
Initial concentrations of each component in the experiment.

	THN	*n*C12	IBB
Upper tube	0.3033	0.3533	0.3433
Bottom tube	0.3633	0.3133	0.3233

3.2. Fitting

Direct determination of the four diffusion coefficients from the experimental results is impossible because a system of two equations contains four unknowns. Four-parameter fittings are not always stable. Because of that, the effect of the fitting procedure on the values of the determined diffusion coefficients is analyzed. Two teams, one from the University of Mondragon, and another from the University of Brussels have tested different fitting procedures.

3.2.1. Fitting tests by "fminsearch" using simultaneously four sets of concentrations

The obtained experimental results provide information about the variation of the concentration of each component with time, $\overline{w}(t)$. The four analytical expressions (11)–(14) determine the function $\overline{\phi}$, which is linked with concentration $\overline{w}(t)$ via matrix $\overline{\overline{P}}$, see Eq. (6). Before applying a transformation from $\overline{\phi}$ to $\overline{w}$ the number of terms of the summation that it was going to be used in Eqs. (11)–(14) should be fixed. In the literature there exist works where only the first term of the series is taken, that corresponds to $n = 0$ [4,11,20]. This approach is correct only if the rest of the terms of the summation are insignificant. Here large number of terms ($n = 100$) were used in order to take into account all experimental points from the beginning of the experiment. The fitting procedure searches diffusion coefficients which correspond to minimal difference between analytical and experimental time-dependent profiles.

In this section, a simultaneous fitting of four sets of concentrations (components 1 and 2 in the upper and the bottom tubes) is discussed. The fitting procedure needs an initial guess from which the program starts searching the solution. The fitting was undertaken by the function "*fminsearch*" of the *MATLAB* software [21] and its results are shown in Fig. 5. The used starting data were: $D_{11} = D_{12} = D_{21} = D_{22} = 1 \times 10^{-9}$.

The fitting procedure converges to a solution which satisfied to the restrictions imposed on diffusion coefficients in ternary mixtures (Eqs. (21)–(23)). The obtained coefficients are given in Table 3 (first row), where THN as component 1 and *n*C12 as component 2.

Several tests were done in order to make sure that the fitting was correct. First, the fitting was repeated with different initial guesses, in order to check that the solution converges to a global minimum instead of a local one. In all cases, the fitting converges to the same set of diffusion coefficients.

Second, reproducibility of the fitting was verified. From the obtained solution, the new points of $w(t)$ that correspond to the obtained diffusion values were calculated. Then, the fitting was applied again. It was expected that the solution obtained would be the same; however, although the obtained curve in the second case coincided with the initial curve (Fig. 6), the values of the diffusion coefficients, especially the ones with lower order, changed noticeably (see first two rows in Table 3).

Although the fitting was converging, it seems that the solution for the fitting is not unique. In the case of D_{11} and D_{12} the variation is small and reasonable; however, in the case of D_{21} and D_{22} the difference is considerable. In addition, D_{11}

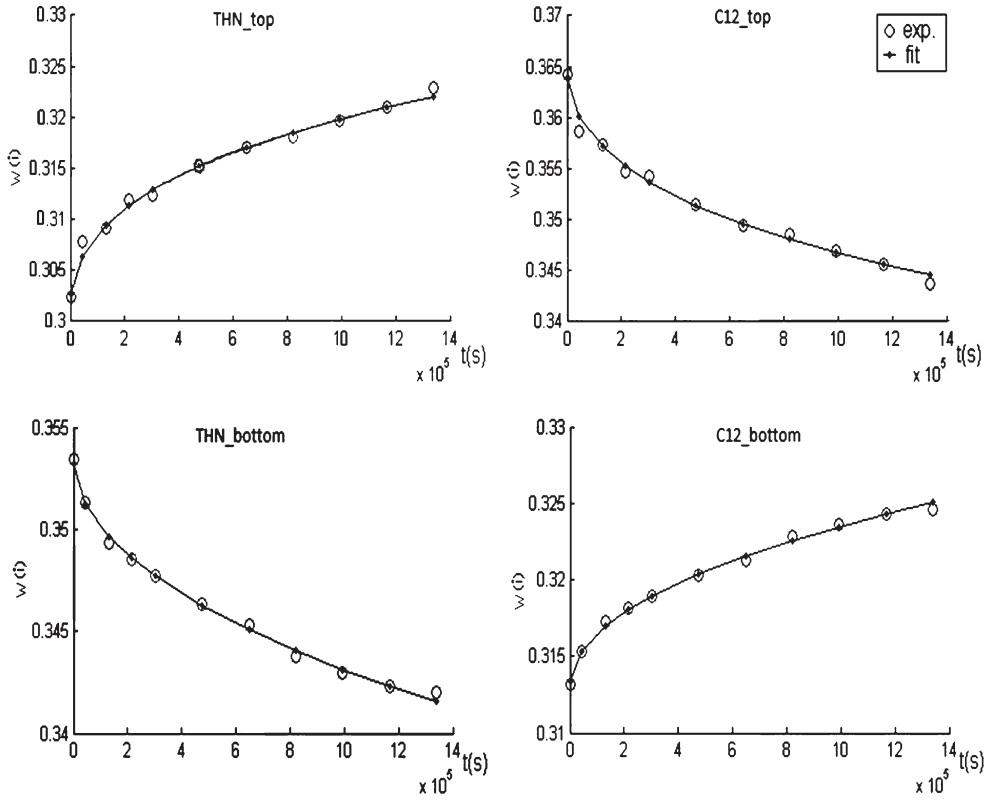

Fig. 5. Simultaneous fitting of four concentrations: components 1 and 2 in the upper and the bottom tubes for THN–*n*C12–IBB mixture with mass fraction of (1:1:1) at 25 °C.

Table 3
Diffusion coefficients obtained by the different fitting procedures for THN–*n*C12–IBB.

Fitting procedure		D_{11} 10^{-9} (m^2/s)	D_{12} 10^{-9} (m^2/s)	D_{21} 10^{-9} (m^2/s)	D_{22} 10^{-9} (m^2/s)	λ_1 10^{-10} (m^2/s)	λ_2 10^{-10} (m^2/s)
"fminsearch"	original fit	6.693	8.135	−0.348	0.252		
	repeated (2nd)	6.638	8.051	−0.213	0.440		
Simplex	2-parameter fit	0.947	10^{-16}	10^{-16}	0.737	7.37	9.47
Trust region method	4-parameter fit	0.982	0.047	∼0	0.74	7.4	9.82
OBD, Ref. [23]						6.81	10.99

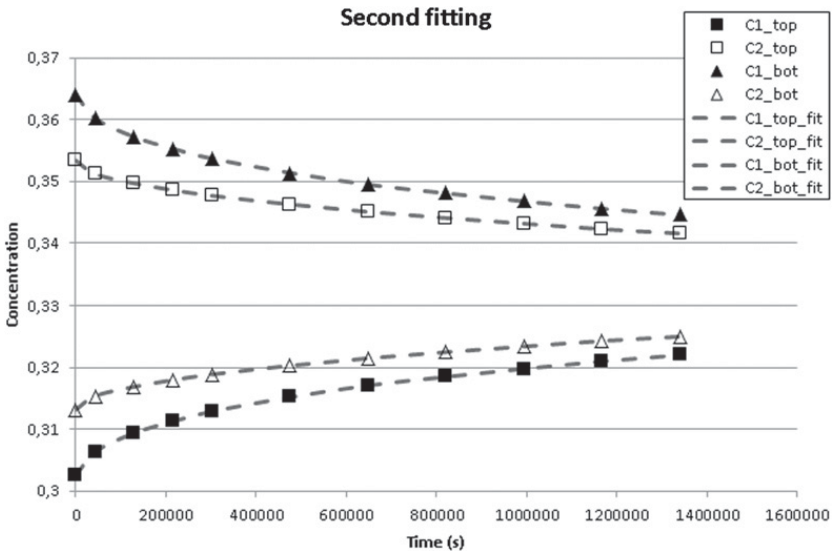

Fig. 6. Results after the second fitting on the calculated points.

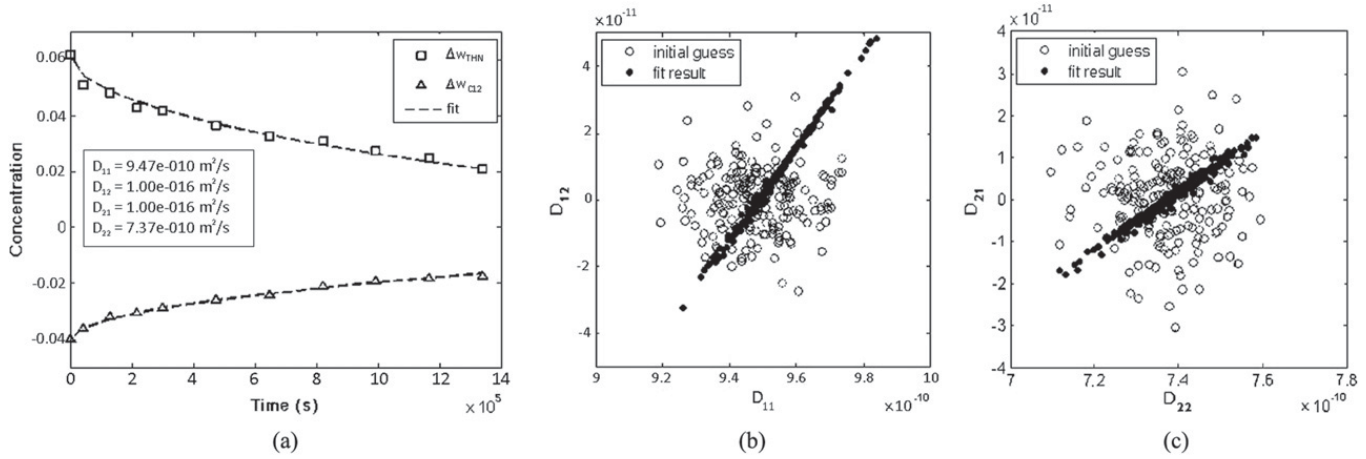

Fig. 7. Results of different fitting procedures: (a) fitting of the experimental points by two-parameter simplex method; (b) and (c) show the dependence of the final fitting results on initial guesses for four-parameter fit by trust region method. Open circles indicate initial guess for pairs of diffusion coefficients (b) D_{12}–D_{11} and (c) D_{21}–D_{22}, while filled circles summarize points to which fitting converges.

and D_{12} are too large in comparison with the largest diffusion coefficients in corresponding binary mixtures [12,14,22]. Therefore, the obtained values for the diffusion coefficients D_{ij} shown in Table 3 cannot be taken as valid, and this requires further investigation.

3.2.2. Fitting tests by simplex and trust region methods using concentration difference

Hereafter the values to be fitted were concentration differences between the upper and bottom parts for components 1 and 2, namely $w_1^{\mathrm{bot}}|_{\mathrm{m}}(t) - w_l^{\mathrm{up}}|_{\mathrm{m}}(t)$ and $w_2^{\mathrm{bot}}|_{\mathrm{m}}(t) - w_2^{\mathrm{up}}|_{\mathrm{m}}(t)$. Two very different fitting algorithms have been used. First is unconstrained Nelder–Mead (*simplex*) method [22] implemented in *"fminsearch"* function of MATLAB. Second is *trust region method*, both unconstrained and constrained, implemented in *"lsqnonlin"* function of MATLAB. Both methods display some advantages and disadvantages, which are discussed in details below.

As the extraction of ternary diffusion coefficients is a very complex task, it is common to divide it on several simple and clear steps. For example, initial step often consists in searching for only diagonal elements of diffusion matrix, assuming cross-diagonal elements vanished. To follow the same approach, D_{12} and D_{21} were fixed to be equal 10^{-16} m^2/s and only D_{11} and D_{22} were varying. In this case, most robust and fast was optimization by simplex method, it converged to the same values of diagonal elements independently of initial guess. Obtained values are reasonable, $D_{11} = 9.47 \times 10^{-10}$ m^2/s and $D_{22} = 7.37 \times 10^{-10}$ m^2/s, see the third line in Table 3. Fitting curves corresponding to these parameters are shown in Fig. 7(a).

But in the next step, when the above diagonal elements were provided as initial guess for four-parameter fit, the *simplex* method fails. In this step the absence of constraints plays a negative role, allowing the *simplex* algorithm to converge to unreasonable values. The *trust region method* appears to be more robust in the case of larger number of fit parameters and better initial guess. To test robustness of the fit, a set of initial guesses generated around 'basic' initial guess with random normal distribution has been used.

Results of the fitting run alone with initial guesses are plotted in parameter space D_{12}–D_{11} and D_{21}–D_{22} in Figs. 7(b, c). Remarkably, fit result forms strait lines in both spaces. Appearance of these lines does not come into surprise as coefficients in both couples 'balance' each other, see Eq. (6). But presence of these lines provides clear insight into problem of appearing and location of unreasonable solutions: all of them seem to converge to the same lines as well, but much far from realistic value.

Among all fit results obtained in the last step one with least magnitude of objective function has been chosen as a provisional result, which is $D_{11} = 9.82 \times 10^{-10}$ m^2/s, $D_{12} = 0.47 \times 10^{-10}$ m^2/s, $D_{21} \sim 0$ m^2/s and $D_{22} = 7.4 \times 10^{-10}$ m^2/s, see the fourth line in Table 3. By the order of the magnitude these values are comparable with diffusion coefficients in corresponding binary mixtures. But strictly speaking these meaningful coefficients cannot be considered as final true value. This conclusion rises from the fact that the trust region method, provided with 'good' initial guess in the vicinity of local minimum of objective function, is unable to find better solution far in parameter space. At the same time, the method fails to converge in case when initial guess is rather far from being good. The results of all the fittings are summarized in Table 3.

Although the results are not reliable, they have been compared to the available results in the literature; for the symmetric point (1:1:1) exists the only one result [23], which was obtained by the Optical Beam Deflection technique in the system with different order of the components (*n*C12–IBB–THN). However, the eigenvalues of diffusion matrix λ_1 and λ_2, Eqs. (4) and (5), do not depend on the order of the components as it is specified in [23].

The comparison of the eigenvalues between our results and those of Ref. [23] (see Table 3) shows a reasonable agreement: λ_1 differs by 8% and λ_2 by 10.5%.

4. Conclusions

An experimental methodology has been developed to determine the variation of the concentration of each component with time. The analytical solution of equations for ternary mixture with boundary conditions corresponding to SST technique has been obtained. Resulting system of two equations contains four unknown diffusion coefficients, D_{ij}. However, four-parameter fitting using "simplex" method and taking into account the restrictions for molecular diffusion coefficients is not enough precise to determine the molecular diffusion coefficients, especially the ones of lower order.

With successfully chosen initial guess the fit by the "trust region method" converges to definite value within close region around this guess; but there is no guarantee that the initial guess is best possible. So, there is some uncertainty still.

Definitely, larger number of experiments would improve the fitting, but it is difficult to define a priori how many experiments are required. This issue can be clarified in the future additional tests.

Another conclusion from the comparison of the results is that researchers should agree on the order of components in ternary mixtures. In recent paper [24] was suggested to choose the denser component as the first one, and then by decreasing of density.

Acknowledgements

This article presents the work done in the framework of the projects GOVSORET3 (PI2011-22), Research Groups (IT557-10) and the Research Fellowship (BFI-2011-295), of the Basque Government; and the project DCMIX of the European Space Agency. MRC, ULB researchers are supported by the PRODEX programme of the Belgian Federal Agency.

References

[1] A. Fick, Über diffusion, Poggendorff's Ann. Phys. 94 (1855) 59–86.
[2] E.L. Cussler, Diffusion Mass Transfer in Fluid Systems, Cambridge University Press, New York, 1997.
[3] A.A. Alizadeh, W.A. Wakeham, Mutual diffusion coefficients for binary mixtures of normal alkanes, Int. J. Thermophys. 3 (1982) 307.
[4] J. Dutrieux, J.K. Platten, G. Chavepeyer, M.M. Bou-Ali, On the measurement of positive Soret coefficients, J. Phys. Chem. B 106 (2002) 6104–6114.
[5] W. Köhler, S. Wiegand (Eds.), Thermal Nonequilibrium Phenomena in Fluid Mixtures, Springer, Berlin, 2002.
[6] R. Taylor, R. Krishna, Multicomponent Mass Transfer, John Wiley & Sons Inc., New York, 1993.
[7] E.L. Cussler, Multicomponent Diffusion, Elsevier Scientific Publishing Company, Amsterdam, 1976.
[8] P.W. Rutten, Diffusion in Liquids, Delft University Press, Delft, 1992.
[9] J.V. Tyrrell, K.R. Harris, Diffusion in Liquids, Butterworth & Co., London, 1984.
[10] P. Blanco, M.M. Bou-Ali, P. Urteaga, Un Dispositivo de Difusion Molecular para determinar el coeficiente de difusión molecular de Mezclas Líquidas a presión atmosférica y a temperatura constante y un método de obtenición del Coeficiente de Difusión Molecular, Patente ES 2351822 (A1), 2011.
[11] J.W. Mutoru, A. Firoozabadi, Form of multicomponent Fickian diffusion coefficients matrix, J. Chem. Thermodyn. 43 (2011) 1192–1203.
[12] D. Alonso de Mezquia, M.M. Bou-Ali, M. Larrañaga, J.A. Madariaga, C. Santamaria, Determination of molecular diffusion coefficient in *n*-alkane binary mixtures: Empirical correlations, J. Phys. Chem. B 116 (2012) 2814–2819.
[13] D. Alonso de Mezquia, P. Blanco, M.M. Bou-Ali, A. Zebib, New technique for measuring the molecular diffusion coefficients of binary liquid mixtures, in: European Thermodynamics Seminar EURO-THERM 84, Namur, Belgium, 2009.
[14] J.K. Platten, M.M. Bou-Ali, P. Costeséque, J. Dutrieux, W. Köhler, S. Wiegand, G. Wittko, Benchmark values for the Soret, thermal diffusion and diffusion coefficients of three binary organic liquid mixtures, Philos. Mag. 83 (2003) 1965–1971.
[15] A. Leahy-Dios, A. Firoozabadi, Effect of molecular shape and size on molecular and thermal diffusion coefficients of binary mixtures, J. Phys. Chem. B 111 (2007) 191–198.
[16] K.J. Zhang, M.E. Briggs, R.W. Gammon, J.V. Sengers, Optical measurement of the Soret coefficient and the diffusion coefficient of liquid mixtures, J. Chem. Phys. 104 (1996) 6881–6892.
[17] P. Kolodner, H. Williams, C. Moe, Optical measurement of the Soret coefficient of ethanol/water solutions, J. Chem. Phys. 88 (1988) 6512–6524.
[18] A. Mialdun, V. Shevtsova, Development of optical digital interferometry technique for measurement of thermodiffusion coefficients, Int. J. Heat Mass Transfer 51 (2008) 3164–3178.
[19] W. Köhler, B. Muller, Soret and mass diffusion coefficients of toluene/*n*-hexane mixtures, J. Chem. Phys. 103 (1995) 4367–4370.
[20] A. Leahy-Dios, M.M. Bou-Ali, J.K. Platten, A. Firoozabadi, Measurements of molecular and thermal diffusion coefficients in ternary mixtures, J. Chem. Phys. 122 (2005) 234502.
[21] MATLAB Version R2011a, The Math Works Inc., Natick, USA, 2011.
[22] A. Mialdun, V. Shevtsova, Measurements of the Soret and diffusion coefficients for benchmark binary mixtures by means of digital interferometry, J. Chem. Phys. 134 (2011) 044524.
[23] A. Königer, H. Wunderlich, W. Köhler, Measurement of diffusion and thermal diffusion in ternary fluid mixtures using a two-color optical beam deflection technique, J. Chem. Phys. 132 (2010) 174506.
[24] A. Mialdun, V. Yasnou, V. Shevtsova, A. Koeniger, W. Koehler, D. Alonso de Mezquia, M.M. Bou-Ali, A comprehensive study of diffusion, thermodiffusion, and Soret coefficients of water–isopropanol mixtures, J. Chem. Phys. 136 (2012) 244512.

D. Determination of the molecular diffusion coefficient in ternary mixtures by the sliding symmetric tubes technique.

Determination of the molecular diffusion coefficients in ternary mixtures by the sliding symmetric tubes technique

Miren Larrañaga,[1] D. Andrew S. Rees,[2] and M. Mounir Bou-Ali[1,a)]
[1]*MGEP Mondragon Goi Eskola Politeknikoa, Mechanical and Industrial Manufacturing Department, Loramendi 4 Apdo. 23, 20500 Mondragon, Spain*
[2]*Department of Mechanical Engineering, University of Bath, Claverton Down, Bath BA2 7AY, United Kingdom*

(Received 21 November 2013; accepted 23 January 2014; published online 6 February 2014)

A new analytical methodology has been developed to determine the diagonal and cross-diagonal molecular diffusion coefficients in ternary mixtures by the Sliding Symmetric Tubes technique. The analytical solution is tested in binary mixtures obtaining good agreement with the results of the literature. Results are presented for the ternary mixture formed by tetralin, isobutylbenzene, and dodecane with an equal mass fraction for all the components (1–1–1) which is held at 25 °C. Diagonal and cross-diagonal coefficients are determined for the three possible orders of components, in order to compare the results with those available in the literature. A comparison with published results shows a good agreement for the eigenvalues of the diffusion matrix, and a reasonable agreement for the diagonal molecular diffusion coefficients. © *2014 AIP Publishing LLC*. [http://dx.doi.org/10.1063/1.4864189]

I. INTRODUCTION

The phenomenon of molecular diffusion in multicomponent mixtures has attracted a great interest within the scientific community, and it has been analyzed in multiple processes of different sectors, such as human biology,[1] materials engineering,[2] or food industry.[3]

In 1855, Fick established the first quantitative relation for molecular diffusion, known as Fick's law,[4] and since then different experimental procedures have been developed in order to determine the molecular diffusion coefficient. In the case of binary mixtures, this phenomenon has been studied in depth and currently there are many well-established and proven experimental techniques which allow the determination of this coefficient. Among them are Thermal Diffusion Forced Rayleigh Scattering (TDFRS) (Ref. 5), Open Ended Capillary (OEC) (Ref. 6), Optical Beam Deflection,[7] Optical Digital Interferometry,[7] techniques that use the Taylor dispersion principle,[8] and the Sliding Symmetric Tubes (SST) technique.[9]

In the case of ternary mixtures, the existence of diagonal and cross-diagonal molecular diffusion coefficients makes their determination considerably more difficult. In the last few years, several works have been published in which the determination of these molecular diffusion coefficients has been attempted; however, the availability of results in the literature is limited, so currently, the reliability of these methods has still to be tested. For example, Königer *et al.*[10] tried to solve the problem applying a second wavelength for the determination by the Two Colour Optical Beam Deflection technique; Mialdun *et al.*[11] devised a new instrument based on interferometry to determine the molecular diffusion coefficients. Leahy-Dios *et al.*[12] used the OEC technique combining the density and refractive index measurements for the determination of the molecular diffusion coefficients and Santos *et al.*[13] and Capuano *et al.*[1] used the Taylor dispersion principle and the Gouy interferometer, respectively. In addition, simulations based on molecular dynamics[14] and prediction models[3] have been undertaken in order to determine the molecular diffusion coefficients in ternary mixtures. In Larrañaga *et al.*,[15] an analytical solution applied to SST technique was developed to determine the diffusion coefficients in ternary mixtures. Recently, Mialdun *et al.*[16] have published a new paper determining the molecular diffusion coefficients in ternary mixtures by two independent experimental techniques: Taylor dispersion technique and digital interferometry applied to a Counter Flow Cell.

As commented in Mialdun and Shevtsova,[17] the correct determination of the molecular diffusion coefficients is very important for the determination of the thermodiffusion coefficients because, except in the case of the thermogravitational column, in the other techniques it is necessary to consider these two diffusion coefficients combined with Soret coefficient, so that the thermodiffusion coefficient for each component may be determined.

Therefore, the principal objective of the present work is the determination of the diagonal and cross-diagonal molecular diffusion coefficients in ternary mixtures by the SST technique. To this end, the mixture formed by 1,2,3,4-tetrahydronaphthaline (THN), isobutylbenzene (IBB), and n-dodecane (nC12), with equal mass fraction and at 25 °C has been used. This mixture was selected by the group which takes part in the project DCMIX (Ref. 18) and which is formed by 14 teams at international level in order to perform analytical, numerical, and experimental studies both in terrestrial conditions and in microgravity, by the installation Selectable Optical Diagnostic Instrument (SODI) in the International Space Station and by applying a purely optical analysis system based on two wavelengths.

a)Author to whom correspondence should be addressed. Electronic mail: mbouali@mondragon.edu

This article is organized as follows. In Sec. II, the methodology, both experimental and analytical, for the determination of the molecular diffusion coefficients by the SST technique is described. In Sec. III, experimental results obtained for both binary and ternary mixtures and the discussion about them are presented. Finally, conclusions are given in Sec. IV.

II. METHODOLOGY

A. Experimental procedure

The SST technique has been successfully applied in the case of binary mixtures[19–21] and it consists of several sets of tubes (Figure 1) which have two positions. In the faced tubes position, the contents of both tubes are in contact and the transport of matter between the tubes arises by molecular diffusion. By contrast, in the separated tubes position the diffusive process is stopped. All the tubes are filled with the same mixture, but with a slight difference of concentration between the upper and bottom tubes. In an experiment, all the sets of tubes are filled in the separated tubes position and they are introduced into a water bath (see Figure 2) with a temperature control of 0.1 °C, which will maintain them at the same temperature throughout the whole experiment. At the beginning of the experiment all the sets are changed to the faced tubes position so that diffusion may be initiated. From that moment, at various predetermined intervals of time, each tube is changed to the separated tubes position, to preserve their contents for later analysis. At the end of the experiment, the variation of the concentration with time is constructed from the concentrations in each of the tubes (see Figure 3).

In order to determine the concentration of each point in a ternary mixture, its density and refractive index are measured by an Anton Paar DMA 5000 vibrating quartz U-tube densimeter with an accuracy of 5×10^{-6} g/cm^3 and by an Anton Paar RXA 156 refractometer with an accuracy of 2×10^{-5}

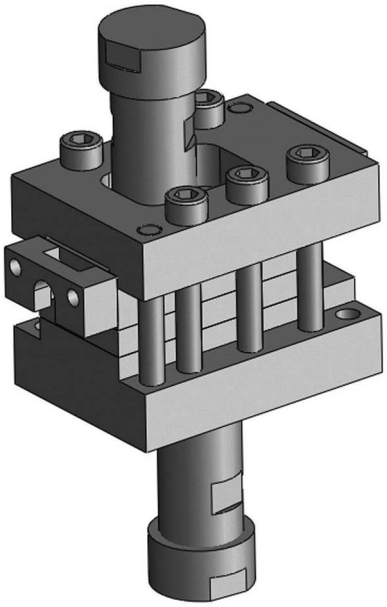

FIG. 1. A set of siding symmetric tubes.

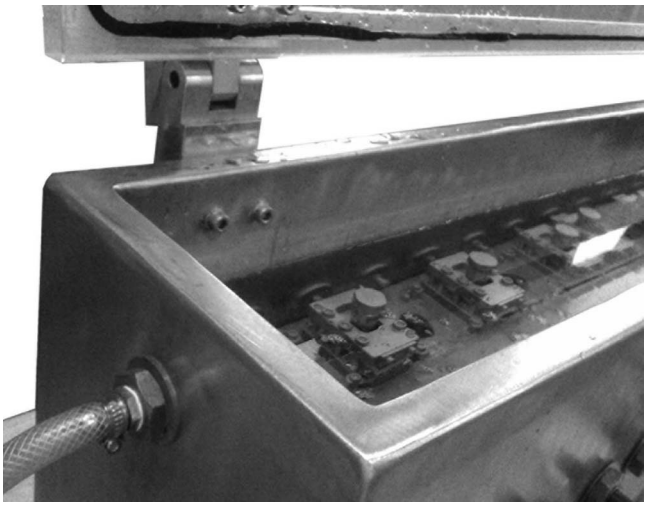

FIG. 2. Installation of the sliding symmetric tubes technique.

RIU, respectively. Mialdun and Shevtsova[17] and Sawicka and Soroka[22] show that these two properties allow the most accurate determination of the concentration of each component. In order to determine the concentration from the density and the refractive index it is necessary to do a prior calibration where measurements are made of the density and the refractive index of 25 mixtures with concentrations that are close to that of the study. Once the calibration coefficients are determined, the concentration of each component, w_i, in each point is calculated by the following equations:

$$w_1 = \frac{c'(\rho - a) - c(n_D - a')}{bc' - b'c}, \tag{1}$$

$$w_2 = \frac{b(n_D - a') - b'(\rho - a)}{bc' - b'c}, \tag{2}$$

$$w_3 = 1 - w_1 - w_2, \tag{3}$$

where ρ and n_D are the density and the refractive index, respectively, and a, a', b, b', c, and c' are the calibration

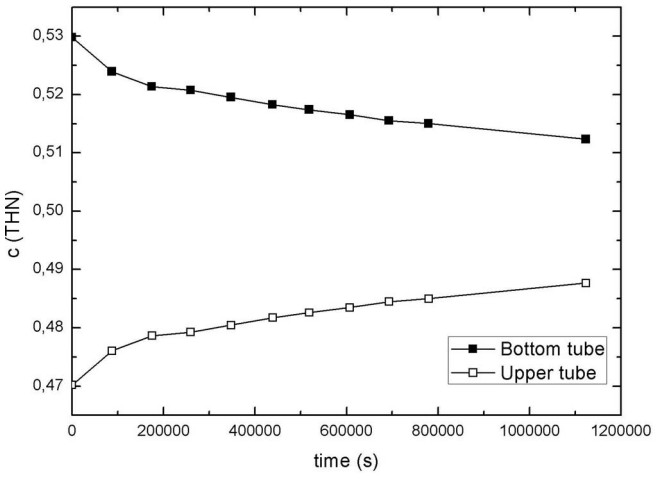

FIG. 3. Variation of the concentration with time in the upper and the bottom tubes determined by the SST technique, for the mixture THN-IBB with 50% mass fraction and at 25 °C.

parameters calculated for the mixture (see Larrañaga *et al.*[15] for details).

B. Analytical solution

First, an analytical solution for binary mixtures was developed, which allowed the determination of the molecular diffusion coefficient from the experimental measurements of the variation of the concentration with time.[19] The working equations are the following:

$$w^{bot}\,|_m(t) - \frac{w_i^{bot} + w_i^{up}}{2} = \frac{4}{\pi^2}\cdot\left(w_i^{bot} - w_i^{up}\right)\cdot\sum_{n=0}^{\infty}\frac{e^{-\left(n+\frac{1}{2}\right)^2\cdot\frac{\pi^2}{L^2}\cdot D\cdot t}}{(2n+1)^2}, \quad (4)$$

$$w^{up}\,|_m(t) - \frac{w_i^{bot} + w_i^{up}}{2} = \frac{4}{\pi^2}\cdot\left(w_i^{up} - w_i^{bot}\right)\cdot\sum_{n=0}^{\infty}\frac{e^{-\left(n+\frac{1}{2}\right)^2\cdot\frac{\pi^2}{L^2}\cdot D\cdot t}}{(2n+1)^2}, \quad (5)$$

where $w^{up}\,|_m(t)$ and $w^{bot}\,|_m(t)$ are the mean concentration in the upper and lower tubes respectively, as functions of time; w_i^{up} and w_i^{bot} are the respective initial concentrations, D is the molecular diffusion coefficient, which is constant in the case of small concentration variations, and L is the length of the tube.

As may be noted, the formulae given in Eqs. (4) and (5) are linearly dependent and therefore it follows, not surprisingly, that the molecular diffusion coefficient must be the same in both tubes for binary mixtures.

In Larrañaga *et al.*,[15] an initial analytical solution for ternary mixtures was obtained by following the same Fourier series procedure as for the case of binary mixtures. The evolution of the mean concentration of component j was found to take the following form:

$$\phi_j^{bot}\big|_m(t) - \frac{\phi_{ji}^{bot} + \phi_{ji}^{up}}{2} = \frac{4}{\pi^2}\cdot\left(\phi_{ji}^{bot} - \phi_{ji}^{up}\right)\cdot\sum_{n=0}^{\infty}\frac{e^{-\left(n+\frac{1}{2}\right)^2\cdot\frac{\pi^2}{L^2}\cdot\lambda j\cdot t}}{(2n+1)^2}, \quad (6)$$

$$\phi_j^{up}\big|_m(t) - \frac{\phi_{ji}^{bot} + \phi_{ji}^{up}}{2} = \frac{4}{\pi^2}\cdot\left(\phi_{ji}^{up} - \phi_{ji}^{bot}\right)\cdot\sum_{n=0}^{\infty}\frac{e^{-\left(n+\frac{1}{2}\right)^2\cdot\frac{\pi^2}{L^2}\cdot\lambda j\cdot t}}{(2n+1)^2}, \quad (7)$$

for $j = 1, 2$ and where $\phi_j^{up/bot}\,|_m(t)$ is the new variable for the mean concentration in the upper and the lower tubes, respectively, $\phi_{ji}^{up/bot}$ is the new variable for the initial concentration in the upper and the lower tubes, respectively, and the λ_j-values are the eigenvalues of the diffusion matrix.

As may be observed, these equations have now become considerably more complicated and in this case there are two linearly independent equations (for each components 1 and 2) with four unknowns (the two diagonal diffusion coefficients and another two cross-diagonal diffusion coefficients). That is why a nonlinear fitting had to be applied in order to determine the diffusion coefficients. Before applying the fitting, the changes of variable were undone, so that the equations became more complicated but we could fit directly the four diffusion coefficients. However, the complexity of the equations made it impossible to achieve reliable results with different fitting methods, as is detailed in Larrañaga *et al.*[15]

That difficulty has motivated the development of a new analytical solution which allows the determination of the diffusion coefficients for both binary and ternary mixtures. The new analytical solution is based on the well-known self-similar solution of Fourier's equation for an impulsively heated solid which is found in Carslaw and Jaeger,[23] and it is described hereafter; the method is illustrated first for binary mixtures and then it is extended to ternary mixtures.

C. New analytical solution for binary mixtures

It is intended to solve Fick's second law,

$$\frac{\partial w}{\partial t} = D\cdot\frac{\partial^2 w}{\partial y^2}, \quad (8)$$

for relatively short times, by which we mean that the developing interface between the upper and lower tubes has not yet reached the far ends of those tubes. In this regime, the evolving front satisfies a self-similar solution for which the following changes of variable are required:

$$\eta = \frac{y}{2\sqrt{Dt}}, \quad (9)$$

$$\tau = \sqrt{t}, \quad (10)$$

where y is the vertical variable. While within the self-similar regime the time-derivative may be neglected and therefore the equation for the concentration transforms to

$$w'' + 2\eta w' = 0, \quad (11)$$

where w' and w'' are the first and the second derivatives of the concentration with respect to η.

The boundary conditions in this case, taking into account the variable transformation, are the following:

$$\begin{aligned} w &\to w_i^{bot} \ \text{ as } \ \eta \to -\infty, \\ w &\to w_i^{up} \ \text{ as } \ \eta \to +\infty, \end{aligned} \quad (12)$$

where w_i^{up} and w_i^{bot} are the initial concentration in the upper and lower tubes, respectively. Upon solving Eq. (11), the following expression for the concentration is obtained:

$$w = w_i^{up} + \frac{w_i^{bot} - w_i^{up}}{2}\operatorname{erfc}(\eta), \quad (13)$$

where $\operatorname{erfc}(\eta)$ is the well-known complementary error function of η.[23]

The mean concentration in each tube is obtained by integrating the solution given in Eq. (13) over the length of the tube, and then dividing it by the length of the tube, L,

$$\frac{1}{L}\int_0^L w\,\mathrm{d}y = w_i^{up} + \frac{\left(w_i^{bot} - w_i^{up}\right)}{L}\sqrt{\frac{Dt}{\pi}}. \quad (14)$$

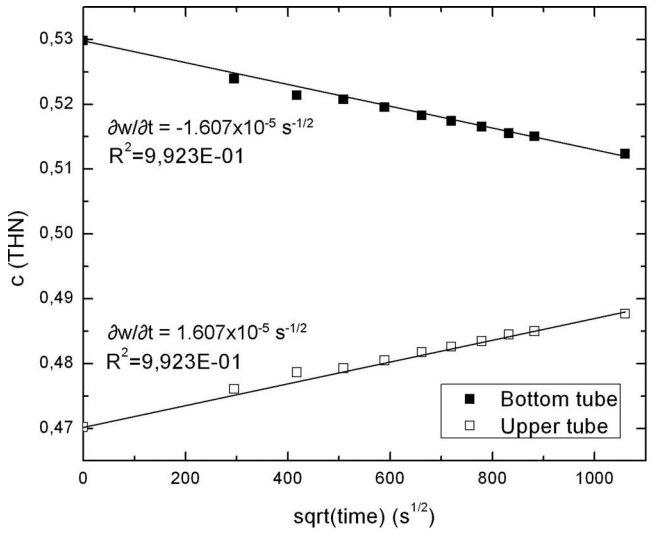

FIG. 4. Variation of the concentration with the square root of time for the mixture THN-IBB at 50% of mass fraction at 25 °C.

It is important to note that Eq. (14) remains valid until the diffusion front (i.e., the region of mixing between the two reservoirs) begins to reach the ends of the tubes. Equation (14) shows that the mean concentration varies linearly with $t^{1/2}$ and therefore Figure 4 has been created to show this linear variation of the upper and lower mean concentrations with the square root of time for the mixture THN-IBB with mass fraction of 50% and at 25 °C. As can be seen, the variations are almost linear and therefore the molecular diffusion coefficient as given by the upper tube data may be determined directly by the following expression:

$$S^{up} = \frac{\left(w_i^{bot} - w_i^{up}\right)}{L}\sqrt{\frac{D}{\pi}}, \tag{15}$$

where S^{up} is the slope of the linear regression formed by the concentration points in the upper tube. If the slope formed by the concentration points in the lower tube is taken, then the diffusion coefficient which is obtained is the same. The presence of linearity in Figure 4 also shows that the diffusion front has not reached the ends of the tubes, and therefore the self-similar solution given in (13) is valid.

D. New analytical solution for ternary mixtures

In the case of ternary mixtures, the procedure is similar to the case of binary mixtures, but it is necessary to use a second change of variable in order to account for the presence of two different eigensolutions of the diffusion matrix, as will be seen. For ternary mixtures, Fick's second law may be written as follows:

$$\frac{\partial w_1}{\partial t} = D_{11}\cdot\frac{\partial^2 w_1}{\partial y^2} + D_{12}\cdot\frac{\partial^2 w_2}{\partial y^2}, \tag{16}$$

$$\frac{\partial w_2}{\partial t} = D_{21}\cdot\frac{\partial^2 w_1}{\partial y^2} + D_{22}\cdot\frac{\partial^2 w_2}{\partial y^2}, \tag{17}$$

where D_{11} and D_{22} are the diagonal diffusion coefficients and D_{12} and D_{21} are the cross-diagonal diffusion coefficients. The variable changes applied in this case are the following:

$$\eta = \frac{y}{2\sqrt{t}}, \tag{18}$$

$$\tau = \sqrt{t}, \tag{19}$$

$$z = \alpha\eta, \tag{20}$$

where α is an eigenvalue which is to be found. Once more we assume that the diffusion front has not reached the extreme ends of the tubes, and therefore the following self-similar equations are obtained for the concentrations of the components 1 and 2:

$$D_{11}\alpha^2 w_1'' + 2z w_1' + D_{12}\alpha^2 w_2'' = 0, \tag{21}$$

$$D_{21}\alpha^2 w_1'' + D_{22}\alpha^2 w_2'' + 2z w_2' = 0, \tag{22}$$

where primes now denote derivatives with respect to the variable z.

The boundary conditions in this case are similar to the ones in the case of binary mixtures:

$$\begin{aligned} &w_1 \to w_{i1}^{bot} \text{ and } w_2 \to w_{i2}^{bot} \text{ as } \eta \to -\infty, \\ &w_1 \to w_{i1}^{up} \text{ and } w_2 \to w_{i2}^{up} \text{ as } \eta \to +\infty, \end{aligned} \tag{23}$$

where w_{i1}^{up}, w_{i1}^{bot}, w_{i2}^{up}, and w_{i2}^{bot} are the initial conditions of the components 1 and 2 in the upper and lower tubes, respectively.

Upon solving Eqs. (21) and (22), the following expressions are obtained for the concentrations of the two components:

$$w_1 = A\,\mathrm{erfc}\,(z_1) + B\,\mathrm{erfc}\,(z_2) + w_{i1}^{up}, \tag{24}$$

$$\begin{aligned} w_2 = {} & A\left(\frac{1 - D_{11}\alpha_1^2}{D_{12}\alpha_1^2}\right)\mathrm{erfc}\,(z_1) \\ & + B\left(\frac{1 - D_{11}\alpha_2^2}{D_{12}\alpha_2^2}\right)\mathrm{erfc}\,(z_2) + w_{i2}^{up}, \end{aligned} \tag{25}$$

where the constants A and B are given by the following functions of the diffusion coefficients and the initial concentrations of the components 1 and 2 in the upper and the lower tubes:

$$A = \frac{D_{12}\alpha_1^2\alpha_2^2\left(w_{i2}^{bot} - w_{i2}^{up}\right) - \alpha_1^2\left(w_{i1}^{bot} - w_{i1}^{up}\right)\left(1 - D_{11}\alpha_2^2\right)}{2\left(\alpha_2^2 - \alpha_1^2\right)}, \tag{26}$$

$$B = \frac{D_{12}\alpha_1^2\alpha_2^2\left(w_{i2}^{bot} - w_{i2}^{up}\right) - \alpha_2^2\left(w_{i1}^{bot} - w_{i1}^{up}\right)\left(1 - D_{11}\alpha_1^2\right)}{2\left(\alpha_1^2 - \alpha_2^2\right)}, \tag{27}$$

the values α_1 and α_2, which are proportional to the eigenvalues of the diffusivity matrix, are given by

$$\alpha_1 = \sqrt{\frac{-(D_{11}+D_{22}) - \sqrt{(D_{11}+D_{22})^2 + 4(D_{12}D_{21} - D_{11}D_{22})}}{2(D_{12}D_{21} - D_{11}D_{22})}}, \tag{28}$$

$$\alpha_2 = \sqrt{\frac{-(D_{11}+D_{22})+\sqrt{(D_{11}+D_{22})^2+4(D_{12}D_{21}-D_{11}D_{22})}}{2(D_{12}D_{21}-D_{11}D_{22})}}, \tag{29}$$

and

$$z_1 = \alpha_1 \eta, \tag{30}$$

$$z_2 = \alpha_2 \eta. \tag{31}$$

As in the case of binary mixtures, the expressions given in Eqs. (24) and (25) are integrated and then divided by the length of each tube to give the mean concentration for each component in each of the tubes:

$$\frac{1}{L}\int_0^L w_1 \mathrm{d}y = w_{i1}^{up} + \frac{2}{L}\sqrt{\frac{t}{\pi}}\left(\frac{A}{\alpha_1}+\frac{B}{\alpha_2}\right), \tag{32}$$

$$\frac{1}{L}\int_0^L w_2 \mathrm{d}y = w_{i2}^{up} + \frac{2}{L}\sqrt{\frac{t}{\pi}}\left(\frac{A}{\alpha_1}\left(\frac{1-D_{11}\alpha_1^2}{D_{12}\alpha_1^2}\right)+\frac{B}{\alpha_2}\left(\frac{1-D_{11}\alpha_2^2}{D_{12}\alpha_2^2}\right)\right). \tag{33}$$

Equations (32) and (33) show that, in the case of ternary mixtures, the concentration of each component also varies linearly with the square root of time. Equations (32) and (33) may be therefore manipulated as before to give the slope of the line corresponding to each component:

$$S_1 = \frac{2}{L\sqrt{\pi}}\left(\frac{A}{\alpha_1}+\frac{B}{\alpha_2}\right), \tag{34}$$

$$S_2 = \frac{2}{L\sqrt{\pi}}\left(\frac{A}{\alpha_1}\left(\frac{1-D_{11}\alpha_1^2}{D_{12}\alpha_1^2}\right)+\frac{B}{\alpha_2}\left(\frac{1-D_{11}\alpha_2^2}{D_{12}\alpha_2^2}\right)\right), \tag{35}$$

where S_1 and S_2 are the slopes formed by the linear regression of the concentration of components 1 and 2, respectively, with respect to the square root of time.

In order to determine the molecular diffusion coefficients in ternary mixtures, it is necessary to have experimental data from two independent experiments of the same mixture where the initial concentrations are different. In this way, a system of four equations (i.e., Eqs. (34) and (35) for two different experiments) and four unknowns (the four diffusion coefficients) is obtained. It is impossible to solve for the four coefficients analytically because the four equations are highly nonlinear, but they may be found very rapidly using a straightforward four-dimensional Newton-Raphson method.

III. RESULTS AND DISCUSSION

In this section, first the molecular diffusion coefficients in binary mixtures determined by the classical and new analytical solutions are shown and compared, and then, the diagonal and cross-diagonal molecular diffusion coefficients in ternary mixtures are determined from the new analytical solution.

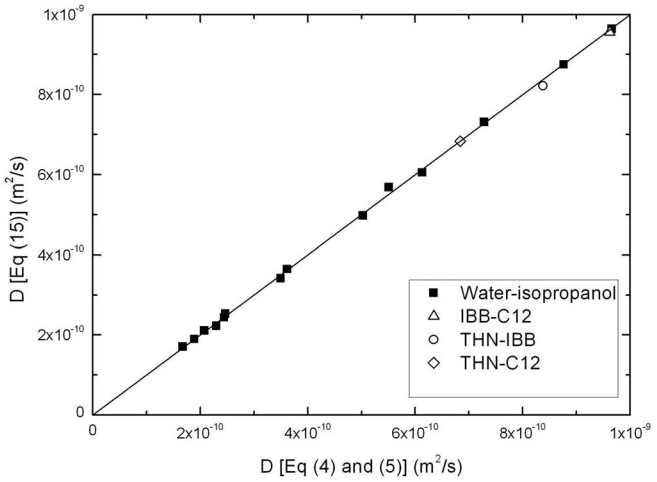

FIG. 5. Comparison of the results obtained by Eqs. (4) and (5), and Eq. (15) for the binary mixtures formed by THN, IBB, and *n*C12 with 50% of mass fraction and the mixture formed by water-isopropanol for many different mass concentrations of water; all cases are at 25 °C.

A. Binary mixtures

In previous works,[19–21] the validity of the SST technique and the classical analytical solution (given by Eqs. (4) and (5)) for the determination of the molecular diffusion coefficients in binary mixtures have been shown to be accurate. Figure 5 compares the results obtained by the present new formulation (given by Eq. (15)) with the ones obtained by the classical solution (given by Eqs. (4) and (5)). The data used are for the binary mixtures formed by THN, IBB, and *n*C12 with 50% of mass fraction and at 25 °C, and for the mixture water-isopropanol for many different mass concentrations of water and at 25 °C.

The very good agreement between the results obtained by the two methods demonstrates the validity of the new analytical solution developed in this work, for the case of binary mixtures.

B. Ternary mixtures

In Larrañaga *et al.*,[15] the determination of the diagonal and cross-diagonal molecular diffusion coefficients using the classical analytical solution (Eqs. (6) and (7)) was attempted. However, as has been pointed out, the establishment of a fitting method which allows reproducible results to be obtained and which does not depend on the fitting conditions was found to be impossible. By contrast, the new analytical solution developed in this work only requires a simple straight-line fit to obtain slopes and then the diffusion coefficients in ternary mixtures may be calculated directly by the Newton-Raphson method.

In this work, the results obtained for the ternary mixture THN-IBB-*n*C12 with equal mass fractions and at 25 °C are shown, and they are compared to the results published in the literature.

The experimental determination of the diagonal and cross-diagonal molecular diffusion coefficients in ternary mixtures requires experimental data from two independent

TABLE I. Initial concentrations and slopes, S ($s^{-1/2}$), for each component in the upper and the bottom tubes, in the two experiments carried out in this work, at 25 °C.

	Expt. 1	Expt. 2
w (THN) up	0.3033	0.3033
w (THN) bot	0.3633	0.3633
w (IBB) up	0.3433	0.3333
w (IBB) bot	0.3233	0.3333
w (C12) up	0.3533	0.3633
w (C12) bot	0.3133	0.3033
S (THN) up ($s^{-1/2}$)	1.58×10^{-5}	1.49×10^{-5}
S (THN) bot ($s^{-1/2}$)	-1.58×10^{-5}	-1.49×10^{-5}
S (C12) up ($s^{-1/2}$)	-0.96×10^{-6}	-1.43×10^{-5}
S (C12) bot ($s^{-1/2}$)	0.96×10^{-6}	1.43×10^{-5}

experiments where the initial concentrations are different. Table I shows the initial concentrations of each component in the two experiments used in this case.

As for the case of binary mixtures, the variation of the concentration with the square root of time is linear. Figure 6 shows some experimental results for the mixture THN-IBB-*n*C12 with equal mass fraction and 25 °C, corresponding to the experiment 1 of Table I.

Prior to showing further results, it is necessary to discuss the implications of the choice of the order of components in a ternary mixture. The four molecular diffusion coefficients which are found depend on which two components of the three are assigned to the variables w_1 and w_2 in the flux Eqs. (36) and (37). This is why special care needs to be taken when results from different scientific groups are compared:

$$J_1 = -\rho\,(D_{11}\nabla w_1 + D_{12}\nabla w_2)\,, \tag{36}$$

$$J_2 = -\rho\,(D_{21}\nabla w_1 + D_{22}\nabla w_2)\,. \tag{37}$$

However, it is quite straightforward to manipulate the pair of coupled Fick's equations for these two components

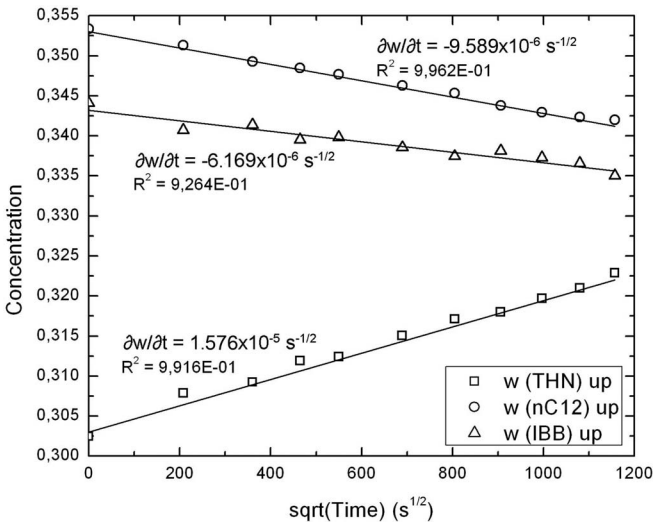

FIG. 6. Variation of the concentration with the square root of time for the components THN, IBB, and *n*C12 at 25 °C, obtained from the upper tube of the SST technique.

TABLE II. Molecular diffusion coefficients determined in this work for the mixture THN-IBB-*n*C12 with equal mass fraction and at 25 °C for the three possible orders of components.

Order of components w_1-w_2-w_3	$D_{11} \times 10^{-10}$ (m^2/s)	$D_{12} \times 10^{-10}$ (m^2/s)	$D_{21} \times 10^{-10}$ (m^2/s)	$D_{22} \times 10^{-10}$ (m^2/s)
THN-IBB-*n*C12	6.16	−4.61	0.37	11.40
THN-*n*C12-IBB	11.30	5.08	0.14	6.65
*n*C12-IBB-THN	6.54	−0.51	−0.37	11.06

into the corresponding forms for either of the other two possible choices of the components as shown in Königer *et al.*[10]

Because of the analysis method used in the present laboratory, the best accuracy was obtained when the components with highest and the lowest densities are chosen, and it is these that were generally chosen to be w_1 and w_2. However, in order to compare the present results with those available in the literature, the molecular diffusion coefficients for all three possible orders of components have been determined experimentally. Table II shows the diagonal and cross-diagonal molecular diffusion coefficients for the three possible orders of components in the mixture.

In the three cases, the molecular diffusion coefficients satisfy the restrictions detailed in Mutoru *et al.*[24]

The literature about molecular diffusion in ternary mixtures of hydrocarbons is very limited. For our same mixture and composition, there are only three works published. Königer *et al.*[10] determined the molecular diffusion coefficients using the two colour optical beam deflection technique (OBD), considering the component order *n*C12-IBB-THN. Mialdun *et al.*[11] measured the molecular diffusion coefficients by a counter flow cell fitted with an optical interferometry device (CFC), and the component order THN-IBB-*n*C12 was preferred. Afterwards, this same team published a new work[16] where two independent techniques were used: the counter flow cell fitted with an optical interferometry device (CFC) and Taylor dispersion technique (TDT). This last work[16] emerges as more confident for the team of Mialdun *et al.*; however, as the published results for molecular diffusion coefficients in ternary mixtures are limited, we have compared the results of the three works available in the literature.

Table III shows the eigenvalues of the diffusion matrix determined here by the SST technique (rows 2, 3, and 4) and the ones determined by OBD (Ref. 10) (row 5), CFC (Ref. 11)

TABLE III. Comparison between the eigenvalues of the diffusion matrix obtained in this work and the results of the literature.

Data source	Order of components w_1-w_2-w_3	$\hat{D}_1 \times 10^{-10}$ (m^2/s)	$\hat{D}_2 \times 10^{-10}$ (m^2/s)
Present study: SST	THN-IBB-*n*C12	6.51	11.10
	THN-*n*C12-IBB	6.49	11.50
	*n*C12-IBB-THN	6.50	11.11
OBD[10]	*n*C12-IBB-THN	6.81	10.99
CFC[11]	THN-IBB-*n*C12	7.26	11.23
TDT[16]	THN-IBB-*n*C12	6.82	9.9
CFC[16]	THN-IBB-*n*C12	7.09	11.17

TABLE IV. Comparison of the diffusion coefficients for the ternary mixture THN-IBB-*n*C12 with equal mass fraction and at 25 °C, where THN and IBB form components w_1 and w_2, respectively.

Data source	Order of components w_1-w_2-w_3	$D_{11} \times 10^{-10}$ (m^2/s)	$D_{12} \times 10^{-10}$ (m^2/s)	$D_{21} \times 10^{-10}$ (m^2/s)	$D_{22} \times 10^{-10}$ (m^2/s)
Present study: SST	THN-IBB-*n*C12	6.16	− 4.61	0.37	11.40
Present study: SST[a]		6.22	− 5.08	0.28	11.73
OBD[10,a]		5.62	− 5.91	1.08	12.18
CFC[11]		6.92	1.06	− 1.37	11.57
TDT[16]		10.31	0.33	− 4.36	6.41
CFC[16]		11.61	0.32	− 6.18	6.65

[a]Data have been transformed for the same order of components (Eqs. (A8)–(A11) in Königer *et al.*[10]).

TABLE V. Comparison of the diffusion coefficients in the ternary mixture THN-IBB-*n*C12 with equal mass fraction and at 25 °C, where *n*C12 and IBB form components w_1 and w_2, respectively.

Data source	Order of components w_1-w_2-w_3	$D_{11} \times 10^{-10}$ (m^2/s)	$D_{12} \times 10^{-10}$ (m^2/s)	$D_{21} \times 10^{-10}$ (m^2/s)	$D_{22} \times 10^{-10}$ (m^2/s)
Present study: SST	*n*C12-IBB-THN	6.54	− 0.51	− 0.37	11.06
Present study: SST,[a]		6.51	− 0.14	− 0.28	11.14
OBD[10]		6.70	0.43	− 1.08	11.10
CFC[11,a]		5.55	− 7.08	1.37	12.94
TDT[16,a]		5.95	− 0.79	4.36	10.77
CFC[16,a]		5.43	− 1.54	6.18	12.83

[a]Data have been transformed for the same order of components (Eqs. (A8)–(A11) in Königer *et al.*[10]).

TABLE VI. Comparison of the diffusion coefficients in the ternary mixture THN-IBB-*n*C12 with equal mass fraction and at 25 °C, where THN and *n*C12 form components w_1 and w_2, respectively.

Data source	Order of components w_1-w_2-w_3	$D_{11} \times 10^{-10}$ (m^2/s)	$D_{12} \times 10^{-10}$ (m^2/s)	$D_{21} \times 10^{-10}$ (m^2/s)	$D_{22} \times 10^{-10}$ (m^2/s)
Present study: SST	THN-*n*C12-IBB	11.30	5.08	0.14	6.65
OBD[10,a]		11.53	5.91	− 0.43	6.27
CFC[11,a]		5.86	− 1.06	7.08	12.63
TDT[16,a]		9.98	− 0.33	0.79	6.74
CFC[16,a]		11.28	− 0.32	1.55	6.97

[a]Data have been transformed for the same order of components (Eqs. (A8)–(A11) in Königer *et al.*[10]).

TABLE VII. Comparison of the Soret coefficients in the ternary mixture THN-IBB-*n*C12 with equal mass fraction and at 25 °C.

Data source	Order of components w_1-w_2-w_3	$S_T^{THN} \times 10^{-3}$ K^{-1}	$S_T^{IBB} \times 10^{-3}$ K^{-1}	$S_T^{nC12} \times 10^{-3}$ K^{-1}
Present study: TGC + SST	THN-IBB-*n*C12	1.83	0.05	− 1.88
	THN-*n*C12-IBB	1.82	0.07	− 1.89
	*n*C12-IBB-THN	1.83	0.05	− 1.88
OBD[10]	*n*C12-IBB-THN	2.11	− 0.96	− 1.15

(row 6), TDT (Ref. 16), and CFC (Ref. 16) (rows 7 and 8). The second column indicates the order in which the components have been taken in each case. The eigenvalues of the diffusion matrix do not depend on the order of the components chosen, so they may be compared directly.

As can be observed, the agreement between the determined eigenvalues is reasonable, obtaining variations between 1% and 12%.

In order to make a comparison between the molecular diffusion coefficients obtained in this work and the ones published in the literature, in the three possible cases of order of components, the transformation of the diffusion matrix detailed in Eqs. (A8)–(A11) of Königer *et al.*[10] has been applied to the results of this work and to the results of the literature, for the cases needed. Table IV shows the results found when the order of components is THN-IBB-*n*C12. Table V shows the results obtained when the order of components considered is *n*C12-IBB-THN. Finally, Table VI shows the results obtained in the case of considering the order of components THN-*n*C12-IBB.

As may be seen in Tables IV–VI, the agreement between the diagonal diffusion coefficients determined in this work and the ones published in the literature is reasonable in most of the cases, especially with the results shown in Königer *et al.*[10] In the case of the cross-diagonal diffusion coefficients, the differences are bigger, appearing in some cases even a disagreement in the sign. The disagreements between the results of the different teams show the difficulty of the determination of the molecular diffusion coefficient in ternary mixtures. It is necessary to continue working in order to optimize the experimental techniques and the corresponding analysis methods. For that purpose, we plan to continue analyzing this mixture but in the whole range of concentrations.

In addition to the comparison of the molecular diffusion coefficients, it is also possible to compare the Soret coefficients of the mixture studied in this work. The Soret coefficient can be determined from the measurements of the thermodiffusion and the molecular diffusion coefficients, by the expression shown in Mialdun and Shevtsova[17] In Blanco *et al.*,[25] this scientific team published the thermodiffusion coefficients for the mixture studied in this work determined by the thermogravitational technique (TGC). The molecular diffusion coefficients determined in this work by the SST technique allow determining Soret coefficients for the mixture THN-IBB-*n*C12 with equal mass fraction, at 25 °C. Table VII shows the results obtained in this work for the three different cases of order of components (rows 2–4) and the results determined experimentally by the OBD technique[10] (row 5).

As may be observed, independently of the order of components chosen, the Soret coefficient corresponding to each coefficient is the same (rows 2–5 of Table VII). The agreement between the results obtained in this work and the ones shown in Königer *et al.*[10] is optimistic in order to continue developing the techniques to determine the transport properties in multicomponent mixtures, taking into account the limited experimental results available for ternary mixtures.

IV. CONCLUSIONS

An analytical method based upon the notion of self-similarity has been developed to enable the determination of molecular diffusion coefficients in ternary mixtures by the SST technique. This method, when combined with a four-dimensional Newton-Raphson scheme, yields the diffusion coefficients very rapidly. The accuracy of these coefficients depends first on the diffusion front not having yet reached the extreme ends of the tubes in our SST experiment, and second on the accuracy of the experimental technique itself. We would claim that both of these conditions are satisfied because the data shown in Figures 4 and 6 yield lines which are almost exactly linear.

In this work, all the diagonal and cross-diagonal molecular diffusion coefficients corresponding to the mixture THN-IBB-*n*C12 with equal mass fraction and at 25 °C have been determined. After comparing these values with the ones shown in the literature, the agreement between the eigenvalues of the diffusion matrix is particularly good and the agreement between the molecular diffusion coefficients is acceptable, especially in the case of the diagonal diffusion coefficients. As can be observed, the cross-diagonal molecular diffusion coefficients are much more sensitive.

ACKNOWLEDGMENTS

The results obtained in this work were obtained in the framework of the following projects: GOVSORET3 (PI2011–22), MICROSCALE, Research Groups (IT557–10), Research Fellowship (BFI-2011–295) and Fellowship for Short Stays (EC-2013–1–72) of Basque Government, and DCMIX (DCMIX-NCR-00022-QS) from the European Space Agency.

[1] F. Capuano, L. Paduano, G. D'Errico, G. Mangiapia, and R. Sartorio, Phys. Chem. Chem. Phys. **13**, 3319–3327 (2011).
[2] T. Takahashi and Y. Minamino, J. Alloys Compounds **545**, 168–175 (2012).
[3] H. Tello Alonso, A. C. Rubiolo, and S. E. Zorrilla, J. Food Eng. **109**, 490–495 (2012).
[4] A. Fick, Ann. Phys. **170**, 59–86 (1855).
[5] P. Blanco, P. Polyakov, M. M. Bou-Ali, and S. Wiegand, J. Phys. Chem. B **112**, 8340–8345 (2008).
[6] J. F. Dutrieux, J. K. Platten, G. Chavepeyer, and M. M. Bou-Ali, J. Phys. Chem. B **106**, 6104–6114 (2002).
[7] M. Gebhardt, W. Köhler, A. Mialdun, V. Yasnou, and V. Shevtsova, J. Chem. Phys. **138**, 114503 (2013).
[8] A. A. Alizadeh, W. A. Wakeham, Int. J. Thermophys. **3**, 307 (1982).
[9] P. Blanco, M. M. Bou-Ali, and P. Urteaga, Patente ES 2351822 (A1) (2011).
[10] A. Königer, H. Wunderlich, and W. Köhler, J. Chem. Phys. **132**, 174506 (2010).
[11] A. Mialdun, V. Yasnou, and V. Shevtsova, C. R. Mecanique **341**, 462–468 (2013).
[12] A. Leahy-Dios, M. M. Bou-Ali, J. K. Platten, and A. Firoozabadi, J. Chem. Phys. **122**, 234502-1–234502-12 (2005).
[13] C. I. Santos, M. A. Esteso, V. M. Lobo, and A. C. Ribeiro, J. Chem. Thermodyn. **59**, 139–143 (2013).
[14] X. Liu, A. Martin-Calvo, E. McGarrity, S. K. Schnell, S. Calero, J-M Simon, D. Bedeaux, S. Kjelstrup, A. Bardow, and T. J. H. Vlugt, Ind. Eng. Chem. Res. **51**, 10247–10258 (2012).
[15] M. Larrañaga, M. M. Bou-Ali, D. Soler, M. Martinez-Agirre, A. Mialdun, and V. Shevtsova, C. R. Mecanique **341**, 356–364 (2013).
[16] A. Mialdun, V. Sechenyh, J. C. Legros, J. M. Ortiz de Zárate, and V. Shevtsova, J. Chem. Phys. **139**, 104903 (2013).
[17] A. Mialdun and V. Shevtsova, J. Chem. Phys. **138**, 161102 (2013).

[18]Diffusion Coefficient Measurements in Ternary Mixtures DCMIX-NCR-00022-QS.
[19]D. Alonso de Mezquia, M. M. Bou-Ali, M. Larrañaga, J. A. Madariaga, and C. Santamaría, J. Phys. Chem. B **116**, 2814–2819 (2012).
[20]D. Alonso de Mezquia, F. Doumenc, and M. M. Bou-Ali, J. Chem. Eng. Data **57**, 776–783 (2012).
[21]A. Mialdun, V. Yasnou, V. Shevtsova, A. Königer, W. Köhler, D. Alonso de Mezquia, and M. M. Bou-Ali, J. Chem. Phys. **136**, 244512 (2012).
[22]M. J. Sawicka and J. A. Soroka, Cent. Eur. J. Chem. **11**(7), 1239–1247 (2013).
[23]H. S. Carslaw and J. C. Jaeger, *Conduction of Heat in Solids* (Clarendon Press, Oxford, 1959), p. 50.
[24]J. W. Mutoru and A. Firoozabadi, J. Chem. Thermodyn. **43**, 1192–1203 (2011).
[25]P. Blanco, M. M. Bou-Ali, J. K. Platten, D. Alonso de Mezquía, J. A. Madariaga, and C. Santamaría, J. Chem. Phys. **132**, 114506 (2010).

E. Effect of thermophysical properties and morphology of the molecular on thermodiffusion coefficient of binary mixtures.

Microgravity Sci. Technol. (2014) 26:29–35
DOI 10.1007/s12217-014-9368-y

ORIGINAL ARTICLE

Effect of Thermophyisical Properties and Morphology of the Molecules on Thermodiffusion Coefficient of Binary Mixtures

Miren Larrañaga · M. Mounir Bou-Ali · Estela Lapeira · Carlos Santamaría · Jose A. Madariaga

Received: 18 December 2013 / Accepted: 5 May 2014 / Published online: 27 May 2014

Abstract In this article, new experimental data of the thermal diffusion coefficient (D_T) of 20 binary mixtures of hexane-hexadecane, decane-hexadecane, toluene-hexadecane and 1-metilnaphtalene-hexadecane at several different compositions and at 298K and atmospheric pressure, are reported. Thermal diffusion coefficients were measured in a thermogravitational column with rectangular configuration. The results obtained show that the mass fraction dependence of thermodiffusion coefficients of the mixture is linear in all the cases. The studied mixtures have a common component, hexadecane, and they can be classified into two groups according to their mass and to the morphology of their components. We also show that the thermal diffusion coefficient and mixture viscosity are related in a different way for mixtures of n-alkanes and for mixtures of aromatic rings.

Keywords Thermophysical properties · Thermodiffusion coefficient · Thermogravitational technique · Binary mixtures

Introduction

The phenomenon of thermodiffusion has generated a great interest in the scientific community, due to its appearance in numerous processes both natural and industrial of different fields such as petroleum industry (Capuano et al. 2011; Tello Alonso et al. 2012; Montel 1998).

In the case of binary mixtures, there are a lot of techniques which allow the determination of the thermodiffusion coefficient, such as Thermal Diffusion Forced Rayleig Scattering (TDFRS) (Leppla and Wiegand 2003), Optical Beam Deflection (OBD) (Königer et al. 2009), Optical Digital Interferometry (ODI) (Mialdun and Shevtsova 2011), modern light scattering techniques (Croccolo et al. 2012) or the Thermogravitational technique (TGC) (Bou-Ali et al. 2003). These experimental techniques were compared and validated by the performance of a Benchmark for binary mixtures (Platten et al. 2003).

The analysis of this phenomenon becomes considerably more complicated when mixtures of more than two components are studied. In that case, orbital laboratories are an ideal environment for the performance of the experiments thanks to the absence of the convection produced by the gravity.

Due to this increasing interest, a cooperative international project supported by the European Space Agency (ESA) was developed. In it, scientists expect to obtain reliable benchmark results by the SODI instrument in the International Space Station (ISS) and validate their ground-based techniques (Mialdun et al. 2012).

With the aim of clarifying the behaviour of the thermodiffusion phenomenon in multicomponent mixtures, studies in binary mixtures about the influence of different properties in the thermodiffusion phenomenon have been carried out. In Madariaga et al. (2010) a correlation that allows the determination of the thermodiffusion coefficient in binary mixtures of n-alkanes at any concentration from the dynamic viscosity, the thermal expansion coefficient and the molecular weight of the mixture was developed. In Leahy-Dios

M. Larrañaga · M. M. Bou-Ali (✉) · E. Lapeira
Mechanical and Manufacturing Department, Engineering Faculty of Mondragon Unibertsitatea, Loramendi 4 Apdo. 23, 20500 Mondragon, Spain
e-mail: mbouali@mondragon.edu

C. Santamaría · J. A. Madariaga
Department of Applied Physics II, University of Basque Country, UPV/EHU, Apdo 644, 48080 Bilbao, Spain

and Firoozabadi (2007) the influence of factors such as the size and the shape of the molecules was analyzed, and later, in Leahy-Dios et al. (2008) the influence of the viscosity was analyzed too. In addition, in other works, the influence of the moment of inertia and the chemical effects was also studied experimentally, by modelling or by simulations (Debuschewitz and Köhler 2001; Villain-Guillot and Würger 2011; Galliéro et al. 2003).

The motivation of this work is to try to expand the knowledge about the influence of different properties on the thermodiffusion coefficient. Therefore, the objective of this work is to analyze the influence of the molecular weight, the viscosity and the morphology of the molecules on the thermodiffusion coefficient.

With the aim of achieving this objective, 4 binary mixtures have been chosen with a common component: hexadecane.

This work is divided as follows. In Section "Experimental Methodology", the experimental methodology followed is described; in Section "Results and Discussion" the obtained results and the discussion about them are shown. Finally, in Section "Conclusions" the conclusions achieved are shown.

Experimental Methodology

Studied Mixtures

In this work the thermogravitational behaviour of four binary systems with different concentrations has been studied. The four systems have a common component, hexadecane. The analyzed systems are: hexadecane-hexane, hexadecane-decane, hexadecane-toluene and hexadecane-1-methylnaphtalene. From here on, hexadecane will be referred as nC16, hexane as nC6, decane as nC10, toluene as Tol and 1-methylnaphtalene as MN. These systems can be grouped by their molecular weight (on the one hand nC16-nC6 and nC16-Tol and on the other hand nC16-nC10 and nC16-MN) and by the morphology of their components (nC16-nC6 and nC16-nC10 are chains and nC16-Tol and nC16-MN are a chain and an aromatic ring). Each system was studied at different concentrations of nC16.

Table 1 shows the concentrations of nC16, the difference of molecular weight between the components of the mixture, $\Delta M = M_{nC16} - M_i$, where M_i is the molecular weight of the second component (Tol, MN, nC6 or nC10), and the configuration of the mixture.

Every product used in this work was purchased from Merck and Aldrich, with purity higher than 99 %. The concentrations of the binary mixture were obtained by weight in a scale with accuracy of 0.0001 g. The necessary volume of mixture for each experiment was of approximately 30 cm^3. The mixtures were prepared introducing first the less volatile component.

Table 1 Description of the analyzed concentrations, the difference of molecular weight and configuration of each mixture

nC16-i	c (nC16)	ΔM	Config,
nC6	0.20	140.27	Chain-Chain
	0.40		
	0.50		
	0.72		
Tol	0.20	134.31	Chain-Ring
	0.30		
	0.40		
	0.50		
	0.60		
	0.80		
nC10	0.20	84.17	Chain-Chain
	0.40		
	0.50		
	0.61		
	0.80		
MN	0.20	84.25	Chain-Ring
	0.40		
	0.50		
	0.60		
	0.80		

Equipment

The determination of the thermodiffusion coefficient in this work was done by the thermogravitational technique (Blanco et al. 2008). By this technique it is possible to determine the thermodiffusion coefficient from the variation of the concentration with the height of the column and some thermophysical properties of the analyzed mixture. The principle of the thermogravitational technique is as follows. Instead of trying to avoid convection in the elemental Soret cell, the thermogravitational technique adds it to the thermodiffusive separation. The liquid is inside a vertical gap with a high aspect ratio $L_z >> L_x$ (where L_z is the height of the column and L_x is the width of the gap), and where the walls are at different and constant temperatures. This horizontal temperature gradient makes, generally, the denser component migrate to the cold wall due to thermodiffusion and at the same time, it is moved to the bottom of the column due to convection. Therefore, a vertical concentration gradient is established through the height of the gap. The theory of the thermogravitational column (Furry et al. 1939) allows

relating the stationary separation with the thermodiffusion coefficient, D_T, by the following expression:

$$\Delta c = -\frac{504 L_z D_{T\nu}}{g L_x^4} c_0(1 - c_0) \quad (1)$$

where Δc is the difference of mass fraction between the top and the bottom of the gap, c_0 is the mass fraction of the initial mixture, $\alpha = -(1/\rho)(\partial\rho/\partial T)$ is the thermal expansion coefficient, ν is the kinematic viscosity and g is the gravity acceleration.

In this work we will take as reference component the denser component in each mixture. When $D_T > 0$the denser component migrates to the cold wall and it is moved to the bottom of the column, increasing the concentration there, so that $\Delta c<0$.

The thermogravitational column used in this work has parallelepiped configuration and it was developed and manufactured in Mondragon Goi Eskola Politeknikoa. It is shown in Fig. 1. The geometric parameters are: $L_z = 0.5 \pm 0.001$ m and $L_x = 1 \times 10^{-3} \pm 5 \times 10^{-6}$ m. The temperatures of the walls were $T_H = 301$ K and $T_C = 295$ K, which implies a mean temperature of 298 K. The column has four outlets of samples distributed evenly along the height of the column.

In order to determine the mass separation between the extremes of the column it was necessary to carry out a prior calibration which relates the mass fraction with a physical property of the mixture, in our case, the density. An Anton Paar DMA 5000 vibrating quartz U-tube densimeter with accuracy of $5\text{x}10^{-6}$ g/cm^3 was used to determine the density of the mixture at different concentrations. From these measurements the mass expansion coefficient may also be determined.

When stationary state is achieved, the vertical density gradient is determined $\partial\rho/\partial z$, by measuring the density of the samples extracted from the four outlets along the height of the column. In every case the variation of the density with the height of the column was linear. As example, Fig. 2 shows the variation of the density with the height for the system MN-nC16 with a 40 % of concentration of nC16.

The stationary separation between the extremes of the column is:

$$\Delta c = -\frac{L_z \partial\rho}{\beta\rho\partial z} \quad (2)$$

where β is the mass expansion coefficient defined by:

$$\beta = \frac{1\partial\rho}{\rho\partial c} \quad (3)$$

Combining Eqs. 2 and 3 we can obtain:

$$D_T = -\frac{g L_x^4}{504} \cdot \frac{\alpha}{c_0(1 - c_0)\beta\mu} \cdot \frac{\partial\rho}{\partial z} \quad (4)$$

Where μ is the dynamic viscosity and $c_0(1 - c_0)$ is the product of the initial concentrations. This equation allows us determining D_T from the measurements of the density of the samples taken from different heights of the column. Considered the experimental errors committed in the measurements of the thermophysical properties, the estimated uncertainty in the determination of the thermodiffusion coefficient is of a 5 %.

Fig. 1 Thermogravitational column with parallelepiped configuration

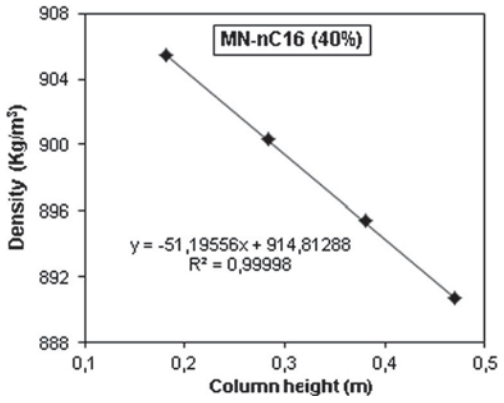

Fig. 2 Variation of the density of the mixture with the height of the column

The dynamic viscosity is determined by two viscometers: a HAAKE falling ball viscometer and a microviscometer Anton Paar AMVn.

Results and Discussion

In this section the results obtained in this work and the discussion generated around them are presented. The density, the mass expansion coefficient, the thermal expansion coefficient, the dynamic viscosity and the thermodiffusion coefficient have been determined for the 20 mixtures presented in the previous section. Table 2 shows the numerical values of these properties and of the mass separation for each mixture.

Figure 3 shows the variation of the density with the concentration of nC16 for the four studied systems. For the systems nC6-nC16 and nC10-nC16 this dependency is linear as it was expected, taking into account the quasi-ideality of the mixtures of n-alkanes. On the contrary, for the systems Tol-nC16 and MN-nC16 this dependency is quadratic, because they are non-ideal mixtures. It is interesting to point out that the four mixtures intersect in the point corresponding to the density of the nC16.

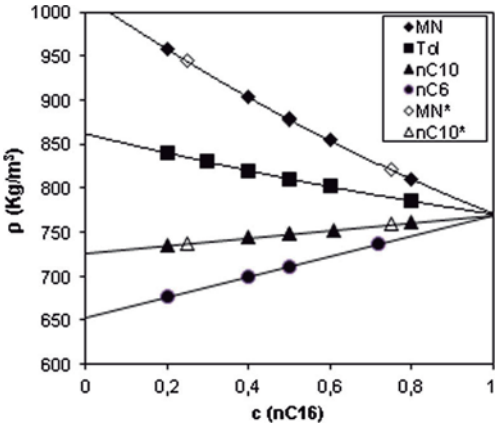

Fig. 3 Variation of the density with the concentration of nC16 for the four systems analyzed. Values with * correspond to the works (Leahy-Dios and Firoozabadi 2007; Leahy-Dios et al. 2008)

In Table 2, the values of β as obtained from the study of the density with the concentration of nC16 are also reported.

Figure 4 shows the results corresponding to the variation of the thermal expansion coefficient with the concentration. The variation of α with the concentration is quasi-linear in every case, and the four lines converge

Table 2 Results of the thermophysical properties, mass separation and thermodiffusion coefficient for the 20 mixtures analyzed in this work at 298 K where c is the mass fraction of nC16

System	c	ρ (kg/m^3)	α x 10^{-3} (K^{-1})	β	μ (mPa·s)	$-\Delta c$ x 10^{-2}	D_T x 10^{-12} (m^2/sK)
Tol-nC16	0.80	785.15	0.929	0.101	1.77	——	——
Tol-nC16	0.60	801.76	0.962	0.108	1.20	——	——
Tol-nC16	0.50	810.65	0.980	0.112	1.02	1.14	1.30
Tol-nC16	0.40	820.00	0.998	0.116	0.87	1.26	1.86
Tol-nC16	0.30	829.78	1.017	0.120	0.76	1.35	2.63
Tol-nC16	0.20	840.00	1.039	0.125	0.68	1.12	3.54
MN-nC16	0.80	809.97	0.877	0.253	2.82	6.61	4.03
MN-nC16	0.60	854.11	0.846	0.273	2.69	9.61	4.19
MN-nC16	0.50	878.45	0.830	0.282	2.62	10.10	4.37
MN-nC16	0.40	903.28	0.810	0.288	2.65	9.88	4.42
MN-nC16	0.20	958.12	0.774	0.304	2.73	6.94	4.66
nC6-nC16	0.72	736.56*	1.009*	0.162*	1.26*	5.55*	6.38*
nC6-nC16	0.50	708.00	1.110	0.161	0.74**	5.08	8.37
nC6-nC16	0.40	699.21	1.140	0.161	0.56	4.16	9.60
nC6-nC16	0.20	676.84	1.233	0.159	0.40	2.18	11.10
nC10-nC16	0.80	761.07	0.917	0.058	2.13	2.39	1.90
nC10-nC16	0.61	752.85*	0.952*	0.059*	1.76*	3.33*	2.23*
nC10-nC16	0.50	747.77	0.966	0.059	1.52**	3.33	2.47
nC10-nC16	0.40	743.66	0.980	0.058	1.28	2.93	2.71
nC10-nC16	0.20	735.00	1.002	0.058	0.99	1.77	3.18

*Blanco et al. (2008)

**Alonso de Mezquia et al. (2012)

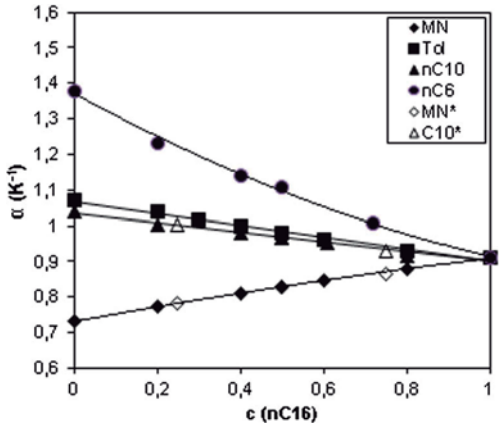

Fig. 4 Variation of the thermal expansion coefficient with the concentration of nC16 for the four mixtures analyzed. Values with * correspond to the works (Leahy-Dios and Firoozabadi 2007; Leahy-Dios et al. 2008)

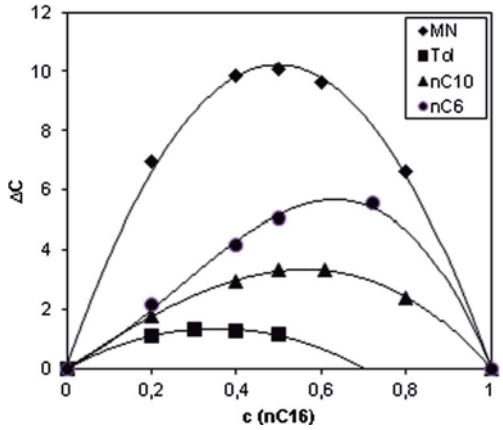

Fig. 6 Variation of the separation along the height of the column, with the concentration of nC16 in the four systems analyzed

to the value corresponding to a 100 % concentration of nC16.

Figure 5 shows the dependency of the dynamic viscosity with the composition of the mixture. In the same way as in the case of density and thermal expansion coefficient, the values of the viscosities in the four systems converge to the value of the viscosity of hexadecane when the compositions of the mixtures tend to 100 %.

In Figs. 3–5 are represented also the values obtained in Leahy-Dios and Firoozabadi (2007) and Leahy-Dios et al. (2008) for these thermophysical properties. The agreement between our values and the ones of those works can be considered excellent.

Moreover, Fig. 6 shows the experimental results obtained in our column for the separation, Δc, for the different mixtures of the four systems. These results are the mean value of at least three different measurements.

With the values of ρ, α, μ and Δc obtained in this work and the geometric constants of our thermogravitational column, the thermodiffusion coefficients can be calculated by Eq. 4. Figure 7 shows the obtained values of D_T. All the values of D_T are positive, which means that in every case the denser and the less dense components enrich the bottom and the top of the column respectively. It is important to point out that with our experimental equipment it has not been possible to measure thermodiffusion coefficients for the mixture Tol-nC16 with concentrations of nC16 higher than 50 %. In these mixtures the separation is very small and the experimental error masks the result. However, the behaviour of D_T in these systems indicates that for concentrations of nC16 higher than 65 % negative values of D_T can be achieved. In any case and for the four systems, the values of D_T decrease with the concentration of nC16, therefore, they decrease with the concentration of the heaviest component.

Considering Fig. 7 it can be observed that the dependency of D_T with the composition is linear for the four systems. Madariaga et al. (2010) showed that the behaviour of the thermodiffusion coefficient with the mass fraction is linear

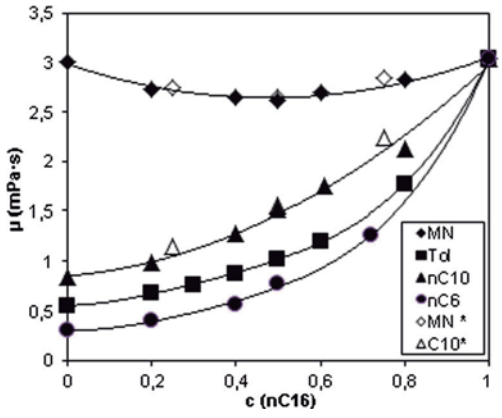

Fig. 5 Variation of the dynamic viscosity with the concentration of nC16 for the four systems analyzed. Values with * correspond to the works (Leahy-Dios and Firoozabadi 2007; Leahy-Dios et al. 2008)

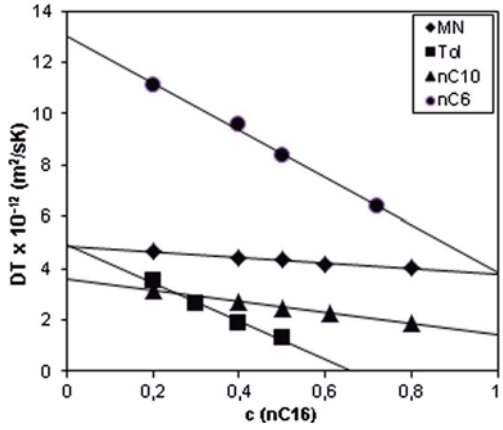

Fig. 7 Variation of the thermodiffusion coefficient with the concentration of nC16 for the four mixtures analyzed

in binary mixtures of n-alkanes. In this work we can confirm this behaviour for the systems nC6-nC16 and nC10-nC16. In this work also, we have shown that this linear behaviour appears also in non-ideal mixtures formed by linear chains and rings such as Tol-nC16 and MN-nC16.

It has to be pointed out that the coefficients D_T for the systems Tol-nC16 and MN-nC16 have the same value when the mass fraction of the hexadecane tends to zero, although their thermophysical properties and molecular weights are different. In other words, toluene and 1-methylnaphtalene have the same response to temperature gradient when hexadecane is present as traces, indicating that the mobility of these components is similar.

With regard to the slopes of the lines that represent the dependency of D_T with mass fraction, the four systems can be classified in two groups. One of the groups is formed by the systems nC6-nC16 and Tol-nC16 which have similar slopes, and the other group is formed by MN-nC16 and nC10-nC16 with similar slopes between them but different to the previous ones. Each group has in common that the difference of molecular weight between their components, ΔM, has similar values (see Table 1). In other words, the slopes of the lines D_T *vs c* are directly related to the values of ΔM.

The thermodiffusive behaviour of the systems formed by n-alkanes, nC6-nC16 and nC10-nC16, is perfectly described by the empirical relations obtained in Madariaga et al. (2010). In this work it is concluded that the values of the coefficient D_T are directly proportional to the difference of molecular weights and to the thermal expansion coefficient, and inversely proportional to the dynamic viscosity (Eq. (5) in Madariaga et al. (2010)). Therefore, for binary mixtures of n-alkanes it is satisfied that:

- When the difference between the molecular weights of the components increases, the mobility of the molecules increases, and therefore, the thermodiffusion coefficient increases too.
- When the dynamic viscosity increases the mobility of the molecules decreases, and the thermodiffusion coefficient decreases too.
- When the thermal expansion coefficient increases, the thermodiffusion coefficient increases too.
- The similarity between the molecules decreases the thermodiffusion coefficient. This is because molecules with the same shape respond in the same way to thermal effects, and therefore, the separation due to the thermodiffusive effect is smaller (Leahy-Dios and Firoozabadi 2007).

It can be observed how when comparing the systems nC6-nC16 and nC10-nC16, the previous considerations about ΔM, viscosity and thermal expansion coefficient encourage the system nC6-nC16 and this is the one which has higher thermodiffusion coefficient (Fig. 6).

On the contrary, the behaviour of the thermodiffusion coefficient comparing systems with an aromatic ring is just the opposite. In these systems, as Fig. 7 shows, the thermodiffusion coefficient increases when viscosity increases and difference between molecular weights of the components and thermal expansion coefficient decrease. For example, the mixture MN-nC16 with a 50 % of mass fraction which has a viscosity of 2.63 mPa·s, has a D_T of 4.37 m^2/sK; however, the system Tol-nC16 with a 50 % of mass fraction, which has a viscosity of 1.02 mPa·s, has a D_T of 1.30 m^2/sK, which is a behaviour completely opposite to the one followed by systems of n-alkanes. A similar situation is found when the influence of α is studied. For the mixture Tol-nC16 with a 50 % of mass fraction α is 0.980 K^{-1} and it has a D_T of 1.30 m^2/sK; on the contrary, the mixture MN-nC16 with a 50 % of mass fraction has a α of 0.830 K^{-1} and a D_T of 4.37 m^2/sK.

Leahy-Dios and Firoozabadi (2007) have disclosed the influence of the molecular shape on the thermodiffusion coefficient. These authors, by experimental measurement of D_T in the series MN-nC_i and nC10-nC_i (I = 5-16) conclude that D_T values are higher in systems formed by MN and n-alkanes than in the ones formed by two n-alkanes. The normal alkanes have a similar configuration and therefore, they respond in the same way to the established thermal gradient, which would explain the low values of D_T in these systems compared to the ones obtained for MN-nC_i. Overall, these conclusions are not maintained for our results. The value of D_T for the system MN-nC16 is higher than the one obtained for the system nC10-nC16, the two systems with similar ΔM. However, for the systems Tol-nC16 and nC6-nC16 with similar values of ΔM the situation is reversed; the value of D_T for the system nC6-nC16 is much higher than the one obtained for the system Tol-nC16. In any case, more studies are needed to confirm the suggestion of Leahy-Dios and Firoozabadi (2007) about the importance of the molecular shape in the thermodiffusion coefficient.

On the other hand, these authors associate the mobility of each component to the Brownian movement of the molecules and it is, ultimately, a function of the viscosity. They also associate the similarity between the components of the mixture to the type of answer to a given force field. In our work, we have checked that in n-alkane mixtures it effectively happens that when molecular weight and viscosity decreases, D_T increases; but in the mixtures of Tol-nC16 and MN-nC16 the behaviour is just the opposite. This different behaviour can be caused by a strong influence of the similarity between the components which counteracts the previous effect, or by other properties that have not been studied in this work.

Conclusions

In this work the thermophysical properties (density, dynamic viscosity and mass and thermal expansion coefficients) and the thermodiffusion coefficient of 20 binary mixtures have been measured. All the mixtures have a common component (hexadecane) and the other component is a n-alkane (hexane or decane) or an aromatic ring (toluene or 1-methylnaphtalene).

For the four studied systems hexane-hexadecane, decane-hexadecane, toluene-hexadecane and 1-methylnaphtalene-hexadecane, it has been shown a linear dependency between the thermodiffusion coefficient and the mass fraction of the mixture. In addition, in the mixtures of hexane and decane, the behaviour is the one predicted by the empirical expressions of Madariaga et al. (2010) for n-alkane binary mixtures. In these mixtures the thermodiffusion coefficient is proportional to the difference of molecular weights of the components and to the quotient between the thermal expansion coefficient and the viscosity. On the contrary, for mixtures where one of the components has an aromatic ring, the behaviour is the opposite; it is proportional to the quotient between the viscosity and the thermal expansion coefficient.

More experiments in non-ideal binary mixtures are needed in order to clarify the influence of different parameters and to determine general trends in these binary mixtures. The knowledge about the behaviour of the thermodiffusion coefficient in binary mixtures will allow having a better basis for the study of ternary mixtures.

Acknowledgments The results presented in this work were obtained in the framework of the following projects: GOVSORET3 (PI2011-22), MICROSCALE (IE13-360), Research Groups (IT557-10), and Research Fellowship (BFI-2011-295) of Basque Government and DCMIX (DCMIX-NCR-00022-QS) from the European Space Agency.

References

Alonso de Mezquia, D., Bou-Ali, M.M., Larrañaga, M., Madariaga, J., Santamaria, C.: Determination of molecular diffusion coefficient in n -alkane binary mixtures: Empirical correlations. J. Phys. Chem. B **116**, 2814–2819 (2012)

Blanco, P., Bou-Ali, M.M., Platten, J.K., Urteaga, P., Madariaga, J.A., Santamaria, C.: Determination of thermal diffusion coefficient in equimolar n-alkane mixtures: Empirical correlations. J. Chem. Phys. **129**, 174504 (2008)

Bou-Ali, M.M., Valencia, J., Madariaga, J.A., Santamaria, C., Ecenarro, O., Dutrieux, J.: Determination of the thermodiffusion coefficient in three binary organic liquid mixtures by the thermogravitational method. Philos. Mag. **83**, 2011–2015 (2003)

Capuano, F., Paduano, L., D'Errico, G., Mangiapia, G., Sartorio, R.: Diffusion in ternary aqueous systems containing human serum albumin and precipitants of different classes. Phys. Chem. Chem. Phys. **13**, 3319–27 (2011)

Croccolo, F., Bataller, H., Scheffold, F.: A light scattering study of non-equilibrium fluctuations in liquid mixtures to measure the Soret and mass diffusion coefficient. J. Chem. Phys. **137**, 234202 (2012)

Debuschewitz, C., Köhler, W.: Molecular origin of thermal diffusion in benzene + cyclohexane mixtures. Phys. Rev. Lett. **87**(1–4), 055901 (2001)

Furry, W., Jones, R., Onsager, L.: On the theory of isotope separation by thermal diffusion. Phys. Rev. E **55**, 1083–1095 (1939)

Galliéro, G., Duguay, B.m., Caltagirone, J.P., Montel, F.: Thermal diffusion sensitivity to the molecular parameters of a binary equimolar mixture, a non-equilibrium molecular dynamics approach. Fluid Phase Equilib. **208**, 171–188 (2003)

Königer, A., Meier, B., Kohler, W.: Measurement of the soret, diffusion, and thermal diffusion coefficients of three binary organic benchmark mixtures and of ethanol-water mixtures using a beam deflection technique. Philos. Mag. **89**(10), 907–923 (2009)

Leahy-Dios, A., Firoozabadi, A.: Molecular and thermal diffusion coefficients of alkane-alkane and alkane-aromatic binary mixtures: Effect of shape and size of molecules. J. Phys. Chem. B **111**(1), 191–198 (2007)

Leahy-Dios, A., Zhuo, L., Firoozabadi, A.: New thermal diffusion coefficient measurements for hydrocarbon binary mixtures: Viscosity and composition dependency. J. Phys. Chem. B **112**, 6442–6447 (2008)

Leppla, C., Wiegand, S.: Investigation of the soret effect in binary liquid mixtures by thermal-diffusion-forced rayleigh scattering (contribution to the benchmark test). Philos. Mag. **83**, 1989–1999 (2003)

Madariaga, J., Santamaria, C., Bou-Ali, M.M., Urteaga, P., Alonso De Mezquia, D.: Measurement of thermodiffusion coefficient in n -alkane binary mixtures: Composition dependence. J. Phys. Chem. B **114**, 6937–6942 (2010)

Mialdun, A., Shevtsova, V.: Measurement of the soret and diffusion coefficients for benchmark binary mixtures by means of digital interferometry. J. Chem. Phys. **134**, 044524 (2011)

Mialdun, A., Yasnou, V., Shevtsova, V., Königer, A., Köhler, W., Alonso de Mezquia, V., Bou-Ali, M.M.: A comprehensive study of diffusion, thermodiffusion, and soret coefficients of water-isopropanol mixtures. J. Chem. Phys. **136**, 244512 (2012)

Montel, F.: La Place de la thermodynamique dans une modelisation de répartitions des espéces d'hydrocarbures dans les réservoirs pétroliers. Incidence sur les problémes de production, Vol. 214 (1998)

Platten, J.K., Bou-Ali, M.M., Costeséque, P., Dutrieux, J., Köhler, W., Leppla, C., Wiegand, S., Wittko, G.G.: Benchmark values for the soret, thermal diffusion and diffusion coefficients of three binary organic liquid mixtures. Philos. Mag. **83**, 1965–1971 (2003)

Tello Alonso, H., Rubiolo, A.C., Zorrilla, S.E.: Prediction of the diffusion coefficients in multicomponent liquid refrigerant solutions. J. Food Eng. **109**, 490–495 (2012)

Villain-Guillot, S., Würger, A.: Thermal diffusion in a binary liquid due to rectified molecular fluctuations. Phys. Rev. E (Stat. Nonlinear Soft Matter Phys.) **83**, 030501 (2011)

F. Contribution to thermodiffusion coefficient measurements in DCMIX project.

International Journal of Thermal Sciences 92 (2015) 14–16

Contents lists available at ScienceDirect

International Journal of Thermal Sciences

journal homepage: www.elsevier.com/locate/ijts

Contribution to thermodiffusion coefficient measurements in DCMIX project

David Alonso de Mezquia [a], Miren Larrañaga [a], M. Mounir Bou-Ali [a, *], J. Antonio Madariaga [b], Carlos Santamaría [b], J. Karl Platten [a]

[a] Mechanical and Manufacturing Department, Engineering Faculty of Mondragon Unibertsitatea, Loramendi 4 Apdo. 23, 20500 Mondragon, Spain
[b] Department of Applied Physics II, University of Basque Country, UPV/EHU, Apdo 644, 48080 Bilbao, Spain

ARTICLE INFO

Article history:
Received 29 May 2014
Received in revised form
18 December 2014
Accepted 13 January 2015
Available online

Keywords:
Thermodiffusion coefficient
Binary mixtures
Ternary mixtures
Thermogravitational column

ABSTRACT

In this work we carefully measured the thermodiffusion coefficient of four ternary mixtures of 1,2,3,4-tetrahydronaphthalene, isobutylbenzene and *n*-dodecane at 25 °C and at mass fractions of: 10/80/10, 10/10/80, 40/20/40 and 45/10/45 using the thermogravitational technique. In order to determine the reproducibility of the measurements we performed three different runs for each mixture. In addition, we have also measured the thermodiffusion coefficient of 13 binary mixtures composed of these components. The obtained values of transport properties for binaries agreed with recent measurements done by optical methods and they allowed analysing the validity of an additive rule to determine the thermodiffusion coefficient of ternary mixtures from binary thermodiffusion data. A good agreement between measured and calculated values of the thermodiffusion coefficient for the four ternary mixtures studied was obtained. This work completes the thermodiffusion results for this hydrocarbon ternary mixture which has been analysed at other two compositions in previous works.

1. Introduction

Soret effect plays an important role in many fields. In particular, in oil reservoirs exploitation and recovery [1,2]. The models developed for the recovery of the fields work in scales of decades and in most of the cases, the operational scenario is predicted using very few data. A similar situation can be found when predicting the initial state of oil reservoirs [3,4]. Thus, the study of this phenomenon is very important for the scientific community.

Due to this interest, the DCMIX project, held by the European Space Agency, was developed. The objective of this project is to quantitatively analyse the thermodiffusion phenomenon in ternary mixtures. In the first stage of the project DCMIX the ternary mixture analysed is the one composed by 1,2,3,4-tetrahydronaphthalene (THN), isobutylbenzene (IBB) and *n*-dodecane (nC_{12}), at six different concentrations and at 25 °C. Recently, a great breakthrough has come across thanks to this project. The first benchmark in ternary mixtures has been developed for the ternary mixture formed by THN-IBB-nC12 at mass fraction of 0.8–0.1–0.1 and at 25 °C [5]. This mixture has been analysed in both ground and microgravity conditions by independent techniques, by six teams.

With the aim of completing the analysis of this ternary mixture, we have measured the thermodiffusion coefficient of four new compositions: 10/80/10, 10/10/80, 40/20/40 and 45/10/45. For that purpose, the thermophysical properties (dynamic viscosity, density, refractive index and thermal expansion coefficient) of these mixtures have been also determined. These results complete the ones published by our team in Refs. [6,7].

In addition, in order to determine the validity of the additive rule proposed by Larre and Platten [8], we have also measured the thermodiffusion coefficient of 13 binary mixtures composed of THN, IBB and nC_{12}. In this case also the thermophysical properties of all these binary mixtures have been determined. The obtained values agree reasonably with the ones recently measured by optical methods [9].

2. Experimental section

The details of the experimental methodology followed in this work can be found in the works [6,7]. First, the thermophysical properties of the mixtures were determined (density, refractive index, dynamic viscosity and thermal expansion coefficient). Then,

* Corresponding author. Tel.: +34 943 79 47 00; fax: +34 943 79 15 36.
E-mail address: mbouali@mondragon.edu (M.M. Bou-Ali).

http://dx.doi.org/10.1016/j.ijthermalsci.2015.01.013
1290-0729/

Table 1
Thermophysical properties at 25 °C for the ternary mixtures studied. Component 1 is THN and component 3 is nC_{12}.

Mixture	c_1	c_3	ρ (kg/m^3)	$\alpha/10^{-3}$ (K^{-1})	μ (mPa s)
THN/IBB/nC_{12}	0.10	0.80	771.944	0.954	1.314
	0.10	0.10	847.553	0.947	1.053
	0.40	0.40	842.524	0.905	1.354
	0.45	0.45	841.822	0.900	1.440

the thermogravitational technique was used to determine the thermodiffusion coefficients of the binary and ternary mixtures analysed in this work, from the measurements of the separation at steady state.

3. Results and discussion

Table 1 shows the thermophysical properties of the four ternary mixtures studied in this work. In addition, Table 2 shows the calibration parameters needed for the determination of the concentration of each component in the mixture [6,7]. In Table 3 the values of density and refractive index gradients for the four ternary mixtures of THN, IBB and nC_{12} studied in this work are shown. In order to test the reproducibility of the results obtained we performed three different runs in the thermogravitational column for each mixture. As can be seen in Table 3 the deviations between the values obtained of these gradients are quite small.

In the same table the values of the concentration gradients obtained from the calibration are given. As can be seen the deviations of these quantities between the different runs were of about 10% for small concentrations of THN and of about 4% for the higher ones. These errors are transmitted to the values of thermodiffusion coefficient which also appear in this table.

Table 4 gives the mean values of the thermodiffusion coefficients in Table 3 for all the ternary mixtures studied. The thermodiffusion coefficient for IBB was calculated using the condition that the sum of the three thermodiffusion coefficients is zero.

As can be seen in Table 4 the thermodiffusion coefficient of the denser component (THN) was always positive and for the lighter component (nC_{12}) was negative. Therefore THN migrates to the cold side and nC_{12} to the warm side. The coefficient of the IBB was, in absolute terms, smaller than the other two, which makes it much more sensitive. In any case the error in the value of this coefficient was large as it is calculated from the data obtained for the other two coefficients.

Larre et al. [8] proposed an additive rule to determine the thermal diffusion coefficient of any component in a ternary mixture from those in the corresponding binary mixtures. In order to check it we measured the thermodiffusion coefficients of the corresponding binary mixtures. We refer to D_T of the denser component which is always positive. The obtained results and the values of the thermophysical properties of these mixtures are given in Table 5. All the results are an average of at least three different measurements being the reproducibility of D_T better than 5%. In Fig. 1 the values of D_T as function of the mass fraction of the denser component for each mixture are plotted. In this Figure the D_T values for these mixtures measured by us in a previous work [6] are also represented. The dashed lines are the second order polynomials proposed by Gebhardt et al. [9] from measurements carried out by two optical methods: optical beam deflection and optical digital interferometry. As can be seen the agreement between our results and those of the literature was very good being the deviations always within the experimental error. It must be noticed that D_T for the mixture THN/nC_{12} is almost constant in the whole range of

Table 3
Thermodiffusion coefficients of ternary mixtures THN/IBB/nC_{12} at 25 °C. $\partial\rho/\partial z$, $\partial n/\partial z$, $\partial c_1/\partial z$ and $\partial c_3/\partial z$ are the density, refractive index and concentration gradients along the column height. Component 1 is THN and component 3 is nC_{12}.

c_1	c_3	$(\partial\rho/\partial z)$ (kg/m^4)	$(\partial n/\partial z)/10^{-2}$ (m^{-1})	$(\partial c_1/\partial z)$ (m^{-1})	$(\partial c_3/\partial z)$ (m^{-1})	$D'_{T,1}/10^{-12}$ (m^2 s^{-1} K^{-1})	$D'_{T,3}/10^{-12}$ (m^2 s^{-1} K^{-1})
0.10	0.80	−10.13	−0.564	−0.0394	0.0702	0.428	−0.767
		−10.23	−0.564	−0.0435	0.0673	0.475	−0.734
		−10.58	−0.582	−0.0463	0.0684	0.501	−0.750
0.10	0.10	−5.93	−0.336	−0.0213	0.0300	0.318	−0.443
		−6.20	−0.353	−0.0213	0.0322	0.318	−0.475
		−6.01	−0.338	−0.0231	0.0291	0.344	−0.430
0.40	0.40	−25.33	−1.390	−0.1097	0.1215	1.201	−1.333
		−25.60	−1.402	−0.1127	0.1210	1.236	−1.327
		−25.86	−1.415	−0.1145	0.1217	1.255	−1.335
0.45	0.45	−29.82	−1.629	−0.1310	0.1426	1.341	−1.459
		−29.42	−1.607	−0.1294	0.1406	1.324	−1.439
		−29.24	−1.596	−0.1291	0.1393	1.324	−1.423

Table 4
Mean values of the thermodiffusion coefficient of the ternary mixture THN/IBB/nC_{12} at 25 °C. Component 1 is THN and component 3 is nC_{12}.

c_1	c_2	c_3	$D'_{T,1}/10^{-12}$ (m^2 s^{-1} K^{-1})	$D'_{T,3}/10^{-12}$ (m^2 s^{-1} K^{-1})	$D'_{T,2}/10^{-12}$ (m^2 s^{-1} K^{-1})
0.10	0.10	0.80	+0.47 ± 0.04	−0.75 ± 0.03	+0.28 ± 0.04
0.10	0.80	0.10	+0.33 ± 0.02	−0.45 ± 0.03	+0.12 ± 0.02
0.40	0.20	0.40	+1.23 ± 0.04	−1.33 ± 0.02	+0.10 ± 0.01
0.45	0.10	0.45	+1.33 ± 0.04	−1.44 ± 0.02	+0.11 ± 0.01

Table 5
Thermophysical properties and thermodiffusion coefficients at 25 °C for the binary mixtures studied. The mass fraction is that of the denser component.

Mixture	c_1	ρ (kg/m^3)	$\alpha/10^{-3}$ (K^{-1})	β	μ (mPa s)	$D_T/10^{-12}$ (m^2 s^{-1} K^{-1})
THN/IBB	0.1111	861.007	0.943	0.129	1.054	3.7 ± 0.2
	0.5000[a]	904.514	0.888	0.128	1.374	2.9 ± 0.1
	0.6666	924.032	0.863	0.129	1.500	2.8 ± 0.1
	0.8181	942.275	0.844	0.131	1.729	2.4 ± 0.1
	0.8889	951.097	0.835	0.130	1.813	2.5 ± 0.1
THN/nC_{12}	0.1111	764.580	0.956	0.236	1.380	6.0 ± 0.3
	0.5000[a]	841.248	0.895	0.257	1.523	6.2 ± 0.3
	0.8889	934.359	0.837	0.287	1.815	6.2 ± 0.3
IBB/nC_{12}	0.1111	754.940	0.969	0.119	1.288	3.2 ± 0.2
	0.1818	761.368	0.968	0.121	1.223	3.3 ± 0.2
	0.3333	775.664	0.964	0.125	1.165	3.6 ± 0.2
	0.5000[a]	792.355	0.961	0.130	1.133	3.9 ± 0.2
	0.8889	835.454	0.959	0.144	1.008	5.0 ± 0.3

[a] Data taken from Ref. [6].

Table 2
Coefficients of the calibration planes of the studied ternary mixtures. Component 1 is THN and component 3 is nC_{12}.

Mixture	c_1	c_3	k_0 (kg/m^3)	k_1 (kg/m^3)	k_2 (kg/m^3)	k'_0	k'_1	k'_2
THN/IBB/nC_{12}	0.10	0.80	838.380	89.227	−94.189	1.476349	0.040406	−0.057613
	0.10	0.10	849.052	105.245	−122.807	1.483803	0.048842	−0.077340
	0.40	0.40	848.077	102.365	−116.189	1.482923	0.047269	−0.071802
	0.45	0.45	847.995	101.875	−115.505	1.483093	0.046719	−0.071310

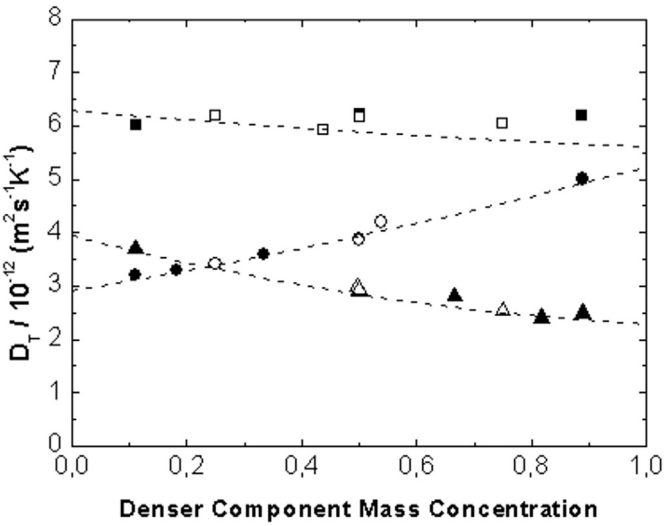

Fig. 1. Measured thermodiffusion coefficients for binary mixtures at 25 °C as function of mass fraction of the denser component for each system: ■:THN/nC12; ▲:THN/IBB and ●: IBB/nC12. Open symbols represent data from Ref. [6]. Dashed lines are the fit of experimental data from Gebhardt et al. [9].

Table 6
Comparison between the experimental data of $D'_{T,i}$ and the one determined using the additive rule of the work [8].

Mixture	c_1	c_3	$D'_{T,1}/10^{-12}$ (m^2 s^{-1} K^{-1})		$D'_{T,3}/10^{-12}$ (m^2 s^{-1} K^{-1})	
			Exp	Eq. [8]	Exp	Eq. [8]
THN/IBB/nC_{12}	0.10	0.80	0.47	0.51	−0.75	−0.74
	0.10	0.10	0.33	0.36	−0.45	−0.46
	0.40	0.40	1.23	1.22	−1.33	−1.28
	0.45	0.45	1.33	1.36	−1.44	−1.40

concentration, while in the case of IBB/nC_{12}, D_T increases with the concentration of the denser component (IBB) and for THN/IBB, D_T decreases with the concentration of the denser component (THN).

With the values of D_T for the binary mixtures we can calculate from the additive rule [8] the thermodiffusion coefficient of the ternary mixtures. In Table 6 we compare the measured and calculated thermodiffusion coefficients of the four ternary mixtures considered. As can be seen the additive rule reproduces the experimental data within a 10% which is a good result considering the experimental error in D_T both in binary and ternary mixtures.

4. Conclusions

In this work we measured in a plane thermogravitational column the thermodiffusion coefficient of four ternary mixtures of THN/IBB/nC_{12} and 13 binary mixtures composed by these components at 25 °C. To determine the reproducibility of the measurements we performed three different runs for each concentration. The results for the binary mixtures agreed with the ones recently measured by optical methods.

As in binary mixtures, in ternary mixtures the denser component (THN) behaves in a thermophobic way and the lighter one (nC_{12}) behaves in a thermophilic way. IBB was also thermophilic. The thermal diffusion coefficient of IBB is, in absolute value, much smaller than the other two coefficients.

The obtained results showed that the additive rule of Larre and Platten [8] reproduces the experimental values of the thermal diffusion coefficient within the error bars.

Acknowledgment

This article presents results that were partly obtained in the framework of the following projects: GOVSORET3 (PI2011-22), MicroCHEAP (IE14-391) and Research Groups (IT557-10) of Basque Government, and DCMIX (DCMIX-NCR-00022-QS) from the European Space Agency.

References

[1] F. Montel, Importance de la thermodiffusion en exploration et production pétroliéres, Entropie 185 (1994) 86–93.
[2] S. Van Vaerenbergh, A. Shapiro, G. Galliero, F. Montel, J.C. Legros, J.P. Caltagarione, J.L. Darion, Z. Saghir, Multicomponent Processes in Crudes: European Space Agency, Special Publication ESA SP 1290, 2005, pp. 202–213.
[3] M. Touzet, G. Galliero, V. Lazzeri, M.Z. Saghir, F. Montel, J.C. Legros, Thermodiffusion: from microgravity experiments to the initial state of petroleum, C. R. Mec. 339 (2011) 318–323.
[4] F. Montel, J. Bickert, A. Lagisquet, G. Galliero, Initial state of petroleum reservoirs: a comprehensive approach, J. Pet. Sci. Technol. 58 (2007) 391–402.
[5] M.M. Bou-Ali, A. Ahadi, D. Alonso de Mezquia, Q. Galand, M. Gebhardt, O. Khlybov, W. Köhler, M. Larrañaga, J.C. Legros, T. Lyubimova, A. Mialdun, I. Ryzhkov, M.Z. Saghir, V. Shevtsova, S. Van Varenbergh, Benchmark values for the Soret, thermodiffusion and molecular diffusion coefficients of the ternary mixture tetralin+isobutylbenzene+n-dodecane with 0.8-0.1-0.1 mass fraction, Eur. Phys. J. E (2015) (Accepted).
[6] P. Blanco, M.M. Bou-Ali, J.K. Platten, D.A. De Mezquia, J.A. Madariaga, C. Santamaría, Thermodiffusion coefficients of binary and ternary hydrocarbon mixtures, J. Chem. Phys. 132 (2010) 114506.
[7] M. Larrañaga, M.M. Bou-Ali, D. Alonso de Mezquia, D.A.S. Rees, J.A. Madariaga, C. Santamaría, J.K. Platten, Contribution to the Benchmark for ternary mixtures: determination of Soret coefficients by the Thermogravitational and the Sliding Symmetric Tubes techniques, Eur. Phys. J. E (2015) (Accepted).
[8] J. Larre, J.K. Platten, G. Chavepeyer, Soret effects in ternary systems heated from below, Int. J. Heat Mass Transfer 40 (1997) 545–555.
[9] M. Gebhardt, W. Köhler, A. Mialdun, V. Yasnou, V. Shevtsova, Diffusion, thermal diffusion and Soret coefficients and optical contrast factors of the binary mixtures of dodecane, isobutylbenzene and 1,2,3,4-tetrahydronaphthalene, J. Chem. Phys. 138 (2013) 114503.

G. Benchmark values for the Soret, Thermodiffusion and molecular diffusion coefficients of the ternary mixture tetralin+isobutylbenzene+n-dodecane with 0.8-0.1-0.1 mass fraction.

Eur. Phys. J. E (2015) **38**: 30
DOI 10.1140/epje/i2015-15030-7

THE EUROPEAN PHYSICAL JOURNAL E

Regular Article

Benchmark values for the Soret, thermodiffusion and molecular diffusion coefficients of the ternary mixture tetralin+isobutylbenzene+n-dodecane with 0.8-0.1-0.1 mass fraction*

M.M. Bou-Ali[1,a], A. Ahadi[2], D. Alonso de Mezquia[1], Q. Galand[3], M. Gebhardt[4], O. Khlybov[5], W. Köhler[4], M. Larrañaga[1], J.C. Legros[3], T. Lyubimova[5], A. Mialdun[3], I. Ryzhkov[6], M.Z. Saghir[2], V. Shevtsova[3], and S. Van Vaerenbergh[3]

[1] MGEP Mondragon Goi Eskola Politeknikoa, Mechanical and Industrial Manufacturing Department, Loramendi 4 Apdo 23, 20500 Mondragon, Spain
[2] Ryerson University, Dept. of Mechanical and industrial Engineering, Toronto, Canada
[3] MRC, EP CP 165/62, Université libre de Bruxelles (ULB), Brussels, Belgium
[4] Physikalisches Institut, Universität Bayreuth, D-95440 Bayreuth, Germany
[5] Institute of Continuous Media Mechanics UB RAS, Perm, Russia
[6] Institute of Computational Modelling SB RAS, Krasnoyarsk, Russia

Received 15 July 2014 and Received in final form 6 November 2014
Published online: 28 April 2015 –

Abstract. With the aim of providing reliable benchmark values, we have measured the Soret, thermodiffusion and molecular diffusion coefficients for the ternary mixture formed by 1,2,3,4-tetrahydronaphthalene, isobutylbenzene and *n*-dodecane for a mass fraction of 0.8-0.1-0.1 and at a temperature of 25 °C. The experimental techniques used by the six participating laboratories are Optical Digital Interferometry, Taylor Dispersion technique, Open Ended Capillary, Optical Beam Deflection, Thermogravitational technique and Sliding Symmetric Tubes technique in ground conditions and Selectable Optical Diagnostic Instrument (SODI) in microgravity conditions. The measurements obtained in the SODI installation have been analyzed independently by four laboratories. Benchmark values are proposed for the thermodiffusion and Soret coefficients and for the eigenvalues of the diffusion matrix in ground conditions, and for Soret coefficients in microgravity conditions.

1 Introduction

Transport properties play an important role in many natural and technological processes and for the fundamental understanding of the behaviour of liquids. Even today the Soret effect, a cross effect between temperature and concentration gradients, is poorly understood in multicomponent mixtures. The mass diffusion flux, $\mathbf{J}_i$, can be induced by both a temperature and a concentration gradient. Considering the linear laws of irreversible thermodynamics, the mass flux equations for components 1 and 2 in a ternary mixture may be written as [1]

$$\mathbf{J}_1 = -\rho D_{11}\boldsymbol{\nabla} c_1 - \rho D_{12}\boldsymbol{\nabla} c_2 - \rho D'_{T,1}\boldsymbol{\nabla} T, \quad (1)$$

$$\mathbf{J}_2 = -\rho D_{21}\boldsymbol{\nabla} c_1 - \rho D_{22}\boldsymbol{\nabla} c_2 - \rho D'_{T,2}\boldsymbol{\nabla} T, \quad (2)$$

where ρ is the density of the mixture, D_{11}, D_{12}, D_{21} and D_{22} are the molecular diffusion coefficients and $D'_{T,1}$ and $D'_{T,2}$ are the thermodiffusion coefficients. The third mass diffusion flux, $\mathbf{J}_3$, is defined from the condition that the fluxes of all the components must sum to zero. In stationary state, we can define the Soret coefficient for components 1 and 2, $S'_{T,1}$, $S'_{T,2}$, as [2]

$$S'_{T,1} = \frac{D'_{T,1}D_{22} - D'_{T,2}D_{12}}{D_{11}D_{22} - D_{12}D_{21}},$$

$$S'_{T,2} = \frac{D'_{T,2}D_{11} - D'_{T,1}D_{21}}{D_{11}D_{22} - D_{12}D_{21}}. \quad (3)$$

The Soret effect appears in many different processes, both natural and technological, of many different fields, such as biology [3] or food industry [4]. In particular, it is of high interest for the oil industry [5], where these data can be used to predict the initial state of oil reservoirs [6,7].

Binary mixtures have been widely studied and there are several works that show both numerical and experi-

* Contribution to the Topical Issue "Thermal non-equilibrium phenomena in multi-component fluids" edited by Fabrizio Croccolo and Henri Bataller.

[a] e-mail: mbouali@mondragon.edu

mental analysis [8–13] that enable the determination of the transport coefficients. The performance of the known Benchmark of Fontainebleau [14–19] came as a great progress. In that work, five groups determined independently the transport coefficients for the three binary mixtures of 1,2,3,4-tetrahydronaphthalene (tetralin), isobutylbenzene and n-dodecane for the mass concentration of 50% at the temperature of 25 °C, validating therefore the techniques and establishing reference values for future works.

But the liquids appearing in nature and in industrial applications usually contain more than just two components and the research focus has shifted to multicomponent systems. Fundamental research in ternary mixtures is needed before going to more complex mixtures. We have to point out that, due to the complexity of the problem, up to now there is no unified theory, as it can be seen, for example, in the differences between the theoretical models proposed by Firoozabadi [20], Kempers [21] and Larre [22]. Moreover, there are some tentative efforts to develop prediction models based on non-equilibrium thermodynamics or on molecular dynamics [23], but they cannot yet be validated. All this necessitates the establishment of a database of reliable experimental results that enables a test of the prediction models and, therefore, the theory.

By the time, some works that provide experimental data in ternary mixtures have been published, but they are very limited and the values given are not always comparable [24–30], so the dispersion in the results is quite high. Thus, it was necessary to coordinate all the experimental teams in order to analyse the same system using different techniques with the aim of comparing and evaluating the obtained results. With this purpose, this benchmark has been promoted in the framework of the project DCMIX jointly sponsored by the European Space Agency (ESA) and the Russian space agency Roscosmos, for comparing not only the results obtained in ground laboratories, but also the results obtained by the SODI installation, on board the International Space Station (ISS) under microgravity conditions.

During the workshop held at Mondragon Unibertsitatea, Mondragon (Spain), in October of 2013, the teams participating in the project DCMIX agreed to carry out the first benchmark for ternary mixtures. The chosen mixture is formed by tetrahydronaphtalene (THN), isobutylbenzene (IBB) and n-dodecane ($n\mathrm{C}_{12}$) at mass fractions of 0.8-0.1-0.1 and at 25 °C. After individual investigations, the results obtained by each team were compared and discussed during the 11th International Meeting on Thermodiffusion (IMT11) held in Bayonne, in June of 2014. The participating teams in this Benchmark are:

- Team headed by W. Köhler (WK), from Universität Bayreuth, Germany.
- Team headed by V. Shevtsova (VS), from Université Libre de Bruxelles (ULB), Belgium.
- Team headed by S. Van Vaerenbergh (SVV), from Université Libre de Bruxelles (ULB), Belgium.
- Team headed by Z. Saghir (ZS), from Ryerson University, Canada.
- Team headed by T. Lyubimova (RAS), from Russian Academy of Science (RAS), Russia.
- Team headed by M.M. Bou-Ali (MBA), from Mondragon Goi Eskola Politeknikoa (MGEP), Spain.

In this work, the obtained results and conclusions are shown, in order to be the reference for future techniques and measurements, as well as for the setting and the development of new prediction models based on the molecular dynamics or on the non-equilibrium thermodynamics.

2 Experimental techniques

The investigated mixture is formed by THN (purity 98+%), IBB (purity 99%) and $n\mathrm{C}_{12}$ (purity 99%), at the mass fraction of 80% of THN, 10% of IBB and 10% of $n\mathrm{C}_{12}$, at the temperature of 25 °C.

The thermodiffusion and Soret coefficients are related through the four isothermal diffusion coefficients that constitute the diffusion matrix, so the determination of the former allows one to find the latter and vice versa. On the one hand, eq. (3) is used to determine Soret coefficients from the independent experimental measurements of thermodiffusion and molecular diffusion coefficients. On the other hand, in order to determine the thermodiffusion coefficients from the independent experimental measurements of the molecular diffusion and Soret coefficients, the following expressions have been used:

$$D'_{T,1} = D_{11}S'_{T,1} + D_{12}S'_{T,2},$$
$$D'_{T,2} = D_{21}S'_{T,1} + D_{22}S'_{T,2}. \quad (4)$$

The eigenvalues of the diffusion matrix are given by the following formulas [28]:

$$\widehat{D_1} = \frac{D_{11} + D_{22} - \sqrt{(D_{11} - D_{22})^2 + 4D_{12}D_{21}}}{2}, \quad (5)$$

$$\widehat{D_2} = \frac{D_{11} + D_{22} + \sqrt{(D_{11} - D_{22})^2 + 4D_{12}D_{21}}}{2}. \quad (6)$$

In the case of the thermodiffusion and Soret coefficients, the results shown are for components 1 and 3, that is, for THN and $n\mathrm{C}_{12}$. As these two components have the highest difference in density and refractive index, the accuracy reached in the analysis of their coefficients is expected to be higher. In order to compare the coefficients corresponding to these two components, the relationships shown in eq. (7) and eq. (8) have been used. These relationships can be easily deduced from the requirement that the sum of the concentrations of the three components in a ternary mixture must be unity:

$$S'_{T,1} + S'_{T,2} + S'_{T,3} = 0, \quad (7)$$

$$D'_{T,1} + D'_{T,2} + D'_{T,3} = 0. \quad (8)$$

In the case of molecular diffusion, the values of coefficients depend on the order of the components. In this work,

the components are ordered in decreasing density, that is, THN-IBB-nC$_{12}$. In order to compare the results of the different teams, the following equations can be used. They enable the transformation of the coefficients from one order of components to another one, as can be seen for the case where components 2 and 3 are permuted [26]:

$$D_{11}^{*} = D_{11} - D_{12}, \tag{9}$$

$$D_{12}^{*} = -D_{12}, \tag{10}$$

$$D_{21}^{*} = D_{22} + D_{12} - D_{21} - D_{11}, \tag{11}$$

$$D_{22}^{*} = D_{22} + D_{12}. \tag{12}$$

The detailed descriptions of the different techniques and analysis methods used can be found in the six papers that are accompanied by this summary paper and are written by the participating teams. In the present work, the techniques used by each team to measure the coefficients in ground conditions and the analysis carried out to obtain the results measured in microgravity conditions are briefly described. Finally, the results proposed as benchmark values are shown.

2.1 Ground conditions

– The team of WK (Universität Bayreuth) has employed two-colour Optical Beam Deflection (OBD) to measure the Soret and thermodiffusion coefficients of the three compounds. Similar to the ODI method employed in Brussels and on board the ISS, this method relies on the different refractive index dispersions of the individual components of the mixture. The concentration changes of the two independent components in the mixture are determined from the refractive index gradients in a Soret cell measured at two different wavelengths. In order to take advantage of the strong dispersion near the UV absorption of aromatic π-electron systems, a blue wavelength of 405 nm has been employed in addition to the red laser at 635 nm. By this, it has been possible to obtain a contrast factor matrix with a condition number of 50, which greatly facilitates its necessary inversion. The Soret coefficients are determined from the asymptotic stationary amplitudes of the measured transient beam deflections.

– The team of VS (Université Libre de Bruxelles) used the Optical Digital Interferometry (ODI) technique to determine the Soret coefficients and the Taylor Dispersion Technique (TDT) to determine the molecular diffusion coefficients. A Mach-Zehnder interferometer was used to examine the separation in a Soret cell with a diffusion path of the same order of magnitude as for the space experiment. Laser diodes of 670 and 925 nm wavelength were used as sources of coherent light. Although the choice of wavelengths was not optimal (the condition number of matrix of contrast factors is around 240 [31]), it was intentionally made to be as close as possible to the space instrument. Experiments with different laser light sources have been carried out individually and were repeated 3 times for each laser. The ODI technique enables tracing of the concentration along the entire diffusion path, thus providing an extended amount of data to be fitted to the full analytical model of the separation process. To characterize the diffusion matrix by Taylor Dispersion Technique (see description of instrument in [27]), small injections of three different concentrations have been made into the laminar flow of the carrier solution created in a thin long capillary. The concentration of diffused injected samples as a function of time was monitored at the end of the capillary by a high-sensitivity differential refractometer operating at near infra-red. The injection of each particular concentration was also repeated 3-4 times.

– The team of SVV (Université Libre de Bruxelles) used the Open Ended Capillary (OEC) technique to determine the molecular diffusion coefficients. In the OEC, a concentration difference is created between a solution contained in capillary tubes and a solution contained in a bath. The liquid of different tubes is sampled over time and their composition is measured *ex situ*. Concentration measurements have been performed by ^{1}H-NMR. The diffusion coefficients are determined by fitting the measured composition evolution. For the results presented here, the precision on the estimated coefficients was improved by fitting simultaneously the data collected in two independent experiments.

– The team of MBA (Mondragon Goi Eskola Politeknikoa) used the thermogravitational technique (TG) [24] to determine the thermodiffusion coefficients from the variation of the concentration with the height of the column and the Sliding Symmetric Tubes (SST) [25] to determine the molecular diffusion coefficients from the variation of the concentration with time. Soret coefficients have been determined by eq. (3), from the measurements of thermodiffusion and molecular diffusion coefficients.

2.2 Microgravity conditions

The Selectable Optical Diagnostic Instrument known (SODI) has successfully been in operation on board the International Space Station since 2009 [32]. The current SODI configuration represents two optical modules accommodating Mach-Zehnder interferometers, suitable for accurate monitoring of refractive index inside transparent test objects [29,33]. One module holds a single-wavelength interferometer, another one features a two-wavelength interferometer with 670 and 935 nm lasers light sources. The latter module is equipped with a lateral translational stage that allows for monitoring of spatially separated cells combined in the so-called cell array. While most parts of the apparatus are fixed for each particular experiment, the cell array with the liquid samples can be changed from one experiment to another. The experiment DCMIX comprises a cell array consisting of 5 cells with ternary solutions (to be monitored by 2-wavelength moving optical module) and one reference binary cell (to be monitored by fixed 1-wavelength module). The cell array filled with the mixtures under investigation is the only part that needs to be uploaded to the ISS prior to the start of the experiments. The first experiment in the series, DCMIX-1, was targeting the THN-IBB-nC$_{12}$ system.

In all DCMIX experiments the mixtures are contained in a 10 mm × 10 mm × 5 mm cell. The mixture chosen for the benchmark was contained in cell #3 of the cell array.

Four teams have independently determined the Soret coefficients from the experiments carried out in the SODI installation. In all cases, the same contrast factors measured in ref. [31] have been used. The teams that have determined the Soret coefficients in microgravity conditions are

- Team of VS (Université Libre de Bruxelles)
- Team of SVV (Université Libre de Bruxelles)
- Team of RAS (Russian Academy of Sciences)
- Team of ZS (Ryerson University).

3 Results

In this section, the results obtained by the participating teams for the transport coefficients are shown. In ground conditions, results obtained for thermodiffusion, molecular diffusion and Soret coefficients and for the eigenvalues of the diffusion matrix are shown, while in microgravity conditions, results for Soret coefficients are provided. Together with the results, the experimental error of each technique is given. In addition, the weighted averages for each coefficient are given. For that, the statistical weights used are directly related to the experimental error of each technique.

3.1 Thermodiffusion coefficient

Here we show the thermodiffusion coefficients determined by the team of VS applying eq. (4) to the results obtained by the ODI and TDT techniques, the thermodiffusion coefficients extracted by the team of WK from OBD measurements, and the thermodiffusion coefficients measured directly by the team of MBA by the TG technique, in all three cases under ground conditions:

Table 1. Thermodiffusion coefficients determined in ground conditions for the mixture THN-IBB-nC$_{12}$ at the mass fraction of 0.8-0.1-0.1 and at 25 °C.

	Technique	$D'_{T,1}\times10^{-12}$ (m^2/s K)	$D'_{T,3}\times10^{-12}$ (m^2/s K)
Ground conditions	ODI+TDT	0.69 ± 0.13	-0.48 ± 0.06
	OBD	0.72 ± 0.26	-0.50 ± 0.16
	TG	0.67 ± 0.05	-0.49 ± 0.06
	Average	0.68 ± 0.05	-0.48 ± 0.04

As can be observed, the agreement between the values independently obtained in the three laboratories, both directly (TG, OBD) and by the combination of two techniques (ODI+TDT), is very good. As reference, we will take the weighted average of the results, with its corresponding weighted deviation (table 1, row 5).

3.2 Molecular diffusion coefficient and eigenvalue of the diffusion matrix

In this section, we present results obtained for the eigenvalues of the diffusion matrix (table 2) and for the corresponding molecular diffusion coefficients (table 3). In ground conditions, they have been directly measured by the team of VS using the TDT technique, by the team of SVV using the OEC technique and by the team of MBA using the SST technique.

Table 2. Eigenvalues of the diffusion matrix measured in ground conditions for the mixture THN-IBB-nC$_{12}$ at the mass fraction of 0.8-0.1-0.1 and at 25 °C.

	Technique	$\widehat{D_1}\times10^{-10}$ (m^2/s)	$\widehat{D_2}\times10^{-10}$ (m^2/s)
Ground conditions	TDT	5.29 ± 0.09	7.30 ± 0.26
	OEC	5.50 ± 0.03	6.60 ± 0.03
	SST	5.43 ± 0.68	8.08 ± 1.02
	Average	5.48 ± 0.03	6.61 ± 0.03

There is a reasonable agreement of the eigenvalues of the diffusion matrix, and the weighted averages with the corresponding weighted deviations have been determined (table 2, row 5). However, the agreement is not good in case of the molecular diffusion coefficients, being the worst in case of the cross-diffusion coefficients, where we can observe even changes in the sign in the results for the coefficient D_{21} (table 3, column 5). It seems that there can be more than one combination of diffusion coefficients in the matrix. Therefore, we propose the eigenvalues of the diffusion matrix as comparable reference parameters, instead of giving reference values for molecular diffusion coefficients.

3.3 Soret coefficients

Here, results for the Soret coefficients are shown. In ground conditions (table 4) they have been directly measured by the team of VS using the ODI technique and by the team of WK using the OBD technique, and they have been determined by applying eq. (3) to the results obtained by the TG and SST techniques. In addition, in microgravity conditions (table 5) Soret coefficients have been determined by teams of RAS, ZS, VS and SVV.

As commented in sect. 2, values are given for THN and nC$_{12}$ (components 1 and 3, respectively), because they are the components chosen to determine the coefficients in most of the techniques. Therefore, experimental errors accumulate in the results for component 2 and the dispersion is higher. However, results for component 2 can be easily calculated by eq. (8).

As can be observed, the values measured in ground conditions are in good agreement. The weighted average of the three independent results has been proposed as the reference. It is interesting to note that consistent results have been obtained by three different methods: by two direct techniques and by the combination of other two independent techniques.

Table 3. Molecular diffusion coefficients for the mixture THN-IBB-nC$_{12}$ at the mass fraction of 0.8-0.1-0.1 and at 25 °C.

	Technique	$D_{11} \times 10^{-10}$ (m^2/s)	$D_{12} \times 10^{-10}$ (m^2/s)	$D_{21} \times 10^{-10}$ (m^2/s)	$D_{22} \times 10^{-10}$ (m^2/s)
Ground conditions	TDT	6.61 ± 0.10	-0.59 ± 0.54	-1.55 ± 0.10	5.98 ± 0.44
	OEC	5.50 ± 0.51	-0.99 ± 0.63	0.002 ± 0.03	6.60 ± 0.37
	SST	5.23 ± 0.66	-1.80 ± 0.23	0.39 ± 0.05	8.28 ± 1.00

Table 4. Soret coefficients measured in ground conditions for the mixture THN-IBB-nC$_{12}$ at the mass fraction of 0.8-0.1-0.1 and at 25°.

	Technique	$S'_{T,1} \times 10^{-3}$ (K^{-1})	$S'_{T,3} \times 10^{-3}$ (K^{-1})
Ground conditions	ODI	1.04 ± 0.15	-0.94 ± 0.10
	OBD	1.20 ± 0.09	-0.86 ± 0.06
	TG+SST	1.19 ± 0.09	-0.91 ± 0.15
	Average	1.17 ± 0.06	-0.88 ± 0.05

Table 5. Soret coefficients measured in microgravity conditions for the mixture THN-IBB-nC$_{12}$ at the mass fraction of 0.8-0.1-0.1 and at 25 °C.

	Technique	$S'_{T,1} \times 10^{-3}$ (K^{-1})	$S'_{T,3} \times 10^{-3}$ (K^{-1})
Microgravity conditions	RAS	1.40 ± 0.16	-0.83 ± 0.10
	ZS	1.37 ± 0.06	-0.57 ± 0.05
	VS	1.43 ± 0.21	-0.66 ± 0.07
	SVV	1.39 ± 0.25	-0.49 ± 0.08
	Average	1.38 ± 0.05	-0.61 ± 0.03

As may be observed from the data in table 5, the Soret coefficients determined in microgravity conditions show acceptable agreement. The differences are larger if we compare them to the coefficients measured in ground conditions. The difference between the results measured in different gravity conditions arises from the fact that the design of the cells for the space instrument was subjected to a set of extra conditions (safety, feasibility, etc.) and from the condition number used. This finally resulted in certain deviations of the visible separation developing in the cell from its analytical model. These deviations can, in principle, be accounted for and a better agreement between all measurements may be achieved. This requires, however, a much more detailed and elaborated processing of the data from the space experiments, which appears not yet feasible at the present time. Simplified processing based on a straightforward fit to the analytical model results in a systematic error of 10–15% (overvalued separation for THN and undervalued separation for nC$_{12}$). It should be noted that the variations of experimental data for the Soret coefficients given in table 5 are not independent. Moreover, they show a linear correlation due to the specific properties of the contrast factor matrix. Further details can be found in the individual contributions of the teams of RAS, VS and WK that accompany this summary paper.

3.4 Benchmark values

In the following table 6 we show the benchmark values of thermodiffusion and Soret coefficients as well as the eigenvalues of diffusion matrix for the mixture THN-IBB-nC$_{12}$ at a mass fraction of 0.8-0.1-0.1 and at 25 °C. Because of the very different experimental boundary conditions, we give separate values for Soret coefficients measured in ground and in microgravity conditions. However, we also present the Soret coefficients for the combined gravity conditions.

Table 6. Benchmark values for the mixture THN-IBB-nC$_{12}$ at a mass fraction of 0.8-0.1-0.1 and at 25 °C.

	$D'_{T,1} \times 10^{-12}$ (m^2/s K)	$D'_{T,3} \times 10^{-12}$ (m^2/s K)
Ground conditions	0.68 ± 0.05	-0.48 ± 0.04
	$\widehat{D_1} \times 10^{-10}$ (m^2/s)	$\widehat{D_2} \times 10^{-10}$ (m^2/s)
Ground conditions	5.48 ± 0.03	6.61 ± 0.03
	$S'_{T,1} \times 10^{-3}$ (K^{-1})	$S'_{T,3} \times 10^{-3}$ (K^{-1})
Ground conditions	1.17 ± 0.06	-0.88 ± 0.05
Microgravity conditions	1.38 ± 0.05	-0.61 ± 0.03
Combined conditions	1.28 ± 0.04	-0.70 ± 0.03

This work has been developed in the framework of the cooperative project DCMIX (AO-2009-0858/1056) of the European Space Agency and the Russian Space Agency (Roscosmos). The Bayreuth team was supported by the Deutsche Forschungsgemeinschaft (KO1541/9-2) and by DLR (50WM1130). The Mondragon team was supported by Micro-CHEAP (IE14-391), Research Groups (IT557-10) and Research Fellowship (BFI-2011-295) of the Basque Government. The Ryerson team acknowledges the financial support of the Canadian Space Agency. The Brussels teams SVV and VS are thankful to the PRODEX programme of the Belgian Federal Science Policy Office and ESA. The Russian team was supported by FGUP TSNIIMASH. The Brussels team VS and Russian Team IR acknowledge the financial support of Wallonie-Bruxelles International, Belgium.

References

1. M.M. Bou-Ali, J.K. Platten, J. Non-Equilib. Thermodyn. **30**, 385 (2005).
2. A. Mialdun, V. Shevtsova, J. Chem. Phys. **138**, 161102 (2013).
3. J.K.G. Dhont, S. Wiegand, S. Duhr, D. Braun, Langmuir **23**, 1674 (2007).
4. H. Tello Alonso, A.C. Rubiolo, S.E. Zorrilla, J. Food Eng. **109**, 490 (2012).
5. F. Montel, Entropie **184/185**, 86 (1994).
6. M. Touzet, G. Galliero, V. Lazzeri, M.Z. Saghir, F. Montel, J.C. Legros, C.R. Méc. **339**, 318 (2011).
7. F. Montel, J. Bickert, A. Lagisquet, G. Galliero, J. Petrol. Sci. Eng. **58**, 391 (2007).
8. A. Mialdun, V. Yasnou, V. Shevtsova, A. Königer, W. Köhler, D. Alonso de Mezquia, M.M. Bou-Ali, J. Chem. Phys. **136**, 244512 (2012).
9. P. Blanco, P. Polyakov, M.M. Bou-Ali, S. Wiegand, J. Phys. Chem. B **112**, 8340 (2008).
10. A. Perronance, C. Leppla, F. Leroy, B. Rousseau, S. Wiegand, J. Chem. Phys. **116**, 3718 (2002).
11. P.A. Artola, B. Rousseau, G. Galliero, J. Am. Chem. Soc. **130**, 10963 (2008).
12. M. Eslamian, M.Z. Saghir, Phys. Rev. E **80**, 011201 (2009).
13. F. Croccolo, H. Bataller, F. Scheffold, J. Chem. Phys. **137**, 234202 (2012).
14. J.K. Platten, M.M. Bou-Ali, P. Costeséque, J. Dutrieux, W. Köhler, C. Leppla, S. Wiegand, G. Wittko, Philos. Mag. **83**, 1965 (2003).
15. G. Wittko, W. Köhler, Philos. Mag. **83**, 1973 (2003).
16. C. Leppla, S. Wiegand, Philos. Mag. **83**, 1989 (2003).
17. J.K. Platten, M.M. Bou-Ali, J.F. Dutrieux, Philos. Mag. **83**, 2001 (2003).
18. M.M. Bou-Ali, J.J. Valencia, J.A. Madariaga, C. Santamaría, O. Ecenarro, J.F. Dutrieux, Philos. Mag. **83**, 2011 (2003).
19. P. Costesèque, J.-C. Loubet, Philos. Mag. **83**, 2017 (2003).
20. K. Ghorayeb, A. Firoozabadi, AlChE J. **46**, 883 (2000).
21. L. Kempers, J. Chem. Phys. **90**, 6541 (1989).
22. J.P. Larre, J.K. Platten, G. Chavepeyer, Int. J. Heat Mass Transfer **40**, 545 (1997).
23. S. Srinisvasan, M.Z. Saghir, J. Non-Equilib. Thermodyn. **36**, 243 (2011).
24. P. Blanco, M.M. Bou-Ali, J.K. Platten, D. Alonso de Mezquía, J.A. Madariaga, C. Santamaría, J. Chem. Phys. **132**, 114506 (2010).
25. M. Larrañaga, D.A.S. Rees, M.M. Bou-Ali, J. Chem. Phys. **140**, 054201 (2014).
26. A. Königer, H. Wunderlich, W. Köhler, J. Chem. Phys. **132**, 174506 (2010).
27. A. Mialdun, V. Sechenyh, J.C. Legros, J.M. Ortiz de Zárate, V. Shevtsova, J. Chem. Phys. **139**, 104903 (2013).
28. A. Leahy-Dios, M.M. Bou-Ali, J.K. Platten, A. Firoozabadi, J. Chem. Phys. **122**, 234502 (2005).
29. A. Ahadi, S. Van Vaerenbergh, M.Z. Saghir, J. Chem. Phys. **138**, 204201 (2013).
30. Q. Galand, S. Van Vaerenbergh, F. Montel, Energy Fuels **22**, 770 (2008).
31. V. Sechenyh, J.-C. Legros, V. Shevtsova, J. Chem. Thermodyn. **62**, 64 (2013).
32. S. Mazzoni, V. Shevtsova, A. Mialdun, D. Melnikov, Yu. Gaponenko, T. Lyubimova, M.Z. Saghir, Europhys. News **41**, 14 (2010).
33. A. Mialdun, C. Minetti, Y. Gaponenko, V. Shevtsova, F. Dubois, Micrograv. Sci. Technol. **25**, 83 (2013).

H. Contribution to the benchmark for ternary mixtures: determination of the Soret coefficients by the thermogravitational and sliding symmetric tubes techniques.

Eur. Phys. J. E (2015) **38**: 28
DOI 10.1140/epje/i2015-15028-1

THE EUROPEAN PHYSICAL JOURNAL E

Regular Article

Contribution to the benchmark for ternary mixtures: Determination of Soret coefficients by the thermogravitational and the sliding symmetric tubes techniques*

Miren Larrañaga[1], M. Mounir Bou-Ali[1,a], David Alonso de Mezquía[1], D. Andrew S. Rees[2], Jose Antonio Madariaga[3], Carlos Santamaría[3], and Jean K. Platten[4]

[1] MGEP Mondragon Goi Eskola Politeknikoa, Mechanical and Industrial Manufacturing Department, Loramendi 4 Apdo 23, 20500 Mondragon, Spain
[2] Department of Mechanical Engineering, University of Bath, Claverton Down, Bath BA2 7AY, United Kingdom
[3] Department of Applied Physics II, University of Basque Country, Apdo. 644, 48080 Bilbao, Spain
[4] University of Mons-Hainaut, B-7000 Mons, Belgium

Received 16 July 2014 and Received in final form 17 November 2014
Published online: 28 April 2015 –

Abstract. This work is part of an international project for the research on the transport properties in ternary mixtures. Six different teams have analysed the same mixture by independent techniques in order to compare the results and validate the techniques. This work is the contribution of the team of Mondragon Unibertsitatea for ground conditions measurements. This team has measured the thermodiffusion coefficients by the thermogravitational techniques and the molecular diffusion coefficients by the Sliding Symmetric Tubes technique. The Soret coefficients have been determined by the combination of the thermodiffusion and molecular diffusion coefficients. The mixture chosen for the study is the one formed by 1,2,3,4-tetrahydronaphtalene, isobutylbenzene and *n*-dodecane at mass fraction of 80% of THN, 10% of IBB and 10% of nC_{12}, and at 25 °C. The good agreement between the results of the different teams shows the validity of the techniques used in this work.

1 Introduction

The research on transport properties in multicomponent mixtures is of great interest in the scientific community, due to their presence in lots of natural and industrial processes.

The case of binary mixtures has been widely studied, and there are several experimental techniques [1,2] and numerical prediction models [3,4] that allow the accurate determination of the diffusion, thermodiffusion and Soret coefficients. Nowadays, the focus is on ternary mixtures, because it is necessary to analyse and understand them before going to multicomponent mixtures. In the last years, some works have been published which try to determine the thermodiffusion, molecular diffusion or Soret coefficients in ternary mixtures [5–14]. However, as they are individual works and not all concerned with the same mixture, there was a high dispersion between the results, so they were not easily comparable. Moreover, the existing differences in the theories about the thermodiffusion phenomenon in ternary mixtures [15–18] show again the need of a database of reliable experimental data. Because of these reasons, and in the framework of the project DCMIX (Diffusion coefficient measurements in ternary mixtures), this Benchmark in ternary mixtures has been developed, where six teams at international level have participated. The present work is published together with other five works corresponding to the other participant teams, and with another one more work in which a summary of the Benchmark is presented.

The purpose of this Benchmark is to analyse independently the same mixture by different techniques so that reliable results of thermodiffusion, molecular diffusion and Soret coefficients are provided. The chosen mixture is formed by 1,2,3,4-tetrahydronaphtalene (THN), isobutylbenzene (IBB) and *n*-dodecane (nC_{12}) at mass fraction of 80% of THN, 10% of IBB and 10% of nC_{12}, and at 25 °C. As was proposed in [2], the order of components chosen is in decreasing order of density, that is, THN-IBB-nC_{12}. The techniques which were employed to analyse this mixture are: Optical Beam Deflection technique (OBD) [6], which determines the Soret coefficients; the Taylor Dispersion instrument (TDT) [5] which determines

* Contribution to the Topical Issue "Thermal non-equilibrium phenomena in multi-component fluids" edited by Fabrizio Croccolo and Henri Bataller.

[a] e-mail: mbouali@mondragon.edu

the molecular diffusion coefficients, Optical Digital Interferometry (ODI) [5], which determines the Soret coefficients; the Open Ended Capillary (OEC) [7] which determines the molecular diffusion coefficients; the thermogravitational technique (TG) [8] which determines the thermodiffusion coefficients; and the Sliding Symmetric Tubes technique (SST) [9], which determines the molecular diffusion coefficients. In addition, measurements have been also performed in the SODI instrument (Selectable Optical Diagnostic Instrument) [18,19] on board the International Space Station (ISS); there, Soret coefficients can be determined in microgravity conditions. The Benchmark results in microgravity conditions have been analysed independently by four teams.

In the present work we present the contribution of the team at Mondragon Unibertsitatea and provide a detailed explanation of the processes used. More specifically, the thermodiffusion coefficients were determined by the thermogravitational technique, the molecular diffusion coefficients were determined by the Sliding Symmetric Tubes technique and Soret coefficients by the combination of the thermodiffusion and molecular diffusion coefficients.

2 Experimental procedure

In this section first, we describe the equipment used to measure the relevant thermophysical properties of the studied mixture composed by THN-IBB-nC$_{12}$ at mass fraction of 0.8-0.1-0.1. We describe also the procedure needed to determine the concentration of each component in a ternary mixture from the density and the refractive index. Then, the thermogravitational technique and Sliding Symmetric Tubes technique are described. Finally, the determination of the Soret coefficient is shown.

2.1 Thermophysical properties and experimental analysis

Before the determination of the thermodiffusion coefficient, it is necessary to determine also the density, the refractive index, the thermal expansion coefficient and the viscosity of the mixture. For the determination of the density an Anton Paar DMA 5000 vibrating quartz U-tube densimeter with accuracy of 5×10^{-6} g/cm^3 was used. By measuring the density at different temperatures (24 °C, 24.5 °C, 25 °C, 25.5 °C, 26 °C) the thermal expansion coefficient was deduced. Coupled to the densimeter is an Anton Paar RXA 156 refractometer with accuracy of 2×10^{-5} RIU, which measures the refractive index. By the measurements of density and refractive index we determine the concentration of the mixture. The dynamic viscosity was measured by an Anton Paar AMVn falling ball microviscometer, which has an accuracy of ±0.002 seconds.

In order to determine the concentration of each component in a ternary mixture it is necessary to carry out a prior calibration. This calibration consists on preparing 25 mixtures with concentration around the concentration of study and measuring their densities and refractive indices. With this data, calibration planes are built (fig. 1 and fig. 2) and from them, calibration parameters can be determined. These coefficients enable the determination of the concentrations of each component in a ternary mixture from the measurements of density and refractive index, by the following equations:

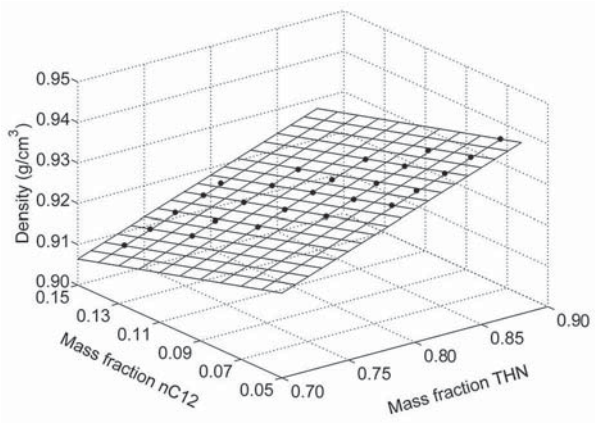

Fig. 1. Calibration plane of density for the mixture THN-IBB-nC$_{12}$ at the mass fraction of 0.8-0.1-0.1 and at 25 °C.

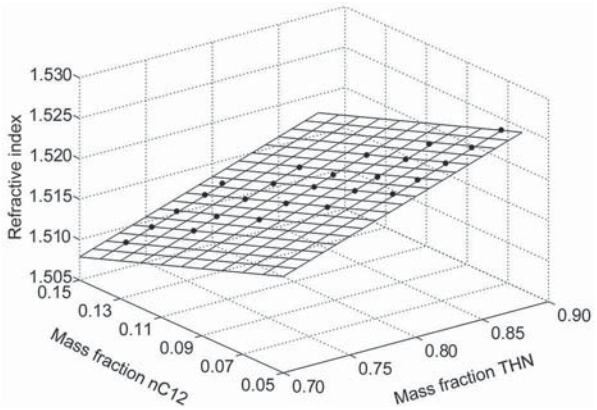

Fig. 2. Calibration plane of refractive index for the mixture THN-IBB-nC$_{12}$ at the mass fraction of 0.8-0.1-0.1 and at 25 °C.

$$c_1 = \frac{c'(\rho - a) - c(n_D - a')}{bc' - b'c}, \tag{1}$$

$$c_2 = \frac{b(n_D - a') - b'(\rho - a)}{bc' - b'c}, \tag{2}$$

$$c_3 = 1 - c_1 - c_2, \tag{3}$$

where c_1, c_2 and c_3 are the concentrations of components 1, 2 and 3, ρ is the density of the mixture, n_D is the refractive index of the mixture, and a, a', b, b', c and c' are the calibration parameters.

So as to validate the calibration, densities and refractive indices corresponding to each concentration are calculated by the calibration parameters. These calculated values are compared to the experimental ones. The maximum error admitted to validate a calibration is 0.5%.

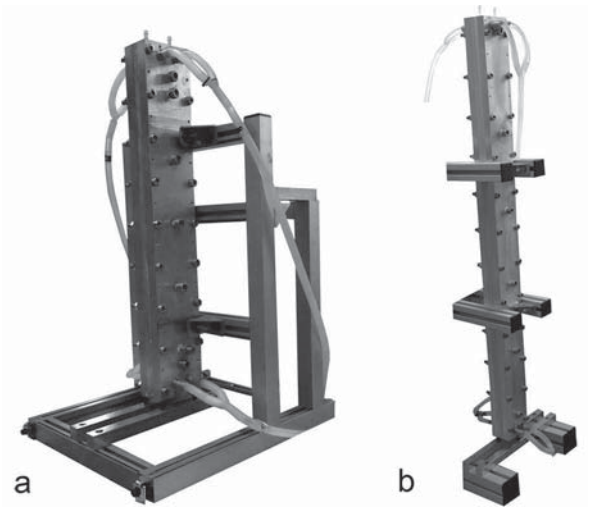

Fig. 3. a) Thermogravitational column of $L_z = 500\,\text{mm}$ (STC). b) Thermogravitational column of $L_z = 980\,\text{mm}$ (LTC).

Table 1. Comparison between Benchmark binary values and the experimental ones obtained by the thermogravitational column of $L_z = 980\,\text{mm}$ (LTC).

Mixture	$D_T \times 10^{-12}$ (m^2/s K) LTC	$D_T \times 10^{-12}$ (m^2/s K) Bench	Diff (%)
THN-IBB (0.5)	2.73 ± 0.05	2.80	2.5
IBB-$n\text{C}_{12}$ (0.5)	3.64 ± 0.06	3.70	1.6
THN-$n\text{C}_{12}$ (0.5)	6.05 ± 0.10	5.90	2.5

2.2 Thermogravitational technique

The thermogravitational technique has been successfully used in several works, both in binary [20,21] and ternary [8] mixtures. In this work two thermogravitational columns have been used: STC and LTC. Both of them have a very similar gap width (STC has $L_x = 1 \pm 0.005\,\text{mm}$ and LTC has $L_x = 1.02 \pm 0.005\,\text{mm}$) but different gap length. The first one has length of $L_z = 500\,\text{mm}$ (fig. 3a), and it has been used in several works [8,22,23], whereas the second one has length of $L_z = 980\,\text{mm}$ (fig. 3b) and therefore, produces a double separation. It has been designed and constructed with the aim of improving the accuracy in the determination of the concentration gradient, which is of particular interest for ternary mixtures.

This new column was validated by measuring the known Benchmark binary mixtures formed by THN, IBB and $n\text{C}_{12}$ at 50% of mass fraction [8]. In all the cases, the differences with the Benchmark values were under 3% (table 1). Independently, in this work, the results obtained with both columns for the studied ternary mixtures are shown.

In the thermogravitational technique, the analysed mixture is placed between two vertical walls at different temperatures. Due to the temperature gradient, generally, the denser component moves toward the colder wall, while the less dense component moves toward the hotter wall, thereby creating a concentration gradient. This gradient generates a diffusive flux in the opposite direction, due to the molecular diffusion effect. In addition, the effect of the gravity generates convective fluxes that amplify the separation along the column. When the ultimate stationary state is reached, density and refractive index are measured at different heights of the column (fig. 4), which enables the determination of the variation of the concentration of each component along the height of the column (fig. 5). These concentration gradients are used to determine the thermodiffusion coefficient for each component, by the following equation [10]:

$$D'_{T,i} = -\frac{L_x^4}{504}\frac{\alpha g}{\upsilon}\frac{\partial c_i}{\partial z}\,, \tag{4}$$

where $D'_{T,i}$ is the thermodiffusion coefficient for component i, L_x is the width of the gap of the column, υ is the kinematic viscosity of the mixture, α is the thermal expansion coefficient, g is gravity and $\partial c_i/\partial z$ is the variation of the concentration with the height of the column.

The experimental error of each of the parameters in eq. (4) must be considered when analysing the uncertainty of the determination of the thermodiffusion coefficients by the thermogravitational technique. As may be noticed, the geometric error of the width of the gap has the greatest influence, and it will appear in all the measurements made by the column. In the case of the thermal expansion coefficient, the accuracy of the densimeter and the error of the linear regression (density *vs.* temperature) were considered. The errors of the density and the dynamic viscosity are directly related to the accuracy of the densimeter and the microviscometer respectively. Finally, in the case of the concentration gradients, two facts were considered: the calibration errors andthe accuracy of the linear regressions (concentration *vs.* height).

2.3 Sliding symmetric tubes technique

This technique has been employed in several works in order to determine the molecular diffusion coefficients in both binary [24] and ternary mixtures [9], where the procedure for determining the molecular diffusion coefficients is widely described. In fig. 6 the installation used for the SST technique is shown.

By this technique, molecular diffusion coefficients can be determined from the variation of the concentration of each component with time. The slopes of the linear regressions formed when showing the variation of the concentration with the square root of time, enable the determination of the molecular diffusion coefficients by the following working equations:

$$S_1 = \frac{2}{L\sqrt{\pi}}\left(\frac{A}{\alpha_1} + \frac{B}{\alpha_2}\right), \tag{5}$$

$$S_2 = \frac{2}{L\sqrt{\pi}}\left(\frac{A}{\alpha_1}\left(\frac{1 - D_{11}\alpha_1^2}{D_{12}\alpha_1^2}\right) + \frac{B}{\alpha_2}\left(\frac{1 - D_{11}\alpha_2^2}{D_{12}\alpha_2^2}\right)\right), \tag{6}$$

where S_1 and S_2 are the slopes formed by the variation of the concentration with the square root of time, L is the

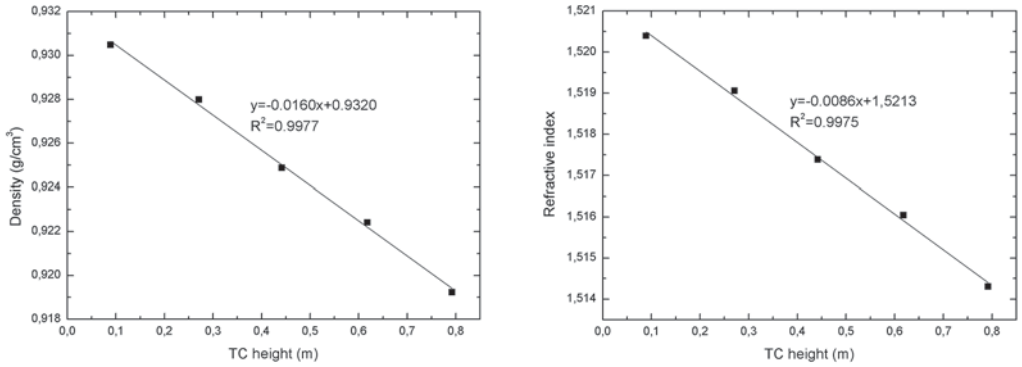

Fig. 4. Variation of the density and the refractive index of the mixture with the height of the column of $L_z = 980\,\text{mm}$.

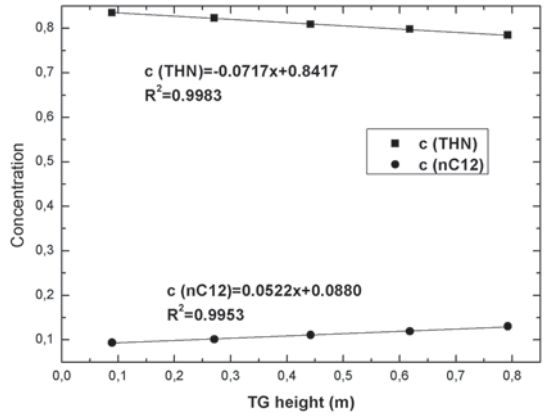

Fig. 5. Variation of the concentration of components 1 and 3 with the height of the column of $L_z = 980\,\text{mm}$.

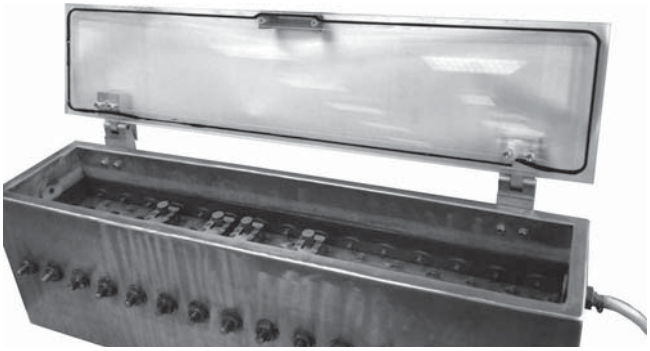

Fig. 6. Installation for the Sliding Symmetric Tubes technique.

length of the tubes, A and B are the integration constants, α_1 and α_2 are function of the eigenvalues of the diffusion matrix, D_{11} and D_{22} are the diagonal diffusion coefficients and D_{12} and D_{21} are the cross-diagonal diffusion coefficients.

As is detailed in [9], two independent experiments with different initial concentrations are needed to determine the molecular diffusion coefficients of a ternary mixture. Thus, we have four equations and four unknowns: the four molecular diffusion coefficients. In order to solve the system, the Newton-Raphson method is used, where the fitting parameters are the four diffusion coefficients. We can control the maximum fitting error in order to be under 1%.

To determine the experimental error in the determination of the molecular diffusion coefficients by the SST technique, three factors may be taken into account: i) the admitted error in the Newton-Raphson fitting, ii) the fitting error of the linear regressions (concentration *vs.* square root of time) and iii) the calibration error.

2.4 Determination of Soret coefficient

The Soret coefficient for each component, $S'_{T,1}$, $S'_{T,2}$, is determined from the results obtained for the molecular diffusion and thermodiffusion coefficients, by means of the following equations [25]:

$$S'_{T,1} = \frac{D'_{T,1}D_{22} - D'_{T,2}D_{12}}{D_{11}D_{22} - D_{12}D_{21}},$$

$$S'_{T,2} = \frac{D'_{T,2}D_{11} - D'_{T,1}D_{21}}{D_{11}D_{22} - D_{12}D_{21}}. \quad (7)$$

The experimental error accumulated in the indirect determination of the Soret coefficient is obtained by applying the rules of error propagation in eq. (7).

3 Results

In this section the results obtained for thermodiffusion, molecular diffusion and Soret coefficients for the mixture THN-IBB-nC$_{12}$ at mass fraction of 0.8-0.1-0.1 and at 25 °C are shown. In addition, the results corresponding to the density, dynamic viscosity, thermal expansion coefficient and calibration parameters used for the determination of the concentrations of each component of the mixture are presented at the beginning.

3.1 Thermophysical properties and calibration parameters

Table 2 gives the density, dynamic viscosity and thermal expansion coefficient of the chosen ternary mixture at the reference concentration.

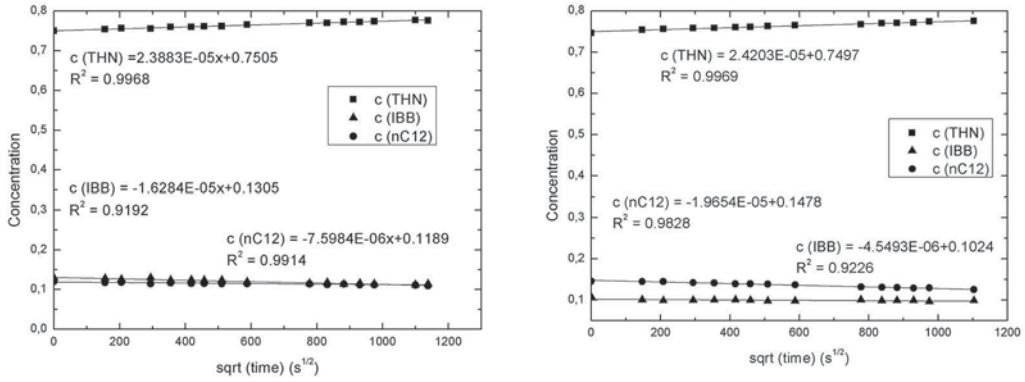

Fig. 7. Variation of the concentration of each component with the square root of the time, for experiments 3 and 4, for the mixture THN-IBB-nC$_{12}$ at mass fraction of 0.8-0.1-0.1 and at 25 °C.

Table 2. Density, thermal expansion coefficient and dynamic viscosity for the ternary mixture THN-IBB-nC$_{12}$ at mass fraction of 0.8-0.1-0.1 and at 25 °C.

THN-IBB-nC$_{12}$ $c_1 - c_2 - c_3$	ρ (kg/m^3)	$\alpha \times 10^{-3}$ (K^{-1})	μ (mPa · s)
0.8-0.1-0.1	925.316	0.848	1.719

Table 3. Calibration parameters for the ternary mixture THN-IBB-nC$_{12}$ at mass fraction of 0.8-0.1-0.1 and at 25 °C.

THN-IBB-nC$_{12}$ c_1-c_2-c_3	a (kg/m^3)	b (kg/m^3)	c (kg/m^3)	a'	b'	c'
0.8-0.1-0.1	845.888	117.569	−145.028	1.48294	0.05497	−0.09042

Then, in table 3 the calibration parameters necessary for the determination of the concentration gradient of each component in the mixture by eq. (1) and eq. (2) are shown.

3.2 Thermodiffusion coefficients

As has been commented previously, in this work the thermodiffusion coefficients have been determined by two different thermogravitational columns: one with length of $L_z = 500$ mm and the other with length of $L_z = 980$ mm. Three independent experiments were performed in each column, from which the mean value is taken as the proposed result for the Benchmark. Table 4 shows the results for the components 1 and 3 (*i.e.* THN and nC$_{12}$). The standard deviation between the six experiments is of 1.4% for component 1 and of 3.6% for component 3 and as can be observed in table 4, these deviations are within the experimental error bar. To determine the uncertainty of the proposed values, the experimental error has been taken into account.

The values of the thermodiffusion coefficient of IBB can be calculated from the condition that the sum of the three thermodiffusion coefficients is zero. In this mixture, this coefficient is positive and smaller than the other two.

3.3 Molecular diffusion coefficients and eigenvalues of the diffusion matrix

As was commented in sect. 2.3, it is necessary to perform two experiments with different initial concentrations in order to determine the molecular diffusion coefficients of one mixture. In this case, in order to check the repeatability of the SST technique, four independent experiments were performed with different initial concentrations. Combining the data of the experiments, four cases of results can be obtained. In the following table 5 the initial concentrations of the four experiments are shown.

As can be observed, in experiments 1 and 3 the concentrations of all the components vary, whereas in experiments 2 and 4, the concentration of the IBB stays constant between the upper and the bottom tubes. In fig. 7 the variation of the concentration of each component with the square root of the time is shown for two independent experiments.

Table 6 gives the results corresponding to the molecular diffusion coefficients and the eigenvalues of the diffusion matrix for the four possible combinations of experiments. In each case, the corresponding experimental error is given. The results shown are for the order of components THN-IBB-nC$_{12}$. The second digit after the decimal point is not relevant in most of the cases, but it has been kept in the results so as to maintain the consistency in this work and in the summary work.

As can be observed, in the case of the eigenvalues the repeatability is convincing, especially for $\widehat{D_1}$. Regarding to the molecular diffusion coefficients, the D_{11} coefficients have an acceptable repeatability, but in the case of the other coefficients the repeatability is worse, finding even changes in the sign in the case of the D_{21} coefficient. Although it may not be wise to calculate the mean values

Table 4. Thermodiffusion coefficients for the ternary mixture THN-IBB-nC$_{12}$ at mass fraction of 0.8-0.1-0.1 and at 25 °C.

	$D'_{T,1} \times 10^{-12}$ (m^2/s K)	$D'_{T,3} \times 10^{-12}$ (m^2/s K)
STC $L_z = 500$ mm	0.68 ± 0.03	-0.49 ± 0.01
	0.66 ± 0.05	-0.45 ± 0.07
	0.66 ± 0.03	-0.46 ± 0.03
LTC $L_z = 980$ mm	0.67 ± 0.04	-0.50 ± 0.03
	0.69 ± 0.03	-0.50 ± 0.03
	0.68 ± 0.04	-0.51 ± 0.03
Proposed values	0.67 ± 0.05	-0.49 ± 0.06

Table 5. Initial concentrations of the experiments carried out by the SST technique.

	Bottom tube			Upper tube		
	THN	IBB	nC$_{12}$	THN	IBB	nC$_{12}$
Exp. 1	0.84	0.08	0.08	0.76	0.12	0.12
Exp. 2	0.84	0.10	0.06	0.76	0.10	0.14
Exp. 3	0.85	0.07	0.08	0.75	0.13	0.12
Exp. 4	0.85	0.10	0.05	0.75	0.10	0.15

Table 6. Molecular diffusion coefficients and eigenvalues of the diffusion matrix for the ternary mixture THN-IBB-nC$_{12}$ at mass fraction of 0.8-0.1-0.1 and at 25 °C.

Experiments	$D_{11} \times 10^{-10}$ (m^2/s)	$D_{12} \times 10^{-10}$ (m^2/s)	$D_{21} \times 10^{-10}$ (m^2/s)	$D_{22} \times 10^{-10}$ (m^2/s)	$\widehat{D_1} \times 10^{-10}$ (m^2/s)	$\widehat{D_2} \times 10^{-10}$ (m^2/s)
1-2	4.91 ± 0.62	-1.97 ± 0.25	0.99 ± 0.12	8.57 ± 1.08	5.56 ± 0.70	7.92 ± 0.99
3-4	5.47 ± 0.69	-1.87 ± 0.23	-0.06 ± 0.01	8.43 ± 1.06	5.43 ± 0.68	8.47 ± 1.06
1-4	5.66 ± 0.71	-0.42 ± 0.53	-0.44 ± 0.05	5.63 ± 0.71	5.22 ± 0.66	6.08 ± 0.76
2-3	4.87 ± 0.61	-2.95 ± 0.37	1.08 ± 0.14	10.49 ± 1.32	5.50 ± 0.67	9.85 ± 0.12
Mean value	5.23 ± 0.66	-1.80 ± 0.23	0.39 ± 0.05	8.28 ± 1.00	5.43 ± 0.68	8.08 ± 1.02

of the diffusion coefficients with such large deviations, we have done it and taken it as a fifth case of results. The purpose of this is to analyse the reliability of the Soret coefficients calculated by eq. (7). The uncertainty given for these mean values is the experimental error.

3.4 Soret coefficients

Soret coefficients have been determined by eq. (7). In the previous section, a bad repeatability of the molecular diffusion coefficients has been observed. Therefore, Soret coefficients have been determined for the four possible results of molecular diffusion coefficients and also for their mean value. In the case of the thermodiffusion coefficient, the mean value of the results obtained by both columns has been used. The results are shown in table 7.

As may be observed, although the molecular diffusion coefficients are quite different, in the case of Soret coefficients essentially the same results are obtained in the five cases. The standard deviation between the five cases is of 2.5% for component 1 and of 4.4% for component 3, and as can be observed in table 7 the deviations are within the experimental error bars. This implies that the molecular diffusion coefficients, especially the cross-diagonal ones, have only a small influence on the Soret coefficients. The values proposed for Soret coefficients are the mean values of the five cases analysed, with the corresponding experimental error.

4 Conclusions

The thermophysical properties, the eigenvalues of the diffusion matrix and the thermodiffusion, molecular diffusion and Soret coefficients have been determined for the ternary mixture THN-IBB-nC$_{12}$ at mass fraction of 0.8-0.1-0.1 and at 25 °C. Table 8 shows the values for the thermodiffusion, molecular diffusion and Soret coefficients and for the eigenvalues of the diffusion matrix proposed by the team of Mondragon Unibertsitatea for the Benchmark.

Table 7. Soret coefficients for each case of molecular diffusion coefficients for the ternary mixture THN-IBB-nC$_{12}$ at mass fraction of 0.8-0.1-0.1 and at 25 °C.

$D'_{T,i}$	D_{ij}	$S'_{T,1} \times 10^{-3}$ (K^{-1})	$S'_{T,3} \times 10^{-3}$ (K^{-1})
Mean value	Exp 1-2	1.23 ± 0.09	-0.87 ± 0.14
	Exp 3-4	1.16 ± 0.09	-0.95 ± 0.16
	Exp 1-4	1.17 ± 0.09	-0.93 ± 0.15
	Exp 2-3	1.20 ± 0.09	-0.90 ± 0.15
	Mean value of D_{ij}	1.19 ± 0.09	-0.91 ± 0.15
	Proposed values	1.19 ± 0.09	-0.91 ± 0.15

Table 8. Proposed values by the team of Mondragon Unibertsitatea for thermodiffusion, molecular diffusion and Soret coefficients and for the eigenvalues of the diffusion matrix, for the ternary mixture THN-IBB-nC$_{12}$ at mass fraction of 0.8-0.1-0.1 and at 25 °C.

$D'_{T,1} \times 10^{-12}$ (m^2/s K)	$D'_{T,3} \times 10^{-12}$ (m^2/s K)		$S'_{T,1} \times 10^{-3}$ (K^{-1})		$S'_{T,3} \times 10^{-3}$ (K^{-1})
0.67 ± 0.05	-0.49 ± 0.06		1.19 ± 0.09		-0.91 ± 0.15
$D_{11} \times 10^{-10}$ (m^2/s)	$D_{12} \times 10^{-10}$ (m^2/s)	$D_{21} \times 10^{-10}$ (m^2/s)	$D_{22} \times 10^{-10}$ (m^2/s)	$\widehat{D_1} \times 10^{-10}$ (m^2/s)	$\widehat{D_2} \times 10^{-10}$ (m^2/s)
5.23 ± 0.66	-1.80 ± 0.23	0.39 ± 0.05	8.28 ± 1.00	5.43 ± 0.68	8.08 ± 1.02

This work has been carried out in the framework of the projects: MicroCHEAP (IE14-391), Research Groups (IT557-10), Research Fellowship (BFI-2011-295) of the Basque Government, and DCMIX (AO-2009-0858/1056) from the European Space Agency and TERDISOMEZ (FIS2014-58950-C2-1-P) of MINECO.

References

1. J.K. Platten, M.M. Bou-Ali, P. Costeséque, J. Dutrieux, W. Köhler, C. Leppla, S. Wiegand, G. Wittko, Philos. Mag. **83**, 1965 (2003).
2. A. Mialdun, V. Yasnou, V. Shevtsova, A. Königer, W. Köhler, D. Alonso de Mezquia, M.M. Bou-Ali, J. Chem. Phys. **136**, 244512 (2012).
3. P.-A. Artola, B. Rousseau, Mol. Phys. **111**, 3394 (2013).
4. G. Galliero, C. Boned, J. Chem. Phys. **129**, 074506 (2008).
5. A. Mialdun, V. Sechenyh, J.C. Legros, J.M. Ortiz de Zárate, V. Shevtsova, J. Chem. Phys. **139**, 104903 (2013).
6. A. Königer, H. Wunderlich, W. Köhler, J. Chem. Phys. **132**, 174506 (2010).
7. Q. Galand, S. Van Vaerenbergh, F. Montel, Energy Fuels **22**, 770 (2008).
8. P. Blanco, M.M. Bou-Ali, J.K. Platten, D. Alonso de Mezquia, J.A. Madariaga, C. Santamaría, J. Chem. Phys. **132**, 114506 (2010).
9. M. Larrañaga, D.A.S. Rees, M.M. Bou-Ali, J. Chem. Phys. **140**, 054201 (2014).
10. M.M. Bou-Ali, J.K. Platten, J. Non-Equilib. Thermodyn. **30**, 385 (2005).
11. F. Capuano, L. Paduano, G. D'Errico, G. Mangiapia, R. Sartorio, Phys. Chem. Chem. Phys. **13**, 3319 (2011).
12. J. Dutrieux, G. Chavepeyer, M. Marcoux, M. Massoutier, Philos. Mag. **83**, 2033 (2003).
13. M. Eslamian, M.Z. Saghir, J. Non-Equilib. Thermodyn. **37**, 329 (2012).
14. A. Leahy-Dios, M.M. Bou-Ali, J.K. Platten, A. Firoozabadi, J. Chem. Phys. **122**, 234502 (2005).
15. K. Ghorayeb, A. Firoozabadi, AlChE **46**, 883 (2000).
16. J.P. Larre, J.K. Platten, G. Chavepeyer, Int. J. Heat Mass Transfer **40**, 545 (1997).
17. L. Kempers, J. Chem. Phys. **90**, 6541 (1989).
18. A. Mialdun, C. Minetti, Y. Gaponenko, V. Shevtsova, F. Dubois, Microgravity Sci. Technol. **25**, 83 (2013).
19. A. Ahadi, M.Z. Saghir, Appl. Therm. Eng. **59**, 72 (2014).
20. P. Blanco, M.M. Bou-Ali, J.K. Platten, P. Urteaga, J.A. Madariaga, C. Santamaría, J. Chem. Phys. **129**, 174504 (2008).
21. M. Larrañaga, M.M. Bou-Ali, E. Lapeira, J.A. Madariaga, C. Santamaría, Microgravity Sci. Technol. **26**, 29 (2014).
22. J.A. Madariaga, C. Santamaría, M.M. Bou-Ali, P. Urteaga, D. Alonso de Mezquia, J. Phys. Chem. B **114**, 6937 (2010).
23. A. Mialdun, V. Yasnou, V. Shevtsova, A. Königer, W. Köhler, D. Alonso de Mezquía, M.M. Bou-Ali, J. Chem. Phys. **136**, 244512 (2012).
24. D. Alonso de Mezquia, M.M. Bou-Ali, M. Larrañaga, J.A. Madariaga, C. Santamaría, J. Phys. Chem. B **116**, 2814 (2012).
25. A. Mialdun, V. Shevtsova, J. Chem. Phys. **138**, 161102 (2013).

I. Soret coefficients of the ternary mixture 1,2,3,4-tetrahydronaphtaline + isobutylbenzene + n-dodecane.

Soret coefficients of the ternary mixture 1, 2, 3, 4-tetrahydronaphthalene + isobutylbenzene + n-dodecane

Miren Larrañaga,[1] M. Mounir Bou-Ali,[1,a)] Ion Lizarraga,[1] Jose Antonio Madariaga,[2] and Carlos Santamaría[2]
[1]*MGEP Mondragon Goi Eskola Politeknikoa, Mechanical and Industrial Manufacturing Department, Loramendi 4 Apdo. 23, 20500 Mondragon, Spain*
[2]*Department of Applied Physics II, University of Basque Country, Apdo. 644, 48080 Bilbao, Spain*

(Received 29 April 2015; accepted 30 June 2015; published online 13 July 2015)

In this work, the transport coefficients of the ternary mixtures of the diffusion coefficient measurements in ternary mixtures 1 project were determined. The analyzed ternary mixtures are formed by 1,2,3,4-tetrahydronaphthalene, isobutylbenzene, and dodecane (nC$_{12}$) at different compositions. In all cases, the analysis was carried out at 25 °C. The thermodiffusion coefficients were measured by a new thermogravitational column, and the molecular diffusion coefficients were determined by the sliding symmetric tubes technique. Finally, the Soret coefficients were ascertained from the measurements of the thermodiffusion and molecular diffusion coefficients. In addition, two new quantitative correlations which enable the prediction of the thermodiffusion and Soret coefficients of a ternary mixture are presented. The comparison between the experimental and the predicted data shows a good agreement. The presented results help to complete the lack of experimental data in ternary mixtures. In addition, this work improves the fundamental understanding of multicomponent mixtures. © *2015 AIP Publishing LLC.* [http://dx.doi.org/10.1063/1.4926654]

I. INTRODUCTION

The study of thermodiffusion phenomenon in multicomponent mixtures has awakened a great level of interest in the scientific community. This is due to their involvement in different fields such as the oil industry,[1] biology,[2] or engineering,[3,4] where the knowledge and understanding of these phenomena can help to optimize many processes and to create new applications. The diffusive mass flux, $\mathbf{J_i}$, may be generated by a temperature and a concentration gradient. Regarding to the linear laws of irreversible thermodynamics, the mass flux equations for components 1 and 2 in a ternary mixture may be written as[5]

$$\mathbf{J}_1 = -\rho D_{11}\nabla c_1 - \rho D_{12}\nabla c_2 - \rho D'_{T,1}\nabla T, \quad (1)$$

$$\mathbf{J}_2 = -\rho D_{21}\nabla c_1 - \rho D_{22}\nabla c_2 - \rho D'_{T,2}\nabla T, \quad (2)$$

where ρ is the density of the mixture, c_1 and c_2 are the two independent mass fractions, D_{11}, D_{12}, D_{21}, and D_{22} are the molecular diffusion coefficients, and $D'_{T,1}$ and $D'_{T,2}$ are the thermodiffusion phenomenological coefficients. The third diffusive mass flux, $\mathbf{J_3}$, is defined from the condition that the fluxes of all the components must sum zero.

Within the last decade, significant progress has been made in the understanding of the thermodiffusion phenomenon in binary mixtures. Currently, there are several experimental techniques that allow us to determine reliably these transport coefficients.[6–8]

However, mixtures with scientific or technological interest are generally formed by more than two components. As the number of components in the mixture increases, the complexity of the problem also increases considerably. With the purpose of achieving a better understanding of the thermodiffusion phenomenon in ternary mixtures, several works[9–15] have been published in recent years.

The most recent breakthrough has been the establishment of the first benchmark in ternary mixtures[16] developed, thanks to the international collaboration project DCMIX (Diffusion Coefficient measurements in ternary MIXtures). This benchmark incorporates the results of six independent teams utilizing different experimental techniques and both in microgravity and ground conditions. Moreover, this serves to validate the different techniques used in the study,[17–22] amongst which are included the two techniques used in this work: thermogravitational (TG) technique and Sliding Symmetric Tubes (SST) technique.

Nevertheless, there is still uncertainty that makes it difficult to identify the results that can be reliably extracted. This happens especially with the determination of the molecular diffusion coefficients, as it was shown by Gebhardt and Köhler,[23] Larrañaga *et al.*,[22] and Bou-Ali *et al.*[16] Therefore, a wide database of reliable experimental results obtained by different techniques and for different types of mixtures is still necessary. This database may be helpful for validating theoretical models that nowadays still do not agree completely.[24–26] Moreover, it is valid for developing numerical models and correlations that enable the prediction of the thermodiffusion coefficients.[27–29]

The aim of this work is to contribute to the experimental database in multicomponent mixtures. For that purpose, new experimental results for five ternary mixtures are provided. These mixtures correspond to the ones of the project DCMIX,

a)Author to whom correspondence should be addressed. Electronic mail: mbouali@mondragon.edu

which are formed by 1,2,3,4-tetrahydronaphthalene (THN), isobutylbenzene (IBB), and dodecane (nC$_{12}$) at different mass concentrations. In all the cases, the analysis has been completed at 25 °C. In this work, THN is considered as component 1, IBB as component 2, and nC$_{12}$ as component 3 in the mixture.

The thermodiffusion coefficients were measured by the thermogravitational technique, by the new long thermogravitational column (LTC) presented and validated by Larrañaga *et al.*[22] The results were compared with the ones published by Alonso de Mezquía *et al.*[10] The molecular diffusion coefficients were determined by the SST technique. Finally, Soret coefficients were determined by the combination of the measurements of thermodiffusion and molecular diffusion. In addition, two new quantitative correlations that allow predicting the thermodiffusion and Soret coefficients of a ternary mixture from the thermodiffusion and Soret coefficients of the corresponding binary mixtures were developed.

II. EXPERIMENTAL PROCEDURE

The ternary mixtures analyzed in this work are all composed of THN, IBB, and nC$_{12}$. We obtained new results of transport coefficients for the first four compositions shown in Table I. In the case of the equimass mixture, we show new results of the thermodiffusion coefficient measured by the LTC and calculate the Soret coefficients from them and from the diffusion coefficients published by Larrañaga *et al.*[9]

Before determining mass transport coefficients in a mixture, it is necessary to define some thermophysical properties of it. To measure the density, we used an Anton Paar DMA 5000 vibrating quartz U-tube densimeter with an accuracy of 5×10^{-3} kg/m^3. The density measurements also provide the thermal expansion coefficient. Coupled to the densimeter, there is an Anton Paar RXA 156 refractometer with accuracy of 2×10^{-5} RIU, which measures the refractive index. Finally, an Anton Paar AMVn microviscometer with an accuracy of ±0.002 s was used for the determination of the dynamic viscosity.

To analyze a ternary mixture, it is also necessary to make a calibration that enables the determination of the concentrations of each component from the measurements of the density and the refractive index, as detailed by Larrañaga *et al.*[22] So as to validate the calibration, the corresponding concentrations to each mixture are calculated by the calibration parameters and the measured densities and refractive indices, and they are compared to the experimental ones. The precision of this procedure is very important for the accuracy of the measurements of the transport coefficients.

TABLE I. Analyzed compositions of the mixture THN-IBB-nC$_{12}$.

c$_1$ (THN)	c$_2$ (IBB)	c$_3$ (nC$_{12}$)
0.10	0.10	0.80
0.45	0.10	0.45
0.40	0.20	0.40
0.10	0.80	0.10
0.33	0.33	0.33

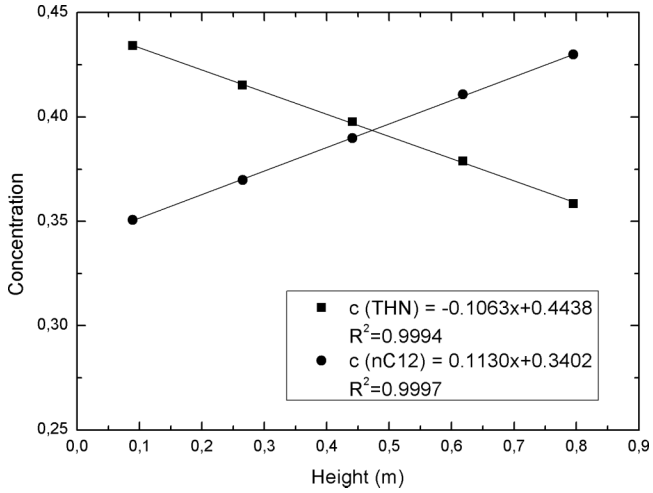

FIG. 1. Variation of the concentration of THN and nC$_{12}$ with the height of the column, for the mixture formed by THN-IBB-nC$_{12}$ at concentration of 0.40-0.20-0.40 and at 25 °C.

A. Thermogravitational technique

The thermogravitational technique was used to determine the thermodiffusion coefficient. This technique has been successfully used in other works, both in binary[29,30] and ternary mixtures.[10,22,31] In this procedure, we measure the variation of the concentration of the mixture along the height of the column. Figure 1 shows the variation of the concentrations of components 1 and 3, that is, THN and nC$_{12}$, in the stationary state. The concentration of component 2 (IBB) may be easily calculated from the statement that the concentrations of the three components must sum unity. These concentration gradients are used to ascertain the thermodiffusion coefficient for each component, by the following equation:

$$D'_{T,i} = -\frac{L_x^4}{504}\frac{g\alpha\rho}{\mu}\frac{\partial C_i}{\partial z}, \tag{3}$$

where L_x is the gap width; g is gravity; α is the thermal expansion coefficient; μ is the dynamic viscosity; and $\partial c_i/\partial z$ is the vertical concentration gradient of component i in the height of the column.

In this work, the new thermogravitational plane column (LTC) presented by Larrañaga *et al.*[22] was used. The gap of the column is 1.02 ± 0.005 mm wide and 980 mm high.

As was explained by Larrañaga *et al.*,[22] the experimental error in each of the parameters in Eq. (3) must be considered when analyzing the uncertainty of the determination of the thermodiffusion coefficients by the thermogravitational technique.

B. SST technique

The SST technique was used to determine the molecular diffusion coefficients. It has been successfully used in several works in both binary[28] and ternary mixtures.[9,22] In this technique, we measure the variation of the concentration of each component with time, an example of which is shown in Figure 2.

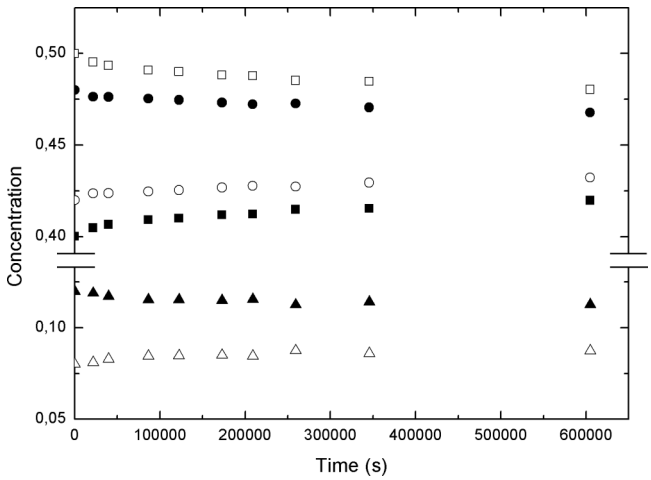

FIG. 2. Variation of the concentration of THN, IBB, and nC$_{12}$ with time, for the mixture with mass fraction 0.45-0.10-0.45, at 25 °C, in the upper and the lower tubes of the SST technique. Squares represent THN, triangles represent IBB, and circles represent nC$_{12}$; in the three cases, filled symbols represent the upper tubes and empty symbols represent the lower tubes.

The variation of the concentration of each component with the square root of the time gives a linear distribution (Figure 3) which enables us to determine the molecular diffusion coefficients. It is important to take into account that the analytical procedure used for the determination of the molecular diffusion coefficients in ternary mixtures is only valid for relatively short times, that is, when the diffusion front has not reached the far ends of the tubes.

As is described in more detail by Larrañaga *et al.*,[9] two experiments with different initial concentrations are needed to determine the molecular diffusion coefficients of one ternary mixture. Thus, we have four equations and four unknowns: the four molecular diffusion coefficients. In order to solve the system, the Newton-Raphson method is used, where the fitting parameters are the four diffusion coefficients.

The uncertainty in the determination of the diffusion coefficients by the SST technique is given by three factors:

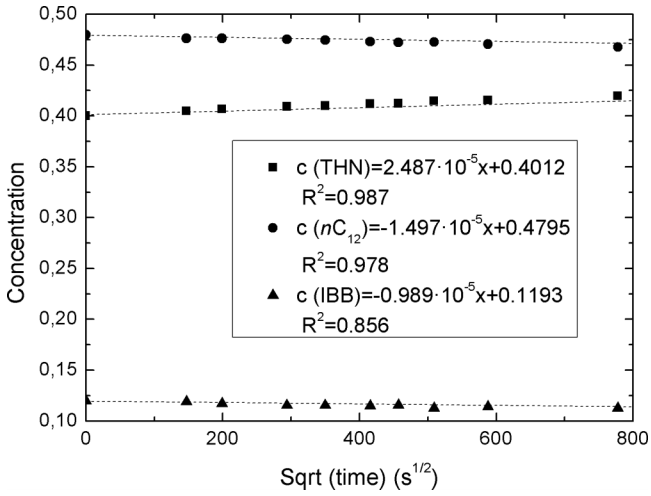

FIG. 3. Variation of the concentration of each component with the square root of time for the mixture formed by THN-IBB-nC$_{12}$ at mass fraction of 0.45-0.10-0.45, at 25 °C, in the upper tubes of the SST technique.

the Newton-Raphson fitting error, the linear regressions fitting error, and the calibration error.

C. Soret effect

The Soret coefficients for each component are determined by Eq. (4),[16] which relates the thermodiffusion and molecular diffusion coefficients with them. Thus, we determine the Soret coefficients by the results obtained by two independent experimental techniques,

$$S'_{T,1} = \frac{D'_{T,1}D_{22} - D'_{T,2}D_{12}}{D_{11}D_{22} - D_{12}D_{21}},$$
$$S'_{T,2} = \frac{D'_{T,2}D_{11} - D'_{T,1}D_{21}}{D_{11}D_{22} - D_{12}D_{21}}. \quad (4)$$

To measure the experimental error accumulated in the indirect determination of the Soret coefficient, the rules of error propagation were used, taking into account Eq. (4).

III. RESULTS AND DISCUSSION

A. Thermodiffusion coefficients

The calibration parameters and the thermophysical properties needed to determine the thermodiffusion coefficients have been taken from Blanco *et al.*[31] for the equimass mixture and from Alonso de Mezquía *et al.*[10] for the other compositions. So as to show the repeatability of the experiment, we performed three independent runs for each mixture.

Table II shows first the results obtained for the density and refractive index gradients, $\partial\rho/\partial z$ and $\partial n_D/\partial z$, by the thermogravitational column with a length of 980 mm (LTC). In the same table, the concentration gradients for components 1 and 3, $\partial c_1/\partial z$ and $\partial c_3/\partial z$, are given. From the measured concentration gradients and the thermophysical properties, we determined the thermodiffusion coefficients for components 1 and 3 by Eq. (3). As may be observed in Table II, the maximum deviation between the different runs was around 4%. The thermodiffusion coefficient for component 2 can be easily calculated from the condition that the sum of the three thermodiffusion coefficients is zero.

The thermodiffusion coefficients presented in this work were already measured by our team by the short thermogravitational column (STC) with length of 500 mm and gap of 1 ± 0.005 mm by Blanco *et al.*[31] for the equimass composition and by Alonso de Mezquía *et al.*[10] for the other compositions. Table III shows the comparison between the mean values of the thermodiffusion measurements made by the LTC in this work and the measurements made by the STC in those two previous works.[10,31]

As may be observed, results obtained by the two columns are similar, as expected. Although the uncertainties are sometimes smaller in the STC, the reproducibility is better in LTC. In some of the measurements made by the STC, we needed to discard one of the points in the height of the column to fit the linear regression, and we also needed to do more experiments to obtain the results. In the LTC, we avoid

TABLE II. Thermodiffusion coefficients for the five compositions analyzed of the ternary mixture THN-IBB-*n*C12 at 25 °C. $\partial\rho/\partial z$, $\partial n_D/\partial z$, $\partial c_1/\partial z$, and $\partial c_3/\partial z$ are the density, refractive index, and concentration gradients along the height of the column, respectively. Component 1 is THN and component 3 is *n*C12.

Composition (c_1-c_3)	$\partial\rho/\partial z$ (kg/m^4)	$\partial n_D/\partial z$ (10^{-2} m^{-1})	$\partial c_1/\partial z$ (m^{-1})	$\partial c_3/\partial z$ (m^{-1})	$D'_{T,1}\times10^{-12}$ (m^2/sK)	$D'_{T,3}\times10^{-12}$ (m^2/sK)
	−9.52	−0.523	−0.0420	0.0613	0.50	−0.72
0.10-0.80	−9.99	−0.548	−0.0443	0.0640	0.52	−0.76
	−10.20	−0.560	−0.0451	0.0655	0.53	−0.77
	−27.59	−1.500	−0.1254	0.1282	1.39	−1.42
0.45-0.45	−26.85	−1.458	−0.1233	0.1237	1.37	−1.37
	−27.22	−1.479	−0.1243	0.1259	1.38	−1.40
	−24.30	−1.326	−0.1097	0.1125	1.30	−1.34
0.40-0.40	−24.02	−1.314	−0.1061	0.1130	1.26	−1.34
	−23.94	−1.301	−0.1114	0.1079	1.32	−1.28
	−5.83	−0.331	−0.0204	0.0300	0.33	−0.48
0.10-0.10	−5.81	−0.332	−0.0195	0.0307	0.31	−0.49
	−5.77	−0.329	−0.0200	0.0301	0.32	−0.48
	−20.35	−1.118	−0.0906	0.0963	1.14	−1.21
0.33-0.33	−20.55	−1.127	−0.0922	0.0965	1.16	−1.21
	−20.44	−1.121	−0.0914	0.0964	1.15	−1.21

these procedure problems because due to its height, the relative separation of the concentration is nearly two times higher than in the STC. This better sensitivity is very interesting for the analysis of ternary mixtures, where the separation is usually smaller than in binary mixtures. Therefore, in future works about ternary mixtures, the measurements will be made by the LTC column.

On the other hand, we have deduced an approximation expression to calculate the thermodiffusion coefficients of a ternary mixture from the thermodiffusion coefficients of its corresponding binaries. Figure 4 shows the experimental results of $D'_{T,1}$ versus the concentrations of components 1 and 3, for the compositions analyzed. The surface $D'_{T,1} = D'_{T,1}(c_1, c_3)$ which contains the experimental points has been drawn taking into account the following boundaries:

$$\begin{aligned} c_1 = 0 &\rightarrow D'_{T,1} = 0, \\ c_1 = 1 &\rightarrow D'_{T,1} = 0, \end{aligned} \tag{5}$$

and the intersection lines of this surface with the planes $c_3 = 0$ and $c_1 + c_3 = 1$ correspond to the values of $D'_{T,1}$ of the binary mixtures 1-2 and 1-3, respectively. By assuming that the intersection lines of the surface with the planes $c_1 = constant$ are approximately straight lines. Therefore, we can tentatively determine $D'_{T,1}$ by the interpolation of each value of c_1 between the boundary values of the thermodiffusion coefficient of component 1 corresponding to the binary mixtures $c_3 = 0$ and $c_3 = 1 - c_1$. Thus, we have the following expression (see the marked triangle in Fig. 4(a)):

$$D'_{T,1} = D'_{T,1-2} + \frac{D'_{T,1-3} - D'_{T,1-2}}{(1 - c_1)} c_3, \tag{6}$$

where c_1 and c_3 are the concentrations of components 1 and 3 in the ternary mixture, and $D'_{T,1-2}$ and $D'_{T,1-3}$ are the thermodiffusion coefficient of the component 1 in the binary mixtures formed by components 1-2 and 1-3, respectively.

In terms of the thermodiffusion coefficients in binary mixtures $D'_{T,i-j}$ and $D_{T,i-j}$ are related by

$$D'_{T,i-j} = D_{T,i-j} c_i (1 - c_i), \tag{7}$$

and Eq. (6) can be written as

$$D'_{T,1} = D_{T,1-2} c_1 c_2 + D_{T,1-3} c_1 c_3, \tag{8}$$

where c_1, c_2, and c_3 are the concentrations of components 1, 2, and 3 in the ternary mixture. This combination rule can be generalized for any $D'_{T,i}$,

$$D'_{T,i} = D_{T,i-j} c_i c_j + D_{T,i-k} c_i c_k. \tag{9}$$

TABLE III. Thermodiffusion coefficients determined by the thermogravitational technique by two different columns. LTC: 980 mm high column and STC: 500 mm high column.

Composition (c_1-c_3)	$D'_{T,THN}\times10^{-12}$ (m^2/sK) LTC	$D'_{T,THN}\times10^{-12}$ (m^2/sK) STC	Difference %	$D'_{T,nC12}\times10^{-12}$ (m^2/sK) LTC	$D'_{T,nC12}\times10^{-12}$ (m^2/sK) STC	Difference %
0.10-0.80	0.52 ± 0.02	0.47 ± 0.04[a]	9.61	−0.75 ± 0.03	−0.75 ± 0.03[a]	0.02
0.45-0.45	1.38 ± 0.07	1.33 ± 0.04[a]	3.62	−1.40 ± 0.05	−1.44 ± 0.02[a]	2.85
0.40-0.40	1.30 ± 0.05	1.23 ± 0.04[a]	5.38	−1.32 ± 0.04	−1.33 ± 0.02[a]	0.75
0.10-0.10	0.32 ± 0.02	0.33 ± 0.02[a]	3.12	−0.49 ± 0.02	−0.45 ± 0.03[a]	8.16
0.33-0.33	1.15 ± 0.06	1.10 ± 0.02[b]	4.34	−1.21 ± 0.05	−1.23 ± 0.02[b]	1.65

[a]Results published by Alonso de Mezquía *et al.*[10]
[b]Results published by Blanco *et al.*[31]

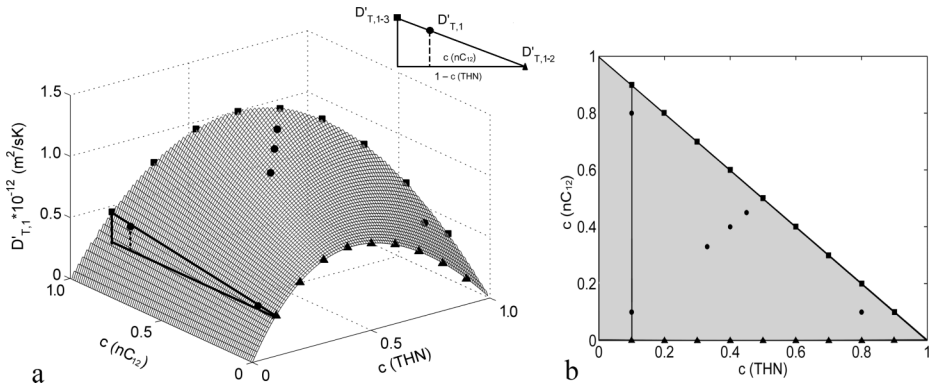

FIG. 4. Thermodiffusion coefficient of component 1 (THN) in function of the mass fractions of components 1 and 3 at 25 °C. Triangles correspond to the binary mixture THN-IBB ($D'_{T,1-2}$), squares correspond to the binary THN-nC12 ($D'_{T,1-3}$), and circles correspond to the ternary mixture THN-IBB-nC12 ($D'_{T,1}$). (a) 3D view. (b) Top view.

This expression is similar to the one developed by Larre *et al.*,[26] but in this case, the thermodiffusion coefficients of the binary mixtures are the corresponding ones to the concentration c_i.

The thermodiffusion coefficients for the ternary mixtures studied in this work were calculated with the new combination rule (Eq. (9)). Table IV provides the comparison between the calculated results and the experimental ones. We include also the results for the benchmark composition, reported by Larrañaga *et al.*[22] To determine the coefficients for the suitable binary compositions, the polynomials presented by Gebhardt *et al.*[7] were used.

As can be observed, the agreement is quite good in general, and the maximum difference with our results is around 12%. The results given by Gebhardt and Köhler[23] for the equimass composition are also in good agreement with our results, within the experimental error. The results obtained by the correlation depend strongly on the prediction polynomials developed by Gebhardt *et al.*;[7] thus, we may conclude that the agreement obtained is very convincing.

B. Molecular diffusion coefficients

Table V shows the results for the eigenvalues of the diffusion matrix for the four ternary mixtures analyzed in this work. Table VI shows the results corresponding to the molecular diffusion coefficients for the mixtures formed by THN-IBB-nC12 (in this order) at different compositions. In these tables are presented also the results for the equimass composition. After a deeper analysis of the time limits valid for the analytical methodology used, the results of molecular diffusion and Soret for this mixture have changed slightly from the ones presented by Larrañaga *et al.*[9] However, the new results for the eigenvalues of the diffusion matrix and for the Soret coefficients are still within the experimental error.

The eigenvalues have proved to be a more reliable parameter when comparing diffusion results in ternary mixtures by Bou-Ali *et al.*[16] As was noted in that work also, there is still uncertainty in the determination of the molecular diffusion coefficients. It seems that there may be more than one possible combination of results. In addition, it was shown by Larrañaga *et al.*[22] that in spite of the differences in the individual coefficients, their influence in the Soret coefficients was the same.

C. Soret coefficients

In Table VII, the Soret coefficients for the five ternary mixtures analyzed are shown. They have been indirectly determined by the Eq. (4) from the values of thermodiffusion (Table III) and molecular diffusion (Table VI) measured in this work.

As noted previously, Soret coefficients were obtained from the measurements made independently by two different techniques. Thus, the comparison of these results with the ones obtained directly by other techniques is very interesting. By the time, there are published results measured by other techniques only for the benchmark composition (Bou-Ali *et al.*[16]) and only one result for the equimass composition measured by the Optical Beam Deflection (OBD) technique, so we still cannot compare the results for the other four compositions.

In addition, in the same way as was done for thermodiffusion coefficients, a combination rule was developed for the prediction of Soret coefficients. It was observed that

TABLE IV. Comparison between the results obtained by the combination rule and the experimental ones.

Composition	$D'_{T,THN}\times10^{-12}$ (m^2/sK)			$D'_{T,nC12}\times10^{-12}$ (m^2/sK)		
(c_1-c_3)	Expt.	Eq. (9)	Difference %	Expt.	Eq. (9)	Difference %
0.10-0.80	0.52	0.53	2.96	−0.75	−0.75	0.14
0.45-0.45	1.38	1.33	3.35	−1.40	−1.37	1.95
0.40-0.40	1.30	1.20	7.60	−1.32	−1.27	3.99
0.10-0.10	0.32	0.36	12.34	−0.49	−0.45	6.90
0.33-0.33	1.15	1.02	11.30	−1.21	−1.12	7.04
0.80-0.10[a]	0.67	0.65	2.96	−0.49	−0.50	2.48

[a]Results published by Larrañaga *et al.*[22]

TABLE V. Eigenvalues of the diffusion matrix for the ternary mixtures formed by THN-IBB-nC$_{12}$ determined by the SST technique, at 25 °C.

Composition (c_1-c_3)	$\widehat{D_1}\times10^{-10}$ (m^2/s)	$\widehat{D_2}\times10^{-10}$ (m^2/s)
0.10-0.80	9 ± 1	11 ± 2
0.45-0.45	7 ± 1	7 ± 1
0.40-0.40	4 ± 1	7 ± 2
0.10-0.10	9 ± 2	12 ± 3
0.33-0.33	5 ± 1	10 ± 3

TABLE VI. Molecular diffusion coefficients for the ternary mixtures formed by THN-IBB-nC$_{12}$ determined by the SST technique, at 25 °C.

Composition (c_1-c_3)	$D_{11}\times10^{-10}$ (m^2/s)	$D_{12}\times10^{-10}$ (m^2/s)	$D_{21}\times10^{-10}$ (m^2/s)	$D_{22}\times10^{-10}$ (m^2/s)
0.10-0.80	10.00 ± 1.00	−0.80 ± 0.10	−1.50 ± 0.20	10.00 ± 1.00
0.45-0.45	7.00 ± 1.00	0.32 ± 0.06	−0.14 ± 0.03	7.00 ± 1.00
0.40-0.40	8.00 ± 2.00	1.30 ± 0.40	−1.30 ± 0.40	4.00 ± 1.00
0.10-0.10	10.00 ± 3.00	−0.21 ± 0.06	−1.70 ± 0.40	7.00 ± 2.00
0.33-0.33	8.00 ± 2.00	−2.30 ± 0.60	−2.00 ± 0.50	6.00 ± 2.00

TABLE VII. Soret coefficients determined indirectly for the ternary mixtures formed by THN-IBB-nC12 at 25 °C.

Composition (c_1-c_3)	$S'_{T,\mathrm{THN}}\times10^{-3}$ (K^{-1})	$S'_{T,n\mathrm{C12}}\times10^{-3}$ (K^{-1})
0.10-0.80	0.54 ± 0.07	−0.90 ± 0.20
0.45-0.45	1.90 ± 0.20	−2.00 ± 0.30
0.40-0.40	1.50 ± 0.40	−2.10 ± 0.60
0.10-0.10	0.31 ± 0.06	−0.60 ± 0.20
0.33-0.33	1.60 ± 0.40	−2.20 ± 0.70

Soret coefficients have a similar distribution to those of the thermodiffusion coefficients in function of the concentrations of their components,

$$S'_{T,i}(c_i,c_j,c_k) = c_ic_jS'_{T,i-j}(c_i) + c_ic_kS'_{T,i-k}(c_i). \quad (10)$$

The Soret coefficients predicted by Eq. (10) are shown in Figure 5, compared to the experimental values obtained in this work. We have included also the experimental point for the equimass composition measured by the OBD technique and given in the most recent paper (Gebhardt and Köhler[23]). This team had published different results for this mixture in a previous paper (Königer *et al.*[11]), but this difference is due to the new contrast factor matrix they have used in the new work (Gebhardt and Köhler[23]). For these values, we have included an experimental error bar of a 7%, which is the experimental error provided by this team for the benchmark mixture (Bou-Ali *et al.*[16]). The binary coefficients that are needed in Eq. (10) were calculated from the prediction polynomials presented by Gebhardt *et al.*[7]

As can be observed, the agreement between experimental and predicted results is good in general, especially if we take into account that the calculated coefficients come from two approximations (the prediction polynomials (Gebhardt *et al.*[7]) and Eq. (10)). In the case of the equimass mixture, we can observe also the acceptable agreement between the new experimental results obtained by the OBD technique and the combination of the thermogravitational and SST techniques.

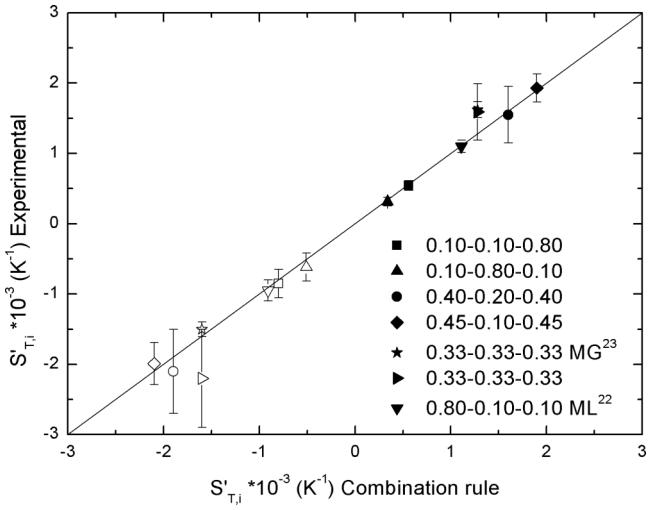

FIG. 5. Comparison between the Soret coefficients obtained experimentally in this work and the ones determined by the combination rule shown in Eq. (10). In all the cases, filled symbols represent the Soret coefficient for component 1, and empty symbols represent the Soret coefficients for component 3.

IV. CONCLUSIONS

Thermodiffusion, molecular diffusion, and Soret coefficients were determined for the ternary mixtures formed by THN-IBB-nC$_{12}$ at mass fractions of 0.10-0.80-0.10, 0.10-0.10-0.80, 0.45-0.10-0.45, and 0.40-0.20-0.40, at 25 °C in all cases. We have achieved the objectives of the project DCMIX1, and we have developed the TG and SST techniques for the analysis of ternary mixtures, so new ternary mixtures will be analyzed in the near future.

Soret coefficients have been determined by the combination of the measurements made by two independent techniques, so it will be very interesting to compare these results with the ones measured directly by other techniques such as OBD, ODI (Optical Digital Interferometry), or SODI (Selectable Optical Diagnostic Instrument), as it was done for the benchmark composition (Bou-Ali *et al.*[16]). By the time, there is only one result published: the Soret coefficients for the equimass composition measured by the OBD technique. The comparison of our experimental results with these ones has shown an acceptable agreement.

In the comparison between the measurements of thermodiffusion made by the two columns, the results were similar, as expected. However, the experimental procedure becomes more complicated in the STC due to the small separation of the ternary mixtures. Therefore, from now on, we will use the column with length of 980 mm in ternary mixtures, in order to obtain more accurate results.

We have developed two combination rules that enable the prediction of the thermodiffusion and Soret coefficients of the ternary mixture analyzed in this work at any mass fraction, from the results of the corresponding binary mixtures. The results of the binary mixtures needed were easily calculated by the polynomials presented by Gebhardt *et al.*[7] Therefore, we

can predict with an acceptable reliability the thermodiffusion and Soret coefficients of the ternary mixture THN-IBB-nC_{12} for any composition. This may be very interesting especially for numerical and theoretical works, in order to compare and prove their models based on non-equilibrium thermodynamics and/or molecular dynamics. In addition, in future works, this combination rule may be extended to other systems to compare the behavior of mixtures of different natures.

ACKNOWLEDGMENTS

This work has been carried out in the framework of the projects: MicroCHEAP (No. IE14-391), Research Groups (No. IT557-10), Research Fellowship (No. BFI-2011-295), and MICROXOM (No. PI 2014_1_70) of the Basque Government; DCMIX (No. AO-2009-0858/1056) from the European Space Agency; and TERDISOMEZ (No. FIS2014-58950-C2-1-P) of MINECO.

[1]S. Van Vaerenbergh, A. Shapiro, G. Galliero, F. Montel, J. C. Legros, J. P. Caltagirone, J. L. Daridon, and Z. Saghir, Eur. Space Agency, [Spec. Publ.] **SP 1290**, 202–213 (2005).
[2]F. Capuano, L. Paduano, G. D'Errico, G. Mangiapia, and R. Sartorio, Phys. Chem. Chem. Phys. **13**, 3319–3327 (2011).
[3]T. Takahashi and Y. Minamino, J. Alloys Compd. **545**, 168–175 (2012).
[4]H. Tello Alonso, A. C. Rubiolo, and S. E. Zorrilla, J. Food Eng. **109**, 490–495 (2011).
[5]M. M. Bou-Ali and J. K. Platten, J. Non-Equilib. Thermodyn. **30**, 385–399 (2005).
[6]A. Mialdun, V. Yasnou, V. Shevtsova, A. Königer, W. Köhler, D. Alonso de Mezquia, and M. M. Bou-Ali, J. Chem. Phys. **136**, 244512 (2012).
[7]M. Gebhardt, W. Köhler, A. Mialdun, V. Yasnou, and V. Shevtsova, J. Chem. Phys. **138**, 114503 (2013).
[8]J. K. Platten, M. M. Bou-Ali, P. Costeséque, J. F. Dutrieux, W. Köhler, C. Leppla, S. Wiegand, and G. Wittko, Philos. Mag. **83**, 1965–1971 (2003).
[9]M. Larrañaga, D. A. S. Rees, and M. M. Bou-Ali, J. Chem. Phys. **140**, 054201 (2014).
[10]D. Alonso de Mezquia, M. Larrañaga, M. M. Bou-Ali, J. A. Madariaga, C. Santamaría, and J. K. Platten, Int. J. Therm. Sci. **92**, 14–16 (2015).
[11]A. Königer, H. Wunderlich, and W. Köhler, J. Chem. Phys. **132**, 174506 (2010).
[12]A. Mialdun, V. Sechenyh, J. C. Legros, J. M. Ortiz de Zárate, and V. Shevtsova, J. Chem. Phys. **139**, 104903 (2013).
[13]A. Mialdun and V. Shevtsova, J. Chem. Phys. **138**, 161102 (2013).
[14]Q. Galand, S. Van Vaerenbergh, and F. Montel, Energy Fuels **22**, 770–774 (2008).
[15]M. Eslamian and M. Z. Saghir, J. Non-Equilib. Thermodyn. **37**, 329–351 (2012).
[16]M. M. Bou-Ali, A. Ahadi, D. Alonso de Mezquia, Q. Galand, M. Gebhardt, O. Khlybov, W. Köhler, M. Larrañaga, J. C. Legros, T. Lyubimova, A. Mialdun, I. Ryzhkov, M. Z. Saghir, V. Shevtsova, and S. Van Varenbergh, Eur. Phys. J. E **38**, 30 (2015).
[17]M. Gebhardt and W. Köhler, Eur. Phys. J. E **38**, 24 (2015).
[18]A. Mialdun, J.-C. Legros, V. Yasnou, V. Sechenyh, and V. Shevtsova, Eur. Phys. J. E **38**, 27 (2015).
[19]A. Ahadi and M. Z. Saghir, Eur. Phys. J. E **38**, 25 (2015).
[20]Q. Galand and S. Van Vaerenbergh, Eur. Phys. J. E **38**, 26 (2015).
[21]O. A. Khlybov, I. I. Ryzhkov, and T. P. Lyubimova, Eur. Phys. J. E **38**, 29 (2015).
[22]M. Larrañaga, M. M. Bou-Ali, D. Alonso de Mezquia, D. A. S. Rees, J. A. Madariaga, C. Santamaría, and J. K. Platten, Eur. Phys. J. E **38**, 28 (2015).
[23]M. Gebhardt and W. Köhler, J. Chem. Phys. **142**, 084506 (2015).
[24]K. Ghorayeb and A. Firoozabadi, AIChE **46**, 883–891 (2000).
[25]L. Kempers, J. Chem. Phys. **90**, 6541 (1989).
[26]J. P. Larre, J. K. Platten, and G. Chavepeyer, Int. J. Heat Mass Transfer **40**, 545 (1997).
[27]S. Srinisvasan and M. Z. Saghir, J. Non-Equilib. Thermodyn. **36**, 243–258 (2011).
[28]D. Alonso de Mezquia, M. M. Bou-Ali, M. Larrañaga, J. A. Madariaga, and C. Santamaría, J. Phys. Chem. B **116**, 2814–2819 (2012).
[29]P. Blanco, M. M. Bou-Ali, J. K. Platten, P. Urteaga, J. A. Madariaga, and C. Santamaria, J. Chem. Phys. **129**, 174504 (2008).
[30]M. Larrañaga, M. M. Bou-Ali, E. Lapeira, C. Santamaría, and J. A. Madariaga, Microgravity Sci. Technol. **26**, 29–35 (2014).
[31]P. Blanco, M. M. Bou-Ali, J. K. Platten, D. A. De Mezquia, J. A. Madariaga, and C. Santamaría, J. Chem. Phys. **132**, 114506 (2010).

J. Thermodiffusion, molecular diffusion and Soret coefficients of aromatic + n-alkane binary mixtures.

Thermodiffusion, molecular diffusion and Soret coefficients of aromatic+n-alkane binary mixtures

M. Larrañaga[1], M. M. Bou-Ali[1], E. Lapeira[1], J. A. Madariaga[2] and C. Santamaría[2].

[1]*MGEP Mondragon Goi Eskola Politeknikoa, Mechanical and Industrial Manufacturing Department, Loramendi 4 Apdo. 23, 20500 Mondragon, Spain.*

[2]*Department of Applied Physics II, University of Basque Country, Apdo. 644, 48080 Bilbao, Spain.*

ABSTRACT

In the present work, we have measured the thermodiffusion coefficient of 51 binary liquid mixtures. This mixtures correspond to the series of the aromatics toluene and 1-methylnaphtalene with n-alkanes nCi (i = 6, 8, 10, 12 and 14) at different concentrations. For that, the thermogravitational technique has been used. It is shown that the thermodiffusion coefficient is a linear function of the mass fraction in all the mixtures. Extrapolating the lines we obtained the thermodiffusion coefficient in dilute solutions of n-alkanes for both toluene and 1-methylnaphtalene. These limiting values showed a linear dependence with the inverse of the product of the molecular weights. In addition, we have also measure the molecular diffusion coefficient of all the mixtures at 0.5 of mass fraction by the Sliding Symmetric Tubes technique. We found that the product of this coefficient with the viscosity at the same concentrations takes a constant value for each of the series considered. Finally, we have also determined the Soret coefficient of the equimass mixtures by the combination of the measurements of thermodiffusion and molecular diffusion coefficients.

K. Analysis of the molecular diffusion coefficient in ternary mixtures by three different techniques.

Analysis of the molecular diffusion coefficient in ternary mixtures by three different techniques.

M. Larrañaga[1], M. Gebhardt[2], T. Triller[2], W. Köhler[2], J.C. Legros[3], A. Mialdun[3], V. Shevtsova[3], M. Mounir Bou-Ali[1].

[1]*MGEP Mondragon Goi Eskola Politeknikoa, Mechanical and Industrial Manufacturing Department, Loramendi 4 Apdo. 23, 20500 Mondragon, Spain*

[2]*Physikalisches Institut, Universität Bayreuth, D-95440 Bayreuth, Germany.*

[3]*MRC, EP CP 165 / 62, Université libre de Bruxelles (ULB), Brussels, Belgium Institution*

ABSTRACT

Molecular diffusion effect takes part in many processes of different areas such as biology or materials engineering. Together with the thermodiffusion phenomenon, it has aroused the interest of the scientific community in the last decade.

As binary mixtures have been studied in-depth and the liquids appearing in natural and in industrial processes usually are multicomponent, most of the efforts in the last years are focused on analysing ternary mixtures. Recently, the first benchmark in ternary mixtures was conducted. In this work, six teams have measured and compared the molecular diffusion, thermodiffusion and Soret coefficients of the ternary mixture formed by 1,2,3,4-tetrahydronaphtalene (THN), isobutylbenzene (IBB) and n-dodecane (nC$_{12}$) at mass concentration of 0.80-0.10-0.10. These measurements have been made by independent techniques and both in ground and microgravity conditions. Results for Soret and thermodiffusion coefficients have shown a very good agreement. However, in the case of molecular diffusion coefficients the differences between the results were larger.

It has been observed that the determination of the molecular diffusion coefficients in ternary mixtures suffers from a significant uncertainty. This has motivated the development of this work, where a deeper analysis of the diffusion phenomenon has been done by different techniques.

The objective of this work is to analyse the determination of the molecular diffusion coefficients by three different techniques: Sliding Symmetric Tubes technique, Optical Beam Deflection technique and Taylor dispersion technique. For that purpose, the analysed mixture is the 0.33-0.33-0.33 concentration of the THN-IBB-nC$_{12}$ system.

The first studies show that there may be more than one combination of coefficients in the diffusion matrix that is in decent agreement with the experimental data. To this day, the eigenvalues of the diffusion matrix have appeared to be more reliable parameters in order to compare different results.

L. Thermodiffusion coefficients of the ternary mixture 1-methylnaphtalene + toluene + n-decane.

Thermodiffusion coefficients of the ternary mixture 1-methylnaphtalene+toluene+n-decane.

Miren Larrañaga[1], M. Mounir Bou-Ali[1], Estela Lapeira[1], Jose Antonio Madariaga[2] and Carlos Santamaría[2].

[1]*MGEP Mondragon Goi Eskola Politeknikoa, Mechanical and Industrial Manufacturing Department, Loramendi 4 Apdo. 23, 20500 Mondragon, Spain*

[2]*Department of Applied Physics II, University of Basque Country, Apdo. 644, 48080 Bilbao, Spain*

ABSTRACT

In this work, we have measured the thermodiffusion coefficient of eight compositions of the ternary system formed by 1-methylnaphtalene, toluene and n-decane at 25°C, by the thermogravitational technique. For that purpose, we have measured also the thermopysical properties of these mixtures.

As it was done for binary mixtures in previous works, we have analysed the effect of different properties of the mixture on the thermodiffusion coefficient, such as viscosity or molecular weight.

On the other hand, we have compared the results obtained in this work with other two ternary mixtures of the literature: tetralin+isobutylbenzene+n-dodecane and toluene+n-dodecane+n-hexane, at different concentrations.